Molecular Dissection of a Nck:WIP:N-WASP signalling Network

Sara Katherine Donnelly

University College London

and

Cancer Research UK London Research Institute

PhD Supervisor: Dr. Michael Way

A thesis submitted for the degree of

Doctor of Philosophy

University College London

September 2012

Declaration

I Sara Katherine Donnelly confirm that the work presented in this thesis is my own. Where information has been derived from other sources, I confirm that this has been indicated in the thesis.

Abstract

Nck and WASP/N-WASP play essential roles in the signalling networks that control Arp2/3 dependent actin polymerisation in a variety of contexts. These include functions downstream of the PDGF, Met and T cell receptors, in endocytosis and in the formation of invadopodia and podosomes. Vaccinia virus exploits a similar signalling network to enhance its cell-to-cell spread. During viral egress newly assembled virus particles fuse with the plasma membrane and activate Src and Abl family kinases. This leads to phosphorylation of a vaccinia protein, A36, and recruitment of a complex of Nck, Grb2, WIP and N-WASP, which activates the Arp2/3 complex to induce the polymerisation of actin tails. The aim of this thesis was to elucidate the exact role of WIP in Nck and N-WASP signalling and furthermore, to understand the connectivity and interplay between the proteins in this important and conserved signalling network.

I found that WIP, or the related protein WIRE, is essential for the induction of actin tails during vaccinia virus infection. I determined that interactions of WIP with the second SH3 domain of Nck and the WH1 domain of N-WASP are crucial for Arp2/3 dependent actin polymerisation. Moreover, in the presence of WIP, the interaction of Nck and N-WASP is dispensable for the actin-based motility of vaccinia virus. Furthermore, in the absence of Grb2, the second SH3 domain of Nck is critical for actin tails formation. My data demonstrates that WIP forms an essential link between Nck and N-WASP that is required to promote Arp2/3 dependent actin polymerisation.

Acknowledgement

First of all, I would like to say that I have loved working in the Way lab and I have never once been sorry that I chose to do my PhD here. I have also loved spending the last four years in London, and I want to thank everyone who has made it such a great time in my life.

Special thanks of course go to Michael, who gave me the chance to work here and has been incredibly supportive throughout my PhD, especially in the last year.

Charlotte, we've been through it all together...and we made it! I know for sure I couldn't have done it without you (especially these last few days of thesis writing, I'm not sure I would have made it without your incredible proof reading skills!). Ashley, I have really loved working with you in the lab and I know that you are a true friend who I will always value. Thanks to Theresa for always being there to sort out all the problems of the lab and for introducing me to the good red wine! Mark deserves special thanks for being an awesome drinking buddy! Amy, I loved working with you and you were also the best neighbour ever! Judy, you always made the lab a more enjoyable place so thank you! Antonio, I always appreciate both your dry wit and incredible range of knowledge. Jazz, thanks for always being encouraging and for lots of laughs in the lab...you are definitely the best "worst post-doc" ever! Xenia, I'm really glad to have met you and I'm sorry we only get to work together for a year. Dave, thank you for making the lab more fun, with your unexpected and hilarious comments! Joe, thanks for livening up the lab and for always being available for random trips to the pub. Thanks to Yutaka for introducing me to some Japanese culture, Kabuki definitely made an impression! Thanks also to Joao and especially to Ina. You both gave me a glimpse of what I could achieve in my four years. Ina, you were a great supervisor and really gave me a good start in the lab. Thanks to Morag and Naoko for always being cheerful and positive!

Finally, the biggest thanks go to my parents and to my sister, Patsy. Without your constant support and encouragement, I definitely would not have made it this far!
Thanks also to Catherine for being a great flatmate throughout my time in London. Thanks to all my other friends both in Ireland and in London for being great distractions when needed. Thanks also go to "the 7th floor crew" for making thesis writing surprisingly fun!

Table of Contents

Table of figures

List of tables

Abbreviations

A-domain	acidic domain
ADF	actin depolymerization factor
ADP	Adenosine 5'-diphosphate
Arp 2/3	actin related proteins 2 and 3
ATP	Adenosine 5'-triphosphate
B-domain	basic domain
bp	base pairs
C-domain	connector domain
CA	connector acidic region
CB	cytoskeleton buffer
CCD	charged coupled device
Cdc	Cell division cycle
CEV	cell-associated enveloped virus
CO_2	carbon dioxide
CRIB	Cdc42 and Rac interactive binding
DAPI	4',6 diamidino-2-phenylindole
DMEM	Dulbecco's modified eagle medium
DMSO	Dimethyl sulfoxide
DNA	deoxyribonucleic acid
dNTP	deoxynucleoside 5'-triphosphate
E.coli	*Escherichia coli*
ECL	enhanced chemiluminescence
EDTA	ethyl diamine N,N,N',N'-tetraacetic acid
EEV	Extracellular enveloped virus
EPEC	Enteropathogenic Escherichia coli
F-actin	filamentous actin
FACS	fluorescence activated cell sorting
FBS	foetal bovine serum
FITC	fluorescin isothiocyanate
FRAP	Fluorescence recovery after photobleaching

FRET	Förster resonance electron transfer
FSM	fluorescent speckle microscopy
G-actin	monomeric actin
GAG	Glycosaminoglycan
GEF	Guanine nucleotide exchange factor
GFP	green fluorescent protein
GTP	Guanosine 5'-triphsphate
HBS	HEPES buffered saline
hpi	hours post infection
HRP	horseradish peroxidase
IEV	intracellular enveloped virus
IF	immunofluorescence
IMV	intracellular mature virus
IP	immunoprecipitation
IV	immature virus
k	rate constant of recovery
kb	kilobase
kDa	kiloDalton
LB	Luria Bertani
M	Molar
MEFs	mouse embryonic fibroblasts
MEM	modified eagle medium
MOI	multiplicity of infection
N-WASP	neural Wiskott Aldrich Syndrome Protein
NPF	nucleating promoting factor
NTP	nucleoside 5'-triphosphate
ºC	degrees Celsius
OD	optical density
PBS	phosphate buffered saline
PCR	polymerase chain reaction
pE/L	early late promoter
Pen	penicillin
PFA	Paraformaldehyde

PFU	plaque forming units
Pi	inorganic phosphate
PIP_2	Phosphatidylinositol 4,5-bisphosphate
pL/L	plasmid lenti lox
pmol	picomolar
PNS	post-nuclear viral stock
PolyPro	poly-proline rich domain
RFP	red fluorescent protein
Rho	Ras homolog gene family
RNAi	Ribonucleic acid interference
ROI	region of interest
rpm	revolutions per minute
RRE	Rev response element
RT	room temperature
RTK	receptor tyrosine kinase
SDS	sodium dodecyl sulphate
Sec	seconds
SH	Src homology
siRNA	small interfering ribonucleic acid
Strep	streptomycin
$t_{1/2}$	half time
TBE	Tris-Borat buffer
V-domain	Verprolin or WH2 domain
v/v	volume per volume
VSV-G	vesicular stomatitis virus –G pseudotyped
w/v	weight/volume
WASP	Wiskott Aldrich-Syndrome Protein
WBD	WASP binding domain
WH	WASP homology domain
WIP	WASP interacting protein
WIRE	WIP related
WR	Western Reserve
YFP	yellow fluorescent protein

Chapter 1. Introduction

1.1 The importance of actin polymerisation

Actin is one of the most abundant proteins in eukaryotic cells and is highly conserved throughout evolution (Erickson, 2007; Firat-Karalar and Welch, 2011). A key characteristic of actin is its ability to polymerise into filaments (Dominguez and Holmes, 2011). This is a dynamic process that occurs in all eukaryotic cells and it is crucial for a wide range of functions that are fundamental to the functioning of the cell and thus the whole organism. For example, actin polymerisation is involved in synapse formation in the brain; in the immune system and in many stages of development (Hotulainen and Hoogenraad, 2010; Reicher and Barda-Saad, 2010; Suzuki et al., 2012). At a subcellular level, the polymerisation of actin at the plasma membrane drives cell migration, while it also plays a major role in endocytosis and membrane trafficking (Ridley, 2011; Anitei and Hoflack, 2012). Furthermore, many cellular organelles are transported in a myosin-dependent manner along actin filaments, and the formation of a contractile ring of actin filaments is required for cytokinesis (Hammer and Sellers, 2012; Pollard and Cooper, 2009). The wide variety of cellular roles that involve actin polymerisation means that tight spatial and temporal control of this process is required. Moreover, deregulation of actin polymerisation results in pathogenesis in many forms, notably in aberrant cell migration and invasion in driving tumour cell metastasis (Nurnberg et al., 2011). A combination of *in vitro* biochemical studies, cellular studies as well as findings in model organisms have led to a good understanding of the principles underlying actin polymerisation, as well as many of the key molecules involved. However, much still remains to be understood and it is only by elucidating the detailed molecular basis of the various signalling networks that control actin polymerisation, as well as the interplay between these networks that a complete understanding of actin polymerisation can be achieved.

1.2 Actin Cytoskeleton

1.2.1 Actin

Actin is a 42kDa protein that has 6 isoforms in mammals – 3 α-isoforms, 1 β-actin isoform and 2 γ-isoforms (Perrin and Ervasti, 2010). Expression of each α-isoform is restricted to skeletal, cardiac or smooth muscle, while one of the γ-isoforms is also specific to smooth muscle. The other γ-isoform and β-actin are ubiquitously expressed. The sequences of these six different isoforms are very similar, with none of them having less then 93% identity to each other. In addition, the majority of the differences lie in the N-termini of the proteins. Studies using knockout mice have revealed that the different actin isoforms have both distinct and overlapping functions (Tondeleir et al., 2009). Knockout of β-actin is embryonically lethal, while loss of the cardiac isoform of α-actin results either in embryonic lethality or perinatal death (Kumar et al., 1997; Shawlot et al., 1998). Loss of the other isoforms results in viable animals that exhibit muscle weakness, reduced stature, deafness or heart defects depending on the specific actin isoform (Perrin and Ervasti, 2010).

1.2.2 The organisation of the actin cytoskeleton

Actin filaments are comprised of two chains of actin monomers that wrap around each other to form a helix (figure 1.1 A) (Hanson and Lowy, 1964). These filaments can be organised in a variety of different ways to form the many actin-based structures in the cell. These structures include lamellipodia, lamella, ruffles, phagocytic and endocytic cups, podosomes and invadopodia, filopodia and microvilli as well as stress fibres (Chhabra and Higgs, 2007; Pellegrin and Mellor, 2007). Lammellipodia are thin sheet like protrusions that are found at the leading edge of migrating cells (Abercrombie et al., 1970a; Svitkina and Borisy, 1999). They are comprised of a dense meshwork of crosslinked actin filaments and are believed to provide the force that drives motile cells forward (Small et al., 2002). The lamella is similar but begins directly behind the lammellipodium and extends back into the cell body. It is also sheet-like but is thicker and less dynamic than the lammelipodium (Chhabra and Higgs, 2007). Ruffles are reminiscent of lammellipodia, but do not adhere to the substrate. There are at least two distinct

populations of ruffles, peripheral and dorsal (Abercrombie et al., 1970b). Peripheral ruffles assemble at the leading edge and move backwards, while dorsal ruffles form as circular structures on the dorsal surface of the cell. Dorsal ruffles are associated with receptor internalisation and possibly macropinocytosis, while peripheral ruffles are only involved in cell migration (Abella et al., 2010a). In phagocytosis, actin polymerisation generates the force required for the cell membrane to envelope extracellular particles and internalise them (Jaumouille and Grinstein, 2011). In addition, during endocytosis, actin polymerisation is required to shape and pinch off vesicles from the plasma membrane (Mooren et al., 2012). Podosomes and invadopodia are specialised adhesive structures that are important for cell migration and invasion (Garcia et al., 2012). Podosomes appear as F-actin rich puncta and seem to function to degrade the extra-cellular matrix to allow cells to migrate through tissues (Cornfine et al., 2011). Invadopodia are similar to podosomes, but are distinct, degradative structures that are only found in cancer cells (Garcia et al., 2012; Oser et al., 2011). Filopodia are thin protrusive spikes that contain parallel bundles of actin filaments (Faix and Rottner, 2006). They generally protrude from the lammellipodium and function as directional sensors during migration (Arjonen et al., 2011; Zheng et al., 1996). Filopodia can also form within the lamellipodium, but they are then referred to as microspikes (Chhabra and Higgs, 2007). Stress fibres are bundles of actin filaments that interact with myosin filaments to form contractile arrays (Pellegrin and Mellor, 2007). They are involved in contracting the rear of the cell and promoting detachment from the substrate during migration (Hotulainen and Lappalainen, 2006).

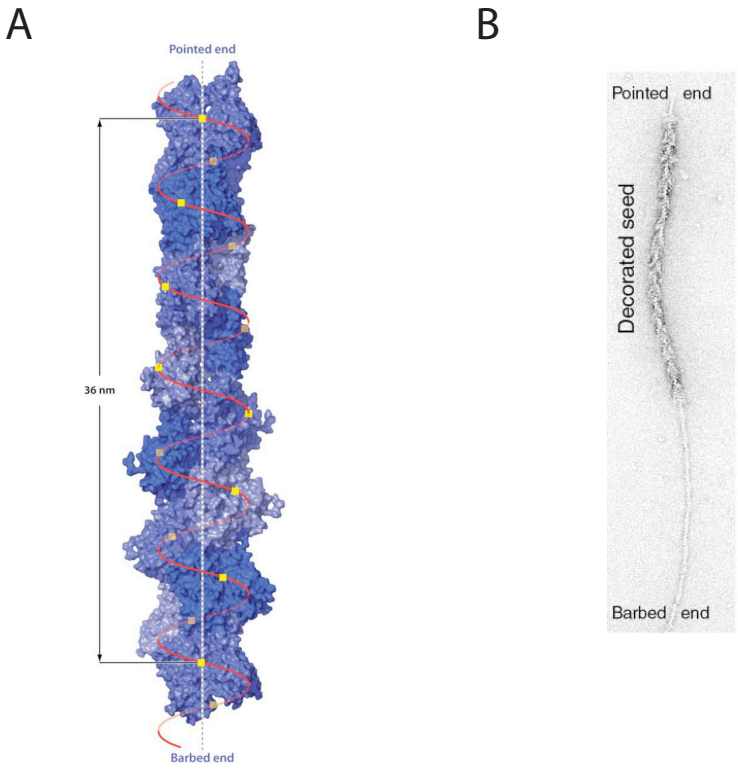

Figure 1.1. The actin filament

(A) The helical structure of an actin filament derived from cryo-electron microscopy. (Taken from Dominguez and Holmes, Actin Structure and Function, Annual review of biophysics, 40, 169-86, (2011). Reproduced with permission of Annual Reviews) **(B)** Electron micrograph of a negatively stained actin filament decorated with the actin binding domain of myosin. Based on this labelling, the terms barbed and pointed end arose. Undecorated filament is newly polymerised actin, highlighting that barbed end growth is more rapid than pointed end growth. Reprinted from Cell, Volume 112, Issue 4, Pollard and Borisy, Cellular Motility Driven by Assembly and Disassembly of Actin Filaments, 453-465, Copyright (2003), with permission from Elsevier.

1.2.3 Actin Polymerisation in vitro

In vitro, above the critical concentration, actin monomers (G-actin) can spontaneously self-assemble or polymerise into polarised filaments with a barbed and a pointed end. These names derive from the appearance of actin filaments decorated with the HMM (heavy meromyosin) fragment of myosin in electron micrographs (Figure 1.1 B) (Huxley, 1963; Woodrum et al., 1975). Different assays are available to measure the rate of actin polymerisation *in vitro,* including fluorescence microsopy and ultracentifugation assays (Amann and Pollard, 2001;

Breitsprecher et al., 2009; Cooper and Pollard, 1982; Fujiwara et al., 2007). However, one of the most sensitive and commonly used techniques is the pyrene-actin assembly assay. In this assay, the polycyclic aromatic hydrocarbon, pyrene is conjugated to actin monomers and the fluorescence is measured over time. The fluorescence intensity pyrene-actin increases 10-20 fold when it is incorporated into filaments (Cooper et al., 1983). This assay has been used to establish the characteristics of actin polymerisation. The rate-limiting step in this process is the establishment of nuclei (nucleation phase), which consist of three actin monomers and act as a stable "seed" from which the rest of the filament can rapidly polymerise (Nishida and Sakai, 1983). Biochemical analysis of the properties of crosslinked actin trimers revealed that they are more effective at nucleating actin polymerisation than either dimers or higher-order oligomers (Gilbert and Frieden, 1983). After nucleation, a period of rapid actin polymerisation occurs, which is referred to as the elongation phase. During this phase, actin monomers can be added to either end of the growing filament, although there is a strong bias for addition of monomers to the barbed ends (or plus ends) of filaments (Figure 1.1 B) (Woodrum et al., 1975). The rate of filament growth is dependent on the concentration of free actin monomers in solution (Pollard, 1983). Eventually, as filaments grow, the concentration of G-actin monomers decreases, and a steady-state is reached where there is no net change in the filament length. The concentration of free actin monomers at this steady-state is known as the critical concentration (C_c) (Figure 1.2 A). At concentrations greater than the C_c, a solution of G-actin will polymerise while at concentrations below this value, G-actin cannot polymerise and F-actin will depolymerise. The C_c at the barbed end is about seven times lower than at the pointed end of the filament, thus actin monomers are added more rapidly to the barbed end of the filament (Pollard and Borisy, 2003; Wegner and Isenberg, 1983).

Structurally, the actin polypeptide chain can be divided into two domains referred to as the inner and outer domains with respect to their position in actin filaments. These domains can each be further sub-divided in two (Figure 1.2 B) (Kabsch et al., 1990). A hinge region links the two major domains but otherwise few contacts are made between them. This results in the formation of two clefts. The upper cleft is the site of nucleotide and magnesium binding, while the lower cleft is site of

interaction with the majority of known actin binding proteins including profilin and the WH2 domain of N-WASP (Chereau et al., 2005; Lee et al., 2007; Mouilleron et al., 2008; Schutt et al., 1993). Actin monomers are bound to ATP or ADP as well as to the divalent cation magnesium. The ability of F-actin to hydrolyse ATP is much greater than that of G-actin, and incorporation of G-actin into filaments results in the rapid hydrolysis of ATP to ADP-Pi, followed by the slow release of Pi (half-lives of 2s and 350s respectively) (Figure 1.2 C) (Blanchoin and Pollard, 2002; Carlier and Pantaloni, 1986). The hydrolysis of ATP in actin filaments is irreversible (Carlier et al., 1988). This leads to a long-lived “cap” of ADP-Pi intermediates at the barbed end of newly assembled filaments. The properties of ATP-actin and ADP-Pi-actin are similar, however, upon release of the phosphate from the monomer, a conformational change occurs that results in more flexible filaments and facilitates the dissociation of ADP-actin from the filament (Janmey et al., 1990; Orlova and Egelman, 1992). The dissociation of ADP-actin from the barbed end of filaments is much more rapid than that of ATP-actin, however, both species dissociate slowly from the pointed ends of filaments (Figure 1.2 D) (Pollard, 1986). This leads to the net incorporation of ATP-bound actin monomers at the barbed ends of filaments. These then undergo ATP-hydolysis and the resulting ADP-actin dissociates from the pointed end of the filament (Fujiwara et al., 2002; Wegner, 1976). This process is referred to as actin filament treadmilling. ATP-hydrolysis drives this treadmilling process, but is not required for nor directly coupled to the polymerisation of actin monomers (De La Cruz et al., 2000; Pardee and Spudich, 1982; Pollard and Weeds, 1984). Instead, hydrolysis can be thought of as an internal timer that denotes the age of the actin filament and results in the activation of processes that lead to actin disassembly in cells.

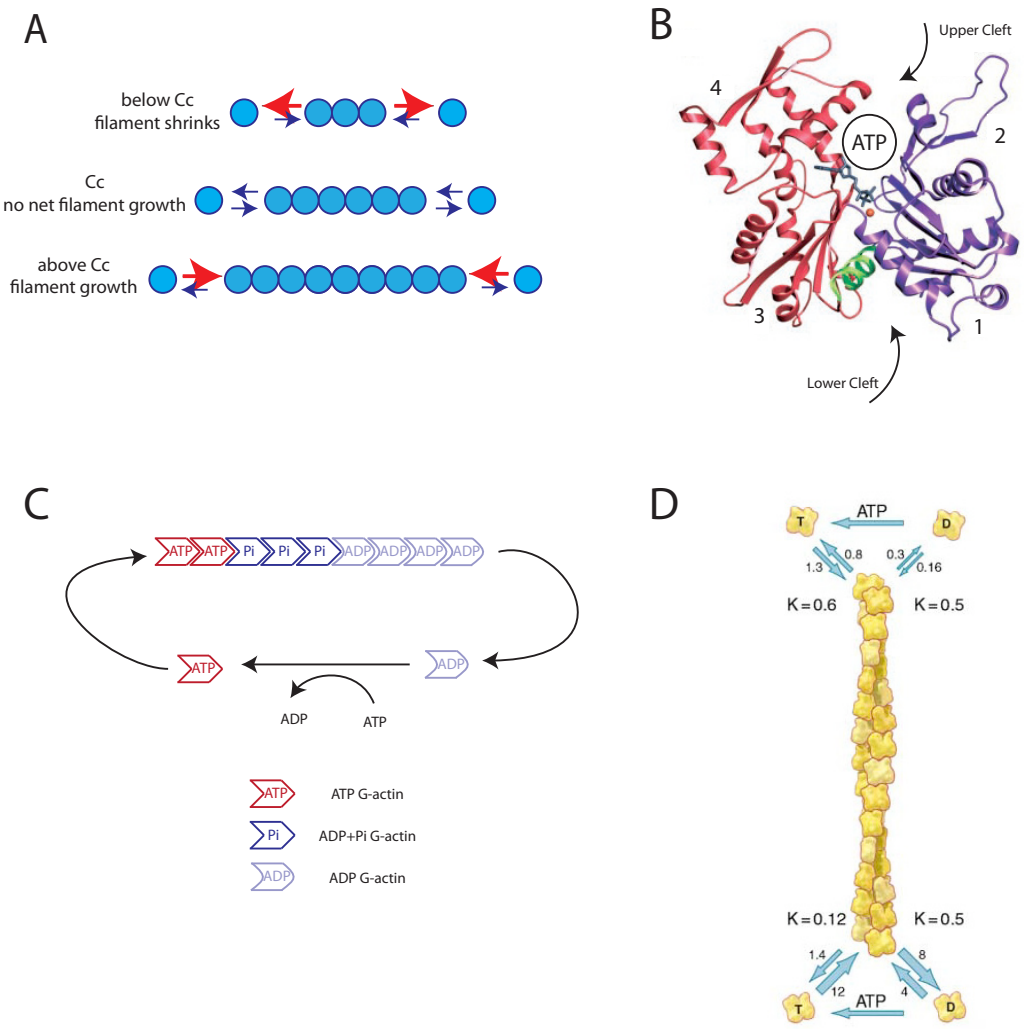

Figure 1.2. Structure and polymerisation of actin

(A) The concentration of free G-actin (the critical concentration Cc) is crucial for controlling the growth of actin filament. Below the Cc, actin will not polymerise. **(B)** Crystal structure of G-actin bound to ATP. The numbers indicate the subdomains of the monomer. The lower cleft, where profilin and WH2 domain containing proteins interact with the monomer is indicated. (This research was originally published in The Journal of Biological Chemistry. Graceffa and Dominguez. Crystal Structure of monomeric actin in the ATP state: Structural basis of nucleiotide dependent actin dynamics. *JBC*. 2003; 278:172-80. © the American Society for Biochemistry and Molecular Biology.)**(C)** Schematic of the treadmilling and ATP hydrolysis cycle that occurs during actin polymerisation (adapted from (Pantaloni et al., 2001)) **(D)** Cartoon of an actin filament. The rates of association and dissociation of ATP and ADP actin monomers from each end of the filament are shown. Reprinted from Cell, Volume 112, Issue 4, Pollard and Borisy, Cellular Motility Driven by Assembly and Disassembly of Actin Filaments, 453-465, Copyright (2003), with permission from Elsevier.

1.2.4 Actin Polymerisation in vivo

Actin filament treadmilling has also been shown to occur *in vivo* (Symons and Mitchison, 1991; Wang, 1985; Watanabe and Mitchison, 2002). Electron microscopy experiments demonstrated that the barbed ends of actin filaments are oriented toward the plasma membrane in the lamellipodia of migrating cells as well in the stationary coelomocytes of sea urchins (Edds, 1993; Small et al., 1978). Photobleaching (FRAP) of actin filaments in the lamellipodia of fibroma cells revealed that new actin monomers were incorporated near the edge of the cell and that the bleached region exhibited retrograde flow towards the cell body (Wang, 1985). Further studies in fibroblasts provided additional evidence for the incorporation of actin monomers at the leading edge of the cell (Symons and Mitchison, 1991). Photoactivation of actin filaments demonstrated that they remain fixed with respect to the substrate in migrating fish keratocytes, regardless of the rate of cell migration (Theriot and Mitchison, 1991). The same study also showed that the actin in the bleached region moves towards the cell body. This data supported a treadmilling model of actin polymerisation, however, it was unclear if actin filaments initiated at the plasma membrane extend through the length of the lamellipodia and if actin monomers treadmill through this entire length.

Fluorescence speckle microscopy has given further insight into this issue (Waterman-Storer et al., 1998). In this technique, a very low level of labelled protein (relative to the endogenous pool) is introduced into cells. The random incorporation of this label into cellular structures allows for low background in fluorescent imaging. Using this approach, actin was shown to move rearward in both the lamellipodia and lamella of cells (Waterman-Storer et al., 1998). In addition, single molecule studies using this technique demonstrated that actin treadmilling occurs in filaments and that the majority of new filaments are initiated in the region immediately adjacent to the plasma membrane (Watanabe and Mitchison, 2002). However, the same study also demonstrated that a basal level of actin polymerisation occurs throughout the lamellipodium (Watanabe and Mitchison, 2002). More recent studies using advanced microscopy techniques including FRAP (fluorescence recovery after photobleaching), photoactivation and FLIP (fluorescence loss in photobleaching), further demonstrated that actin is primarily

incorporated into filaments at the leading edge of cells and that treadmilling occurs (Lai et al., 2008; Millius et al., 2012).

1.3 Factors Regulating Actin Polymerisation

Despite evidence demonstrating that actin treadmilling occurs in cells, the slow rate of actin treadmilling observed *in vitro* could not explain the rapid actin rearrangements that occur in cells or the observed rates of cell migration (Pollard and Borisy, 2003). For example, the rate of treadmilling *in vitro* has been measured at about 0.008 μm/minute compared with around 0.80 μm/minute in cells (Bonder et al., 1983; Wang, 1985). This discrepancy indicates that other regulatory proteins must facilitate cellular actin polymerisation. The minimum requirements for actin-based motility have been demonstrated by *in vitro* reconstitution of the motility of the bacterium *Listeria monocytogenes* (Cameron et al., 1999; Loisel et al., 1999; Welch et al., 1997b; Welch et al., 1998). The key proteins that are required to promote actin-based motility in this case are: an actin nucleator, a nucleation-promoting factor, profilin, capping protein and ADF/cofilin (Loisel et al., 1999). These will be discussed in more detail in the following sections.

1.3.1 Actin Nucleators

In vitro, actin polymerisation occurs rapidly only after the establishment of nuclei comprising of trimers of actin monomers (Gilbert and Frieden, 1983). The formation of the trimer is very inefficient, thus factors have evolved to overcome this kinetically unfavourable step. These are known as actin nucleators. The major classes of actin nucleators are: the Arp2/3 complex, the formins and the WH2 domain-containing nucleators (Campellone and Welch, 2010). The Arp2/3 complex was the first actin nucleator discovered, and as it is the most relevant to this thesis, will be discussed in detail in chapter 1.4.

1.3.1.1 The Formins

The formins are a family of proteins that have both actin nucleation and elongation activity (Paul and Pollard, 2008). Formins induce unbranched actin filaments and the defining feature of these proteins is the presence of conserved formin

homology domains (FH1 and FH2) (Li and Higgs, 2003; Pruyne et al., 2002; Romero et al., 2004). The FH2 domain is sufficient to induce the polymerisation of purified actin, however the mechanism of actin nucleation and elongation *in vivo* has not been fully elucidated (Figure 1.3 A) (Sagot et al., 2002). FH2 domains appear to bind to the barbed ends of filaments and compete with other barbed end capping proteins, thereby preventing them from inhibiting elongation of the filament (Pruyne et al., 2002). At the same time, the FH2 domains facilitate the addition of actin monomers to the filament. Crystal structures of FH2 domains indicate that they are homodimers that exist as a ring that can bind two actin monomers simultaneously and mimic the short-pitch actin dimers that exist in filaments (Otomo et al., 2005). The FH2-ring binds to the barbed end of filaments in either a closed or an open conformation (Otomo et al., 2005). In the closed conformation, the FH2 dimer caps the end of the filament, while in the open conformation; actin monomers can be added to the filament although the mechanism of this is unclear. Meanwhile, the FH1 domain, which is adjacent to the FH2 domain, binds to profilin (Paul and Pollard, 2008). Thus the FH1 domain supplies the monomers directly to the FH2 domain for incorporation into the filament, resulting in more rapid elongation (Figure 1.3 B) (Courtemanche and Pollard, 2012).

The formins are divided into several classes based on the sequences of the FH2 domain. These are the DRFs (Diaphanous related formins), which include mDia1-3, the FRLs (formin related in leukocytes) and DAAM (dishevelled-associated activator of morphogenesis) proteins, the FMN (formin) and FHOD (FH1 and FH2 domain containing) proteins as well as Delphilin, INF1 and INF2 (inverted formins) (Campellone and Welch, 2010). Outside of the conserved FH1 and FH2 domains, the formins are large proteins containing a variety of different domains. This diversity allows formins to interact with a wide range of binding partners that regulate their functions in many cellular processes, including cell division, migration, morphogenesis and adhesion (Chesarone et al., 2010). Finally, in addition to their role as actin nucleators, some of the formins, including mDia1 and 2) have also been shown to directly regulate the function of microtubules (Bartolini and Gundersen, 2010).

1.3.1.2 WH2-containing nucleators

The WH2 domain containing nucleators comprise the Spire and Leiomoden families of proteins, as well as Cordon-Bleu (COBL) (Figure 1.3 C) (Ahuja et al., 2007; Conley et al., 2001; Quinlan et al., 2005). These actin nucleators have been identified in the last seven years and are less well characterised than the formins or the Arp2/3 complex.

Spire was first identified as an essential factor in the development of drosophila oocytes and embryos (Quinlan et al., 2005). Spire contains four tandem WH2 (WASP Homology 2) domains that bind actin and are required for its actin nucleating activity *in vitro* (Quinlan et al., 2005). Structural studies demonstrated that Spire creates an actin nucleus by tethering three monomers together in either a side-to-side conformation or a straight longitudinal arrangement (Ducka et al., 2010). These structures are thought to represent different steps of the normal actin filament nucleation process. The nucleating ability of Spire is thought to be a result of its ability to form an actin nucleus that resembles one strand of the long pitch actin helix in a filament. In addition, Spire can cap the pointed ends of actin filaments and inhibit disassembly (Quinlan et al., 2005). Spire interacts with Cappuccino (a drosophila formin) and this interaction promotes actin nucleation by spire, while inhibiting the ability of Cappuccino to nucleate actin polymerisation (Quinlan et al., 2007). This finding hints at the complex layers of regulation that influence actin polymerisation *in vivo*. Spire has also recently been shown to play roles in neuronal morphogenesis and heart development in drosophila (Gates et al., 2011; Xu et al., 2012a). Furthermore, Spire-type actin nucleators have also been found to play a critical role in the asymmetric division of oocytes in mice (Pfender et al., 2011).

The Leiomoden family of nucleators are related to tropomodulin and are specifically expressed in muscle cells (Conley et al., 2001). The members of the leiomoden family have an actin-binding domain in the flexible N-terminus, a central leucine rich repeat (LRR) region and a C-terminal WH2 domain. As these three domains can all interact with actin monomers, they are thought to function in the assembly of

an actin trimer that nucleates actin polymerisation, which then proceeds from the barbed end (Chereau et al., 2008).

Cordon-bleu or COBL is a vertebrate specific actin nucleator that is highly expressed in the brain (Ahuja et al., 2007). COBL contains three WH2 domains that function together to nucleate actin polymerisation by binding actin monomers in a trimeric arrangement that allows for elongation from the barbed end of the filament (Ahuja et al., 2007; Husson et al., 2011; Qualmann and Kessels, 2009). The actin nucleation ability of low concentrations of COBL is as high as that of the Arp2/3 complex, although at high concentrations COBL sequesters actin monomers and inhbits actin polymerisation. Physiologically, COBL has been shown to play a role in regulating the morphology of neuronal cells as overexpression of COBL results in an increased number of dendrites as well as increasing axonal branching (Ahuja et al., 2007; Schwintzer et al., 2011).

Recently, JMY has also been shown to have actin nucleating ability (Zuchero et al., 2009). JMY nucleates actin using a combination of three tandem WH2 domains as well as a linker region, in a manner reminiscent to spire (Firat-Karalar et al., 2011). Interestingly, JMY is also a nucleating promoting factor that can increase the activity of the Arp2/3 complex (Zuchero et al., 2009).

APC (adenomatous polyposis coli), an established regulator of microtubule dynamics, has also been shown to contain actin-nucleating activity (Munemitsu et al., 1994). This requires the basic C-terminal region of the protein, which interacts directly with G-actin, despite lacking any similarity to WH2 domains (Okada et al., 2010). APC has also been shown to synergise with the formin, mDia1 to promote actin polymerisation (Breitsprecher et al., 2012).

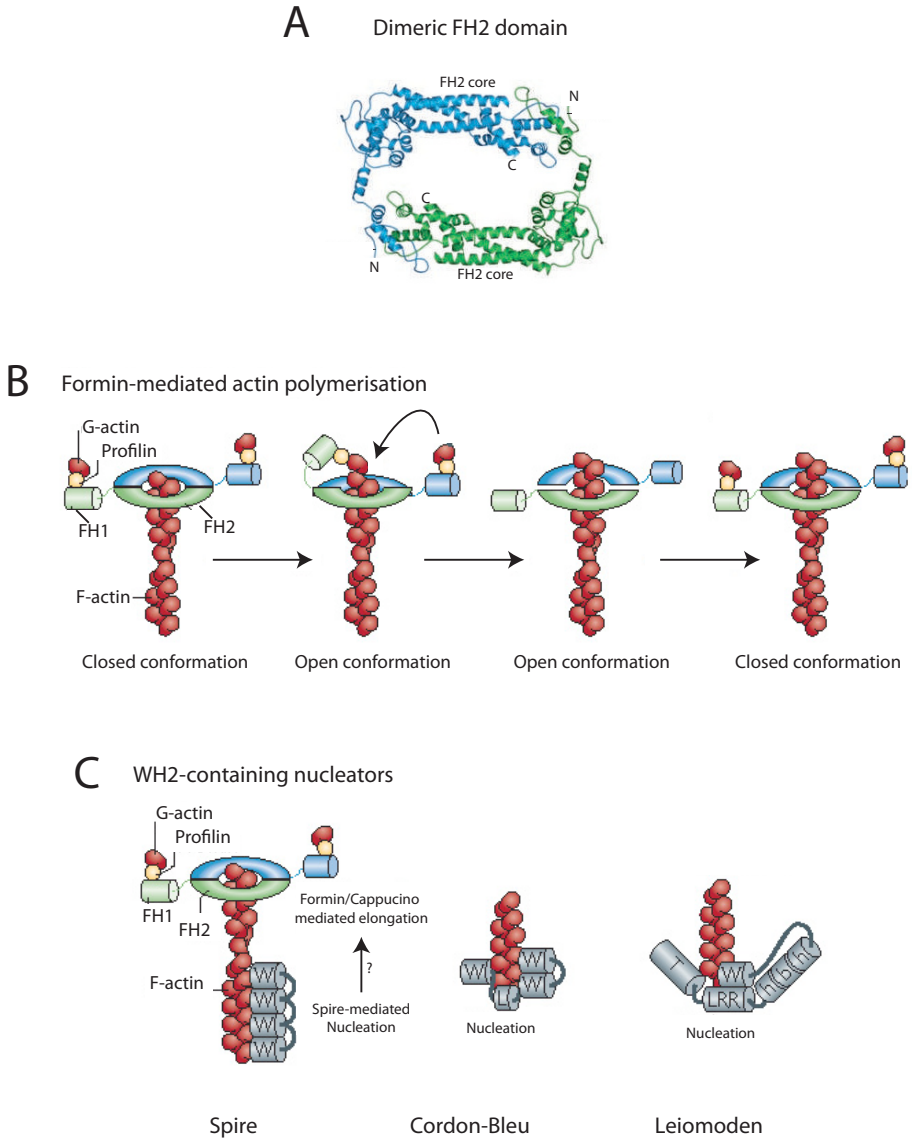

Figure 1.3. Nucleation of actin by formins

(A) Structure of the dimeric FH2 domain from *S.cerevisiae* Bni1. **(B)** An FH2 dimer binds to the barbed end of an actin filament, as the FH1 domains recruit profilin-actin. The profilin-actin is added to the barbed end, either before or after the FH2 domain steps towards the barbed end. The second FH2 then repeats this process. In the closed conformation, the formin prevents actin filament capping by other factors. **(C)** Schematic of actin nucleation by the WH2 domain containing nucleators Spire, Cordon-Bleu and Leiomoden. Spire has been found to cooperate with formins in actin polymerisation. Reprinted by permission from Macmillan Publishers Ltd: Nature Reviews Molecular Cell Biology Campellone and Welch, A nucleator arms race: cellular control of actin assembly, copyright (2010)

1.3.2 Profilin

The profilins are a family of small proteins (~16kDa) that are conserved in eukaryotes and form a 1:1 complex with monomeric G-actin (Carlsson et al., 1976). This complex inhibits spontaneous actin polymerisation *in vitro* (Carlsson et al., 1977). The profilin family consists of four isoforms, of which only profilin I is ubiquitously expressed (Obermann et al., 2005; Witke, 2004). The importance of profilin I is demonstrated by the fact that homozygous knockout mice die at the embryonic two cell stage due to cytokinesis failure (Witke et al., 2001). A major function of profilin is to facilitate the nucleotide exchange of actin monomers (Figure 1.4) (Blanchoin and Pollard, 1998; Lu and Pollard, 2001; Porta and Borgstahl, 2012). This occurs because profilin both decreases the affinity of actin for ADP and transiently stabilises actin in an open conformation that permits the exchange of nucleotides with the surrounding environment (Selden et al., 1999l; Porta and Borgstahl, 2012). In addition, profilin prevents ADP-actin binding to either the barbed or the pointed ends of filaments, thus sequestering ADP-actin. The combined action of profilin leads to the accumulation of a large pool of ATP-actin monomers that are ready to be incorporated into actin filaments. Furthermore, profilin-bound ATP-actin complexes can only be added to the barbed ends of filaments (Pollard and Cooper, 1984; Tilney et al., 1983). In this way, profilin directs the addition of actin monomers in a manner that is consistent with the observed treadmilling of actin filaments in cells (Lai et al., 2008; Waterman-Storer et al., 1998).

1.3.3 ADF/Cofilin

The ADF/cofilin family of proteins is conserved from yeast to humans and in vertebrates consists of three members – ADF (actin depolymerising factor), cofilin 1(non-muscle) and cofilin 2 (muscle-specific) (Bernstein and Bamburg, 2010). ADF/cofilin can interact with both filamentous (F-) actin and monomeric G-actin (Blanchoin and Pollard, 1998). The primary function of ADF/cofilin is to promote the disassembly of actin filaments both by filament severing and by increasing the dissociation of actin monomers from the pointed ends of filaments (Figure 1.4) (Andrianantoandro and Pollard, 2006; Carlier et al., 1997). ADF/cofilin preferentially

interacts with ADP-bound F-actin and upon binding causes a localised twist in the structure of the filament at the site of interaction, which weakens the longitudinal contacts between the monomers and promotes severing (Galkin et al., 2011; McGough et al., 1997; Okreglak and Drubin, 2007). The hydrolysis of ATP and slow released of inorganic phosphate (Pi) from actin filaments can be thought of as a molecular clock denoting the age of the filament, thus ADF/cofilin binds preferentially to older filaments. Furthermore, although it binds ADP-Pi filaments with a lower affinity, ADF/cofilin also promotes the release of Pi from these filaments resulting in increased filament aging and the accumulation of ADP-bound actin molecules that are able to disassemble from the filament (Blanchoin and Pollard, 1999). In this way ADF/cofilin promotes actin polymerisation both by increasing the number of uncapped barbed ends that are available for elongation and also the concentration of free actin monomers in the cell. Interestingly, at high concentrations ADF/cofilin has also been shown to have some actin nucleating capacity, which may also contribute to its ability to promote actin polymerisation (Andrianantoandro and Pollard, 2006). Filament severing occurs at the boundaries between regions of the filament that have bound ADF/cofilin and those that are undecorated, thus ADF/cofilin also regulates the length of the filament to be severed (Suarez et al., 2011).

In addition to its activity in filament severing, ADF/cofilin also binds to G-actin. Preferential binding of ADP-G-actin is observed and this interaction prevents the free exchange of ADP for ATP (Blanchoin and Pollard, 1998; Kardos et al., 2009). Profilin has been shown to synergise with ADF/cofilin *in vivo* to increase actin dynamics (Didry et al., 1998). In yeast, another protein, Srv/CAP, links the activities of profilin and cofilin (Balcer et al., 2003). Srv/CAP promotes the dissociation of actin monomers from cofilin, while concurrently promoting their association with profilin, thus facilitating the exchange of ADP for ATP (Balcer et al., 2003). The presence of a conserved Srv2/CAP protein in humans suggests that this may be a common mechanism of action (Moriyama and Yahara, 2002). The activity of ADF/cofilin is necessary to promote actin polymerisation during many cellular processes including endocytosis and cell migration (Okreglak and Drubin, 2007; Pollard and Borisy, 2003). ADF/cofilin is localised throughout the lamellipodia of migrating cells, where it exhibits dynamics consistent with a role in promoting actin

filament disassembly (Lai et al., 2008). Overexpression of ADF/cofilin also increases the rate of motility of *dictyostelium* (Aizawa et al., 1996). In addition, ADF/cofilin is important for the actin-based motility of *Listeria* and *Rickettsia* (Loisel et al., 1999; Serio et al., 2010).

1.3.4 Capping Protein

Capping proteins (CP) are another family of proteins that promote actin polymerisation. They are conserved in eukaryotes and exist as functional α/β heterodimers (Cooper and Sept, 2008). The α-subunits range in size from 32-36kDa, while the β-subunits are slightly smaller at 28-32kDa. CP binds to the barbed ends of actin filaments and prevents both the addition and loss of actin monomers (Isenberg et al., 1980; Wear et al., 2003). Capping of actin filaments controls the rate of filament elongation as well as limiting the length of the actin filaments (Figure 1.4). This is beneficial in situations such as cell migration, where actin filaments are required to generate force (Pollard and Borisy, 2003). Short filaments are stiffer than long filaments and therefore push the membrane forward more efficiently (Mogilner and Oster, 1996).

Capping of the barbed ends of filaments results in depolymerisation of those filaments from their pointed end (Pantaloni et al., 2000). This results in more free ADP-actin monomers, which can be converted to ATP-actin by profilin, and are then available for incorporation into new filaments (section 1.3.3). As the rate of polymerisation is proportional to the concentration of ATP-actin monomers, this leads to an increase in the rate of polymerisation of uncapped filaments. Carlier and Pantaloni coined the phrase " the funnelled treadmilling model" to describe this mechanism, by which capping protein regulates the delivery of actin monomers to uncapped filaments so that rapid elongation can occur, for example, at the leading edge (Carlier and Pantaloni, 1997; Pantaloni et al., 2001). A more recent study has challenged this model and instead proposes that capping protein cooperates with the Arp2/3 complex to increase the nucleation of actin filaments (Akin and Mullins, 2008).

The localisation of capping protein is limited to the leading edge of migrating cells (Lai et al., 2008; Mejillano et al., 2004). This is consistent with its role in promoting actin polymerisation by interaction with the barbed ends of filaments. In further support of this role, the level of expression of capping protein in *dictyostelium* controls the rate of motility (Hug et al., 1995). The actin-based motility of *Listeria* and *Shigella* requires capping protein and the rate of this motility increases with increasing concentrations of capping protein (Loisel et al., 1999). At extremely high levels of capping protein, no motility is observed, probably because all of the barbed ends are capped and actin filament disassembly is favoured.

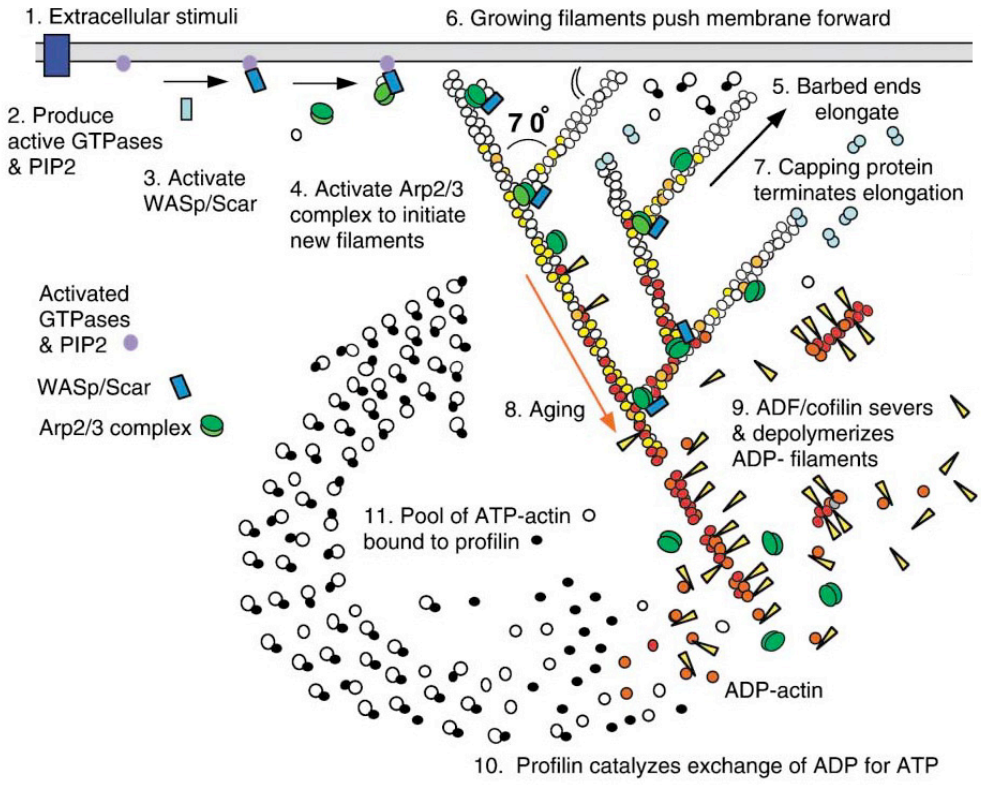

Figure 1.4. The regulation of actin polymerisation *in vivo*

Schematic depicting a proposed model for the regulation of actin polymerisation and actin filament treadmilling at the plasma membrane of a cell. The roles of profilin, ADF-cofilin and capping protein are indicated. Reprinted from Cell, Volume 112, Issue 4, Pollard and Borisy, Cellular Motility Driven by Assembly and Disassembly of Actin Filaments, 453-465, Copyright (2003), with permission from Elsevier.

1.4 The Arp2/3 Complex

1.4.1 Structure and branching ability of the Arp2/3 complex

The Arp2/3 complex was the first actin nucleator identified and is the best studied of these factors (Goley and Welch, 2006; Machesky et al., 1994). This large (220kDa), seven subunit complex was initially purified from *Acanthamoeba* extracts using a profilin affinity column (Machesky et al., 1994). The Arp2/3 complex has subsequently been identified in other organisms including yeast, xenopus and humans (Ma et al., 1998; Welch et al., 1997a; Winter et al., 1997). Arp2 (actin related protein 2) and Arp3 have 47% and 40% identity to actin respectively and are members of protein families that are highly conserved in eukaryotes (Kelleher et al., 1995). The other five members of the complex are designated ARPC1, ARPC2, ARPC3, ARPC4 and ARPC5 (Pollard, 2007). The similarities of Arp2 and Arp3 to actin led to the hypothesis that together these proteins mimic the formation of an actin dimer. This overcomes the kinetic barrier that prevents the spontaneous polymerisation of actin and provides a template from which a new filament can elongate (Goley and Welch, 2006; Higgs and Pollard, 1999; Machesky et al., 1994). Subsequent studies confirmed the *in vitro* nucleation ability of the Arp2/3 complex and also revealed that it is involved in the formation of arrays of branched actin filaments (Bailly et al., 1999; Blanchoin et al., 2000; Mullins et al., 1998; Pollard and Borisy, 2003; Svitkina and Borisy, 1999).

The Arp2/3 complex is unique in its ability to induce the formation of branched actin filaments. Both TIRF fluorescence and electron microscopy has been used to visualise branched, Arp2/3 dependent actin polymerisation *in vitro* (Amann and Pollard, 2001; Mullins et al., 1998). Furthermore, ultrastructural studies of lamellipodia using electron microscopy revealed dense arrays of branched filaments, in which the Arp2/3 complex could be visualised at branch points (Svitkina and Borisy, 1999; Svitkina et al., 1997). A subsequent study demonstrated that the branching activity of the Arp2/3 complex is required to provide the protrusive force required in the lamellipodia of migrating cells (Bailly et al., 2001). In addition, depletion of the Arp2/3 complex in fibroblasts revealed that it is essential for the establishment of lammellipodia (Wu et al., 2012). While these

studies highlight the physiological importance of branched actin filaments, the mechanism of branching remains elusive. In recent years, 3D reconstruction after electron tomography has given fresh insight the branched arrays of actin filaments. An initial study controversially suggested that branches were not present in the lammellipodia of cells (Urban et al., 2010). However, further analysis by the same group confirmed that branched filaments are present, albeit at lower frequency than previously described (Vinzenz et al., 2012).

Two models of Arp2/3 complex dependent actin nucleation have been proposed. These are the barbed-end branching model and the dendritic model of actin nucleation (Mullins et al., 1998; Pantaloni et al., 2000). The barbed end branching model suggested that the activated Arp2/3 complex interacts with the barbed ends of filaments, thereby incorporating into the mother filament and causing the elongation of two filaments from this point. This theory was based on biochemical observations showing the activity of the Arp2/3 complex depends on the number of filaments rather than on their length and that the capping of barbed ends inhibits branching (Pantaloni et al., 2000). In contrast, the dendritic model of nucleation suggested that the interaction of the Arp2/3 complex with the sides of pre-existing actin filaments and nucleated a side-branch (Mullins et al., 1998; Mullins et al., 1997). Support for this model came from TIRF microscopy studies of Arp2/3 dependent filament nucleation *in vitro*, which demonstrated that new branches were initiated from the sides of actin filaments (Amann and Pollard, 2001; Blanchoin et al., 2000). In addition, structural studies also support the dendritic model of nucleation and thus it is favoured over the former model (Boczkowska et al., 2008; Rouiller et al., 2008).

The first crystal structure of the Arp2/3 complex revealed that Arp2 and Arp3 lie head-to-tail with each other but are too far apart to serve as the nucleus for polymerisation of a new actin filament (Figure 1.5 A) (Robinson et al., 2001). This structure is proposed to represent the inactive form of the Arp2/3 complex and provided an explanation for the low nucleation activity of the purified complex *in vitro* (Mullins et al., 1998; Welch et al., 1998). This model suggests that other cellular signals result in a conformational change that brings the Arp2 and Arp3 subunits into proximity, thus allowing them to nucleate an actin filament (Figure 1.5

A). While a crystal structure of the active Arp2/3 complex has not yet been obtained, electron microscopy (EM) studies have given insight into the function of the complex (Rouiller et al., 2008; Xu et al., 2012b). Fitting of the crystal structure of the inactive Arp2/3 complex into EM reconstructions of an actin filament branch revealed density mismatches that are consistent with the complex undergoing a conformational change upon activation (Figure 1.5 B) (Rouiller et al., 2008). In this study, Arp2 and Arp3 are clearly shown to act as the first two subunits at the pointed end of the daughter filament, thus promoting barbed-end elongation. Molecular dynamics simulations of the activation of the Arp2/3 complex also support this theory (Dalhaimer and Pollard, 2010).

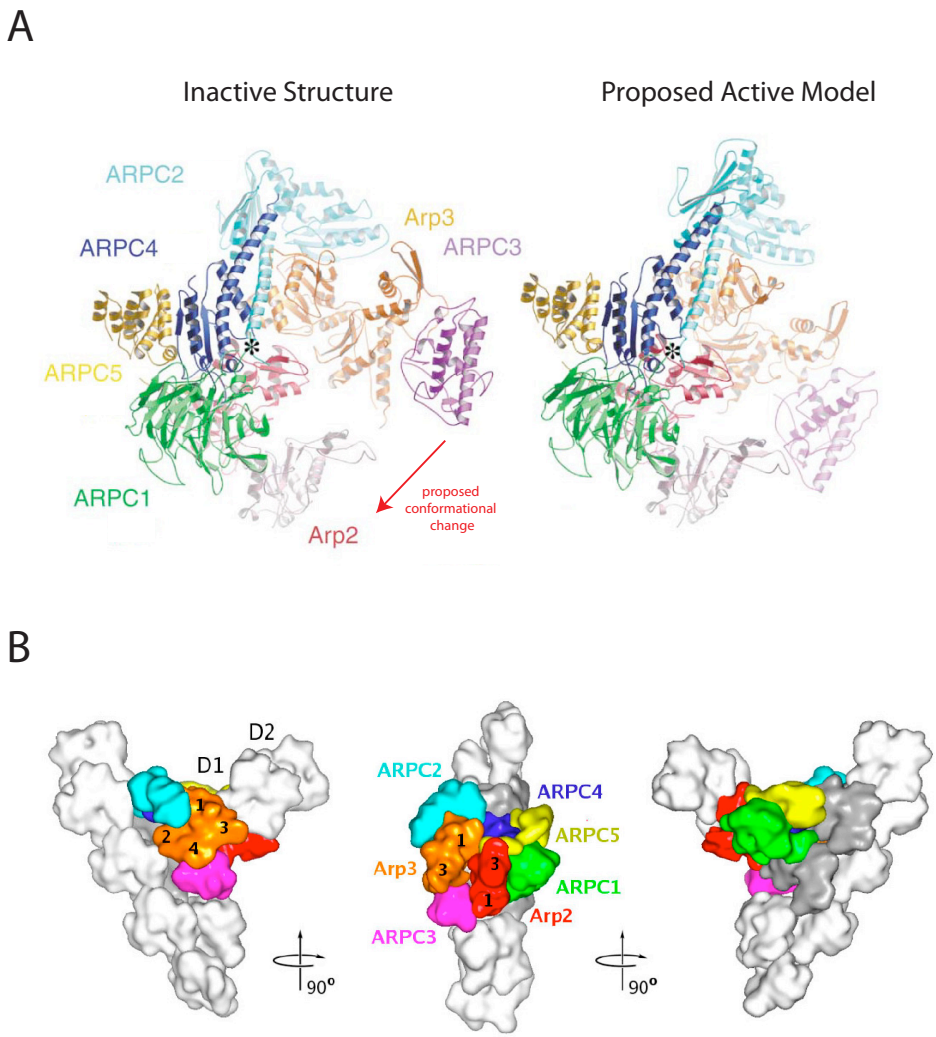

Figure 1.5. The Arp2/3 Complex

(A) Ribbon diagram of the crystal structure of the inactive Arp2/3 complex. The proposed conformational change and the projected active structure are also shown. The names of all the subunits are indicated. **(B)** Representation of the best fit of the crystal structure of the Arp2/3 complex at the branch junction of an actin filament. Actin subunits are depicted in white or gray. D1 and D2 indicates the first two subunits of the daughter filament. D1 and D2 are the first two subunits in the daughter filament. The Arp2/3 complex is labelled and shown in colour. The three views are related by 90° clockwise rotations. ©Rouiller et al., 2008. Originally published in *Journal of cell biology*. 180:887-95.

1.4.2 Activation of the Arp2/3 complex

Purified Arp2/3 complex exhibits a low level of intrinsic actin nucleating activity (Mullins et al., 1998; Welch et al., 1998). Furthermore, Arp2 and Arp3 are positioned too far apart in the crystal structure of the complex to fulfil their proposed role as a pseudo-actin dimer and promote filament nucleation (Robinson et al., 2001). Thus, it was suggested that other cellular signals are required to induce a conformational change in the Arp2/3 complex and stimulate its nucleation activity.

1.4.3 Activation by Nucleation-Promoting Factors (NPFs)

The first evidence for a protein that could activate the Arp2/3 complex came from studies of the actin-based motility of *Listeria*. The bacterial protein ActA was found to activate the actin nucleating ability of the Arp2/3 complex *in vitro* and to promote motility of the bacteria (Welch et al., 1997b; Welch et al., 1998). The discovery of this bacterial activator of the Arp2/3 complex was strong evidence that other cellular proteins might exist that perform analagous functions in, for example, the lamellipodia of migrating cells. Many proteins that perform this function have now been identified. These are known as nucleation-promoting factors or NPFs (Figure 1.6 A) (Campellone and Welch, 2010; Le Clainche and Carlier, 2008; Veltman and Insall, 2010). Proteins of this type are divided into two classes. The class I NPFs are the largest group and comprise a number of proteins, all of which contain a WCA domain that harbours their Arp2/3 complex activation ability (Derivery and Gautreau, 2010). Cortactin and its related protein, HS1 (haematopoetic-specific protein 1) are members of the class II family of NPFs (Campellone and Welch, 2010).

The Class I NPFs are further divided into five groups: N-WASP/WASP (Neural-/Wiskott Aldrich Syndrome Protein), WAVE/SCAR (WASP-family verprolin homology protein/ suppressor of cAMP receptor), WASH (WASP and SCAR homologue), WHAMM (WASP homologue associated with actin, membranes and microtubules) and JMY (Junction-mediating regulatory protein) (Bear et al., 1998; Campellone et al., 2008b; Derry et al., 1994; Linardopoulou et al., 2007; Miki et al., 1996; Zuchero et al., 2009). All these proteins contain a C-terminal WCA domain consisting of one or more WH2 domains (also known as verprolin (V) domains), a

connector (C) region and an acidic (A) region (Figure 1.6 A). Together these form a conserved domain that activates the actin nucleating ability of the Arp2/3 complex (Higgs et al., 1999; Machesky and Insall, 1998; Rohatgi et al., 1999; Winter et al., 1999). The WH2 domain binds to actin monomers and is not actually required for the interaction of the WCA with the Arp2/3 complex (Gaucher et al., 2012; Machesky and Insall, 1998; Miki and Takenawa, 1998). Instead, the WH2 domain is proposed to deliver actin monomers to the Arp2/3 complex to enhance the initiation of the new branch (Chereau et al., 2005; Pollard, 2007). The CA region interacts directly with multiple subunits of the Arp2/3 complex. Electron microscopy indicated that the WCA binds to the Arp2/3 complex in a cleft that exists between Arp2 and Arp3 (Rodal et al., 2005). Chemical crosslinking studies revealed that contacts are formed between the WCA of NPFs and Arp2, Arp3, ARPC1, ARPC4 and ARPC5 (Weaver et al., 2002; Zalevsky et al., 2001a; Zalevsky et al., 2001b). Further studies using NMR confirmed that the C-termini of both the A and C regions are likely to interact with ARPC3 (Kreishman-Deitrick et al., 2005). In addition, the C region also interacts ARPC1 (Kelly et al., 2006). Differences in activity between NPFs may be partially explained by their ability to contact different subunits of the Arp2/3 complex. For example, the WCA of N-WASP contacts more subunits than the WCA of SCAR and also has 70-fold higher activity towards the Arp2/3 complex than SCAR (Zalevsky et al., 2001b). This is consistent with the hypothesis that the interaction of the WCA domain with the ARP2/3 complex results in a conformational change that leads to its activation (Goley et al., 2004; Kreishman-Deitrick et al., 2005; Machesky and Insall, 1998; Marchand et al., 2001; Panchal et al., 2003; Xu et al., 2012b). As N-WASP is the most relevant NPF to this thesis, it will be discussed in more detail in section 1.5.

The class II NPFs, cortactin and HS1 are much less potent activators of the Arp2/3 complex (Campellone and Welch, 2010). These proteins have acidic regions at their N-termini (NTA domain) that interact with and activate the Arp2/3 complex (Weaver et al., 2001). Unlike the class I NPFs; they harbour repetitive sequences that bind F-actin (Uruno et al., 2003; Weed et al., 2000). Cortactin co-operates with N-WASP to increase Arp2/3 mediated actin nucleation as well as stabilising actin filament branches by inhibiting the dissociation of the Arp2/3 complex (Weaver et al., 2001). Cortactin is an important regulator of many cellular processes including

invadopodia formation, endocytosis and in cell migration (Cao et al., 2003; Kirkbride et al., 2011). HS1, which is haematopoietic specific, is closely related to cortactin and thus can activate the Arp2/3 complex and interact with F-actin (Uruno et al., 2003). It has recently been found to be important for neutrophil chemotaxis (Cavnar et al., 2012).

In recent years, a further level of Arp2/3 complex regulation has emerged. Dimers of WCA domains were found to have an increased ability to activate the Arp2/3 complex, when compared with monomeric WCA domains (Higgs and Pollard, 2000; Padrick et al., 2008). These dimers bound to two sites in the Arp2/3 complex (Padrick et al., 2011). It appears that one WCA interacts with the canonical WCA binding site, while the other interacts with the cortactin-binding site in the Arp2/3 complex (Padrick et al., 2008). The identification of a second WCA binding site resolves some of the conflicting data that arose from the aforementioned cross-linking studies (Weaver et al., 2002; Zalevsky et al., 2001a; Zalevsky et al., 2001b). Experiments exploiting the ability of an agent that transfers biotin labels to subunits within 17Å were used to show that Arp2 and ARPC1 are likely to comprise one binding site, while Arp3 and ARPC3 bind to another WCA (Padrick et al., 2011). The high affinity WCA canonical binding site comprises Arp3 and ArpC3 (Xu et al., 2012b). Maximal activation of the Arp2/3 complex appears to require the delivery of actin monomers to the Arp2/3 complex by both WCA domains, although the delivery of actin to the Arp3 subunit is more critical for actin polymerisation (Padrick et al., 2011). A recent study has determined the ratio of N-WASP to the Arp2/3 complex in actin comets that were induced by antibody-mediated clustering of Nck SH3 domains at the plasma membrane (Ditlev et al., 2012). Twice as much N-WASP as Arp2/3 complex was observed, indicating that two WCA domains could indeed interact with each Arp2/3 complex.

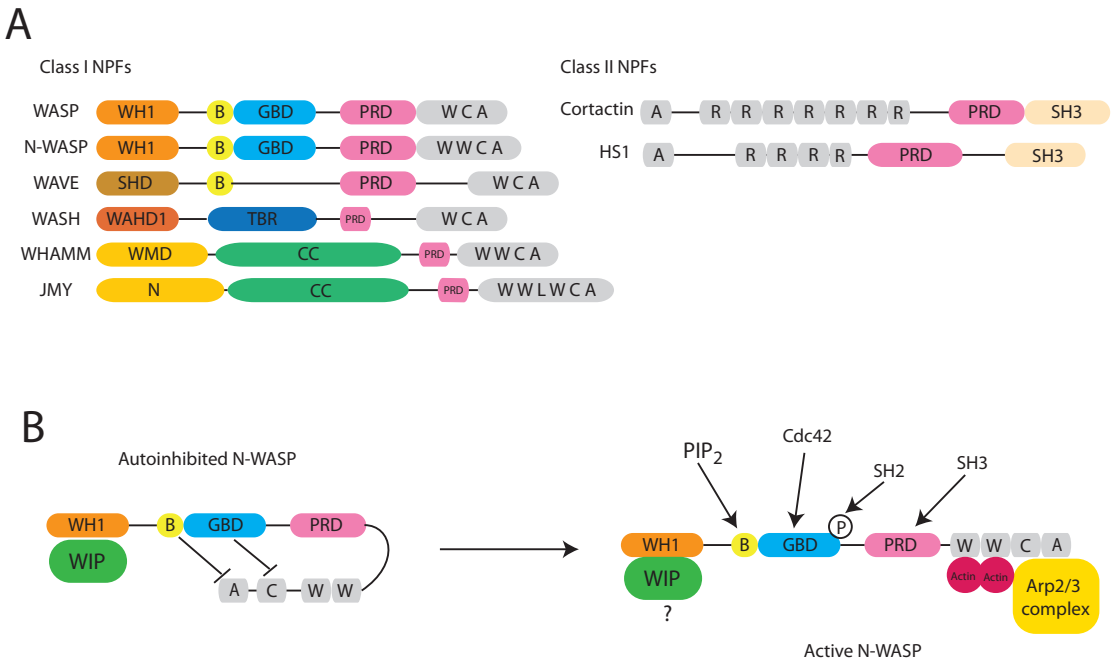

Figure 1.6. Activation of N-WASP

(A) Schematic representation of the class I and class II nucleation promoting factors (NPFs). WH1 (WASP Homology 1), B (Basic domain), GBD (GTPase Binding domain), PRD (Proline Rich Domain), W (WH2/WASP Homology 2 Domain), C (Connector), A (Acidic), SHD (Scar Homology Domain), WAHD1 (WASH Homology Domain 1), TBR (Tubulin Binding Region), WMD (WHAMM-membrane interaction-domain), CC (Coiled Coil Domain), L (Linker), R (Repeat), SH3 (Src Homology 3 domain). (B) Schematic representation of the activation of N-WASP by molecules such as PIP2, Cdc42, SH2 and SH3 domain containing proteins. Binding of these molecules relieves the autoinhibitory intramolecular interaction in N-WASP.

1.4.4 Other regulators of the Arp2/3 complex

In addition to NPFs, ATP also regulates the activity of the Arp2/3 complex. FRET (Forster Resonance Energy Transfer) experiments demonstrated that the conformation of the Arp2/3 complex changes upon nucleotide binding (Goley et al., 2004). Moreover, in the absence of hydrolysable ATP, actin nucleation does not occur (Dayel et al., 2001). While both Arp2 and Arp3 bind ATP, the interaction of Arp2 and ATP is dependent on the presence of a WCA domain (Le Clainche et al.,

2001). Furthermore, hydrolysis of ATP by Arp2, but not by Arp3, is required for actin polymerisation (Le Clainche et al., 2001). Thus, WCA domains and ATP appear to cooperate in regulating the activity of the complex. The Arp2/3 complex also has higher affinity for WCA domains in the presence of saturating concentrations of ATP (Dayel et al., 2001). This data suggests that hydrolysis of ATP could regulate the dissociation of the Arp2/3 complex from its upstream regulators.

The presence of actin filaments also increases the rate of nucleation of WCA activated Arp2/3 complex, although the final number of filaments generated is not altered (Higgs et al., 1999). The affinity of the WCA of WASP for the Arp2/3 complex was found to be higher in the presence of preformed actin filaments (Marchand et al., 2001). Thus it is likely that the interaction of the Arp2/3 complex with the sides of actin filaments results in a conformational change that stabilises NPF binding. Data from electron microscopy studies detailing the conformation of the Arp2/3 complex at the mother filament reinforces this model. All seven subunits of the Arp2/3 complex were found to contact the mother filament, although ArpC2 and ArpC4 comprise the main interacting surface (Rouiller et al., 2008; Xu et al., 2012b).

Phosphorylation of the Arp2/3 complex at a number of positions has also been shown to play a role in regulating its activity. The phosphorylation of threonine 21 of ARPC1 by p21 activated kinase (PAK) regulates the association of this subunit with the Arp2/3 complex (Vadlamudi et al., 2004). Moreover, expression of a non-phosphorylatable mutant of ArpC1 results in a decrease in cell migration. Arp2 is also phosphorylated on threonine (T237 and T238) and tyrosine (Y202) residues (LeClaire et al., 2008). This study showed that phosphorylation of the Arp2/3 complex is required for its actin nucleating activity *in vitro*. Loss of phosphorylation does not actually affect the interaction of the complex with the WCA domains of N-WASP or SCAR, but does inhibit WCA mediated activation of the Arp2/3 complex (Narayanan et al., 2011). Molecular dynamics simulations revealed that phosphorylation of Arp2 leads to conformational changes in the Arp2/3 complex that would facilitate activation by WCA domains (Narayanan et al., 2011). Phosphorylation of the Arp2/3 complex is also necessary to facilitate the interaction

of the complex with the pointed end of actin filaments (LeClaire et al., 2008). Consistent with a role in regulating its actin nucleating activity, phosphorylation of the Arp2/3 complex was shown to be essential for lamellipodia formation in *Drosophila* S2 cells (LeClaire et al., 2008).

In recent years, Coronin 1B has emerged as multifunctional regulator of the Arp2/3 complex. Coronin is the first and as yet only protein identified as an inhibitor of the Arp2/3 complex *in vitro* (Humphries et al., 2002). The roles of coronin are complex, on one hand it protects newly formed ATP-actin filaments from cofilin mediated severing, but it can also synergise with cofilin to promote the disassembly of older actin filaments (Chan et al., 2011). Coronin also promotes the dissociation of the Arp2/3 complex from actin filaments (Cai et al., 2008). The ability of coronin to inhibit actin nucleation by the Arp2/3 complex and to promote the breakdown of older actin filament networks is likely important to allow the recycling of both actin and the Arp2/3 complex within the cell. This would then facilitate the polymerisation of new actin filaments at sites where they are required, for example, at the leading edge of migrating cells (Chan et al., 2011). Overall, the regulation of the Arp2/3 complex by a combination of different factors is consistent with its important role in many crucial cellular processes, which require very fine spatial and temporal regulation of its function.

1.5 WASP and N-WASP

N-WASP is one of the most well characterised NPFs. It is conserved in eukaryotes and is expressed in most cell types (Miki et al., 1996; Snapper et al., 2001). This is in contrast to the closely related protein WASP, which was identified first, but is restricted to haematopoietic cell types (Derry et al., 1994; Symons et al., 1996). Loss of WASP results in the impairment of phagocytosis, the functioning of T lymphocytes, chemotaxis and cell migration, which leads to immune defects that manifest as Wiskott Aldrich Syndrome (WAS) in humans (Bouma et al., 2009; Jones et al., 2002; Snapper et al., 1998; Zhang et al., 1999). In contrast, the loss of N-WASP causes abnormalities in both the brain and the heart, resulting in embryonic lethality in mice by E12 (Snapper et al., 2001). N-WASP plays important roles in a multitude of cellular processes including phagocytosis, endocytosis, the

formation of membrane ruffles and filopodia, in podosomes and invadopodia as well as the stabilisation of epithelial cell junctions and in pathogen induced actin polymerisation (Dart et al., 2012; Kovacs et al., 2011; Legg et al., 2007; Miki et al., 1998; Nusblat et al., 2011; Park and Cox, 2009; Qualmann and Kessels, 2002; Snapper et al., 2001; Yamaguchi et al., 2005).

1.5.1 N-WASP Structure and Autoinhibition

As WASP and N-WASP have similar mechanisms of regulation, I will largely focus on N-WASP as it is the most relevant to this thesis. N-WASP contains a number of conserved domains (Figure 1.6 A). It consists of an N-terminal WH1 (WASP homology 1) domain followed by the basic region (B), the GTPase-binding domain (GBD) that is also referred to as the CRIB (Cdc42 and Rac interactive binding) domain, a proline rich domain (PRD) and the C-terminal WCA domain, which activates the Arp2/3 complex. The major binding partners of the WH1 domain are the verprolins (WIP, WIRE and CR16 – see section 1.7). The WH1 domain has a similar structural fold to the EVH1 domain that is found in Ena/Vasp proteins (Fedorov et al., 1999; Prehoda et al., 1999; Volkman et al., 2002). However, the WH1 domain binds preferentially to sequences that are distinct from the canonical FPPPP motif that is favoured by EVH1 domains (Peterson et al., 2007; Volkman et al., 2002; Zettl and Way, 2002). A combination of biochemistry and NMR was used to determine the molecular basis of the interaction of WIP with N-WASP (Peterson et al., 2007; Volkman et al., 2002; Zettl and Way, 2002). The minimal WIP peptide required for interaction with N-WASP is longer than those required for binding to other EVH1 domains (Peterson et al., 2007). A 34 amino acid long region from WIP wraps more than half way around the WH1 domain of N-WASP, making extensive contacts with the surface of this domain (Peterson et al., 2007; Volkman et al., 2002). Three major regions are involved in the binding of the WH1 domain to the WASP Binding Domain (WBD) of WIP. Two conserved phenylalanines at positions 454 and 456 in WIP are both necessary and sufficient for binding to the WH1 domain (Zettl and Way, 2002). These interact with a hydrophobic surface of the WH1 domain that contains valine 42 and alanine 119 (Peterson et al., 2007). The second region involves an LPPP motif in WIP, which adopts a type II polyproline helical conformation and surrounds tryptophan 54 of N-WASP (Volkman et al.,

2002). Mutation of tryptophan 54 to alanine is sufficient to abrogate the interaction between the WH1 domain and WIP (Moreau et al., 2000; Zettl and Way, 2002). Finally, glutamate 90 of N-WASP forms a salt bridge with lysine 478 of WIP (Peterson et al., 2007). Neither the second nor the third region alone can mediate the interaction of the WH1 domain and WIP, although together they are sufficient for binding (Peterson et al., 2007). The importance of each of these regions for maintaining the interaction of N-WASP and WIP *in vivo* was assessed using vaccinia virus actin tail formation as a read out. Expression of the WBD of WIP inhibits vaccinia virus from inducing actin tails by preventing N-WASP recruitment (Moreau et al., 2000). Mutating the conserved phenylalanines of the first region, or proline 465 in the second region results in a dramatic decrease in the ability of the WBD to block actin tail formation, indicating that these regions are required for the interaction with the WH1 domain of N-WASP (Peterson et al., 2007; Zettl and Way, 2002). In contrast, mutating lysine 477 of the WBD results in only a 50% increase in actin tail formation, suggesting that this residue is not essential for WIP binding to N-WASP (Peterson et al., 2007). Interestingly, a large number of the causative mutations of Wiskott Aldrich Syndrome (WAS) map to the WH1 domain (Jin et al., 2004; Volkman et al., 2002). Introduction of mutations found in WASP, which are known to cause Wiskott Aldrich Syndrome, into N-WASP (C35W, R76C and E123K) disrupts the interaction with WIP and results in the loss of WH1 domain recruitment to vaccinia virus (Moreau et al., 2000). Taken together, this data highlights the critical importance of the interaction between WIP and N-WASP in regulating N-WASP function.

Contacts between the GBD and the WCA domain result in autoinhibition of WASP/N-WASP (Figure 1.6 B). These interactions mask the WCA and prevent it from interacting with the Arp2/3 complex (Kim et al., 2000; Miki et al., 1998; Prehoda et al., 2000; Rohatgi et al., 2000). The basic region adjacent to the GBD is also involved in maintaining the autoinhibited state of WASP/N-WASP (Prehoda et al., 2000; Rohatgi et al., 2000). Multiple signals contribute to the activation of N-WASP by relieving its autoinhibition (Figure 1.6 B). The Rho GTPase Cdc42 and phosphatidylinositol (4,5)-bisphosphate (PIP_2) were two of the first characterised activators of WASP/N-WASP. Active (GTP bound) Cdc42 binds to the GBD of N-WASP, while the basic domain interacts with PIP_2 (Miki et al., 1998;

Papayannopoulos et al., 2005; Rohatgi et al., 2000; Rohatgi et al., 1999). An NMR structure of the GBD of WASP revealed that the GDB is intrinsically unstructured but upon binding to the WCA, it assumes a more ordered conformation, which is distinct from its structure when bound to Cdc42 (Kim et al., 2000). Furthermore the GBD cannot bind to both Cdc42 and the WCA simultaneously (Kim et al., 2000; Miki et al., 1998). This suggests that Cdc42 activates N-WASP by competing with the WCA for binding to the GBD. When Cdc42 is bound to the GBD, the WCA domain is free to interact with and activate the Arp2/3 complex. An alternative mechanism has been proposed in which the autoinhibited N-WASP molecule is already bound to the Arp2/3 complex (Prehoda et al., 2000). No definitive evidence has discriminated between these two models, however, the final output is similar in both, as exogenous signals must relieve the autoinhibition of N-WASP before it can activate the Arp2/3 complex.

The basic domain of N-WASP contributes to the stability of the autoinhibited conformation by interacting with the A region of the WCA (Prehoda et al., 2000; Rohatgi et al., 2000). Consistent with this PIP_2 synergizes with Cdc42 to potently activate N-WASP (Rohatgi et al., 2000). Furthermore, a peptide comprising the GBD and the basic region is required to maximally inhibit the WCA, while the GBD alone is not sufficient (Prehoda et al., 2000). The proline rich region that links the GBD to the WCA is also the site of interaction of myriad SH3 domain containing adaptors. These include Nck, Grb2, the F-BAR proteins Toca-1 and FBP-17, Abi1, Syndapin, SNX9 and Abp1 (Carlier et al., 2000; Ho et al., 2004; Innocenti et al., 2005; Kessels and Qualmann, 2004; Pinyol et al., 2007; Rohatgi et al., 2001; Shin et al., 2007; Takano et al., 2008). Thus, although the proline rich region does not directly participate in the intramolecular interaction between the WCA and the GBD, binding of the aforementioned proteins can destabilise these autoinhibitory contacts and release the WCA (Rohatgi et al., 2001; Tomasevic et al., 2007). Nck and PIP_2 synergise to activate N-WASP in a Cdc42 independent manner, while Grb2 functions with Cdc42 to enhance activation (Carlier et al., 2000; Rohatgi et al., 2001). Thus multiple signalling inputs can act cooperatively to stimulate N-WASP-Arp2/3 dependent actin polymerisation.

The importance of the interaction of N-WASP and WIP was further highlighted when it was found that WIP inhibits the ability of N-WASP to activate the Arp2/3 complex (Ho et al., 2004; Martinez-Quiles et al., 2001). *In vitro* actin polymerisation assays demonstrated that the activation of N-WASP by Cdc42 is inhibited by WIP in a dose dependent manner (Martinez-Quiles et al., 2001). Activation of the Arp2/3 complex by the VCA domain of N-WASP is not affected by the presence of WIP, indicating that the interaction of WIP with N-WASP is specifically required to mediate the inhibitory effect of WIP (Martinez-Quiles et al., 2001). The mechanism of this inhibition is not well understood. A number of molecules have been demonstrated to relieve the inhibition of N-WASP by WIP. PIP_2 is sufficient to allow activation of N-WASP by Cdc42, even in the presence of very high concentrations of WIP (Martinez-Quiles et al., 2001). Furthermore, Toca-1 (transducer of Cdc42 activity) was found to relieve the inhibitory effects of WIP and promote activation of N-WASP by Cdc42 (Ho et al., 2004). This study also demonstrated that Toca-1 could synergise with PIP_2 in activating N-WASP. Toca-1 binds to N-WASP via its SH3 domain, as well as to Cdc42, resulting in the formation of a tripartite complex that relieves the autoinhibition of N-WASP, thereby allowing it to activate the Arp2/3 complex (Bu et al., 2010; Ho et al., 2004). Toca-1 and a related protein FBP-17 can also promote the activation of the N-WASP/WIP complex in the presence of liposomes (Takano et al., 2008). This activation is independent of the presence of Cdc42 or PIP2, but does depend on the curvature of the liposomal membrane with larger diameter vesicles resulting in increased activation of N-WASP (Takano et al., 2008). Furthermore binding of both Toca-1/FBP-17 and N-WASP to the membrane was also required for maximal activation (Takano et al., 2008). WIP was also shown to interact with both the membrane and with the SH3 domain of Toca-1/FBP-17 (Takano et al., 2008). This may contribute to the activation of the N-WASP-WIP complex perhaps by facilitating a conformational change that promotes N-WASP activation at the plasma membrane.

Phosphorylation of WASP and N-WASP has emerged as another important mechanism involved in regulating the function of these proteins. Activation of both the B-cell receptor (BCR) and the T-cell receptor (TCR) results in phosphorylation of WASP on tyrosine 291 by Btk or Fyn (Baba et al., 1999; Badour et al., 2004). Similarly, the Src family kinase, Hck phosphorylates WASP at the same site,

thereby enhancing its ability to induce the formation of filopodia (Cory et al., 2002). Tyrosine 291 lies within the GBD of WASP and phosphorylation of this residue was found to decrease the affinity of the GDB for the WCA domain of WASP (Torres and Rosen, 2003). This study also demonstrated that phosphorylation of WASP occurred only after prior binding of Cdc42 to WASP. Thus it is thought that after the release of autoinhibition of WASP by active Cdc42, phosphorylation of Y291 by Src family kinases results in prolonged activation of WASP (Torres and Rosen, 2003). Furthermore, after phosphorylation, the SH2 domain of Src family kinases can bind to the phosphorylated tyrosine and further activate WASP (Torres and Rosen, 2003). This lead to the proposal that phosphorylation acts a form of “molecular memory”, as only a subset of WASP molecules, which have previously been phosphorylated, can respond to the SH2 binding signal. A subsequent study showed that N-WASP activity is controlled by a similar mechanism involving the phosphorylation of the equivalent tyrosine 256 (Torres and Rosen, 2006). Phosphorylation of N-WASP is important for neurite outgrowth in PC12 cells (Suetsugu et al., 2002). Expression of an N-WASP mutant that cannot be phosphorylated resulted in the inhibition of neurite outgrowth, as did treatment with inhibitors of Src family kinases (Suetsugu et al., 2002). Thus WASP family proteins are regulated by the integration of multiple signals leading to the tight spatial and temporal control of their activation. Different regulatory mechanisms predominate in different contexts, for example the phosphorylation of WASP/N-WASP is more important downstream of the TCR or for neurite extension, while activation by Cdc42 is key for the induction of N-WASP dependent filopodia in Cos7 cells (Badour et al., 2004; Miki et al., 1998; Suetsugu et al., 2002).

In addition to supplying actin monomers for incorporation into the growing actin filament, the WH2 domains of N-WASP have also been shown to mediate the attachment of the actin filament network to membranes (Co et al., 2007). Furthermore, the interaction of N-WASP with the actin filament network promotes the clustering of the protein on moving lipid vesicles (Co et al., 2007; Delatour et al., 2008). Abrogation of the ability of the WH2 domains to interact with the barbed ends of the actin filaments results in a more rapid rate of exchange of N-WASP at vaccinia virus particles undergoing actin-based motility (Weisswange et al., 2009). This destabilisation of N-WASP leads to shorter actin tails that move more rapidly.

In addition, podosome formation in Src transformed cells was disrupted when N-WASP could not interact with actin via its WH2 domains (Co et al., 2007). This suggests that the downstream actin filament network regulates N-WASP in a positive feedback loop that both stabilises and increases the local density of N-WASP. Furthermore, N-WASP competes with capping protein to bind the barbed ends of actin filaments, thus promoting filament elongation.

1.5.2 Oligomerization

In recent years, the oligomerization of N-WASP has been identified as an important mechanism for controlling its function (Padrick et al., 2008; Padrick and Rosen, 2010). This stems from the observation that dimerization of N-WASP WCA domains increases their ability to activate the Arp2/3 complex (Higgs and Pollard, 2000; Padrick et al., 2008). Furthermore, each Arp2/3 complex is bound and activated by two WCA domains (Padrick et al., 2008; Padrick et al., 2011; Ti et al., 2011). Many N-WASP binding partners contain multiple domains that could simultaneously interact with multiple N-WASP molecules, thereby increasing the local density of N-WASP and facilitating the interaction of multiple WCA domains with the Arp2/3 complex (Padrick et al., 2008; Padrick et al., 2011). These include the bacterial protein $EspF_u$ and SH3 domain containing proteins such as Nck and Grb2 (Campellone et al., 2008a; Carlier et al., 2000; Cheng et al., 2008; Rohatgi et al., 2001). Enterohaemorrhagic *E. coli* (EHEC) is a food-borne pathogen that induces the formation of N-WASP dependent actin pedestals upon adhering to the surface of cells. $EspF_u$ contains a sequence that mimics the structure of the WCA domain of N-WASP (Cheng et al., 2008; Sallee et al., 2008). This sequence binds to the GDB of N-WASP and displaces the WCA domain, thus activating N-WASP. $EspF_u$ contains 2-8 repeats of this sequence depending on the strain of the bacteria (Campellone et al., 2008a). Actin polymerisation can be induced by artificially clustering the EspFu repeats at the plasma membrane and it was found that increasing their number correlates with increasing amounts of actin polymerisation (Campellone et al., 2008a). This suggests that not only does EspFu activate N-WASP by relieving its autoinhibition, but that it also clusters multiple N-WASP molecules thereby increasing the probability that two WCA domains will be able to interact with each Arp2/3 complex (Padrick et al., 2008; Padrick and Rosen, 2010).

A similar mechanism can be envisaged for proteins such as Nck that contain three SH3 domains (Buday et al., 2002; Li et al., 2012). In fact, dimerization of a Nck SH3 domain increased the activation of the Arp2/3 complex by N-WASP above that of a the monomeric SH3 domain (Padrick et al., 2008).

The spatial organisation of N-WASP at the plasma membrane is also important for regulating its activity. Larger liposomes resulted in increased activation of the Arp2/3 complex by N-WASP compared to that observed with smaller liposomes (Takano et al., 2008). This makes sense in light of the oligomerisation of the protein as not only would the density of N-WASP molecules be important for activation, they would also need to be positioned correctly so that two molecules of N-WASP could interact with each Arp2/3 complex. In addition, synthetic ActA dimers were shown to have increased Arp2/3 activation ability *in vitro* (Footer et al., 2008). ActA is a *Listeria* protein that mimics the WCA domain of N-WASP to activate the Arp2/3 complex (Welch et al., 1997b; Welch et al., 1998). Interestingly, although ActA does not actually dimerise, the density of molecules expressed on the suface of the bacterium is such that their proximity would allow them to function as a dimer and therefore maximally activate the Arp2/3 complex (Footer et al., 2008). Furthermore, N-WASP proteins exhibit a high local density on rocketing PIP_2 vesicles that is consistent with them functioning as dimers in order to achieve maximal activation of the Arp2/3 complex (Co et al., 2007; Delatour et al., 2008).

1.6 The Verprolins

Verprolin was first identified as a regulator of the actin cytoskeleton in yeast (Donnelly et al., 1993). It has subsequently been implicated in bipolar bud site selection and in the establishment of a polarised actin cytoskeleton in *S. cerevisiae* (Vaduva et al., 1997). Verprolin also interacts with the type I myosin, myo5p, and is required for the correct localisation of this protein (Anderson et al., 1998). Furthermore, verprolin is essential for endocytosis and cytokinesis (Munn and Thanabalu, 2009; Naqvi et al., 2001; Naqvi et al., 1998; Thanabalu and Munn, 2001). Verprolin is highly proline rich and interacts with both actin and the yeast homologue of WASP/N-WASP, Las17p (Naqvi et al., 1998). In mammals, the verprolin family of proteins consists of WIP, WIRE and CR16 (Aspenstrom, 2005;

Garcia et al., 2012). The mammalian verprolins contain two WH2 actin-binding domains, a central proline rich region and a C-terminal WBD (WASP binding domain) (Aspenstrom, 2005). Interestingly, WIP rescues the defects in polarity, growth and endocytosis that arise in yeast lacking verprolin indicating that the two proteins are indeed functional homologues (Vaduva et al., 1999).

1.6.1 WIP

WIP was initially identified in a yeast two-hybrid screen for WASP interacting partners (Ramesh et al., 1997; Stewart et al., 1999). WIP mRNA is widely expressed in human tissues, with especially high levels detected in peripheral blood mononuclear cells and in the spleen (Ramesh et al., 1997). Two additional isoforms of WIP have been identified. Prpl2 has an additional sequence that arises from a rare alternative splicing event that results in the insertion of exon 6a into the protein (Anton et al., 2007). The function of Prpl2 is unknown. The second isoform is termed miniWIP and is a truncation of WIP that lacks the WBD and is expressed in peripheral blood cells but not in fibroblasts (Koduru et al., 2007). Its physiological role remains to be determined.

WIP is a key regulator of the actin cytoskeleton. Overexpression of WIP results in an overall increase in F-actin content as well as the formation of actin-rich projections or filopodia in both BJAB cells and fibroblasts (Martinez-Quiles et al., 2001; Ramesh et al., 1997). The increased amount of F-actin is dependent on the N-terminus of WIP, which harbours two actin binding WH2 domains and a profilin interaction motif (Ramesh et al., 1997). In addition, WIP interacts with F-actin and is clearly localised to actin stress fibres in fibroblasts (Martinez-Quiles et al., 2001; Vetterkind et al., 2002). Overexpression of WIP in fibroblasts results in an elongation of cells as well as decreased adhesion and spreading (Lanzardo et al., 2007). Conversely, loss of WIP lead to increased adhesion, as well as a faster rate of migration than observed for control cells in scratch assays (Lanzardo et al., 2007).

WIP can also interact with the type II NPF cortactin and increase its ability to activate the Arp2/3 complex (Kinley et al., 2003). Consistent with this, co-

expression of WIP and cortactin results in increased membrane protrusion (Kinley et al., 2003). Loss of WIP also induces a mislocalisation of cortactin in dendritic cells resulting in the loss of cell polarity and aberrant membrane protrusion and ruffling (Chou et al., 2006). In addition, WIP has also been shown to increase the formation of dorsal ruffles in response to PDGF stimulation (Anton et al., 2003). This is dependent on the interaction of WIP with both actin and Abp1 (actin binding protein 1), but not with cortactin (Anton et al., 2003; Cortesio et al., 2010). WIP also interacts with the SH2-SH3 adaptor, Nck (Anton et al., 1998). Nck and WIP function together in invadopodia formation (Yamaguchi et al., 2005). Vaccinia virus also recruits Nck and WIP during actin tail formation and this will be discussed in more depth in section 1.8 (Frischknecht et al., 1999b; Moreau et al., 2000; Zettl and Way, 2002).

The C-terminal region of WIP interacts with the WH1 domain of both WASP and N-WASP (Section 1.5.1) (Martinez-Quiles et al., 2001; Ramesh et al., 1997). The interaction of WIP and WASP is crucial for maintaining expression levels of WASP in haematopoietic cells, as WIP protects WASP from proteosomal degradation (de la Fuente et al., 2007). Accordingly, in lymphocytes more than 95% of WIP and WASP exist in a complex (Sasahara et al., 2002). WIP also protects WASP from calpain-mediated degradation *in vitro*, although this is physiologically relevant only in activated lymphocytes (de la Fuente et al., 2007). Recently, a study has shown that in β1- integrin -/- cells, N-WASP expression is decreased and that this reduction can be rescued by the overexpression of WIP (King et al., 2011). In addition, this study showed that treatment of β1-integrin +/+ cells with RNAi against WIP resulted in decreased expression of N-WASP. However, the interaction of N-WASP with WIP does not seem to be critical for maintaining its level of expression, as WIP-/- fibroblasts still had normal levels of N-WASP (de la Fuente et al., 2007). Loss of WASP expression results in Wiskott Aldrich syndrome (WAS), and the majority of mutations causing this disease are found in the WH1 domain of WASP (Jin et al., 2004; Thrasher and Burns, 2010; Volkman et al., 2002). Interestingly, a recent study revealed that a mutation in WIP, which prevents its expression, also results in a similar condition (Lanzi et al., 2012). Moreover, WIP null mice have a progressive immunological disorder that is very similar to WAS (Curcio et al., 2007).

WIP has recently been found to be a negative regulator of neuronal maturation (Franco et al., 2012). WIP-/- mice were found to have brain hypertrophy, specifically an increase in the volume of the forebrain, as a result of increased neurite branching. Hippocampal neurons derived from these mice displayed accelerated development, which is dependent on N-WASP. This prompted the authors to propose that loss of WIP leads to inappropriate “hyper activation” of N-WASP, resulting in increased actin polymerisation and concomitant neuritogenesis (Franco et al., 2012). In *Drosophila*, WIP has been shown to interact with Blown Fuse (Jin et al., 2011). Interestingly, this protein competes with WIP for binding to WASP. In the absence of Blown Fuse, the rates of exchange of both WIP and WASP are decreased, as is the percentage recovery of the proteins. This leads to decreased actin polymerisation and impaired myoblast fusion. This finding raises the interesting possibility of a similar mechanism of regulation of N-WASP in vertebrates mediated by a homologue of Blown Fuse, although as yet no such protein has been identified (Jin et al., 2011).

1.6.1.1 WIP and the immune system

Consistent with its role as a chaperone of WASP, WIP has myriad roles in the immune system (Noy et al., 2012). T lymphocytes derived from WIP-/- mice are defective in their response to T cell receptor (TCR) ligation (Anton et al., 2002). After activation of the receptor, these cells are unable secrete IL-2, induce actin polymerisation or proliferate. The ability of the WIP-WASP complex to induce actin polymerisation and mediate IL-2 production are believed to be distinct as loss of the VCA domain of WASP affects the ability of the complex to increase F-actin content, but not to stimulate IL-2 production (Silvin et al., 2001). WIP was found to participate in IL-2 secretion via multiple WASP dependent pathways. WIP cooperates with Vav, a guanine nucleotide exchange factor, to induce NF-AT/AP1-mediated gene transcription via a mechanism that requires the interaction of WIP and WASP (Savoy et al., 2000). Another pathway involves the formation of a complex of WIP, WASP and the Src family kinase, Fyn (Sato et al., 2011). Inhibition of the formation of this complex resulted in decreased NF-AT activation and the loss of IL-2 production and suggesting that together WIP, WASP and Fyn are important for mediating TCR signalling. WIP also interacts with CrkL, an SH2-

SH3 adaptor and is important for recruiting WASP to the immune synapse after TCR activation (Sasahara et al., 2002). After ligation of the TCR, ZAP70 is recruited and phosphorylated providing a platform for the recruitment of CrkL via its SH2 domain. The SH3 domain of CrkL then recruits the WIP-WASP complex. Abrogation of this recruitment leads to a defects in both actin polymerisation and IL-2 production. WIP is also phosphorylated by PKCθ after TCR ligation (Sasahara et al., 2002). This was initially believed to result in the disruption of the WIP-WASP complex, however, further studies demonstrated that this was not the case (Dong et al., 2007; Koduru et al., 2007). Thus, the role of WIP phosphorylation downstream of the TCR remains unclear.

WIP-/- mice display distinct phenotypes that are not observed in WASP -/- mice, indicating that WIP has functions outside of its role in protecting WASP from degradation (Curcio et al., 2007). The failure of lymphocytes to proliferate in response to TCR activation is observed in cells lacking WIP, but not WASP (Le Bras et al., 2009). Furthermore, the chemotactic response of T-cell is decreased by 50% in cells lacking WIP (Gallego et al., 2006). Interestingly, while loss of both WIP and WASP results in an even more severe defect in chemotaxis, the loss of WASP alone does not show this phenotype. In addition, the loss of WIP severely impairs the formation of the immune synapse, however, WASP deficient cells form these structures normally and induce actin polymerisation (Gallego et al., 2006). Taken together, these observations suggest that WIP has functions that are independent of its interaction with WASP.

WIP also appears to regulate B-lymphocyte development in a WASP independent manner (Becker-Herman et al., 2011; Noy et al., 2012). WIP-/- mice have fewer B-cells, although those that are present exhibit an increased response to B cell receptor (BCR) activation by non-specific stimuli, such as LPS (Anton et al., 2002; Curcio et al., 2007). The actin cytoskeleton is also disrupted in WIP-/- B cells suggesting that the control of actin polymerisation by WIP is involved in negative regulation of the BCR (Anton et al., 2002). WIP also regulates the abundance of natural killer (NK) cells, which are involved in the destruction of virally infected or cancer cells. Loss of WIP in patients with a severe immunodeficiency resembling WAS, results in an increased number of NK cells, although the function of these

cells is drastically impaired (Lanzi et al., 2012). Furthermore, overexpression of WIP leads to an increase in NK cell dependent cytotoxicity (Krzewski et al., 2008). WIP forms a complex with WASP and myosin IIa in NK cells that is recruited to sites of cell-cell contacts and induces actin polymerisation (Krzewski et al., 2006). Thus, as in T and B-lymphocytes, the defects observed in WIP-/- NK cells are likely the result of impaired actin polymerisation.

1.6.1.2 The role of WIP in podosomes and invadopodia

Podosomes are specialised adhesive structures that are important for cell migration (Garcia et al., 2012). These structures appear to have the capacity to degrade the extra-cellular matrix and thus allow cells to overcome physical barriers that block their path and migrate through tissues (Cornfine et al., 2011). Podosomes are found in many migratory cell types including phagocytes, dendritic cells and macrophages, which are involved in immune surveillance (Murphy and Courtneidge, 2011; Noy et al., 2012). They consist of an F-actin rich core, surrounded by proteins involved in adhesion, enzymes that degrade the extracellular matrix (ECM) and proteins involved in remodelling the cell membrane (Garcia et al., 2012). WASP and the Arp2/3 complex control actin polymerisation at podosomes, and in recent years WIP has also emerged as a major regulator of the organisation and function of podosomes (Banon-Rodriguez et al., 2011; Chou et al., 2006; Tsuboi, 2006). In the absence of WIP, dendritic cells cannot induce the formation of podosomes (Chou et al., 2006). Furthermore, WIP is required for the secretion of matrix metalloproteinases (MMPs) from dendritic cells. MMPs are the key proteins involved in the degradation of the matrix by podosomes (Banon-Rodriguez et al., 2011). The interaction of WIP with cortactin is also important for podosome function (Banon-Rodriguez et al., 2011; Chou et al., 2006). While podosomes are induced in the absence of this interaction, there is a dramatic reduction in their ability to degrade the ECM (Banon-Rodriguez et al., 2011). The podosomes also appear smaller and have decreased F-actin content consistent with the observation that cortactin is relocalised to the plasma membrane in the absence of WIP, leading to increased membrane ruffling and protrusion (Banon-Rodriguez et al., 2011; Chou et al., 2006). Loss of WIP also impairs the formation of a polarised and defined leading edge (Chou et al., 2006). Podosomes are usually short-lived structures

with a half-life of 30s -5 minutes. In the absence of WIP, podosomes are not formed, instead large stable focal adhesion like structures, with a half-life of 30-60 minutes, are observed (Chou et al., 2006). Disrupting the interaction of WASP and WIP decreases the efficiency of podosome formation; moreover, WASP-/- cells lack the ability to form podosomes (Jones et al., 2002; Olivier et al., 2006; Tsuboi, 2006). Therefore, many of the defects in podosome formation observed upon the loss of WIP could be explained by the role of WIP in preventing WASP degradation (de la Fuente et al., 2007). However, clear evidence has demonstrated that this is not the only role of WIP in podosome formation. Expression of WASP in WIP-/- dendritic cells that had been treated with proteosome and calpain inhibitors was not sufficient to rescue podosome formation (Chou et al., 2006). Instead it was found that WIP is required for the correct localisation WASP to sites of actin polymerisation. WIP has also been shown to have a role in the formation of invadopodia (Yamaguchi et al., 2005). Invadopodia are also actin rich structures that degrade the extracellular matix (Murphy and Courtneidge, 2011). They are related to podosomes but occur only in cancer cells, where they are thought to play an important role in tumour cell metastasis (Garcia et al., 2012). Disruption of the interaction between WIP and N-WASP by expression of the WBD of WIP resulted in a marked decrease in invadopodia formation (Yamaguchi et al., 2005). Abrogation of the interaction between WIP and cortactin did not interfere with the formation of invadopodia, indicating that while similar, podosomes and invadopodia are differently regulated (Banon-Rodriguez et al., 2011; Yamaguchi et al., 2005). Consistent with a role in invadopodia formation, further evidence has arisen in recent years that points to a role for WIP in invasive and metastatic cancers. Gene expression microarray analysis has revealed a correlation between low expression of WIP and improved prognosis for a variety of cancers (Staub et al., 2009). Furthermore, increased WIP expression has also been associated with epithelial-mesenchymal transition (EMT) (Gu et al., 2007).

1.6.2 WIRE

WIRE (WIP related protein), also known as WICH (WIP and CR16 homologous) was identified as a homologue of WIP in two independent studies (Aspenstrom, 2002; Kato et al., 2002). WIRE has about 40% sequence identity to WIP and is

very proline rich (Aspenstrom, 2002). It is expressed widely, with particularly high protein expression observed in the brain, colon, lung and stomach (Kato et al., 2002). WIRE binds to both actin monomers and filaments and stabilises these filaments by decreasing the rate of actin depolymerisation (Kato et al., 2002). Another study demonstrated that WIRE crosslinks actin filaments *in vitro* (Kato and Takenawa, 2005). Consistent with this, the same study showed that overexpression of WIRE in fibroblasts induces the formation of thick actin filament bundles. WIRE has also been implicated both in actin rearrangements downstream of the PDGF receptor as well as in endocytosis of the receptor itself (Aspenstrom, 2002, 2004). In porcine aortic endothelial (PAE) cells overexpressing the PDGFβ receptor, ectopic WIRE resulted in depolymerisation of actin stress fibres, while at the same time inducing small actin puncta and membrane ruffles (Aspenstrom, 2002).

Like WIP, WIRE interacts with both WASP and N-WASP, although there is evidence that it may preferentially bind to N-WASP (Aspenstrom, 2002, 2004; Kato et al., 2002). WIRE and N-WASP have been shown to function together in a number of situations. Endocytosis of the PDGF receptor by WIRE is dependent on its interaction with N-WASP (Aspenstrom, 2004). In addition, co-expression of WIRE and N-WASP cells results in the formation of actin microspikes/filopodia, although neither protein alone is sufficient to produce this phenotype unless the cells have been stimulated with EGF or PDGF-BB (Aspenstrom, 2002; Kato et al., 2002). Interestingly, the ability of WIRE to induce filopodia was subsequently found to be independent of a direct interaction with N-WASP, although an intact WIRE WH2 domain was required (Aspenstrom, 2004). This seemingly contradictory data can be explained by the interaction of WIRE and IRSp53 (Misra et al., 2010). IRSp53 binds to active GTP-bound Cdc42 and contains an IMD/BAR (IRSp53 and Missing in Metastasis homology domain/ Bin–amphipysin–Rvs167) domain, which is involved in linking the actin cytoskeleton to membranes (Scita et al., 2008). In the absence of N-WASP, co-expression of WIRE and IRSp53 results in the induction of Cdc42-dependent filopodia (Misra et al., 2010). This process requires both the SH3 domain of IRSp53 and the actin binding WH2 domain of WIRE. Furthermore, IRSp53 also interacts with N-WASP and together these proteins induce filopodia formation (Lim et al., 2008). Thus it is plausible that IRSp53 mediates the

cooperative increase in filopodia induction observed upon co-expression of WIRE and N-WASP. Alternatively as WIP has also been shown to induce filopodia in concert with N-WASP; co-expression of WIRE and N-WASP may result in the up regulation of two distinct pathways that lead to filopodia formation (Martinez-Quiles et al., 2001; Vetterkind et al., 2002).

Interestingly, WIP does not synergise with IRSp53 to induce filopodia, thus demonstrating that WIP and WIRE can perform distinct cellular functions (Misra et al., 2010). Another example of a pathway that specifically requires the presence of WIRE, but not WIP, is found at adherens junctions (Kovacs et al., 2011). In this case, WIRE cooperates with N-WASP to maintain the actin structures of the zonula adherens. Paradoxically, the ability of N-WASP to activate the Arp2/3 complex is not required in this case, indicating that N-WASP is not involved in the nucleation of these filaments. Instead, N-WASP and WIRE participate in a non-canonical post-nucleation pathway that stabilises newly formed actin filaments and promotes their incorporation into apical actin rings (Kovacs et al., 2011).

Other WIRE binding partners include profilin and Nck (Aspenstrom, 2002). Profilin immunoprecipitates with an N-terminal fragment of WIRE, but not with the full-length protein. This suggests that another level of regulation exists in which the N-terminal segment of WIRE is masked, preventing it from interacting with profilin. However a physiological function for this interaction has not been elucidated. Co-expression of Nck and WIRE results in the formation of large, arrow shaped focal adhesions (Aspenstrom, 2002). Based on this data, Nck was proposed to recruit WIRE to focal adhesions, however, further studies are required to verify that this is the case.

1.6.3 CR16

CR16 (corticosteroids and regional expression 16) was initially identified in a rat hippocampal cDNA library and its mRNA expression is regulated by glutocorticoid receptor (Masters et al., 1996; Nichols et al., 1990). CR16 mRNA has been detected in the brain, lung, testes and heart but is not observed in the spleen, liver or kidney (Masters et al., 1996). Similarly, the CR16 protein is highly expressed in

brain, while lower expression is detectable in the heart, lung and testes (Ho et al., 2001; Suetsugu et al., 2007). CR16 interacts with the WH1 domain of N-WASP via its C-terminal region. Interestingly, the presence of CR16 in *in vitro* actin polymerisation assays did not inhibit the ability of N-WASP to activate the Arp2/3 complex, indicating that CR16 and WIP may fulfil different functions in this pathway (Ho et al., 2004; Ho et al., 2001). In addition to the interaction with N-WASP, CR16 contains WH2 domains and can also bind both G and F-actin. Furthemore, CR16 interacts with multiple SH3 domain containing proteins including Src, Abl and PLCγ (Ho et al., 2001; Weiler et al., 1996). CR16 can also be phosphorylated *in vitro* by MAP kinase although the biological relevance of this interaction has not yet been established (Weiler et al., 1996). CR16 can partially compensate for the loss of verprolin in yeast (Meng et al., 2007). Expression of CR16 rescues the defects in growth and endocytosis that result from the loss of verprolin, however the polarisation of actin patches is not restored (Meng et al., 2007). This study also demonstrated that the actin binding WH2 domains of CR16 are not required for the functioning of the protein, as it was found that N-terminal proline motifs that are specific to CR16 can compensate for the loss of actin binding. The mechanism of this redundancy is unclear, although it may involve Myo3p, which interacts with this proline rich region of CR16 (Meng et al., 2007). Despite, the high levels of CR16 present in neuronal tissues, no gross brain abnormalities are observed in CR16 knockout mice (Suetsugu et al., 2007). As WIP and WIRE are also expressed in the brain, they may be able to compensate for the loss of CR16. In contrast, the loss of CR16 in mice results in male specific sterility due to defects in spermatogenesis. CR16 and N-WASP were found in complex in testes and lower levels of N-WASP were observed in the absence of CR16 indicating that these proteins function together in spermatogenesis (Suetsugu et al., 2007). Consistent with this, a recent study demonstrated that lower levels of CR16 and N-WASP are expressed in the testes of men with idiopathic azoospermia (Xiang et al., 2011).

1.7 Receptor signalling to the actin cytoskeleton

In order to function, a cell must process the external signals it receives and mount the appropriate response. This is achieved via signalling cascades that involve transmembrane receptor proteins and adaptor proteins that connect the external

environment to numerous signalling pathways including the N-WASP and Arp2/3 complex dependent actin polymerisation machinery. One class of transmembrane receptors implicated in the regulation of actin polymerisation is the receptor tyrosine kinases (RTKs). These include the epidermal growth factor receptor (EGFR), the platelet derived growth factor receptor (PDGFR), the T cell receptors (TCR), and the Met receptor (Abella et al., 2010b; Anton et al., 2003; Dustin and Depoil, 2011; Kempiak et al., 2003). Pathogens including EPEC and vaccinia virus also encode proteins that mimic receptor tyrosine kinases in order to induce actin polymerisation in host cells (Frischknecht et al., 1999b; Hayward et al., 2006; Kenny et al., 1997). In general, RTKs consist of an extracellular ligand binding domain, a single transmembrane domain and a cytoplasmic tail that frequently harbours the protein tyrosine kinase activity as well as other C-terminal and juxtamembrane regulatory regions (Hubbard and Miller, 2007; Lemmon and Schlessinger, 2010). Upon activation by ligand binding, receptor dimerization or oligomerization occurs and results in a conformational change that activates the kinase activity of the cytoplasmic domain of the receptor. This results in the phosphorylation of multiple sites in the cytoplasmic region of the dimer/oligomer and the RTKs can now function as a recruitment and activation platforms for other cellular proteins (Lemmon and Schlessinger, 2010). One important class of proteins that link cell surface receptors to the cytoskeleton are the SH2-SH3 adaptor proteins, for example Nck and Grb2 (Buday et al., 2002; Mayer, 2001; Pawson, 2007; Reebye et al., 2012).

1.7.1 SH2 domains

SH2 (Src homology 2) domains are small, independently folding, modular domains that bind directly to phosphotyrosine motifs (Waksman et al., 1992). SH2 domains were first identified in the $p130^{Gag\text{-}Fps}$ oncoprotein in Fujinama sarcoma virus and are highly conserved among cytoplasmic protein tyrosine kinases (Mayer et al., 1988a; Sadowski et al., 1986). They are found in a diverse set of proteins including adaptors suck as Nck, Grb2 and Crk, the p85 subunit of PI3Kinase, the tyrosine phosphatase SHP-2 and Vav, a small GTPase guanine nucleotide exchange factor (GEF) (Buday et al., 2002; Matozaki et al., 2009; Mayer et al., 1988b; Pawson, 2004, 2007; Tybulewicz et al., 2003). A key feature of the structure of SH2 domains

is an invariant arginine in the binding pocket that accommodates the phosphorylated tyrosine (Waksman et al., 1992). Furthermore, SH2 domains have a second more variable binding region that interacts with residues adjacent to the phosphorylated tyrosine and confers the different binding specificities that are observed for the various SH2 domains (Eck et al., 1993; Waksman et al., 1993). Altering a single residue in this region is sufficient to change the selectivity of the SH2 domain and modify its cellular function (Marengere et al., 1994). The residues immediately C-terminal to the phosphorylated tyrosine are critical for determining the SH2 domain specificity (Songyang et al., 1993). For example, the SH2 domain of Nck has a strong preference for interacting with the sequence YDxV, whereas Grb2 can bind to a wider variety of motifs containing the sequence YxNx (Frese et al., 2006; Kessels et al., 2002; Songyang et al., 1993; Songyang et al., 1994).

1.7.2 SH3 domains

In contrast to SH2 domains, SH3 domains are part of a superfamily of proline recognition domains (PRD), which includes WW, EVH1, GYF, profilin, Cap-gly and UEV domains (Kay, 2012; Li, 2005). These are the most abundant protein interaction domains in metazoans (Castagnoli et al., 2004). SH3 domains are approximately 60 residues in length and like SH2 domains; they interact with sequences containing a core motif flanked by residues that confer specificity (Saksela and Permi, 2012). The canonical SH3 ligand is a short proline rich peptide that contains the sequence PxxP and adopts a left-handed polyproline type II helix (Ren et al., 1993; Sparks et al., 1996; Yu et al., 1994). The structure of the SH3 domain is a β-barrel that contains five anti-parallel β-strands (Musacchio et al., 1992). The binding surface of the domain consists of three main features, two hydrophobic grooves that are lined with aromatic residues, which accommodate the xP peptides of the canonical motif and a specificity pocket that is formed by residues from the RT and nSrc loops (Feng et al., 1994; Lim et al., 1994; Musacchio et al., 1992; Noble et al., 1993; Yu et al., 1994). As the hydrophobic grooves lack defined features that would allow recognition of subtle differences between different PxxP motifs, the specificity pocket is crucial for determining the range of binding partners of an SH3 domain. Consistent with this, the substitution of a single residue within this specificity pocket is sufficient to alter the binding

preferences of an SH3 domain (Weng et al., 1995). Negative regulation of interactions between SH3 domains and their binding partners can be controlled by phosphorylation of conserved tyrosines within the binding pocket (Tatarova et al., 2012).

Many SH3 domains bind either type I or type II proline motifs (Tong et al., 2002; Zarrinpar et al., 2003). Class I motifs are characterised by the sequence R/KxxPxxP, while class II ligands are typified by PxxPxR sequences (Alexandropoulos et al., 1995; Feng et al., 1994). Both classes have similar binding affinities for SH3 domains that lie in the range of 1-200μM (Mayer, 2001). As PxxP motifs can bind the SH3 domain in two opposite orientations, an important function of the R/K residues in these motifs are to position the proline rich ligand correctly with respect to the binding groove in the SH3 domain (Feng et al., 1994; Lim et al., 1994). Interestingly the SH3 domains of Fyn and Fyb, were shown to interact with SKAP55 via an RKxxYxxY motif suggesting that prolines are not absolutely required for SH3 domain interactions (Kang et al., 2000). This was further reinforced by the discovery of other atypical SH3 ligands including SH2 domains, LIM domains and PX domains (Hiroaki et al., 2001; Latour et al., 2003; Vaynberg et al., 2005). Another example of this is the interaction of the GADS SH3 domain with SLP-76 via an RxxK motif (Liu et al., 2003). Interestingly, the SH3 domain of Pex13p was shown to bind both canonical and non-canonical ligands via distinct surfaces (Barnett et al., 2000; Douangamath et al., 2002). Futhermore, IRTKS (insulin receptor tyrosine kinase substrate) has recently been shown to bind to tandem PxxP motifs in EspFu, suggesting that the complexity of SH3 interacting partners may be even greater that previously imagined (Aitio et al., 2010).

1.7.3 Nck

The Nck family of adaptors has two members, Nck1 and Nck2, which have 68% amino acid identity (Braverman and Quilliam, 1999; Buday et al., 2002; Chen et al., 1998). They are both widely expressed and at least partially functionally redundant. Nck adaptors consist of three SH3 domains followed by a C-terminal SH2 domain. Knockout of either Nck1 or Nck2 alone yields healthy, fertile mice that have no

gross abnormalities, while the double knockout is embryonically lethal by E12.5 (Bladt et al., 2003). Fibroblasts derived from Nck1/2 null mice have defects in cytoskeletal organisation and cell migration. Furthermore, loss of Dock (the *Drosophila* Nck homologue), results in defects in axonal guidance and targeting in photoreceptor cells (Garrity et al., 1996). The ability of Nck to interact with both phosphotyrosine motifs in RTKs like the PDGFR, the TCR and the Met receptor, and the proline rich regions domains in N-WASP and WIP make it a crucial link in regulating cytoskeletal remodelling in response to extracellular signals (Abella et al., 2010b; Anton et al., 1998; Lettau et al., 2009; Rohatgi et al., 2001; Ruusala et al., 2008). Furthermore, Nck can interact with phophotyrosine motifs on other non-receptor proteins that are involved in cytoskeletal organisation including cortactin, Tks5 and SLP76 (Oser et al., 2010; Pauker et al., 2011; Stylli et al., 2009). Nck activates N-WASP by interacting with its proline rich region and relieving its autoinhibition in a synergistic manner with PIP_2 (Rohatgi et al., 2001; Tomasevic et al., 2007). Moreover, clustering of the three SH3 domains of Nck at the plasma membrane is sufficient to induce localised actin polymerisation in an N-WASP dependent manner (Rivera et al., 2004; Rivera et al., 2009). In addition, recruitment of Nck by multiple phosphorylated tyrosines on the nephrin receptor is essential for actin polymerisation in a mechanism that requires the second and third SH3 domains of Nck (Blasutig et al., 2008). PAK (p21 activated kinase) activation at the plasma membrane occurs in response to Nck recruitment (Lu et al., 1997). Nck and PAK participate in processes as diverse as the regulation of focal adhesion assembly and synaptic transmission (Stoletov et al., 2001; Thevenot et al., 2011). Downstream of the TCR, Nck co-operates with ADAP to stabilise the interaction of SLP76 and WASP during TCR activation (Pauker et al., 2011). Furthermore, Nck functions with WIP and N-WASP to promote the actin-based motility of PIP_2 rich vesicles as well that of pathogens such as vaccinia virus (Benesch et al., 2002; Frischknecht et al., 1999b; Moreau et al., 2000; Weisswange et al., 2009). In addition, Nck regulates the formation of invadopodia via interactions with cortactin and Tks5 as well as with WIP and N-WASP, which are also essential for this process (Oser et al., 2010; Stylli et al., 2009; Yamaguchi et al., 2005). Thus, Nck functions as a crucial linker between a multitude of plasma membrane receptors and the actin cytoskeleton in a vast range of physiological processes.

1.8 Comparison of pathogens that hijack the cellular actin polymerisation machinery

A wide variety of bacterial and viral pathogens exploit Arp2/3 complex dependent actin polymerisation to enhance their pathogenesis. *Listeria monocytogenes*, *Shigella flexneri, Burkholderia pseudomallei* and *Mycobacterium marinum* all induce actin polymerisation in order to propel the bacteria through the cytoplasm of the cell (Bernardini et al., 1989; Kespichayawattana et al., 2000; Knutton et al., 1989; Mounier et al., 1990; Stamm et al., 2005; Tilney and Portnoy, 1989). In contrast, EPEC and EHEC adhere to the surface of cells and induce the formation of actin rich pedestals beneath the bacteria (Campellone et al., 2008a; da Silva et al., 1989; Lommel et al., 2004; Phillips et al., 2004; Wong et al., 2012). This structure is referred to as an attaching and effacing (A/E) lesion and is important to promote efficient colonization by the bacteria (Wong et al., 2011). Furthermore, after replication within host cells, vaccinia and other vertebrate poxviruses fuse with the plasma membrane and induce the formation of actin tails that enhance their cell-to-cell spread (section 1.8.1) (Cudmore et al., 1995; Dodding and Way, 2009; Rietdorf et al., 2001).

Listeria monocytogenes encodes a direct activator of the Arp2/3 complex, known as ActA (Loisel et al., 1999; Welch et al., 1997b; Welch et al., 1998). *In vitro* assays in which beads were coated with purified ActA demonstrated that it is sufficient to reconstitute actin-based motility in cytoplasmic extracts (Cameron et al., 1999). Subsequently, ActA was found to contain regions of homology to WASP family proteins, that mimic the WCA domain and bind directly the Arp2/3 complex to stimulate its actin nucleation activity (Boujemaa-Paterski et al., 2001; Skoble et al., 2000; Zalevsky et al., 2001a). Interestingly, like the WCA domain of WASP/N-WASP, phosphorylation of ActA positively regulates actin tail formation by increasing its affinity for the Arp2/3 complex (Chong et al., 2009). VASP, capping protein and ADF/cofilin have also been shown to play important roles in *Listeria* actin tail formation (Li et al., 2008; Loisel et al., 1999; Skoble et al., 2001).

In contrast to *Listeria*, *Shigella* encodes, IcsA, a protein that activates N-WASP. Consistent with this, *Shigella* does not induce actin tail formation in the absence of

N-WASP (Suzuki et al., 2002). IcsA contains glycine-rich repeats that interact with both the GBD and WH1 domains of N-WASP in order to promotes its activation (Egile et al., 1999; Goldberg and Theriot, 1995; Lommel et al., 2001; Moreau et al., 2000; Suzuki et al., 1998; Suzuki et al., 2000; Suzuki et al., 2002). IcsA is both necessary and sufficient for *Shigella* actin-based motility (Goldberg and Theriot, 1995; Loisel et al., 1999). Cdc42 is not required for actin based motility of the bacteria, although it is important for the entry of *Shigella* into cells (Moreau et al., 2000; Shibata et al., 2002). In addition, both WIP and Nck are recruited to *Shigella*, however dominant negative constructs of these proteins did not affect the formation of actin tails (Moreau et al., 2000). Transient recruitment of Toca-1 is also required for the initiation of actin polymerisation by *Shigella* (Leung et al., 2008). This recruitment is dependent on type III secreted effector proteins but not IcsA. Furthermore, Toca-1 was shown to be necessary to relieve the auto-inhibitory conformation of N-WASP, presumably to facilitate the interaction of IcsA with the GBD (Leung et al., 2008).

Actin pedestal formation by EPEC and EHEC has evolved to mimic receptor tyrosine kinase signalling (Hayward et al., 2006). Both types of bacteria secrete effector proteins into the cell that are required for actin pedestal formation (Kenny et al., 1997). One such protein, which is essential for actin polymerisation is Tir (translocated intimin receptor), a transmembrane protein that has a hairpin topology with both the N and C-terminal regions exposed to the cytosol (DeVinney et al., 1999; Hartland et al., 1999). The extracellular portion of Tir interacts with intimin, a protein located in the outer membrane of the bacteria (Kenny et al., 1997; Rosenshine et al., 1996). The induction of pedestals by EPEC and EHEC then proceeds by different mechanisms, although in both cases N-WASP and the Arp2/3 complex are required (Kalman et al., 1999; Lommel et al., 2004; Lommel et al., 2001). In EPEC, Tir is tyrosine phosphorylated by Src and Abl family kinases resulting in the recruitment of Nck by tyrosine 474 (Gruenheid et al., 2001; Kenny, 1999; Phillips et al., 2004; Swimm et al., 2004). Nck is crucial for robust actin pedestal formation and is required for the recruitment of N-WASP and the Arp2/3 complex to sites of pedestal formation (Gruenheid et al., 2001). In the absence of Nck, EPEC can still induce actin polymerisation, albeit with fourfold lower efficiency (Campellone et al., 2004). N-WASP and the Arp2/3 complex are recruited to

pedestals in the absence of Nck, and phosphorylation of another tyrosine in Tir (454) is also involved in this secondary pathway of pedestal formation (Campellone and Leong, 2005). The importance of phosphorylated tyrosine 454 suggests that another SH2 adaptor is involved in this mechanism of actin polymerisation; however, the identity of this protein remains unknown (Campellone and Leong, 2005).

In contrast to EPEC, EHEC requires a second bacterial protein, EspFu (*E. coli*-secreted protein F-like protein encoded on prophage U), to induce actin polymerisation (Campellone et al., 2004). EspFu interacts with both Tir and N-WASP and activates N-WASP by competing with the WCA domain for GBD binding (Campellone et al., 2008a; Campellone et al., 2004; Cheng et al., 2008; Sallee et al., 2008). IRSp53 and the related protein, IRTKS, mediate recruitment of EspFu to bacteria by interacting both with tyrosine 458 of Tir and with the proline rich region of EspFu (Vingadassalom et al., 2009; Weiss et al., 2009). Tyrosine 458 of EHEC Tir is part of an NPY motif, which is also conserved in EPEC Tir (NPY 454). Interestingly in Nck deficient cells, expression of EspFu rescues the ability of EPEC to induce actin pedestal formation to near wild type levels suggesting that the origins of this actin polymerisation pathway are common to both EPEC and EHEC (Brady et al., 2007; Campellone et al., 2004). Although Y454 can be phosphorylated in EPEC infected cells, substitution of this tyrosine for phenylalanine results in a minor, although significant, defect in actin pedestal formation in both EHEC and EPEC. This indicates that tyrosine phosphorylation is not essential for EspFu recruitment to Tir (Brady et al., 2007). Surprisingly, recent data has demonstrated that while N-WASP is required for translocation of Tir and EspFu into cells, it is not essential for actin pedestal formation (Vingadassalom et al., 2010). Clustering of the C-terminal repeats of EspFu in N-WASP-/- cells was sufficient to induce actin polymerisation. Despite this, loss of N-WASP does lead to a decrease in the efficiency of pedestal formation, and the Arp2/3 complex is still essential for the formation of pedestals. This data raises the interesting possibility that another unknown factor plays a major role in stimulating Arp2/3 dependent actin polymerisation during EHEC infection (Vingadassalom et al., 2010). EPEC and EHEC both recruit WIP to sites of actin pedestal formation (Lommel et al., 2004). Recruitment of WIP involves both Tir and another bacterial protein, EspH,

(Wong et al., 2012). It seems that WIP then interacts with N-WASP and mediates actin polymerisation independently of Nck. Consistent with this mechanism, expression of the WBD of WIP, which disrupts the interaction of WIP and N-WASP eliminates EspH dependent actin polymerisation (Wong et al., 2012).

1.8.1 Vaccinia Virus

Vaccinia virus is a member of the orthopox genus of poxviridae (Roberts and Smith, 2008). It is large, brick shaped, enveloped virus with dimensions of approximately 250nm by 200nm (Goebel et al., 1990). It is a double-stranded DNA virus that replicates entirely in the cytoplasm of host cells. The virus enters the cell primarily by macropinocytosis, a specialised form of endocytosis that results in the engulfment of large amounts of fluid (Mercer and Helenius, 2008; Schmidt et al., 2011). In addition, virus particles can also enter the cell by direct fusion with the plasma membrane (Armstrong et al., 1973; Carter et al., 2005). After entry, the viral core is transported to the perinuclear region of the cell in a microtubule dependent manner where it establishes a compartment known as the virus factory where replication occurs (Carter et al., 2003; Domi and Beaud, 2000; Tolonen et al., 2001). A subset of newly replicated virus particles, knowns as IMVs (intracellular mature virus), leave the virus factory and become wrapped in a double membrane derived from the endosomal network or the trans-golgi, resulting in the formation of intracellular enveloped virus (IEV) particles (Dodding et al., 2009; Hiller and Weber, 1985; Roberts and Smith, 2008; Schmelz et al., 1994; Tooze et al., 1993). IEVs are transported on microtubules in a kinesin-1 dependent manner to the cell periphery where the outer membrane of the virus fuses with the plasma membrane, resulting in the liberation of an enveloped virus particle that remains attached to the cell surface (Arakawa et al., 2007a; Arakawa et al., 2007b; Dodding et al., 2011; Hollinshead et al., 2001; Morgan et al., 2010; Rietdorf et al., 2001). The extracellular form of the virus particle is referred to as a CEV (cell-associated enveloped virus). CEVs then signal back into the cell to induce the formation of an actin tail that propels the virus particle away from the plasma membrane towards neighbouring cells to enhance the spread of infection. The importance of actin tails in cell-to-cell spread of the virus is demonstrated by the small plaque phenotype of mutant viruses that cannot induce actin tails (Blasco and Moss, 1992; Herrera et al.,

1998; Mathew et al., 1998; Rodger and Smith, 2002; Rottger et al., 1999). Interestingly, vaccinia virus also uses actin tails to infect distantly located cells in order to substantially increase the rate of infection (Doceul et al., 2012; Doceul et al., 2010). Doceul and colleagues found that if a virus particle contacted an already infected cell, it would induce an actin tail, and “surf” across the plasma membrane until it came into contact with another uninfected cell. The virus particle can then infect this cell and establish a virus factory.

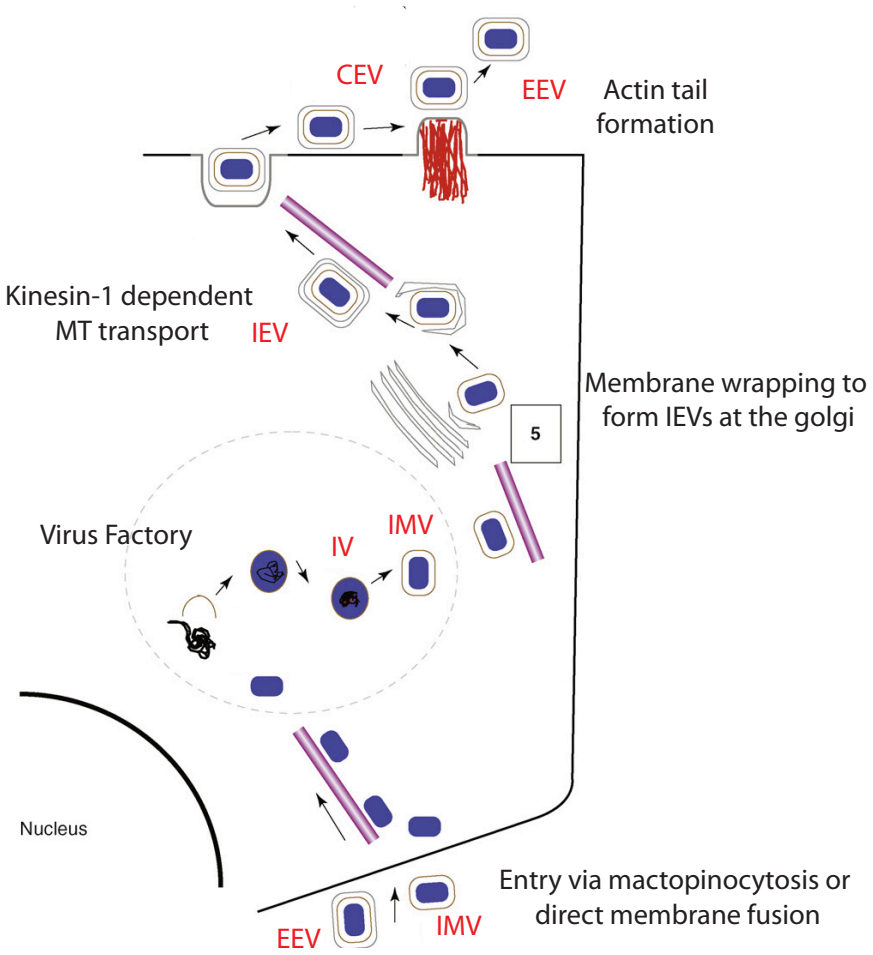

Figure 1.7. The life cycle of vaccinia virus

Schematic representation of the life cycle of vaccinia virus. Virus particles bind to and enter the cell by macropinocytosis or direct membrane fusion. The core of the virus is transported on microtubules to the perinuclear region where the virus factory is established. Within the virus factory, the viral core is uncoated and transcription of viral DNA and replication of virus particles occur. This results in the formation of IMVs, a subset of which are transported to the Golgi where they become wrapped in a double membrane to form IEVs. These are transported on microtubules in a kinesin-1 dependent manner to the cell periphery where they fuse with the plasma membrane and reside on the cell surface in the form of CEVs. These particles signal back inside the cell to induce the formation of actin tails, which generate the force to propel them into neighbouring cells. IMV (intracellular mature virus), IEV (intracellular enveloped virus), CEV (Cell-associated enveloped virus). **(**Roberts and Smith, Vaccinia virus morphogenesis and dissemination, Trends in Microbiology, (2008) 16(10): 472-9. Reproduced with permission of ELSEVIER LTD. in the format reuse in a thesis/dissertation via Copyright Clearance Center.

1.8.2 Actin tail formation

After fusion with the plasma membrane, vaccinia virus particles (CEVs) induce an outside-in signalling cascade that locally stimulates actin polymerisation. The viral protein A36 is critical for the induction of actin tails (Frischknecht et al., 1999b; Rottger et al., 1999). It is a 45kDa, type 1b transmembrane protein that is specifically localised to IEVs (van Eijl et al., 2000). A36 becomes incorporated into the plasma membrane upon fusion of IEVs and remains localised underneath the CEV (van Eijl et al., 2000). CEVs induce the activation of Src and Abl family kinases via an unknown mechanism that is dependent on the SCR repeats of the vaccinia protein B5 (Newsome et al., 2004; Newsome et al., 2006). Recently, CK2 (Casein Kinase 2), a serine/threonine kinase has also been implicated in the recruitment of activated Src to vaccinia virus particles (Alvarez and Agaisse, 2012). Activated Src then phosphorylates A36 on two tyrosines in its cytoplasmic domain (Frischknecht et al., 1999a; Frischknecht et al., 1999b; Scaplehorn et al., 2002). In this way, vaccinia virus mimics receptor tyrosine kinase signalling (Munter et al., 2006; Reeves et al., 2005). Phosphorylation of A36 on Y112 results in the recruitment of a complex of Nck, WIP and N-WASP that function together to activate the Arp2/3 complex and induce actin polymerisation (Frischknecht et al., 1999b; Moreau et al., 2000). Nck and N-WASP are essential for actin tail formation (Snapper et al., 2001; Weisswange et al., 2009). In contrast, it still remains to be established if WIP is essential. Furthermore, Nck is thought to be the major factor that activates N-WASP at virus particles. Although Cdc42 is localised to virus particle inducing actin tails, it is not thought to play a role in their formation, as expression of dominant negative Cdc42, or treatment of cells with toxin B, did not affect the ability of vaccinia virus to induce actin tails (Moreau et al., 2000). Expression of the WBD of WIP in vaccinia infected HeLa cells results in the loss of recruitment of N-WASP and a decrease in the efficiency of actin tail formation (Moreau et al., 2000; Zettl and Way, 2002). Consistent with this, the WH1 domain of N-WASP is also important for its recruitment. This suggests that the localisation of N-WASP to virus particles may depend on the presence of WIP. However, in the absence of N-WASP, only Nck localises to vaccinia virus, suggesting that WIP and N-WASP may be recruited as a complex (Weisswange et al., 2009). Thus, the

precise mechanism of recruitment of WIP and N-WASP still remains to be fully clarified.

Phosphorylation of tyrosine 132 of A36 results in the recruitment of Grb2, which functions as a secondary adaptor in actin tail formation (Scaplehorn et al., 2002). Recruitment of Grb2 also depends on an interaction with the proline rich region of N-WASP (Scaplehorn et al., 2002; Weisswange et al., 2009). Grb2 is not essential for inducing actin tail formation, however its presence enhances the efficiency of this process and leads to an increase in the number of actin tails induced (Scaplehorn et al., 2002). Recent work has demonstrated that the dynamics of the vaccinia actin-signalling network are very rapid (Weisswange et al., 2009). FRAP experiments revealed that Nck and WIP have similar rates of exchange of ~800ms, while Grb2 is much more dynamic with a rate of exchange of ~140ms. Surprisingly, N-WASP exchanges more 3.5 times more slowly, despite its role as the most downstream component of the complex. It was found that N-WASP is stabilised by interactions with both Grb2 and actin filaments and furthermore that the rate of N-WASP exchange was the primary determinant of the rate of actin based motility of vaccinia virus particles (Weisswange et al., 2009). Loss of Grb2 recruitment also resulted in the more rapid exchange of both Nck and WIP (Weisswange et al., 2009). Thus Grb2 stabilises the actin-signalling network at virus particles. Grb2 can also activate N-WASP, although it is not clear whether this is important in vaccinia induced actin tail formation (Carlier et al., 2000; Tomasevic et al., 2007).

1.9 The Aim of this thesis

Studies examining how the actin cytoskeleton is exploited by viral and bacterial pathogens have been an invaluable tool in understanding cellular mechanisms regulating actin polymerisation. The aim of my thesis was to use vaccinia virus to further understand how a phosphotyrosine based signalling network functions to activate Arp2/3 dependent actin polymerisation. In particular, my aim was to elucidate the exact role of WIP in Nck and N-WASP signalling and furthermore, to understand the connectivity and interplay between the proteins in this important and conserved signalling network.

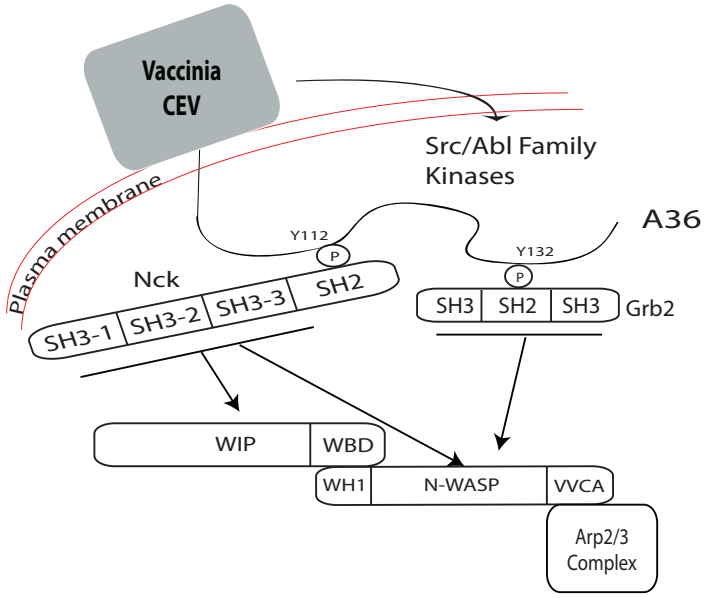

Figure 1.8. Vaccinia Virus Actin Signalling Network

Schematic representation of A36 and the cellular proteins required for actin based motility of vaccinia virus. Activation of Src and Abl family kinases results in phosphorylation of A36 on two tyrosines 112 and 132. This results in the recruitment of a complex of Nck, Grb2, WIP, and N-WASP, which function together to stimulate the Arp2/3 complex and induce actin tail formation. Nck and N-WASP are essential for actin polymerisation while Grb2 functions as a secondary adaptor to enhance actin tail formation. SH (Src Homology), WBD (WASP Binding Domain), V (verprolin/WH2), C (connector), A (acidic). Arrows indicate potential interactions.

Chapter 2. Materials & Methods

2.1 General Buffers and culture media

Most generic buffers and media were provided by the in-house service at CRUK. The recipes for the relevant reagents are listed below. All other buffers will be described in the relevant section.

2.1.1 General Buffers

Phosphate Buffered Saline A (PBSA)

8g Sodium chloride, NaCl

0.25g Potassium chloride, KCl

1.43g Sodium phosphate dibasic, Na_2HPO_4

0.25g Potassium phosphate monobasic, KH_2PO_4, pH 7.2

2.1.2 Cell Culture Media

Trypsin Solution : 0.25% in Tris Saline

Tris Saline (TS)

8g NaCl

2ml 19% (w/v) KCl solution

0.1g $Na_2H_2PO_4$

1g D-Glucose

3g Trizma Base

1.5ml 1% (w/v) Phenol red solution

0.06g Penicillin

0.1g Streptomycin

Versene Solution

8g NaCl

0.2g KCl

1.15g Na_2HPO_4

0.2g KH_2PO_4 , pH 7.2

0.2g Ethyldiaminotetraacetic acid disodium (EDTA) salt

1.5ml 1% (w/v) Phenol red solution

2.1.3 Bacteriological Media

Luria-Bertani (LB) Medium

10g Bacto-tryptone

5g Bacto-yeast extract

10g NaCl

LB Agar

15g of Bacto-agar was dissolved in 1 litre of LB medium.

2.2 Cell Culture

2.2.1 Culturing and Freezing Stocks

All cell lines used in this thesis, as well as details of their corresponding media, are listed in Table 2.1.

Cell were cultured in media containing FCS and antibiotics (complete media) at 37°C and 5% CO_2. Generally cells were grown to approximately 70% confluency in 10cm dishes and passaged every 2-3 days. To passage cells, the media was aspirated, the plate was washed once with PBS (HeLa, 293T, N-WASP-/- MEFs) or Versene (Nck-/- MEFs, WIP-/- MEFs) and then 2ml of 0.05% trypsin was added to the dish. After ~5 minutes at 37°C, cells were resuspended in complete media and added to a new dish in the required confluency. All cell lines except WIP-/- and WIP wild type MEFs were cultured in 10% FCS. The WIP cell lines were cultured in 15% serum.

To generate frozen stocks, cells from a 70% confluent 10cm dish, were trypsinised as described above, resuspended in complete media and then centrifuged at 100g for 5 minutes. Cell pellets were resuspended in FCS supplemented with 10% DMSO, transferred to cryovials and placed in the -80°C. After 1-2 weeks, cells were transferred to liquid nitrogen for long-term storage. Frozen cells were recovered by thawing an aliquot in a 37°C water bath and then transferring to a 10cm dish

containing complete media. Once the cells had attached to the dish, the media was changed to remove the DMSO.

Table 2.1. Cell lines and media

Cell Line	Species	Medium	Serum	Antibiotics	Source
HeLa	Human	MEM	10% FCS[3]	Pen/Strep[4]	EMBL, Heidelberg
293FT	Human	DMEM[1]	10% FCS[3]	Pen/Strep[4]	Invitrogen
BSC-1	Monkey	DMEM[2]	10% FCS[3]	Pen/Strep[4]	ATCC
N-WASP-/-	Mouse	DMEM[1]	10% FCS[3]	Pen/Strep[4]	S.Snapper
19-IRES Nck 1/2-/-	Mouse	DMEM[1]	10% FCS[3]	Pen/Strep[4]	T. Pawson
WIP WT	Mouse	DMEM[1]	15% FCS[3]	Pen/Strep[4]	N. Ramesh
WIP-/- KO7	Mouse	DMEM[1]	15% FCS[3]	Pen/Strep[4]	N. Ramesh

Notes

[1]Dulbecco's modified eagle medium 4500mg/dm^3 glucose from Invitrogen (Cat..)

[2]Dulbecco's modified eagle medium 1000mg/dm^3 glucose from Invitrogen (Cat..)

[3]Foetal Calf Serum from PAA Laboratories (A15-041)

[4]100units/ml penicillin G sodium, 100µg/ml streptomycin sulphate, from 100x stock, Invitrogen (15140-122).

2.3 Transfection

Different transfection reagents were used depending on the assay and the cell type.

2.3.1 Calcium Phosphate

The ProFection mammalian transfection system from Promega was used for calcium phosphate transfection of 293FT during lentiviral production using the pL/L system. Media was changed on the cells to be transfected 4 hours before addition of the complexes. To transfect a 6cm dish, 20µg of DNA and 37µl of 2M CaCl2 were diluted to a final volume of 300µl in dH20, while 300µl of 2X HBS was added to another tube. After 20 minutes, the DNA mixture was added drop-wise to the HBS with gentle vortexing. 30 minutes later, after mixing by pipetting, the complexes were added to the cells and the plate was gently swirled to ensure an even distribution.

2.3.2 Effectene

Effectene (Qiagen) was used for the transfection of infected cells with pE/L vectors during vaccinia virus infection. In general, cells were transfected 5 hours post infection and fixed 4-5 hours later. Cells were usually plated at $1x10^5$ cells the day prior to the transfection. For a 3cm dish, 400ng of DNA was diluted in 100µl of EC Buffer, 3.2µl of enhancer was added and the mixture was vortexed before incubation at room temperature for 5 minutes. 5µl of effectene was added to the mixture, which was then vortexed for 10 seconds and incubated at room temperature for 10 minutes before mixing by pipetting. The mixture was added directly to the cells. Due to the short period before fixation, it was not necessary to change the media.

2.3.3 Lipofectamine 2000

This method of transfection was used to transfect 293FT cells during the production of lentivirus using the pLVX system. For a 10cm dish, 20µg of DNA was diluted in 0.5ml of Opti-MEM (Invitrogen) while 60µl of lipofectamine 2000 was diluted in 0.5ml of Opti-MEM in a separate tube. After 5 minutes, the lipofectamine 2000 was added to the DNA mixture and this was then incubated at room temperature for 30

minutes. The mixture was then added directly to the cells, which had been seeded the previous day in complete media.

2.3.4 Hiperfect

Hiperfect was used for transfection of cells with siRNA. The standard fast-forward protocol was used as follows. For a 3cm dish: 2µl of a 20µM stock of siRNA was diluted in 100µl of complete media, prior to the addition of 12µl of Hiperfect. The mixture was vortexed and incubated for 5 minutes at room temperature. During this time, the relevant cell line was trypsinised and plated at a density of $7x10^4$ cells in a final volume of 2ml of complete media. The transfection mixture was then added directly to the cells. Cells were incubated for 24-72 hours before transferring to coverslips/Matek dishes for immunofluorescence or live cell imaging or being processed for Western Blot analysis.

2.3.4.1 WIRE RNAi

Two independent siRNA oligos targeting mouse WIRE were purchased from Dharmacon (siGENOME siRNA - Mouse 1110014J05RIK D-041519-01/02). The AllStars negative control siRNA from Qiagen was used to control for non-specific effects and toxicity of the siRNA.. WIP-/- cells were treated with RNAi for 48hrs, before infection with vaccinia virus for 9-10 hours. For rescue experiments, human GFP-WIP (or WIP mutant) was transfected into infected cells 5 hours post infection, using effectene as described above. The human WIP construct was not targeted by the mouse siRNA.

2.4 Vaccinia Virus

The wild type strain of vaccinia virus used in this thesis was Western Reserve (WR). Any other viruses used are listed below.

Table 2.2. Viruses used in this thesis

Vaccinia virus strain	Generated by	Reference/Figure
WR/RFP-A3L	S. Schleich	Figure 3.7
A36R-Y132F	N. Scaplehorn	Figure 3.8
A36R-Y132F/RFP-A3L	I. Weisswange	Figure 3.10

2.4.1 Virus Stock Preparation

Cells were infected using post-nuclear stocks (PNS) of vaccinia virus. Stocks were prepared by infecting 5-10x15cm dishes of 80% confluent HeLa cells with the required virus. Cells were infected in complete media at an MOI of 0.05. Infection was allowed to proceed for 2-3 days until virtually all cells were infected. The level of infection was assessed using a standard wide field tissue culture microscope equipped with at 10X PH-1 objective. To collect the virus, the medium was aspirated and all dishes were scraped and combined into 10-20ml of PBSA. This was centrifuged at 1700rpm for 5 minutes at 4°C. The PBSA was removed and the pellet was resuspended in 250µl of ice-cold viral lysis buffer per 10cm dish. This suspension was then frozen at -20°C, usually overnight. Once thawed, the cell membranes and nuclei were sheared by 8-10 times through a needle. The suspension was then centrifuged at 13000 rpm for 5 minutes at 4°C and the supernatant was collected. This supernatant was divided into 100µl aliquots and stored at -80°C.

Viral Lysis Buffer
10mM Tris.HCl, pH9.0
10mM KCL
3mM Magnesium acetate

2.4.2 Infection

To infect cells, a 100µl aliquot of the PNS preparation was thawed at 37°C and then sonicated for 20 seconds. This vial was then kept at -20°C as a working stock for a number of weeks-months, with little effect on the infection efficiency. The stock was sonicated before each infection was carried out. In order to maintain consistency between experiments, the titre of each virus was calculated using a plaque assay (Chapter 2.4.3). This method allows calculation of the plaque forming units of virus/ml, from which the multiplicity of infection (MOI) can be determined. Generally an MOI of 2-3 was used to infect cells for immunofluorescence or live-cell imaging.

Cells were plated at a density of $1x10^5$ in a 3cm dish, the day prior to infection, which resulted in about 60% confluency. To infect the cells, the media was aspirated and the cells were washed once with serum free media. Serum free media containing the appropriate amount of virus was then added to the cells for 1 hour, after which the media was replaced with complete media. WIP-/- or WIP WT cells were usually infected for 9-10 hours before fixation or live imaging, while Nck-/- and N-WASP-/- cells were infected for 15-16 hours due to the delay in the virus life cycle that was observed in these cell lines. For these cell lines, the cells were usually plated at a density of $1x10^5$ cells per 3cm dish in the morning, and the infection was carried out in the evening to proceed overnight.

2.4.3 Plaque Assay

Plaque assays were used to measure the titre of a viral stock in order to determine the plaque forming units (PFU) so that the correct amount of virus could be used to infect cells. BSC-1 cells were grown to a confluent monolayer in 3cm format and then infected with vaccinia virus using the standard protocol described above (Section 2.4.2). To ensure the formation of single plaques, a 1:10 dilution series was prepared and 6 different dilutions of virus were used to infect cells. One hour after infection, an overlay consisting of sterile 0.9% low melting-temperature agarose in MEM with 2% FCS and Pen/strep was added to the cells. This overlay limits the dissemination of the virus to direct cell-cell spread. The cells were maintained in a 37°C incubator for 72 hours before fixation with 3% PFA.

To determine the titre of the virus, the agarose overlay was removed and the cell monolayer was washed once with PBSA and then stained in 0.1% crystal violet in 20% ethanol for 30 minutes. The cells were then washed extensively with distilled water and the number of plaques was counted.

2.5 Stable Cell lines

Two different lentiviral systems were used to generate the stable cell lines used in this thesis.

2.5.1 pL/L 3.7 Vector

The Nck-/- cell lines expressing various constructs of GFP-Nck were generated using this method.

293FT cells were plated in 6cm dishes at a density of $2x10^6$ cells. Calcium phosphate was used to transfect each dish with 5µg of the pL/L construct of interest as well as 5µg of each of the lentiviral packaging vectors RRE, RER and VSVG. The following morning the media was changed to fresh warm complete media supplemented with 10mM Sodium Butyrate to induce viral transcription. After 8-10 hours this media was replaced with 3ml of complete media. The following day, this media was taken up in a syringe and passed through a 0.45µm filter to remove any particles of 293FT cells, and then added to the cells to be infected. These cells were plated at ~50% confluency in a 3cm dish on the day prior to infection (for most cell lines this is $5x10^4$ cells in a 3cm dish) The virus containing media was left on the cells for two days, after which fresh media was added and the cells were amplified as required. Infection efficiency was assessed by checking for fluorescence using a Zeiss Axioplan Upright equipped with a 25x lens, before cells stably expressing the protein of interest were prepared for FACS sorting.

2.5.1.1 Fluorescence activated cell sorting (FACS)

Fluorescence activated cell sorting (FACS) was used to obtain a population of cells that all expressed the GFP positive construct of interest. This was carried out by the FACS Facility at CRUK. The cells to be sorted were trypsinised and harvested by centrifugation at 100g for 5 minutes. The cell pellet was resuspended in PBSA supplemented with 1% FCS and then filtered through a cell strainer to ensure a single cell suspension. For each cell line a negative control was prepared in the same way to set up the FACS machine, this consisted of the same cells, which had not been infected with lentivirus and were thus not expressing a fluorescent protein. For each cell line, a 15cm dish was sorted (around $2x10^7$ cells) and the collected GFP positive cells were subsequently grown up and stocks were frozen for storage in liquid nitrogen. Cell lines created using this method are listed in Table 2.3.

Table 2.3. Stable cell lines generated with pL/L system

Cell Line	Protein Introduced	Species of Introduced Protein
Nck-/-	GFP-Nck1-Δ1	Human
Nck-/-	GFP-Nck1-Δ2	Human
Nck-/-	GFP-Nck1- Δ3	Human
Nck-/-	GFP-Nck1-ΔSH2	Human
Nck-/-	GFP-Nck1-Δ1+2	Human
Nck-/-	GFP-Nck1-Δ1+3	Human
Nck-/-	GFP-Nck1-Δ2+3	Human
Nck-/-	GFP-Nck1-Δ1+2+3	Human

2.5.2 pLVX-puromycin system

During my time in the Way lab, a new system of creating stable cell lines using lentivirus was adopted. This uses the pLVX vector from Clontech, which contains a puromycin resistance cassette, which allows for rapid selection of stably transfected cells by treating with puromycin, thereby removing the need for FACS sorting. To generate stable cell lines using this method, 293FT cells were seeded in a 10cm dish at a density of $4x10^6$ (70-80% confluent). The following evening, the cells were co-transfected with 10µg of the construct of interest in the pLVX vector, 7µg of the pPAX and 3µg of the pMDG2.3 packaging vectors using lipofectamine 2000. The next morning, the media was replaced with 7mls of complete media. Lentivirus can be harvested twice from these cells over the following two days. To harvest the virus, the media was taken up in a syringe and passed through a 0.45µm Millex HV filter (Millipore#SLHV033RB). The media was replaced on the 293FT the process was repeated the following day. The virus from either day can be used to infect the cells of interest, or combined. The cells to be infected were plated at 50% confluency in a 3cm dish and 2ml of the lentivirus containing media was used to infect them. The rest of the lentivirus was stored at 4°C for a few days or at -20°C or -80°C for the long term. The cells were incubated with the virus containing media for 2 days before selection with puromycin.

To select for cells that stably express the protein of interest, the appropriate amount of puromycin was determined by performing a kill curve in which the cell line to be infected with lentivirus was treated with various amounts of puromycin. For N-WASP-/- cells, 1µg/ml puromycin was found to be sufficient to kill all cells after 3-4 days of treatment. After treatment of the infected cells with puromycin for 3 days, the cells were checked for fluorescence and then grown up to establish stocks of the cell lines for future use. The cell lines generated by this method are listed in Table 2.4

Table 2.4. Cell lines generated by puromycin selection

Cell Line	Protein Introduced	Species of Introduced Protein
N-WASP-/-	GFP N-WASP	Rat
N-WASP-/-	GFP N-WASPΔNck	Rat

2.6 Molecular Biology

2.6.1 General buffers and solutions

5X TBE

54g Tris Base

27.5g Boric acid

20ml of 0.5M EDTA

make up to a final volume of 1L with distilled water

5X DNA Loading Buffer

0.25% (w/v) Bromophenol Blue

15% (v/v) Glycerol

These were diluted in 5X TBE.

2.6.2 Expression Vectors

Three different vectors were used to express proteins. The pE/L vector, which is a synthetic early/late vaccinia virus promoter was used for protein expression in mammalian cells during vaccinia virus infection (Chakrabarti et al., 1997). For creating stable cell lines the modified pL/L3.7 or pLVX vector was used. Finally, the

pMW172 vector, which contains a leaky T7 promoter, was used for bacterial expression of protein (Way et al., 1990). These vectors contained either a GFP or His tag at the N-terminus of the protein of interest. The constructs used in this thesis are listed in table 2.5 below:

Table 2.5. Expression vectors

Vector	Figure	Created by
pE/L GFP stop	3.5	Rietdorf et al., 2001
pE/L GFP WIP	3.5	M. Zettl
pE/L GFP WIRE	3.5	M. Zettl
pE/L GFP WIP P253A P256A	4.2	S. Donnelly
pE/L GFP WIP P332A P335A	4.2	S. Donnelly
pE/L GFP WIPΔNck (P253A P256A+ P332A P335A)	4.2	S. Donnelly
pE/L GFP WIP FFAA	4.7	M. Zettl
pE/L GFP WIPΔNck +FFAA	4.11	S. Donnelly
pE/L N-WASP	5.2	Frischknecht et al., 1999b
pE/L GFP N-WASP P276A P279A	5.2	S. Donnelly
pE/L GFP N-WASP P297A P300A	5.2	S. Donnelly
pE/L GFP N-WASPΔNck (P276A P279A +P297A P300A)	5.2	S. Donnelly
pE/L GFP Nck1	6.2	Frischknecht et al., 1999b
pE/L GFP Nck1ΔSH3-1	6.2	N. Scaplehorn
pE/L GFP Nck1ΔSH3-2	6.2	N. Scaplehorn
pE/L GFP Nck1ΔSH3-3	6.2	N. Scaplehorn
pE/L GFP Nck1ΔSH2	6.2	N. Scaplehorn
pE/L GFP Nck1ΔSH3-1+2	6.2	S. Donnelly
pE/L GFP Nck1ΔSH3-1+3	6.2	S. Donnelly
pE/L GFP Nck1ΔSH3-2+3	6.2	S. Donnelly
pE/L GFP Nck1ΔSH3-1+2+3	6.2	S. Donnelly
pMW His Nck 1		N. Scaplehorn
pL/L3.7 GFP Nck1ΔSH3-1	6.2	S. Donnelly
pL/L3.7 GFP Nck1ΔSH3-2	6.2	S. Donnelly

pL/L3.7 GFP Nck1ΔSH3-3	6.2	S. Donnelly
pL/L3.7 GFP Nck1ΔSH2	6.2	S. Donnelly
pL/L3.7 GFP Nck1ΔSH3-1+2	6.2	S. Donnelly
pL/L3.7 GFP Nck1ΔSH3-1+3	6.2	S. Donnelly
pL/L3.7 GFP Nck1ΔSH3-2+3	6.2	S. Donnelly
pL/L3.7 GFP Nck1ΔSH3-1+2+3	6.2	S. Donnelly
pLVX-puro GFP N-WASP	5.3	S. Donnelly
pLVX-puro GFP N-WASPΔNck	5.3	S. Donnelly
pE/L GFP Grb2	3.11	N. Scaplehorn

2.6.3 Site Directed Mutagenesis

Site directed mutagenesis was used to introduce specific point mutations into a construct of interest. Primer pairs were designed to cover the sequence of interest and to contain the point mutation. The mutation was always in the centre of the primer, with at least 10 base pairs on either side. Longer primers were ordered if more than one point mutation was being introduced. Primers were designed according to Stratagene guidelines.

PCR reactions were carried out using Phusion High-Fidelity DNA Polymerase (NEB) and the following reaction was prepared:

50-100ng of dsDNA template

10µl of 5X reaction buffer

125ng of forward oligonucleotide primer

125ng of reverse oligonucleotide primer

1µl of 25mM dNTP mix (6.25 mM of each dNTP)

1µl (2 units) of Phusion Polymerase

made up to a final volume of 50µl with dH_20

PCR reactions were carried out on an Applied Biosystems GeneAmp PCR machine using the following cycling conditions:

1. 98°C 30 seconds

2. 98°C 10 seconds
   55°C 30 seconds
   68°C 30 seconds/kb of plasmid length

3. 68°C 10 minutes

Section 2 was repeated 16-20 times depending on the type of mutation (more cycles for more mutations).

After the PCR reaction, 1µl of Dpn1 restriction enzyme was added to the reaction and this was incubated at 37°C. Dpn1 specifically digests methylated DNA, thus only the template DNA will be digested by this enzyme. DNA was precipitated by the addition of Sodium acetate at a final concentration of 0.3M and 2.5 volumes of 100% ethanol at -20°C for at least 1 hour. The mixture was centrifuged for 20 minutes at 13,000rpm at 4°C, the pellet was washed with 70% ethanol and centrifuged again for 10 minutes. After drying, the DNA was resuspended in 10µl of dH_20 and transformed into competent *E. coli*. The primers used for site directed mutagenesis in this thesis are listed in table 2.6

Table 2.6. Primers used for Site Directed Mutagenesis

Construct	Primer sequence
pE/L GFP WIP P253A P256A	CGGCCTCCCCTGGCGCCTACCGCCAGCAGGGCCTTG
pE/L GFP WIP P332A P335A	CAATGACGAAACCGCAAGACTCGCACAGCGGAATCTG
pE/L GFP N-WASP P276A P279A	GCAAGCACCACCAGCTCCTCCAGCCTCAAGAGGAGGAC
pE/L GFP N-WASP P297A P300A	CAGCTCAGGCCCTGCTCCCCCTGCTGCCCGTGGAAGGG

Mutated constructs were created from the wild type pE/L construct, verified by sequencing, and sub-cloned into other vectors if necessary. Where double mutants were constructed, as in the case of pE/L GFP WIPΔNck or pE/L GFP N-WASPΔNck, the mutations were introduced sequentially. For pE/L GFP WIPΔNck +FFAA, the two Nck binding mutations were introduced into pE/L GFP WIP FFAA.

2.6.4 Overlap PCR

This method was used to generate the double and triple Nck SH3 mutants. Constructs containing the single point mutations had previously been generated in the lab. Two sets of internal primers were ordered in order to create the necessary combinations of mutations. To create chimearas combining the mutations of interest three PCRs were carried out. The first two PCR reactions amplified the segments of the gene containing the point mutations. These PCR products were gel purified and third PCR was carried out using a 1:1 mixture of these products as a template. In this PCR the forward and reverse primers containing the N and C-terminal restriction sites were used and the resulting product was cloned into pE/L. For each reaction, 100µl PCR reaction were prepared containing
100ng of a pre-existing construct, 10pmol of each primer, 1x Taqplus Precision DNA polymerase buffer, 5units Taqplus Precision DNA polymerase (Stratagene) and 25nmol dNTP mix.

The following cycling conditions were used as standard:

1. 95°C 5 minutes

2. 95°C 30 seconds
   55°C 30 seconds
   72°C 1 minute/kb of plasmid length

3. 72°C 7 minutes

Section 2 was repeated 25 times.

The primers used in these PCRs are listed in table 2.7

Table 2.7. Primers used to create Nck mutants

Primer Name	Sequence
Nck 300 For	tttcaggggaacgtctctatgacc
Nck 300 Rev	tttggtcatagagacgttcccctg
Nck 550 For	tttcaataacctaaatactgggca
Nck 550 Rev	ttttgcccagtatttaggttattg

2.6.5 Subcloning

New constructs were generated using either a sequence verified insert, which had been sub-cloned before or by cloning a PCR amplified gene from an existing vector. The restriction enzymes were purchased all from New England Biolabs (Table 2.8).

Insert and vector were digested in a total volume of 40µl containing the two enzymes, the correct buffer for the enzymes and 1µg of DNA. The reaction was incubated for 1hour at 37ºC. The reaction was loaded on a 1% agarose/TBE gel. Bands corresponding to the predicted insert/vector were cut out from the gel, purified with the Qiagen QIAquick gel extraction kit and eluted from the column in 30µl of distilled water. A 10µl ligation reaction was set up containing the digested vector DNA (100-500ng), an excess of purified insert DNA, 200units T4 DNA ligase and 1x ligase buffer (New England Biolabs). The reaction was incubated for at least 30min at room temperature (or overnight at 16ºC) before transformation into 30µl of chemically competent *E.coli* (Chapter 2.6.6). Colonies were screened using either PCR reactions directly from the colonies (Chapter 2.6.8) or by digestion of minipreps (Chapter 2.6.9).

2.6.6 Plasmid DNA transformation of bacteria

To transform DNA into bacteria, 10µl of ligation reaction or 50ng of plasmid DNA was incubated with 30µl of *E. coli* on ice for 10 minutes. The bacteria were subjected to a 45 second heat shock at 42°C and then replaced on ice for 1 minute. 100µl of antibiotic free LB was added to the transformation mixture and this was

incubated at 37°C for 20 minutes with shaking. The mixture was then spread on pre-warmed LB-agar plates containing the required antibiotic (usually 100µg/ml ampicillin).

2.6.7 Preparation of chemically competent bacteria

Chemically competent bacteria (XL-10 or BL-21) were prepared by inoculating 500ml of LB media with a 2ml culture that had been grown overnight. The culture was incubated with shaking at 37ºC until an OD600 of 0.5 was reached, which indicates that the bacteria are in an exponential growth phase. The bacteria culture was then incubated for 30min on ice, before centrifugation at 2500rpm for 12 minutes. The pellet was resuspended in 20ml of RF1 buffer, incubated on ice for a further 15min and centrifuged at 2500rpm for 9 minutes. The pellet was resuspended in 7ml of RF2 buffer and the suspension was stored at -80ºC in 100µl aliquots.

RF1 Buffer

12g Rubidium chloride, RbCl
9g Manganese chloride, $MnCl_2$
2.94g Potassium acetate
150g Glycerol, pH 5.8
The reagents were dissolved in 900ml of distilled water and the pH was adjusted to pH 5.8 with acetic acid, before increasing the volume to 1L. The buffer was filtered through a 0.22µm filter and stored at 4°C.

RF2 Buffer

2.09g MOPS
1.2g RbCl
11g Calcium chloride, $CaCl_2$
150g Glycerol, pH 6.8
The reagents were dissolved in 900ml of distilled water and sodium hydroxide was used to adjust the pH to 6.8, before the volume was adjusted to 1L. The buffer was filtered through a 0.22µm filter and stored at 4°C.

2.6.8 Colony Screening PCR

PCR was also used to screen colonies for the correct insert after transformation of ligation reactions (Chapter 2.6.5). A 25µl PCR reaction was prepared containing 10pmol of each primer,1X PCR buffer (Thermo Scientific), 0.25µl dNTP mix and 1.25units SimpleRed Taq polymerase (Thermo Scientific). The colonies were picked with a 10µl tip and transferred to a PCR tube containing 20µl of dH_20. The tip was then transferred to a 5ml LB/Amp culture for DNA preparation. The reaction was performed on an Applied Biosystems GeneAmp PCR machine using standard conditions and analysed on a 1% agarose gel.

The following cycling conditions were used as standard:

1. 95°C 5 minutes

2. 95°C 30 seconds
   55°C 30 seconds
   72°C 1 minute/kb of plasmid length

3. 72°C 7 minutes

Section 2 was repeated 25 times.

2.6.9 Plasmid DNA preparation

For large-scale plasmid DNA preparation over night cultures were grown from single colonies. 5ml or 50ml cultures were used for mini and midi preparations respectively. The bacteria cultures were centrifuged at 2500rpm for 20 minutes and the pellets were processed as described in the manufacturers instructions for Qiagen Plasmid Miniprep and Midiprep Kits.

2.6.10 DNA Sequencing

Oligonucleotide primers matching sequences in the regions of the vector flanking the insert as well as every 500bp in the insert were used for sequencing. Each reaction contained 200ng plasmid DNA, 3.2pmol oligonucleotide primer, 8µl BDT reaction mix (Big Dye Terminator Cycle sequencing kit) and 10µl of distilled water. The reaction was cleaned up using the Qiagen Dye-Ex 2.0 Spin kit, and vacuum dried. The samples were sequenced using an Applied Biosystems DNA sequencer

by the Sequencing facility at CRUK. The resulting sequences were analyzed using the DNAstar software package. Primers used for sequencing are listed in table 2.9.

2.7 Biochemistry

2.7.1 Whole cell lysate

Mammalian cells were washed once in PBSA before lysing in the appropriate amount of final sample buffer (FSB). Cells were scraped in FSB and transferred to a microcentifuge tube, before boiling for 5 minutes at 95ºC. 0.5µl of D4527 deoxyribonuclease I (DNase I) was added to the lysate to digest DNA where required. Lysates were stored at -20ºC until required.

2X Final Sample Buffer
50% Glycerol
3% SDS
50mM Tris.HCl pH6.8
2% β-mercaptoethanol
Bromophenol Blue

2.7.2 SDS-PAGE

Pre-cast NuPAGE 4-12% Bis-Tris 1.0mm gels (Invitrogen) were used in all cases. Generally, gels were run using MES running buffer (Invitrogen) at 200V for 40 minutes. After separation of samples, gels were either subjected to immunoblot analysis or stained with Coomassie (0.5% Coomassie Brialliant Blue, 50% Methanol, 10% acetic acid) to visualize protein. Gels were then destained for 30 minutes in high destain (50% methanol, 10% acetic acid) followed by low destain (5% methanol, 10% acetic acid) until protein bands were visualized.

20X MES Running Buffer (Invitrogen)
97.6g MES (1M)
60.6g Tris Base (1M)
10.0g SDS (69.3mM)
3.0g EDTA (20.5mM)

2.7.3 Immunoblot analysis

After separation by SDS-PAGE, proteins were transferred onto nitrocellulose membranes using the iBlot and the iBlot gel transfer kit (Invitrogen). Ponceau S was used to check for successful transfer and to control for equal sample loading. The membrane was blocked for 30 minutes in blocking buffer (5% milk in PBSA, 0.1% Tween20 (Sigma)) and incubated with primary antibody (in blocking buffer) for 1 hour at room temperature or overnight at 4ºC. The membrane was washed 3x10 minutes in in PBSA+0.1% Tween20 (PBS-T) before incubation with HRP conjugated secondary antibody (in blocking buffer) for 30 minutes. The membrane was again washed 3x10 minutes in PBS-T before incubation with ECL, according to the manufacturers instructions (Amersham Bioscences). The membrane was then exposed in Hyperfilm-ECL (Amersham Biosciences) and developed using an IGP Compacct automated developer (IPG limited).

Table 2.8. Primary antibodies used for immunoblot analysis

Antibody	Species	Dilution	Origin
GFP (3E1)	Mouse monoclonal	1:1000	CRUK
His	Mouse monoclonal	1:2000	Sigma
Nck	Rabbit polyclonal	1:1000	Millipore
WIRE 19-39 4G	Rabbit polyclonal	1:500	Way Lab
Grb2	Rabbit polyclonal	1:2000	BD Biosciences
N-WASP	Rat polyclonal	1:1000	Way Lab
RFP (mCherry)	Rabbit polyclonal	1:1000	Chemicon

2.7.4 Expression and purification of His-Nck for far western analysis

2.7.4.1 Leaky Protein Expression

Chemically competent BL21 (DE3) Rosetta *E. coli* were transformed with the pMW172-His-Nck1. A 4ml starter culture (LB-ampicillin) was inoculated using bacteria from a single colony. This was grown for at least 3 hours at 37ºC with vigorous shaking. This was then used to inoculate a 1 L culture (LB/ampicillin), which was grown overnight at 30ºC with shaking. Bacteria were harvested by

centrifugation at 3000rpm for 20 minutes at 4ºC. The resultant pellet was snap frozen in liquid nitrogen. After thawing at room temperature, the pellet was resuspended in 25ml of bacterial lysis buffer (50mM Tris pH 8.0, 150mM NaCl, 25% sucrose, 1x Complete EDTA-free protease inhibitor (Roche)). This was incubated with 2mg of lysozyme for 30 minutes at room temperature. 240 µl of 1 M MgCl2, 24µl of 1M MnCl2 and 10µl of 10mg/ml DNase I were added to lysate, which was then incubated for another 30 minutes at room temperature. This was then centrifuged for 30 minutes at 10,000 rpm at 4ºC and the resultant supernatant was retained as the bacterial soluble fraction. This was snap frozen and stored in aliquots at -20ºC until needed.

2.7.4.2 Purification of His-Nck

25mM Imidazole (pH 8.0) and 10% glycerol were added to the bacterial soluble fraction containing His-Nck. The final concentration of NaCl was increased to 500mM. Ni-NTA resin was washed 3X in wash buffer (500mM NaCl, 10 % Glycerol, 50 mM Tris pH8.0, 25 mM imidazole pH 8.0, 0.1 % Triton X-100) before adding to the bacterial soluble fraction. This was incubated at 4ºC for 1 hour on a rotating wheel, before the resin was pelleted by centrifugation at 2000rpm. The resin was washed 3X in wash buffer prior to elution of bound His-Nck. His-Nck1 was eluted from the resin using 4 washes of 600µl of elution buffer (250mM Imidazole pH8.0, 50mM Tris HCl pH8.0). The eluted fractions were then passed through a PD-10 desalting column according to the manufacturers instructions (GE Healthcare). Protein concentrations were measured by spectrophotometry (absorbance at 280nm) using a NanoDrop spectrophotometer (Thermo Scientific).

2.7.4.3 *Probing peptide arrays*

The WIP and N-WASP peptide arrays were generated by the peptide synthesis laboratory at Cancer Research UK. All arrays comprised 15 amino acid long peptides that were synthesized and spotted onto a cellulose membrane. Adjacent peptides were shifted by 3 amino acids each time. To carry out far western analysis, the dried peptide arrays were moistened by washing with 100% ethanol and then washed 3 times in PBS-T for 10 minutes each time. The array was then blocked for

at least 1 hour in blocking buffer (5% milk in PBS-T), before probing with His-Nck. His-Nck was diluted in blocking buffer to a final concentration of 2µg/ml. The peptide array was then incubated upside-down on parafilm in a plastic box with 2-3ml of the diluted purified protein for 1 hour at 4ºC. The array was washed 5X10 minutes in blocking buffer before being incubated with rabbit anti-His antibody (1:5000) for 1 hour at room temperature. After 5X10 minute washes with blocking buffer, the membrane was incubated with goat anti-rabbit HRP conjugated secondary antibody for 45 minutes. This was followed by 5X10 minute washes in PBS-T and one 10-minute wash with PBS-T containing 500mM NaCl, to reduce non-specific binding. Peptide arrays were then developed using ECL as described in Chapter 2.7.3.

2.7.5 Immunoprecipitation

GFP-WIP immunoprecipitations were carried out using mouse monoclonal anti-GFP antibody 4E12 (Cancer Research UK). For each condition, a 10 cm dish of confluent HeLa cells expressing the GFP-tagged protein of interest was lysed in 1ml of lysis buffer (20mM Tris pH 7.5, 150 mM NaCl, 10 % Glycerol, 1mM EDTA, 1.5 mM $MgCl_2$, 1% NP-40, 1x protease inhibitors), centrifuged for 10 minutes at 13,000 rpm, and then incubated with 30µl of prewashed Protein-G resin (Pierce) for 1 hour at 4ºC on a rotating wheel. The resin was pelleted at 2000 rpm and the cell lysates were transferred to a fresh tube. 100µl of lysate was retained as input. 2µg of GFP antibody was added to the lysate, which was subsequently rotated at 4ºC overnight. 30µl of prewashed protein G resin was incubated with each sample for 1 hour at 4ºC with rotation. The resin was pelleted at 2000rpm and washed 3X in lysis buffer, before boiling in FSB and analysed by SDS-PAGE and immunoblotting. GFP-N-WASP immunoprecipitations were performed using the GFP-Trap (Chromotek), according to the manufacturers instructions, except that 10µl of resin was used per sample.

2.7.6 Peptide pulldown assays

Peptides were obtained from the peptide synthesis facility and coupled via an N-terminal cysteine residue to SulfoLink resin according to the manufacturers

instructions (Pierce/Thermo Scientific). Coupled peptides were washed in wash buffer (150mM NaCl, 10% Glycerol, 50mM Tris pH 8.0, 0.1% Triton-X 100) before incubation for 1 hour at 4ºC with bacterial soluble fraction expressing His-Nck1 (Chapter 2.4.7.1). The peptide couple resin was pelleted at 1000rpm and washed 3 times in wash buffer, before boiling in FSB and subjection to SDS-PAGE. Gels were coomassie stained to visualise bound protein (Chapter 2.7.2).

2.8 Immunofluorescence

2.8.1 General buffers and solutions

1X Cytoskeletal Buffer (CB)

10mM MES pH 6.1

150mM NaCl

5mM EGTA

5mM $MgCl_2$

5mM Glucose

These reagents were dissolved in distilled water.

Immunofluorescence (IF) blocking buffer

1% BSA

2% FBS

These reagents were dissolved in 1X CB.

Mowiol

Mowiol (2.4g) and Glycerol (6g) were dissolved in 6ml of distilled water. This mixture was incubated for 2 hours at room temperature before 12ml of 200mM Tris-HCl (pH 8.5) was added. The resultant solution was stirred for 10 minutes at 60ºC, before being centrifuged at 5000rpm for 5 minutes and stored in 500µl aliquots at -20ºC.

3% Paraformaldehyde (PFA)

15g of paraformaldehyde was added to 500ml PBS. The solution was stirred and gently heated. 1M NaOH tablets were added until the PFA dissolved. After cooling

to room temperature, the pH was adjusted to 7.5 and the solution was passed through a 0.45 filter, before being stored at -20ºC.

2.8.2 Fixation

Paraformaldehyde (PFA) was used to fix cells for immunofluorescence analysis. Cells were washed once in PBSA, then incubated with 3% PFA for 10 minutes, before washing 3X in PBS and storing at 4ºC until needed.

2.8.3 Staining and mounting

Generally, cells on coverslips were blocked for 20-30 minutes in IF blocking buffer, before incubation with the B5 primary antibody for at least 40 minutes to detect extracellular virus particles. Coverslips were washed 3X in PBSA and then permeabilized for 45 seconds with 0.1% Triton X100 in PBSA. After permeabilization, cells were again blocked for 20-30 minutes before incubation with another primary antibody or secondary antibody, again in blocking buffer. Coverslips were washed 3X in PBSA and then 1X in distilled water before mounting on microscopy slides with Molwiol. F-actin was stained with Phalloidin, which was diluted, 1:800 in blocking buffer and added at the same time as the secondary antibody. If an extracellular virus stain was not required, cells were permeabilised directly after fixation and IF was carried out as normal.

Table 2.9. Primary antibodies used for immunofluorescence

Antibody	Species	Fixation	Dilution	Origin
B5	Rat monoclonal	PFA	1:500	Dr. Gerhardt Hiller
Nck	Rabbit polyclonal	PFA	1:200	Millipore
WIRE (19-39)	Rabbit polyclonal	PFA	1:200	Way Lab
N-WASP	Rat polyclonal	PFA	1:200	Way Lab
Texas Red Phalloidin		PFA	1:800	Molecular Probes

2.9 Microscopy

2.9.1 Microscopes

2.9.1.1 Zeiss Axioplan Upright

For fixed samples, a Zeiss Axioplan2 equipped with a Photometrics Cool Snap HQ cooled CCD camera, external Prior Scientific filter wheels (DAPI; FITC; Texas Red;Cy5) and a 63x/ 1.4 Plan Apochromat objective was used. The system was purchased from Zeiss and Universal Imaging Corporation Ltd and was controlled with MetaMorph 6.3r7 software. Images were later analysed using the MetaMorph 6.3r7 software and processed with the Adobe software package (Adobe Systems Incorporated, San Jose, CA, USA).

2.9.1.2 Zeiss Inverted

Live cell imaging was carried out on a Zeiss Axiovert 200 equipped with a Photometrics Cool Snap HQ cooled CCD camera, a Photometrics Cascade II camera, external Prior Scientific filter wheels (GFP, RFP) and a Plan-Apochromat 63x/1.4 Oil objective was used. The system was purchased from Zeiss and Universal Imaging Corporation Ltd and was controlled by MetaMorph 6.3r7 software. Movies and Images were analysed using the MetaMorph software and processed with the Adobe software package.

2.9.1.3 Spinning Disk Confocal

Live imaging and FRAP was carried our ion a Zeiss Axio Observer Microscope equipped with a Plan-Achromat 63x/1.40 Ph3 M27 Oil lens (Carl Zeiss, Germany) and an Evolve 512 camera (Photometrics, AZ) and a Yokagawa CSUX spinning disk. The system was controlled by Slidebook 5.0 (3i intelligent imaging innovations, USA). Movies and images were analysed using Slidebook 5.0 or MetaMorph software.

2.9.2 Quantification of actin tail formation

Cells were fixed 10 hours (WIP-/- cells) or 15 hours (Nck-/-; N-WASP-/- cells) post infection (Chapter 2.7.1). Actin tails are induced only by a subset of vaccinia virus

particles known as CEVs (Cell-associated enveloped virions). After replication, these virions are transported to the cell periphery where they fuse with the plasma membrane and remain attached to its extracellular surface. Only cells with extracellular virus particles were scored for actin tails. In order to specifically detect these extracellular virus particles, the anti-B5 antibody was used. B5 is a viral protein that specifically localizes to virus particles in the later stages of the viral life cycle. Labeling the cell with the anti-B5 antibody prior to permeabilisation enables detection of only CEVs. To visualize actin tails, cells were permeabilised for 1 minute with 0.1% triton-x in PBS and then stained with fluorescently conjugated phalloidin. For the percentage of cells with actin tails, 100 cells on each of three independent days were scored for the presence or absence of actin tails. To determine the average number of actin tails per cells, the number of actin tails in 30 randomly selected cells over three independent experiments were quantified. The experiments were performed as previously described (Frischknecht et al., 1999b; Scaplehorn et al., 2002). Finally, to determine the average length of actin tails, the length of 50 actin tails in 5 cells was measured in each of three independent experiments.

2.9.3 Quantification of actin tail speed

To measure the speed of actin tails in WIP-/- or N-WASP-/- cells, the cells were infected with with WR expressing RFP-A3 or A36-Y132F expressing RFP-A3. The RFP signal was acquired concurrently with the GFP signal of WIP, N-WASP or the mutant protein of interest. As these GFP proteins specifically localize to virus particles that can form actin tails, tracking particles that are both GFP and RFP results in a measurement of the rate of actin based motility. Movies of 5-10 cells were acquired with a rate of 1 frame/second and virus particles were tracked for at least 30 seconds using MetaMorph or Slidebook5.0 software, depending on whether they were acquired on the Zeiss inverted or Spinning Disc confocal (Chapter 2.91.2 and 2.9.1.3). The experiment was repeated 3 times. For actin tails in the WT and WIP-/- cells, actin tails were visualized using phase constrast microscopy.

2.9.4 FRAP

To analyse the dynamic behaviour of the proteins in the vaccinia signalling network FRAP (Fluorescence recovery after photobleaching) was carried out. This technique is used to determine the mobility of a protein in a cell. FRAP experiments are carried out by bleaching the signal from a fluorescently tagged protein in a small region of the cell, in my case the signal localised to the virus particle, and monitoring the recovery of this signal over time. A lack of recovery indicates that the protein exists in an immobile pool as the photobleached population does not dissociate and therefore the remaining fluorescent population cannot replace it. The proportion of the protein pool that is not replaced is known as the immobile fraction (Figure 2.1). A large immobile fraction indicates that the protein of interest is tightly associated with a cellular structure. The rate constant of recovery (k) can also be measured and from this the half-time of fluorescence recovery ($t_{1/2}$) can be calculated. The $t_{1/2}$ is the time taken for the fluorescent signal to recover to half the maximum intensity reached after photobleaching. The $t_{1/2}$ is used as a read out for the mobility of the protein of interest, with a shorter $t_{1/2}$ indicating that the protein is more dynamic.

To carry out FRAP experiments cells were infected with WR/RFP-A3 virus. WIP-/- cells, treated with WIRE siRNA, were transfected 5 hours post infection with the GFP-tagged protein of interest and FRAP was carried out 4 hours later. For the N-WASP-/- cells that stably express GFP-N-WASP or GFP-N-WASP∆Nck, FRAP was carried out 15 hours post infection. Images were acquired on a spinning disc confocal microscope (Section 2.9.1.3), with images acquired every 350ms. The exposure time for each channel was 100ms. The GFP signal was bleached using 5 iterations of the 488 laser at 100% power, which resulted in a post-bleach intensity of approximately 30%. The size of the bleached region and the time interval was kept consistent for all movies. The fluorescence intensity of bleached particles in FRAP movies was measured using the Slidebook software. A threshold was set manually for each movie and the intensity of particles was determined in each frame. The fluorescence intensity of a background region was also determined. This was subtracted from the fluorescence intensity of the GFP signal at the virus particle. The data was normalised to the pre-bleach images. Kinetic modelling of

the normalised data was carried out using Prism5 and the equation $I_{(t)}$= (Imax-Imin)(1-e^{-kt}) + Imin , where I=intensity and t=time (Weisswange et al., 2009). The rate constant of recovery (k) and the maximum (%) recovery after photobleaching (compared to the pre-bleach image) were calculated from the best-fit curve (Figure 2.1). The half-time of fluorescence recovery was calculated from the rate constant of recovery ($T_{1/2}$ = ln2/k). In each experiment around 20 virus particles were bleached in at least 5 different cells. The experiment was repeated on three independent days.

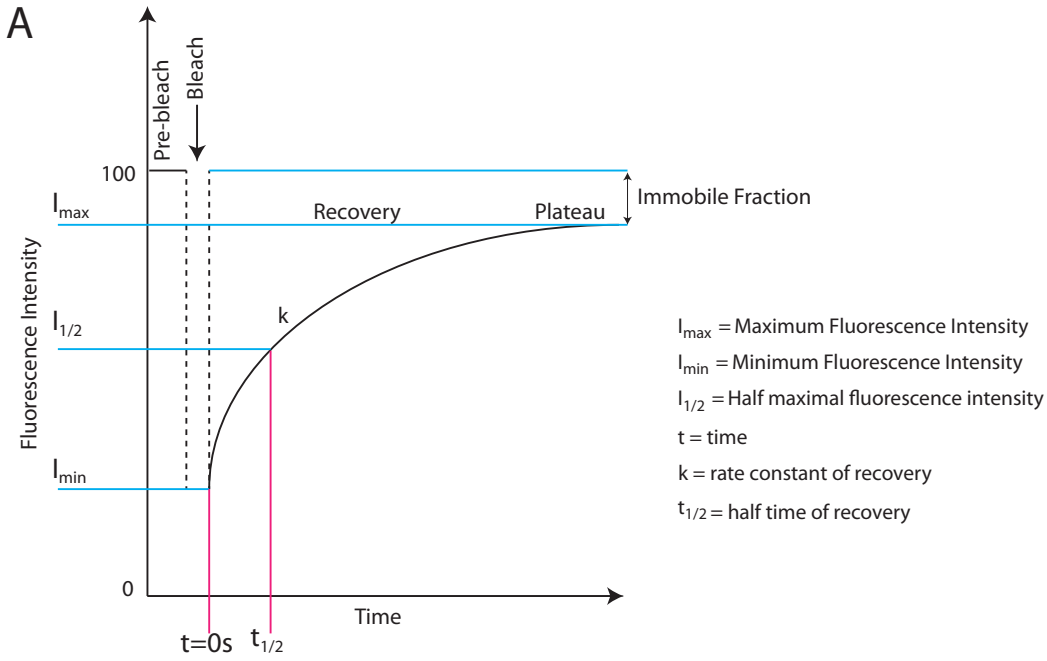

B

$$I_{(t)}=(I_{max}-I_{min})(1-e^{-kt})+I_{min}$$

$$t_{(1/2)} = \frac{\ln 2}{k}$$

Figure 2.1. Schematic of an idealised FRAP curve

(A) Schematic representation of an idealised FRAP analysis curve. The intensity measurements are plotted on the Y-axis, while the time is plotted on the X-axis. The intensity values are normalised against those of the pre-bleach image, which is set to 100. This graph allows calculation of the maximum intensity reached after the recovery reaches a plateau (I_{max}) and the first intensity measurement obtained after the bleach (I_{min}). Non-linear regression curve-fitting was performed using Prism 5.0 and the equation shown in **(B)**. From the best-fit curve, values for I_{max}, I_{min} and the rate constant of recovery (k) can be calculated. The half time of fluorescence recovery ($t_{1/2}$) can then be determined as shown. The $t_{1/2}$ is the time taken for the fluorescence intensity to reach half the maximum fluorescence recovery ($I_{1/2}$).

2.9.5 Statistical analysis of microscopy data

Data in all graphs are presented as mean and standard error of the mean as indicated. Prism 5.0 (GraphPad Software, CA) was used to perform standard statistical analysis of measured data sets. When two data sets were compared a Student's t-test was performed. If more than two data sets were compared with each other a One Way ANOVA test followed by a Tukey multiple comparison test was performed. Statistical analysis of fitted FRAP data was performed using the "Do the best fit values of selected parameters differ between data sets" function in Prism 5.0. All experiments were repeated 3 times on three independent days, unless otherwise stated. A p value of <0.05 is considered statistically significant. * indicates $p<0.05$, ** indicates $p<0.01$ and *** indicates $p<0.001$

Chapter 3. WIP or WIRE is required for vaccinia induced actin polymerisation.

3.1 Introduction

Previous work has shown that Nck and N-WASP are essential for vaccinia-induced actin tail formation (Frischknecht et al., 1999b; Moreau et al., 2000; Weisswange et al., 2009). In contrast, Grb2 is neither essential nor sufficient for actin tail formation, but instead acts as a secondary adaptor to increase the efficiency of the process (Scaplehorn et al., 2002; Weisswange et al., 2009). Despite the robust localisation of WIP to the tips of vaccinia-induced actin tails and evidence that over-expression of the WASP binding domain of WIP acts as a dominant negative to inhibit actin tail formation (Moreau et al., 2000), the role of WIP in actin tail formation remains unclear.

WIP is a member of the verprolin family of proteins that was initially identified as a binding partner of WASP/N-WASP (Aspenstrom, 2005; Ramesh et al., 1997). These proteins participate in many actin dependent cellular processes, including in the induction of filopodia, in pathogen induced actin rearrangements and downstream of receptor tyrosine kinases (Anton et al., 2003; Martinez-Quiles et al., 2001; Moreau et al., 2000; Wong et al., 2012). The role of N-WASP in Arp2/3 complex-dependent actin polymerisation is clear, however the importance of WIP in modulating the activity of N-WASP in cells is not well understood (Campellone and Welch, 2010).

I took advantage of WIP-/- cells to determine if WIP plays an essential role in Nck and N-WASP signalling networks during vaccinia virus actin-based motility.

3.2 WIP is essential for actin tail formation

To gain insight into the role of WIP during the actin-based motility of vaccinia virus, I investigated whether actin tail formation is dependent on the expression of WIP. I obtained mouse embryonic fibroblasts that lack expression of WIP from Raif Geha (Immunology Division, Children's Hospital, Boston). Infection of these cells with WR

(Western Reserve, wild type strain of vaccinia) revealed that at 9 hours post infection, Extracellular virus particles or CEVs (Cell-associated enveloped virus particles) were present on the plasma membrane. These were detected using an antibody against the vaccinia B5 protein (Figure 3.1A). B5 only localised to the IEV (intracellular enveloped virus) and CEV forms of the virus in the later stages of its life cycle. Staining with this antibody prior to cellular permeabilisation specifically reveals the plasma membrane associated CEVs. Control cells (WT), which were obtained from a wild type littermate, showed similar amounts of CEVs (Figure 3.1 A). Actin tails are induced by a signalling pathway initiated by CEVs, which results in the recruitment of the cellular vaccinia virus actin polymerisation complex, comprised of Nck, N-WASP, WIP and Grb2, to the plasma membrane underneath the CEV. However the presence of these CEVs does not mean that this complex is present or that an actin tail will be formed. Thus I stained cells with Texas Red-conjugated phalloidin to visualize the actin cytoskeleton and found that actin tails were formed in both WT and WIP-/- cells. Quantification of the average number of actin tails formed per cell showed that similar numbers of actin tails were induced in control and WIP-/- cells (Figure 3.1A, B). However, compared to those in control cells, actin tails in WIP-/- cells were significantly shorter (3.24 ± 0.25 and 1.64 ± 0.23 μm respectively).

I used live cell imaging to determine if the shorter actin tails in WIP-/- cells exhibit altered rates of actin-based motility of vaccinia virus. To perform live imaging, I infected WT or WIP-/- cells with a recombinant virus, in which the viral core protein A3 had been tagged with RFP (WR/RFP-A3). Actin tails were visualised using phase contrast microscopy. Cells were imaged at 9 hours post infection and images were acquired every second for 3 minutes. In order to avoid the speed of actin-based motility being affected by virus particle collisions, the speed of RFP-virus particles inducing actin tails was tracked for 30 seconds. This analysis revealed that loss of WIP expression leads to a slower average speed of actin tail movement than is observed in WT cells (0.10 ± 0.01 and 0.14 ± 0.01 μm/s respectively) (Figure 3.1 B).

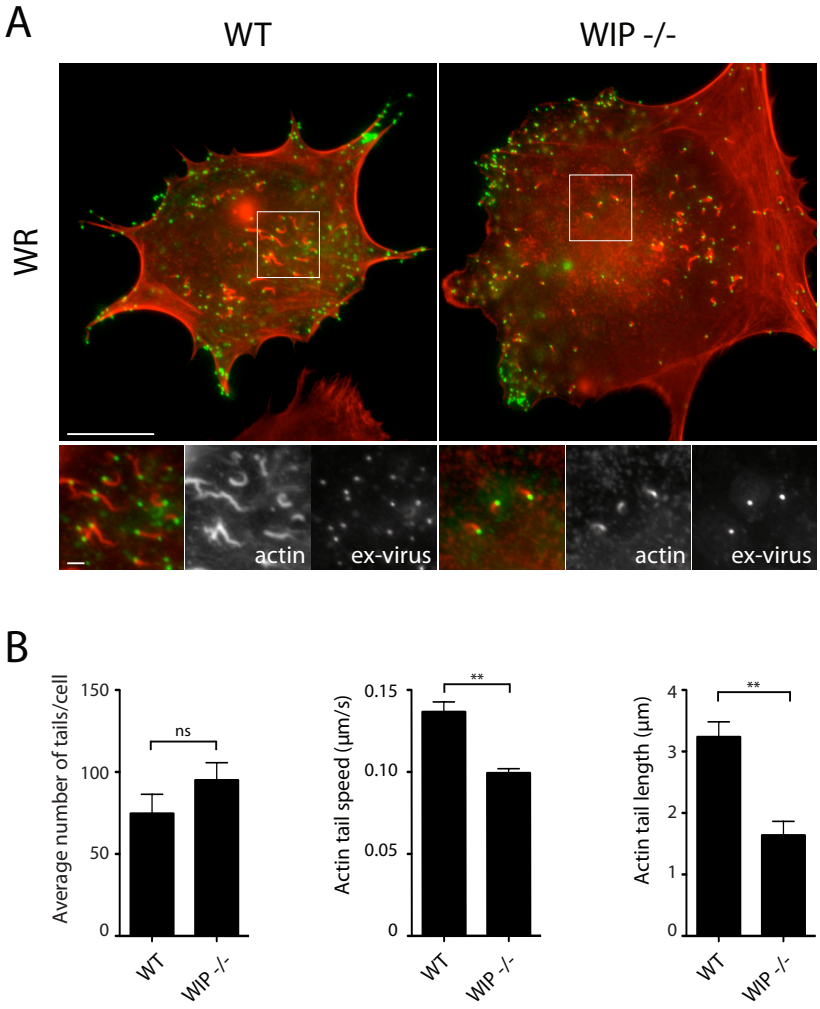

Figure 3.1. Loss of WIP impairs actin tail formation

(A) Immunofluorescence images showing the formation of shorter actin tails by WR in WIP-/- compared to WT cells. Extra-cellular virus particles (ex-virus) are detected using an antibody against the viral protein B5, prior to permeabilisation. Higher magnification panels correspond to the boxes in the main panels. Scale bars = 20 and 2 µm. **(B)** The average number of actin tails per cell is similar in both WT and WIP-/- cells infected with WR. Error bars represent the standard error of the mean (SEM) from 4 independent experiments. Quantification of the rate of actin-based motility reveals that actin tails move more slowly in WIP-/- cells. Error bars are the SEM from 3 experiments in which 50 actin tails in 5 cells were tracked. Quantification of the average length of actin tails shows that actin tails are shorter in WIP-/- compared with WT cells. Error bars represent SEM from 3 independent experiments. ns = not significant, ** = $p<0.01$.

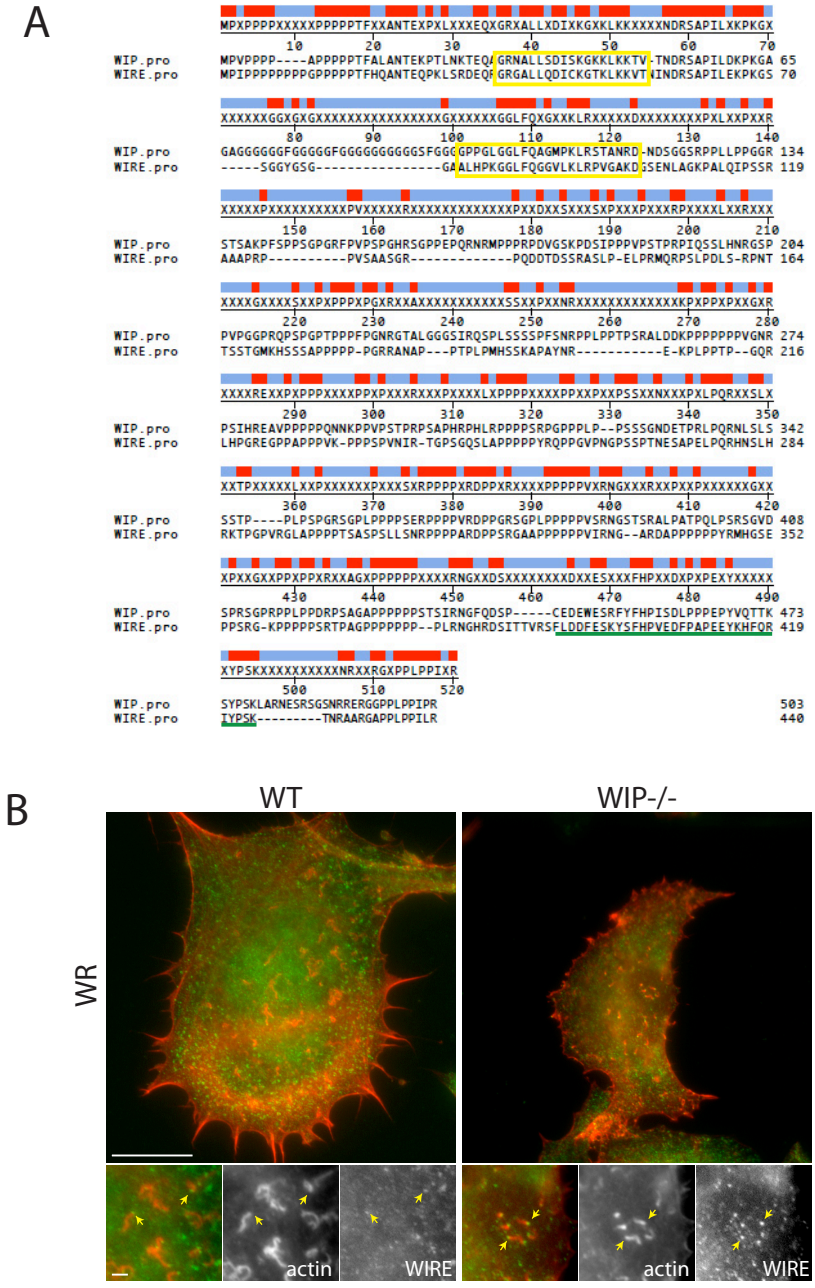

Figure 3.2. Endogenous WIRE is recruited to actin tails

(A) ClustalW sequence alignment showing sequence homology between human WIP and WIRE protein sequences. Red indicates identical residues. The WH2 domains (actin binding) are indicated by yellow boxes and the WASP binding domain (WBD) is underlined in green. **(B)** Immunofluorescence images of WT and WIP-/- cells in which the recruitment of endogenous WIRE to the tips of actin tails is indicated by yellow arrows. Scale bars = 20 and 2μm.

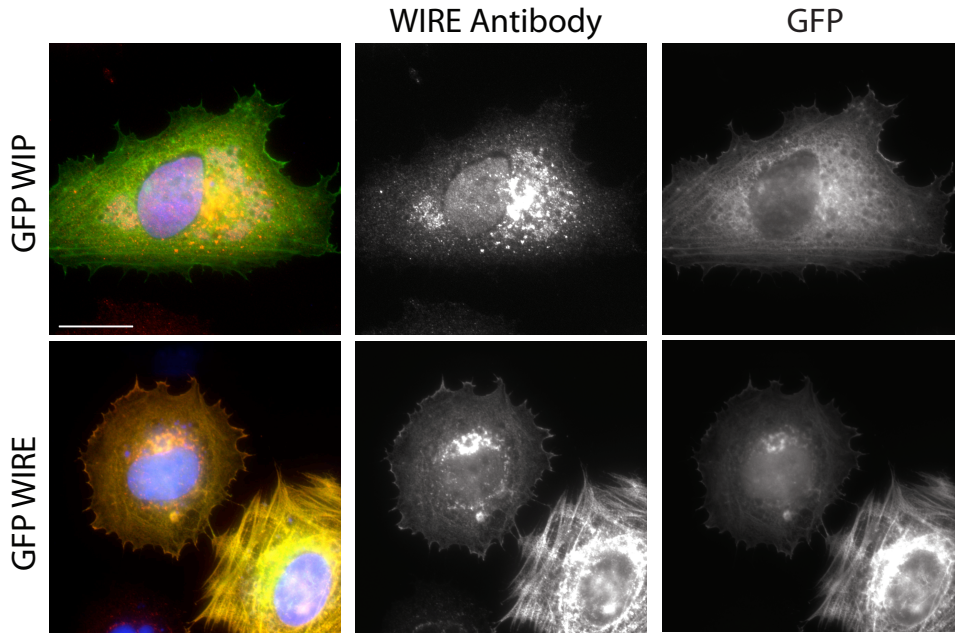

Figure 3.3. The WIRE antibody is specific.

Immunofluorescence images showing that the WIRE antibody specifically co-localises with GFP WIRE but not GFP WIP expressed in HeLa cells. Scale bar = 10μm.

3.2.1 WIRE can functionally replace WIP in actin tail formation

WIP is a member of the verprolin family of proteins, which in humans comprises two other members – WIRE/WICH and CR16. The expression of CR16 is largely restricted to the brain, heart, lungs, colon and testes, while WIRE, like WIP, is ubiquitously expressed (Aspenstrom, 2002; Ho et al., 2001; Kato et al., 2002; Ramesh et al., 1997). WIRE is a proline rich protein that shares ~40% sequence identity with WIP (Figure 3.2 A). A region of very high similarity is found in the C-terminus of the proteins. In both WIP and WIRE, this domain has been shown to bind N-WASP and thus is named the WASP binding domain (WBD) (Kato et al., 2002; Martinez-Quiles et al., 2001). WIP and WIRE both contain several potential SH3-domain binding sites and have been shown to bind to Nck (Anton et al., 1998; Aspenstrom, 2002). Due to the similarities in domain organisation, I hypothesised that WIRE might functionally replace WIP in actin tail formation. Immunofluorescence analysis reveals that endogenous WIRE is localised beneath actin tail inducing virus particles in WIP-/- cells (Figure 3.2 B). WIRE is also

localised to virus particles in WT cells, however the localisation is much more robust in the absence of WIP. This suggests that WIRE does not compete efficiently with WIP for recruitment to vaccinia virus. Staining cells that were expressing GFP-WIP or GFP-WIRE confirmed the specificity of WIRE antibody. The WIRE antibody specifically co-localised with the GFP-WIRE but not the GFP-WIP signal (Figure 3.3).

To determine whether the actin tails seen in WIP-/- cells are dependent on WIRE, iI depleted WIRE using two independent siRNA oligonucleotides. Immunofluorescence analysis showed that in the absence of both WIP and WIRE, vaccinia virus induces significantly fewer actin tails (Figure 3.4 A, C). The efficiency of knockdown was assessed by immunoblot analysis of lysates from cells transfected with either WIRE siRNA or a control non-targeting siRNA. WIRE expression was significantly reduced in siRNA-treated cells after 72 hours (Figure 3.4 B). I did not observe a decrease in N-WASP expression in these cells in the absence of WIP and WIRE (Figure 3.4 B). This suggests that the expression of WIP or WIRE is not required to prevent the degradation of N-WASP by calpain and the proteosome, as is the case for WASP (de la Fuente et al., 2007). The number of cells with actin tails was reduced from 90.75 ± 2.7 % in control cells to 18.76 ± 9.0% and 20.67 ± 8.2% in cells treated with each of the siRNA oligonucleotides targeting WIRE (Figure 3.4 C). In addition the number of actin tails per cell dropped from an average of 40.64 ± 2.26 actin tails per cell in the control, to 4.85 ± 1.01 or 3.49 ± 0.87 tails per cell in the absence of WIRE, with the majority of WIRE depleted cells lacking actin tails (Figure 3.4 C). A similar amount of extra-cellular virus was observed in control and RNAi treated cells, indicating that the failure to induce actin tails is specifically due to changes in the vaccinia actin polymerisation complex and not the result of a more general effect on the viral life cycle (Figure 3.4 B and data not shown).

To ensure that the observed consequences of the siRNA depletion of WIRE are specific, I performed a rescue experiment. GFP-tagged human WIP or WIRE were transfected into WIP-/- cells that had been treated with WIRE siRNA. As the WIP-/- cells are derived from mice, siRNA oligonucleotides were chosen that specifically target mouse, but not human, WIRE mRNA. The human WIP construct is also not

targeted by the WIRE siRNA. Expression of either GFP-WIP or WIRE, but not GFP alone, resulted in the rescue of actin tail formation in these cells (Figure 3.5 A). The percentage of cells with actin tails was increased from 14.00 ± 1.50% in cells transfected with GFP alone to 88.00 ± 1.52% or 85.00 ± 0.58% in cells transfected with GFP-WIP and GFP-WIRE, respectively (Figure 3.5 B). Actin tails in WIRE siRNA treated cells transfected with GFP-WIRE measured 1.25 ± 0.03μm in length. This is similar to the length of actin tails seen in WIP-/- cells that had been treated with the control siRNA and transfected with GFP alone (1.17 ± 0.03μm). This indicates that the shorter actin tails seen in WIP-/- cells are dependent on WIRE. Expression of GFP-WIP in WIP-/- cells treated with WIRE siRNA resulted in actin tails measuring 2.23 ± 0.04μm in length. This is significantly longer than the actin tails induced by GFP-WIRE, although not as long as those seen in the WT cells (Figure 3.2A). This difference in length may be the result of differences in expression levels of WIP in the WT cell line and in those cells rescued with GFP-WIP or because the GFP tag slightly interferes with the function of the protein. Treatment of the cells with siRNA or transfection with DNA may also result in slight toxicity that impairs the formation of actin tails. Another possibility arises from the observation that WIRE is weakly recruited to virus particles in WT cells. This indicates that both WIP and WIRE may act in actin tail formation in this case. The presence of a mixture of different complexes comprising WIP: N-WASP and WIRE: N-WASP at virus particles could result in differences in actin polymerisation that are not observed in WIRE depleted WIP-/- cells rescued with GFP-WIP. To test this hypothesis and to determine whether WIRE plays an important role in actin tail formation in the presence of WIP, WIRE was depleted in the WT cell line. No difference was observed in the percentage of infected cells inducing actin tails or in the length of the actin tails in these cells (Figure 3.6 A, B, C). This shows that WIRE is only essential for actin tail formation in the absence of WIP and that its recruitment to virus particles does not interfere with WIP dependent actin polymerisation.

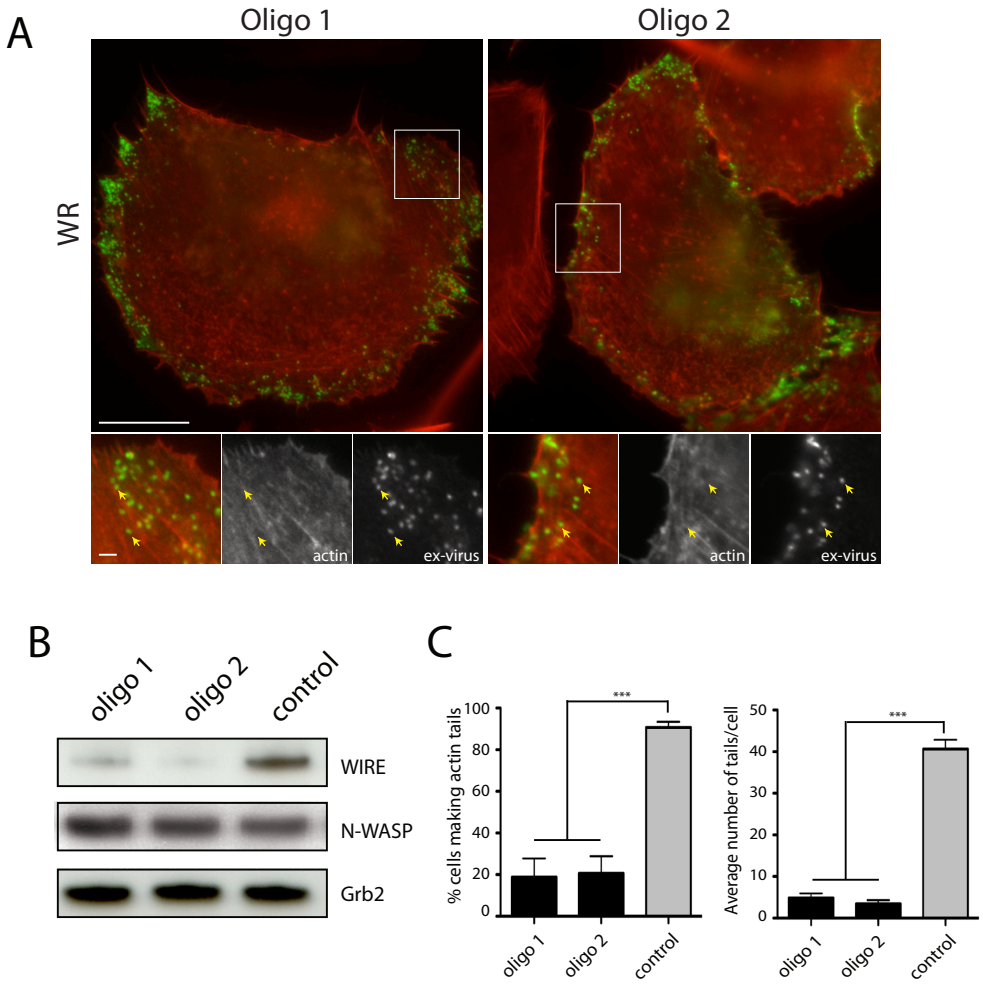

Figure 3.4. Depletion of WIRE in WIP-/- cells results in the loss of actin tail formation.

(A) Immunofluorescence images showing that actin tails are not induced in WR infected WIP-/- cells treated with two independent oligos targeting WIRE. The higher magnification panels correspond to the boxes in the main panels. Scale bars = 20 and 2 μm. **(B)** Immunoblot analysis with the indicated antibodies (right) showing the level of WIRE after siRNA treatment with the indicated WIRE oligos (top). Knockdown of WIRE does not affect levels of N-WASP. Grb2 is used as a loading control. **(C)** WR can induce actin tail formation in less than less than 20% of WIP-/- cells that have been treated with WIRE siRNA (black bars) compared with 90% of control cells (grey bars) (left panel). The WR infected WIP-/- cells lacking WIRE that make tails have an average of 3-4 actin tails per cell (right panel). Error bars represent the SEM of 3 independent experiments. *** = $p<0.001$.

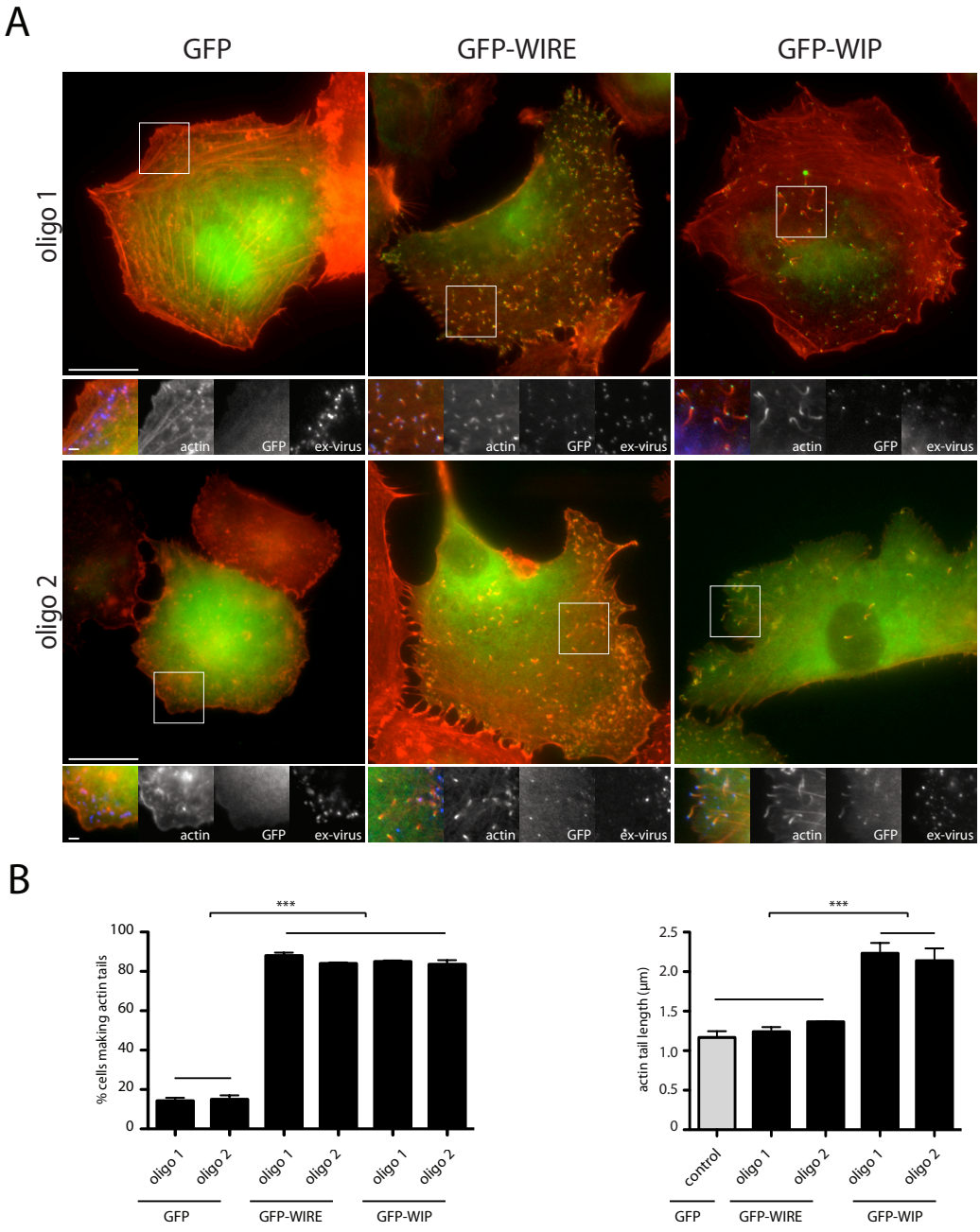

Figure 3.5. Expression of GFP-WIP or GFP-WIRE rescues actin tails in WIP-/- cells treated with WIRE siRNA.

(A) Images show GFP-WIRE or GFP-WIP, but not GFP, rescue WR actin tail formation in WIP-/- cells, in which endogenous WIRE has been depleted. Scale bars = 20 and 2 µm. **(B)** Graph shows that expression of GFP-WIRE or GFP-WIP in WIP-/- cells lacking endogenous WIRE rescues actin tail formation to similar levels (left panel). Actin tails induced by GFP-WIP are longer than those induced by GFP-WIP (right panel). Error bars represent SEM of 3 independent experiments. ***=p<0.001 as determined by a one way Anova.

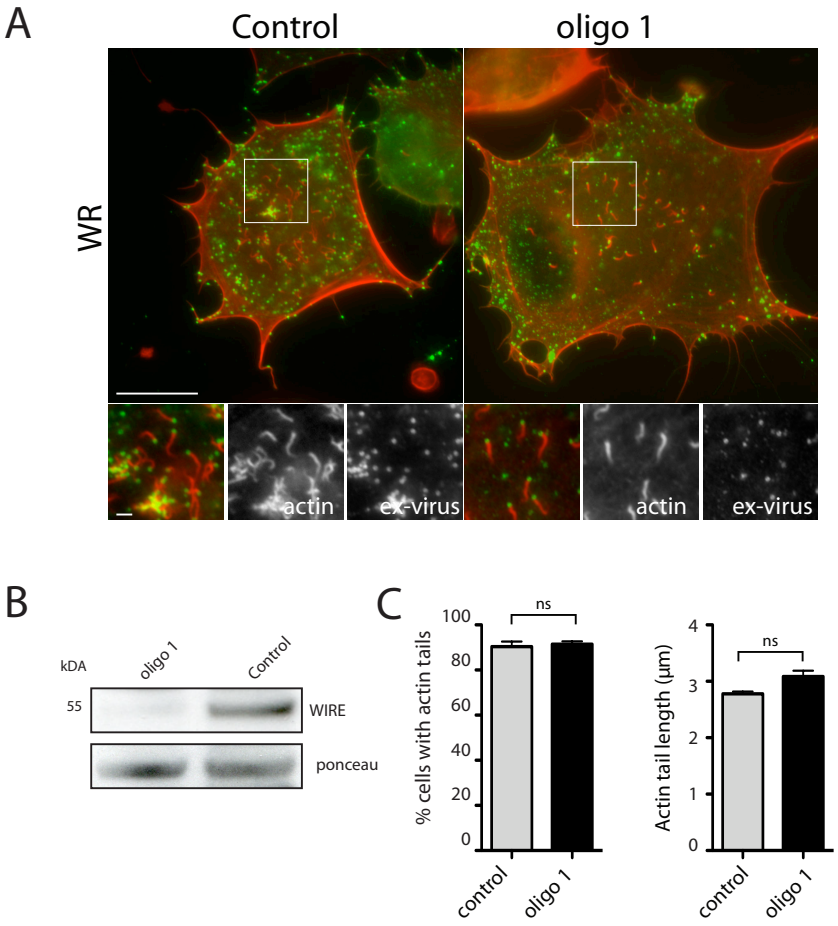

Figure 3.6. WIRE is not required for actin tail formation if WIP is present

(A) Immunofluorescence images show that actin tails are similar in WR infected WT cells treated with control or WIRE siRNA. Scale bars = 20 and 2 µm. **(B)** Immunoblot analysis showing that WIRE is depleted in WT cells after 72 hours. **(C)** No difference in the percentage of WR infected WT cells inducing actin tails (left panel) or the length of actin tails (right panel) is observed in control (grey bars) or WIRE knock down (black bars) conditions. Error bars represent the SEM of 3 independent experiments. ns = not significant.

3.2.2 WIRE is less stable than WIP

Despite the similarities between WIP and WIRE, they have different effects on actin tails. WIRE dependent actin tails are shorter and move more slowly than actin tails in cells expressing WIP (Figure 3.2). To gain further insight into the functioning of WIP and WIRE, I decided to investigate the dynamics of these proteins. FRAP (Fluorescence recovery after photobleaching) was used for this analysis. This technique is used to determine the mobility of a protein in a cell. FRAP experiments are carried out by bleaching the signal from a fluorescently tagged protein in a small region of the cell and monitoring the recovery of this signal over time. A lack of recovery indicates that the protein exists in an immobile pool as the photobleached population does not dissociate and therefore the remaining fluorescent population cannot replace it. The rate of recovery of the fluorescent signal gives a measurement of the dynamic behaviour of the protein of interest. This type of analysis has previously been used to show that the components of the vaccinia virus actin polymerisation complex are very dynamic and that the speed of actin tails is dependent on the rate of exchange of N-WASP at the virus particle (Weisswange et al., 2009).

To carry out FRAP experiments WIP-/- cells in which WIRE had been depleted were infected with WR/RFP-A3 virus. Cells were transfected with the GFP tagged construct of interest five hours post infection and FRAP was carried out four hours later. Images were acquired on a spinning disc confocal microscope, with one image acquired every ~300ms. The GFP signal was bleached using 5 iterations of the 488 laser at 100% power, which resulted in a post-bleach intensity of approximately 30% (Chapter 2.9.4). Analysis of the dynamics of GFP-WIP showed that the half-time of fluorescence recovery was 0.93 ± 0.06 seconds (Figure 3.7 A). The rate of exchange was previously measured in the presence of endogenous WIP in HeLa cells and a similar rate of exchange was observed (0.77 ± 0.06) (Weisswange et al., 2009). Interestingly, the half-time of recovery of WIRE was measured at 0.41 ± 0.03 seconds, indicating that WIRE is less stable in the vaccinia virus actin polymerisation complex than WIP (Figure 3.7 A). The fluorescence intensity of WIP and WIRE recovered to 94.5 ± 0.7 and 93.7 ± 0.5%, respectively. This indicates that neither protein maintains an immobile population at

the virus particle. Although this recovery is not quite 100%, it is likely that this is due to minor photo-damage over the course of the movie. It was not possible to correct for this because it was necessary to acquire a small area to facilitate fast imaging and accurate bleaching of virus particles. This means that a reference point that could be used to correct for photo-damage was lacking.

The speed of actin-based motility of vaccinia virus being propelled by WIP- or WIRE-dependent actin tails was also measured (Figure 3.7 B). Experiments were carried out in the same manner as the FRAP experiments. As GFP-WIP and WIRE are localised to the tips of actin tails, speeds of actin-based motility were determined by tracking only those RFP-tagged virus particles that co-localised with a GFP signal. Images were acquired on a spinning disc confocal at rate of one image per second and particles were tracked for 30 seconds (Chapter 2.9.3) Actin tails in cells expressing GFP-WIP moved at an average speed of 0.15 ± 0.01 μm/s, while in cells expressing GFP-WIRE, the actin tails moved slightly faster at 0.16 ± 0.01 μm/s. These speeds are slightly faster than those measured in the WT and WIP-/- cell lines (Figure 3.1). In addition, little difference is observed between the GFP-WIP and GFP-WIRE induced actin tails. As with the difference in tail length observed in the WT cells when compared to the rescued knockout cells (Section 3.2.1), the differences in speed may be due differences in the expression levels of endogenous protein compared to the GFP-tagged protein, because the presence of the GFP-tag interferes with the function of the protein or because of the treatment of the cells with transfection reagents.

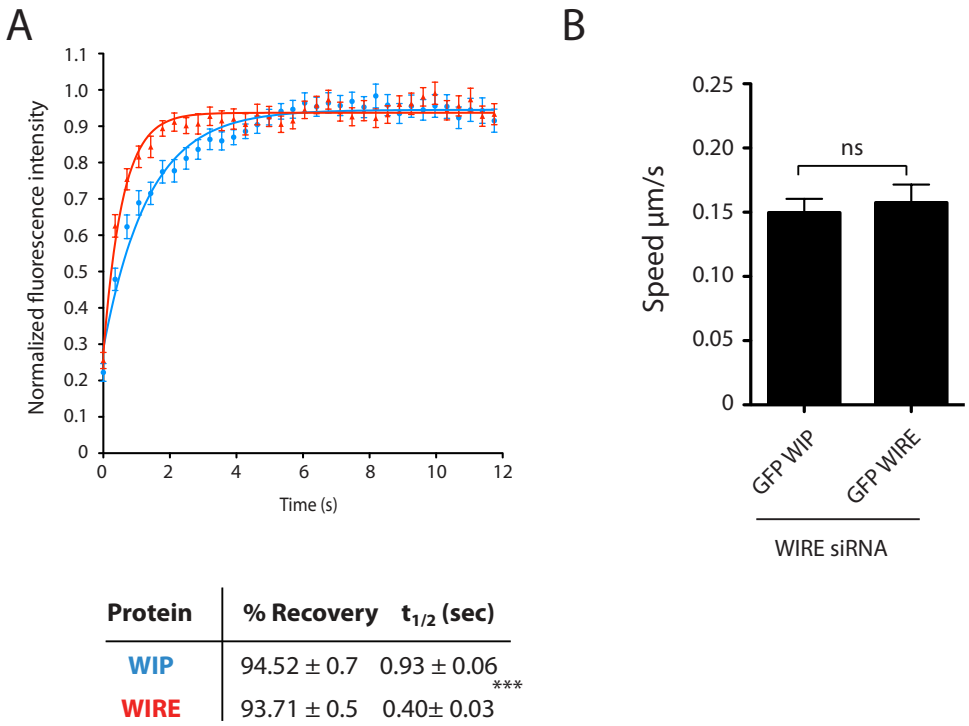

Protein	% Recovery	$t_{1/2}$ (sec)
WIP	94.52 ± 0.7	0.93 ± 0.06 ***
WIRE	93.71 ± 0.5	0.40± 0.03

Figure 3.7. WIRE is less stable than WIP

(A) The graph shows the normalized intensity values for WIP (blue) or WIRE (red) over time. Best fit curves are also shown for each protein. Comparison of the recovery kinetics of GFP-WIP or WIRE in WR infected WIP-/- cells lacking WIRE reveals that WIRE has a more rapid rate of exchange than WIP. n = 43 from 3 independent experiments. **(B)** Actin tails in WR infected WIP-/- cells treated with WIRE siRNA and expressing GFP-WIP or GFP-WIRE have similar speeds. Error bars represent the SEM of three independent experiments. ns = not significant. *** = p<0.001

3.2.3 Grb2 co-operates with WIP, but not WIRE to enhance actin tail formation

Grb2 enhances actin tail formation by stabilising the rate of exchange of Nck, WIP and N-WASP in the vaccinia virus actin polymerisation complex (Weisswange et al., 2009). To gain further insight into the function of WIP, we investigated the formation of actin tails in WIP-/- cells using a virus that cannot recruit Grb2 (A36-Y132F). This virus contains a point mutation, which replaces tyrosine 132 of A36 with a phenylalanine, rendering it deficient in phosphorylation by Src and Abl family kinases during infection (Newsome et al., 2004; Newsome et al., 2006; Scaplehorn et al., 2002). Infection of WT cells with the A36-Y132F virus resulted in the formation shorter and slower moving actin tails than those formed in WR infections (Figure 3.8 A, B and Figure 3.2 B). However, in WIP-/- cells A36-Y132F induced actin tails were a similar length and moved at a similar speed to the WR induced actin tails (Figure 3.8 A, B and Figure 3.2 B). Thus, loss of Grb2 recruitment impacts on WIP dependent but not WIRE dependent actin tails. (Figure 3.8 A, B).

As expected, siRNA of WIRE in these cells resulted in much less actin tail formation during A36-Y132F infection (Figure 3.9 A, B). The percentage of cells with actin tails is 7.00 ± 0.58 in WIRE siRNA treated cells, which is fewer than those seen in WIRE knockdown cells in WR infection (18.76 ± 9.0% and 20.67 ± 8.2%) (Figure 3.4 C). This agrees with previous data showing that fewer actin tails are induced during A36-Y132F infection (Scaplehorn et al., 2002). This more dramatic phenotype reinforces the evidence that Grb2 acts to stabilise the vaccinia virus actin polymerisation complex.

Actin tail formation was rescued by ectopic expression of either GFP-WIP or WIRE. In this case, the actin tails induced by GFP-WIP expression measured 1.29 ± 0.15μm, which is similar to the length of the actin tails seen in either WIP-/- cells treated with control siRNA (1.18 ± 0.14μm), or knockdown cells rescued with GFP-WIRE (1.38 ± 0.19 μm) (Figure 3.9 A, B). FRAP analysis of GFP-WIP and WIRE in WIP-/- cells treated with WIRE siRNA, revealed that in the absence of Grb2 recruitment to virus particles, WIP is more dynamic, with a half-time of recovery of 0.56 ± 0.04 seconds. In contrast, the rate of exchange of WIRE is similar, although

slightly slower, to the value measured during WR infection with a half-time of 0.55 ± 0.04 (Figure 3.7 A, 3.10 A). The maximum fluorescence recovery of WIP was 96.69 ± 0.6%, which is similar to that measured in WR infected cells (Figure 3.7 A). However, GFP-WIRE was found to recover less than in WR infected cells, with the maximum fluorescence recovery in A36-Y132F infected cells measuring 88.95 ± 0.5% compared to 93.71 ± 0.5% during WR infection. One reason for this may be increased photo-damage in this sample. However, previous data has shown that WIP does not recover in the absence of active actin polymerisation (Weisswange et al., 2009). Due to the similarities between WIP and WIRE it is likely that the recovery of WIRE would also be affected by differences in actin polymerisation. Thus this defect in WIRE recovery, in the absence of Grb2 recruitment, may indicate that there is less active actin polymerisation occurring at virus particles.

The speed of both WIP and WIRE dependent actin tails was also similar having average velocities of 0.19 ± 0.01μm/s and 0.18 ± 0.04μm/s, respectively (Figure 3.10B). An increased speed of actin tails during A36-Y132F infection has previously been observed (Weisswange et al., 2009). My data shows that the increase in actin-based motility in the absence of Grb2 recruitment is greater in WIP dependent actin tails (1.3 fold) than in actin tails induced by WIRE (1.1 fold) (compare Figure 3.7 B and 3.10B). Once again, the loss of Grb2 recruitment affects the WIP dependent actin tails more than the WIRE dependent actin tails. This results in the WIP and WIRE dependent actin tails exhibiting similar characteristics in the absence of Grb2. Taken together, my data suggests that Grb2 co-operates with WIP but not WIRE to induce actin tail formation.

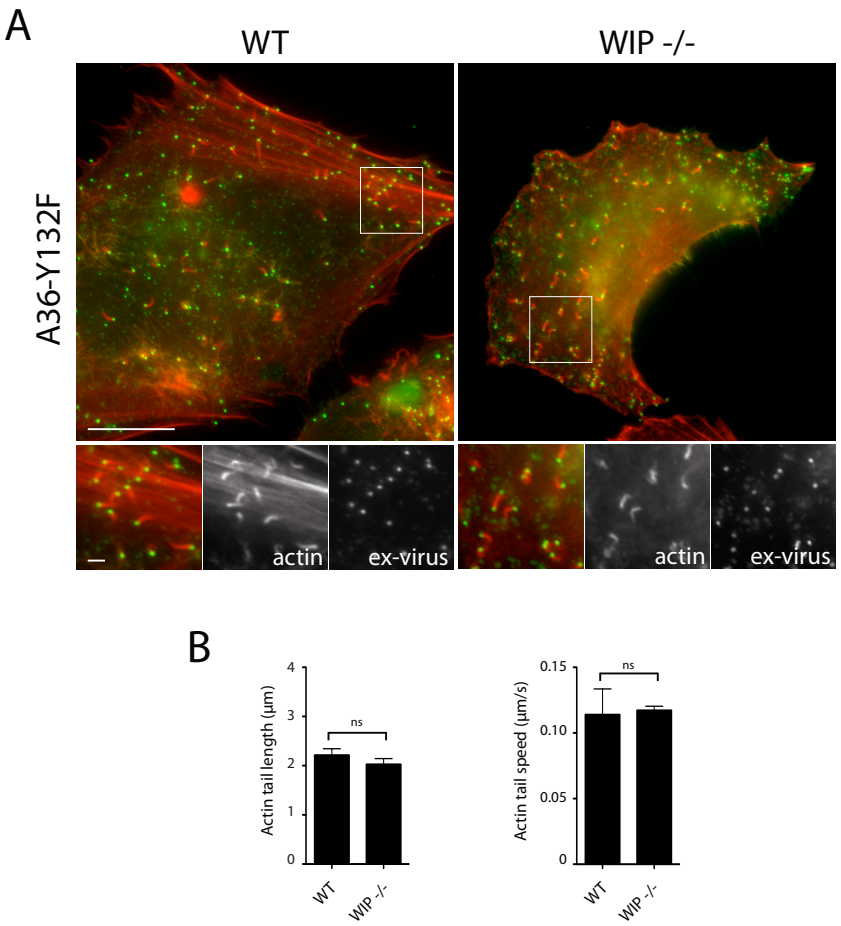

Figure 3.8. Lack of Grb2 recruitment results in shorter actin tails in WT but not WIP-/- cells

(A) Immunofluorescence images showing the formation of actin tails in both WIP-/- and WT cells infected with the A36-Y132F virus, which cannot recruit Grb2. Higher magnification panels correspond to the boxes in the main panels. Scale bars = 20 and 2 µm. **(B)** In WT and WIP-/- cells infected with the A36-Y132F virus, actin tails are the same length (left panel). In the absence of Grb2 recruitment, virus particles in both WT and WIP-/- cells exhibit similar rates of actin-based motility (right panel). Error bars represent the SEM from 3 independent experiments in which 50 actin tails from 5 cells were tracked. ns = not significant

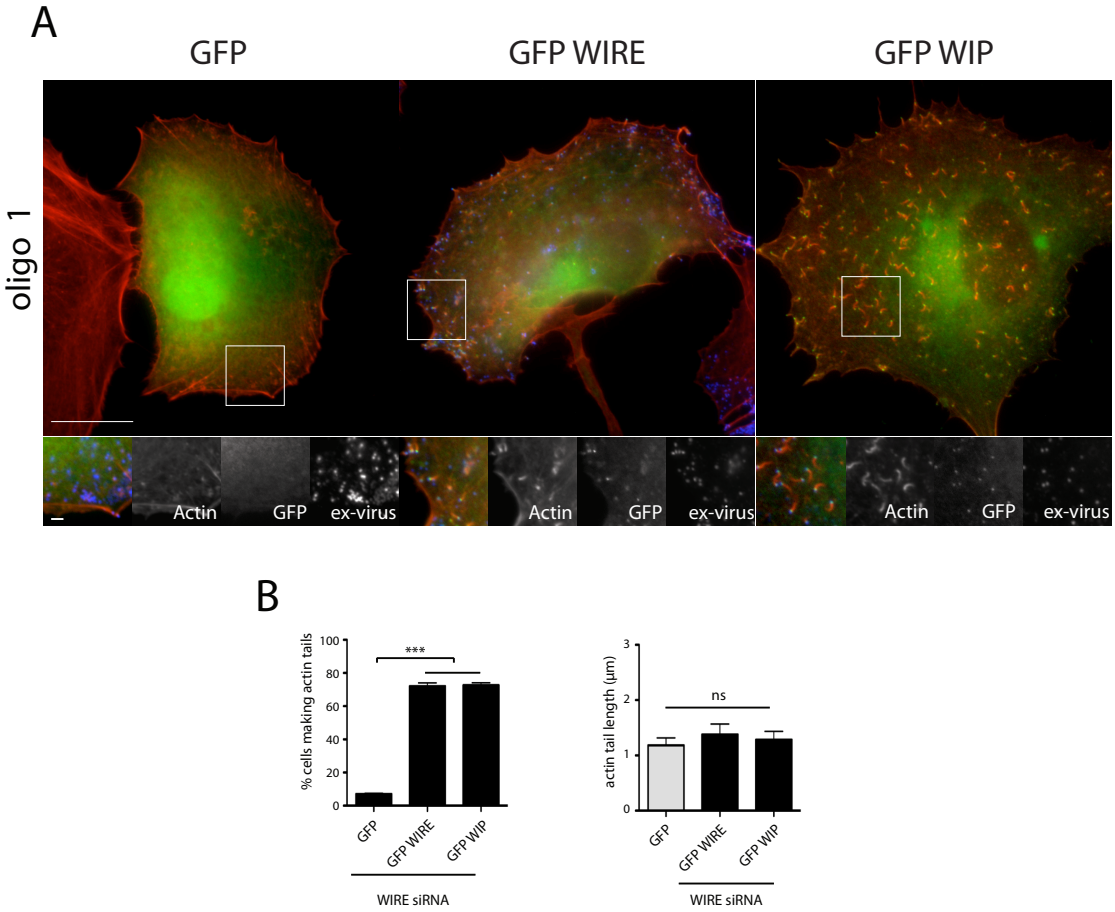

Figure 3.9. In the absence of Grb2 recruitment, actin tails are similar lengths in cell expressing either GFP-WIP or GFP-WIRE

(A) Images show that GFP-WIRE or GFP-WIP, but not GFP, can rescue actin tail formation in WIP-/- cells lacking WIRE during infection with the A36-Y132F virus. The higher magnification panels correspond to the boxes in the main panels. Scale bars = 20 and 2 µm. **(B)** Graph shows that expression of GFP-WIRE or GFP-WIP in WIP-/- cells lacking endogenous WIRE rescues actin tail formation to similar levels (left panel). In the absence of Grb2 recruitment, actin tails induced by GFP-WIP are the same length as those induced by GFP-WIRE in WIRE depleted (black bars) or as control siRNA treated (grey bars) WIP-/- cells expressing GFP (right panel). Error bars represent SEM of 3 independent experiments. *** = $p<0.001$; ns=not significant.

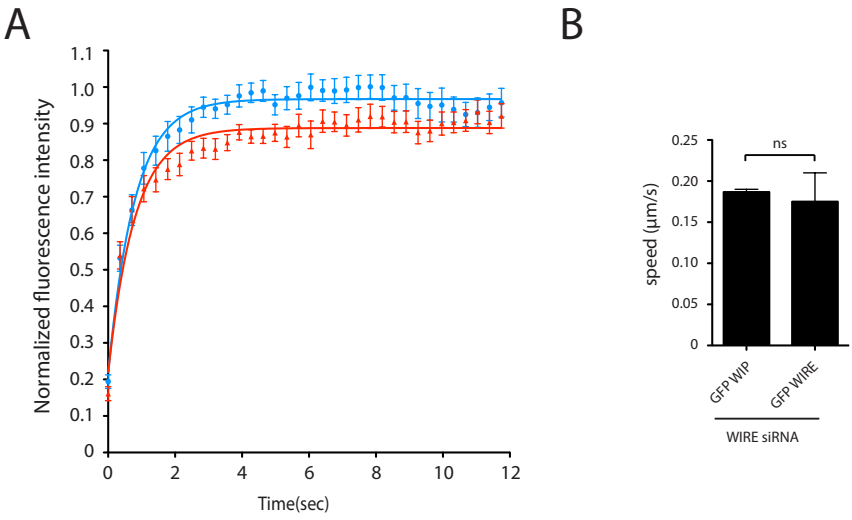

Protein	% Recovery	$t_{1/2}$ (sec)
WIP	96.69 ± 0.6	0.56 ± 0.04
WIRE	88.95 ± 0.5	0.55 ± 0.04

Figure 3.10. WIP and WIRE have similar dynamics in the absence of Grb2 recruitment

(A) The graph shows the normalized intensity values for WIP (blue) or WIRE (red) over time. Best fit curves are also shown for each protein. Comparison of the recovery kinetics of GFP-WIP or WIRE in A36-Y132F infected WIP-/- cells lacking WIRE, reveals that WIP and WIRE have similar rates of exchange. n = 41 (WIP) and 48 (WIRE) from 3 independent experiments. **(B)** Actin tails in WR infected WIP-/- cells treated with WIRE siRNA and expressing GFP-WIP or GFP-WIRE have similar speeds. Error bars represent the SEM of three independent experiments. ns = not significant.

3.3 Localisation of Nck, N-WASP and Grb2 to virus particles in the absence of WIP

Previous studies in N-WASP-/- cells have indicated that Nck is localised to virus particles in the absence of the other members of the actin polymerisation complex (Weisswange et al., 2009). However, the localisation of WIP and Grb2 was shown to depend on the presence of N-WASP (Weisswange et al., 2009). In addition, N-WASP constructs lacking the WIP interacting WH1 domain, were not localised to actin tails in HeLa cells (Moreau et al., 2000). This data suggests that WIP and N-WASP are recruited to virus particles as a complex. To further investigate this hypothesis and determine if the recruitment of the other members of the vaccinia actin polymerisation complex is dependent on WIP, I examined the localisation of Nck, N-WASP and Grb2 in both WT and WIP-/- cells.

As expected, during WR infection of WT cells, endogenous Nck and N-WASP were robustly recruited to actin tails (Figure 3.11 A, B). The localisation of endogenous Grb2 could not be verified, as an antibody that worked well for immunofluorescence was not available. However GFP-Grb2 was recruited to actin tails (Figure 3.11 C). Nck and N-WASP were also recruited to actin tails in WT cells during infection with A36-Y132F virus, while Grb2 was not (Figure 3.12 A, B, C). As expected, no difference in the localisation of Nck, N-WASP or Grb2 was observed in either viral background when WIRE was depleted in these cells (Figures 3.11, 3.12 A, B, C).

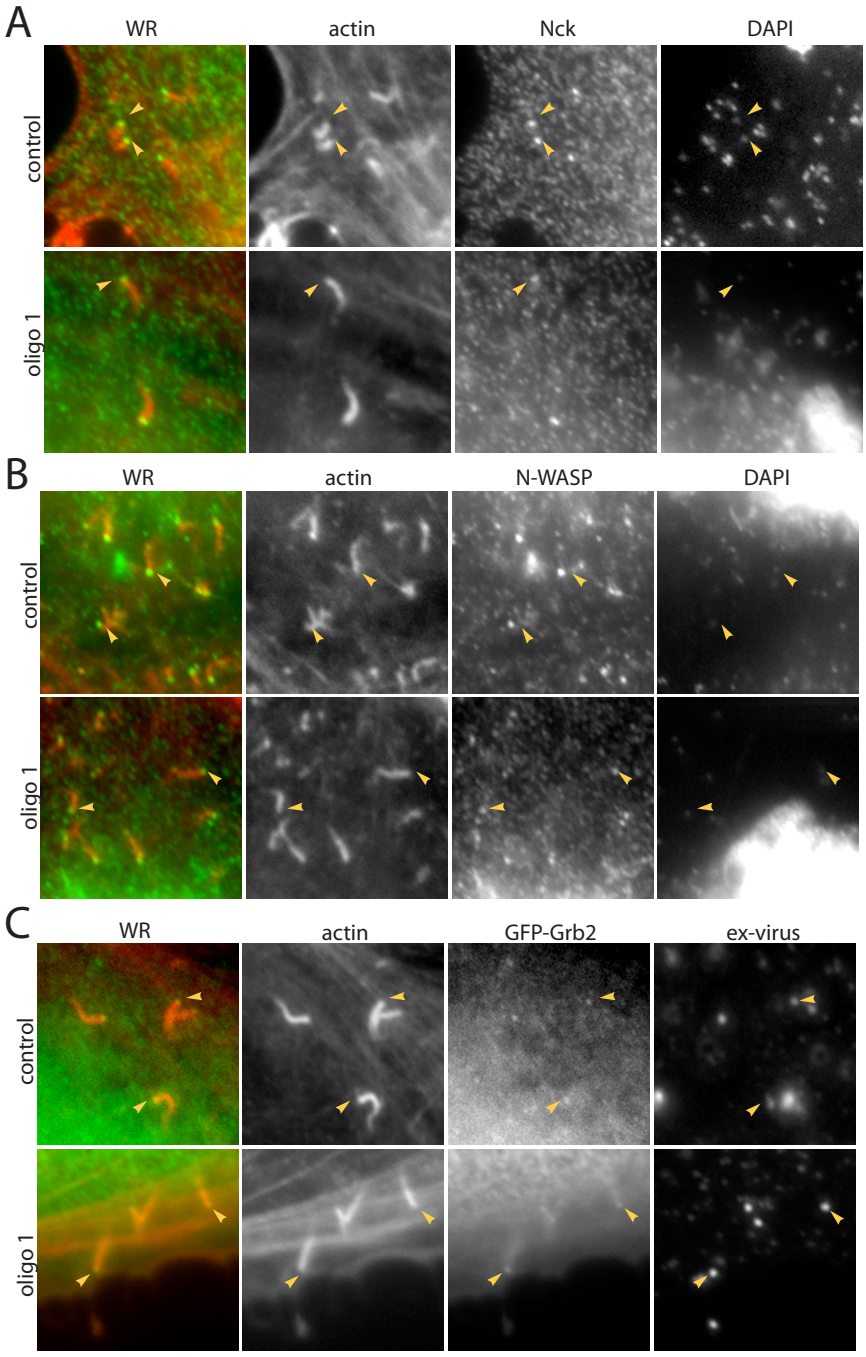

Figure 3.11. Localisation of Nck, N-WASP and Grb2 to actin tails in WT cells

Immunofluorescence images reveal that endogenous Nck (A), endogenous N-WASP (B) and GFP-Grb2 (C) are localised to actin tails in WT cells infected with WR. Treatment of WT cells with WIRE siRNA does not affect the localisation of Nck, N-WASP or GFP-Grb2 (A, B, C lower panels). Scale bar = 2 μm.

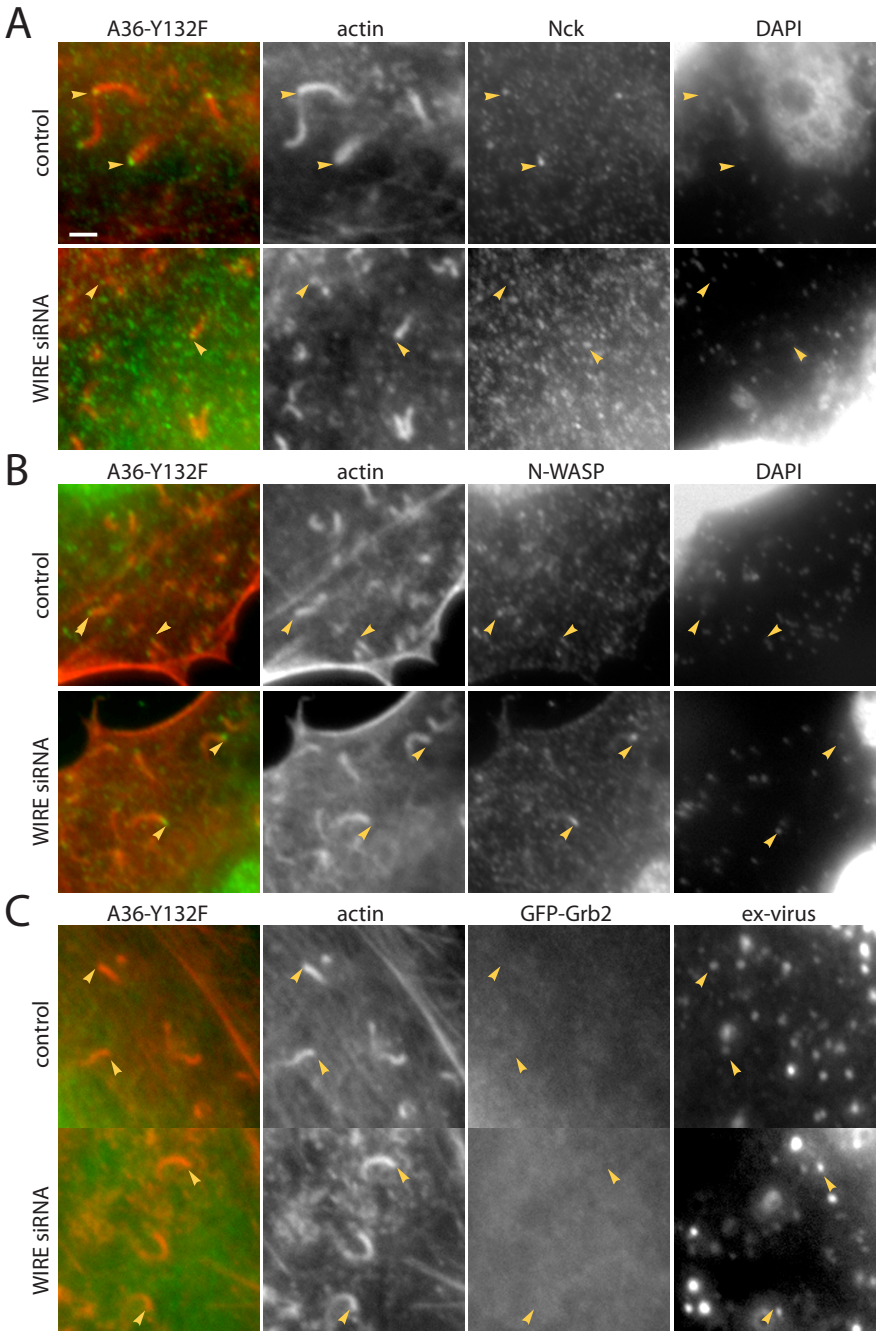

Figure 3.12. Localisation of Nck and N-WASP to WT cells in the absence of Grb2

Immunofluorescence images reveal that endogenous Nck (A), endogenous N-WASP (B) but not GFP-Grb2 (C) are localised to actin tails in WT cells infected with the A36-Y132F virus. Treatment of WT cells with WIRE siRNA does not affect the localisation of Nck, N-WASP or GFP-Grb2 (A, B, C lower panels). Scale bar = 2 μm.

Nck, N-WASP and GFP-Grb2 were robustly localised to the tips of actin tails in WIP-/- cells treated with control siRNA, further demonstrating that WIRE functionally replaces WIP in actin tail formation (Figure 3.13 A, B, C). As expected, actin tails were not observed in WIP-/- cells treated with WIRE siRNA. Virus particles were stained with DAPI and the localisation of Nck and N-WASP was examined. DAPI was used as a marker for virus particles to minimize the chances of cross-reactivity, particularly between the B5 and N-WASP antibodies, as both were raised in rat. As expected from the experiments in N-WASP-/- cells, Nck was recruited to virus particles in cells lacking expression of both WIP and WIRE (Figure 3.13 A). This data confirms that Nck is recruited to virus particles independently of both WIP and N-WASP.

N-WASP was not recruited to virus particles in the absence of WIP and WIRE (Figure 3.13 B). Occasionally, N-WASP was observed localised to a few virus particles (~5% of virus particles compared with 30% in control cells, data not shown). This recruitment was very weak compared to that seen in the control and is probably due to incomplete depletion of WIRE in the WIP-/- cells. Alternatively, the interaction of Nck with N-WASP could mediate this recruitment. However, it is clear that the major pathway of N-WASP recruitment is dependent on WIP. This suggests that WIP and N-WASP are recruited to virus particles as a complex. In addition, GFP-Grb2 was not localised to virus particles in WIP-/- cells treated with WIRE siRNA (Figure 3.13 C). This is consistent with data showing that recruitment of Grb2 is dependent on an interaction with the proline rich region of N-WASP (Scaplehorn et al., 2002). In the absence of Grb2 recruitment, robust localisation of Nck was still observed at virus particles (Figure 3.13 A). As expected, neither N-WASP nor Grb2 were recruited to virus particles during A36-Y132F infection (Figure 3.13 B, C).

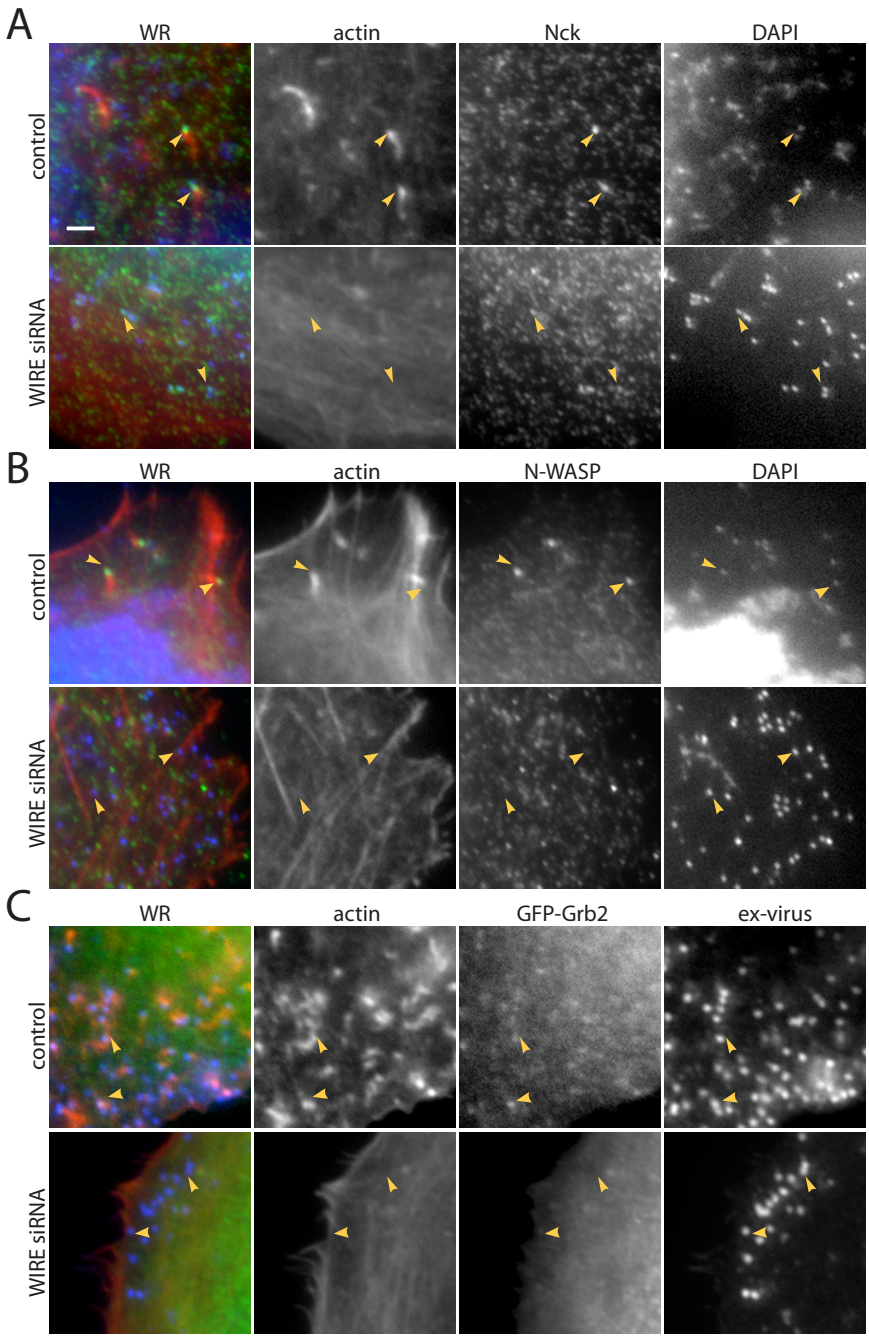

Figure 3.13. Nck but not N-WASP or Grb2 is localised to virus particles in the absence of WIP and WIRE

Immunofluorescence images reveal that endogenous Nck (A), endogenous N-WASP (B) and GFP-Grb2 (C) are localised to actin tails in WR infected WIP-/- cells. Treatment of WIP-/- cells with WIRE siRNA does not affect the localisation of Nck, but N-WASP and GFP-Grb2 are no longer observed at virus particles which are stained with DAPI or the B5 antibody (A, B, C lower panels). Scale bar = 2 μm.

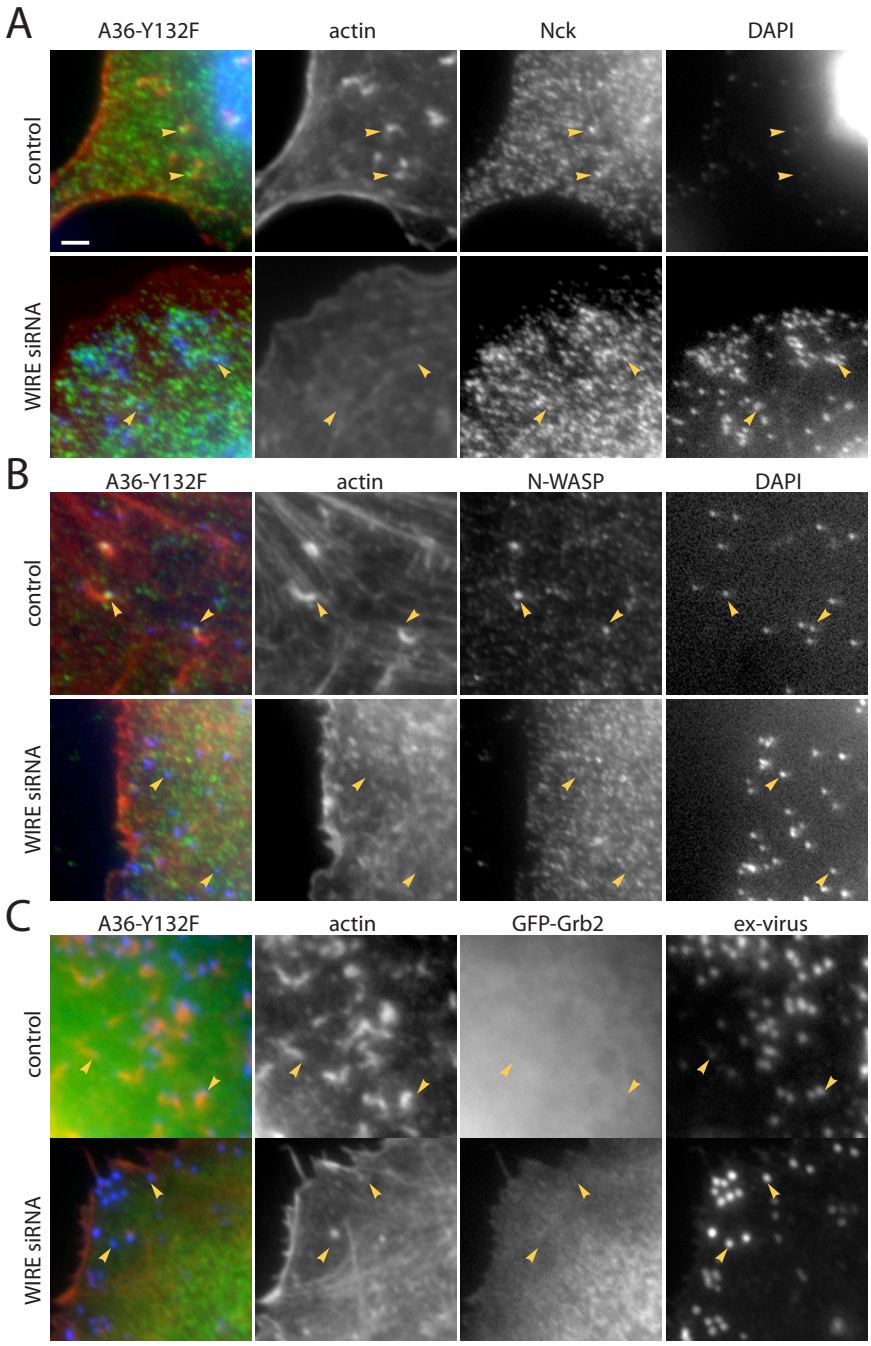

Figure 3.14. Nck is localised to virus particles in the absence of Grb2, WIP and WIRE

Immunofluorescence images reveal that endogenous Nck (A), endogenous N-WASP (B) but not GFP-Grb2 (C) are localised to actin tails in A36-Y132F infected WIP-/- cells. Treatment of WIP-/- cells with WIRE siRNA does not affect the localisation of Nck, but N-WASP and GFP-Grb2 are no longer observed at virus particles which are stained with DAPI or the B5 antibody (A, B, C lower panels). Scale bar = 2 μm.

3.4 Summary

The role of WIP in vaccinia virus actin tail formation has previously been unclear. I have now demonstrated that WIP is essential for actin tail formation, although the related protein WIRE can compensate for the loss of WIP in actin tail formation. I have also shown that neither WIP nor WIRE is required to maintain a stable pool of N-WASP expression in cells. In addition, the rate of exchange of WIP in the absence of endogenous protein was found to agree with values previously measured in HeLa cells (Weisswange et al., 2009). I found that WIRE is less efficient than WIP in inducing actin polymerisation, most likely as a result of its faster rate of exchange in the vaccinia actin polymerisation complex. WIP induced actin tails are sensitive to the loss of Grb2 recruitment during A36-Y132F infection, however WIRE dependent tails are unaffected. This suggests that Grb2 acts to stabilise WIP, but not WIRE, possibly via a direct interaction with WIP. I have also shown that the localisation of Nck to virus particles is not dependent on WIP or WIRE. However, in the absence of WIP and WIRE, neither N-WASP nor Grb2 are efficiently recruited to virus particles. This is consistent with WIP and N-WASP being recruited as a complex.

In the next chapter, I will further investigate the role of WIP by determining the function of its interactions with other members of the vaccinia virus actin polymerisation complex.

Chapter 4. WIP links Nck and N-WASP during vaccinia induced actin tail formation

4.1 Introduction

In the previous chapter, I showed that in the absence of WIRE, WIP is essential for actin tail formation. However, exactly how WIP promotes actin tail formation remains elusive. WIP interacts with Nck and N-WASP, both of which play essential roles in the formation of actin tails. Therefore, I hypothesised that understanding the functions of these interactions would give insights into role of WIP in actin polymerisation. WIP is thought to link Nck and N-WASP in reorganisation of the actin cytoskeleton during rocketing of PIP_2 induced vesicles and in the formation of invadopodia and vaccinia actin tails (Benesch et al., 2002; Moreau et al., 2000; Yamaguchi et al., 2005). However these studies were carried out using dominant negative mutants in cells expressing endogenous WIP. Another study showed that in dendritic cells lacking expression of WIP, WASP was not properly localised to podosomes (Chou et al., 2006). In this chapter, I will take advantage of the WIP-/- cells to dissect the interactions of WIP with both Nck and N-WASP in detail.

4.2 Characterisation of the interaction between WIP and Nck

In order to assess the function of the Nck-WIP interaction in actin tail formation, I set out to define the Nck binding site in WIP. The interaction of Nck and WIP is dependent on the SH3 domains of Nck (Anton et al., 1998). SH3 domains are known to interact with short, linear proline rich motifs, which contain a core PxxP motif (where x is any residue) (Ren et al., 1993; Yu et al., 1994). Residues flanking this minimal binding site confer specificity to these interactions (Weng et al., 1995). WIP is very proline-rich (~30%) and contains multiple potential SH3 domain interacting motifs (Ramesh et al., 1997). To identify potential Nck binding sites in WIP, I performed far-western analysis of a peptide array covering the entire sequence of WIP (Figure 4.1 A, B). The short linear binding motifs favoured by SH3 domains makes them particularly suitable for this type of analysis (Volkmer, 2009).

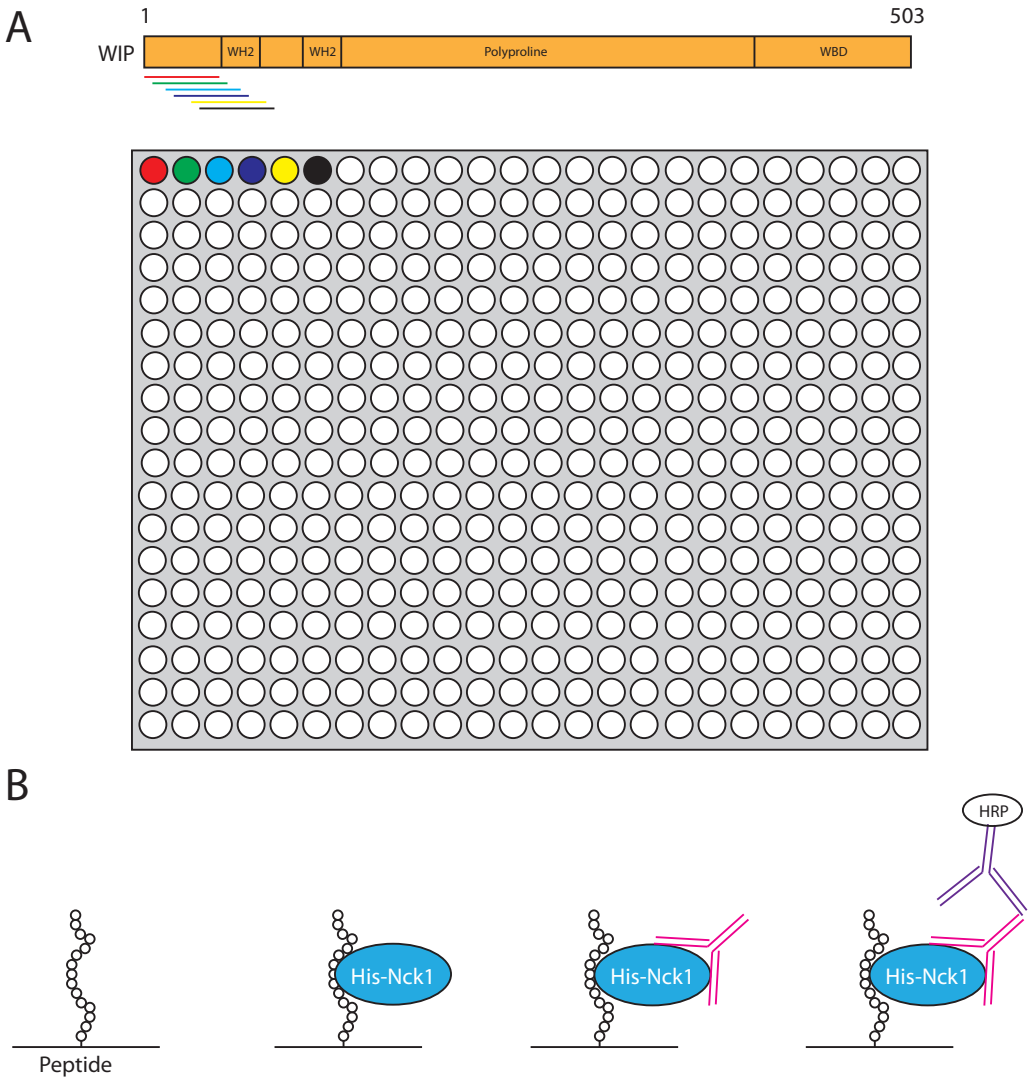

Figure 4.1. Schematic representation of the Far Western Approach used to map the Nck binding site in WIP

(A) Overlapping peptides corresponding to the complete amino acid sequence of WIP were synthesised on a cellulose membrane. Each peptide was 15 residues in length and adjacent peptides were shifted by 3 amino acids. **(B)** The peptide array was probed with His-Nck1 and potential interactions were detected by immunoblot using an anti-His antibody (pink) followed by a secondary antibody conjugated to HRP (purple).

Full-length, His-tagged Nck1 was expressed in BL21 DE3 (Rosetta) *E.coli* and affinity purified using a nickel resin (Chapter 2.7.4) (Figure 4.2 A). A peptide array containing 15-mer peptides shifted by 3 amino acids each time was incubated with 2µg/ml of His-Nck for 1 hour at 4°C and then subjected to immunoblot analysis using an anti-His antibody. Two strong interaction spots were identified (Figure 4.2 B). These potential binding sites both contained the canonical SH3 domain interaction motif – PxxP. More specifically, both peptides contain a PxxPxRxL motif. The presence of an arginine downstream of the PxxP motif is a common specificity determinant in SH3-proline interactions (Lim et al., 1994). To confirm the interaction of these peptides with Nck, I performed pulldowns and found that both peptides retained His-Nck1 from bacterial soluble fraction. Substitution of the two key prolines in the PxxP motif with alanine prevented this interaction (Figure 4.2 C). To verify that these sequences were responsible for the interaction of Nck and WIP in the context of full-length proteins in cells, I carried out immunoprecipitation experiments. GFP-WIP or GFP-WIP mutants, in which the key prolines were substituted with alanine, were immunoprecipitated from HeLa cells. Endogenous Nck bound to GFP-WIP and mutation of the prolines in either of the identified binding sites weakened this interaction. Mutation of both PxxP motifs (GFP-WIP∆Nck) was required to abrogate the interaction of Nck and WIP (Figure 4.3 A). In the same experiment, Nck also bound to GFP-WIRE, confirming previous reports of the interaction between these proteins (Aspenstrom, 2002). In addition, endogenous N-WASP co-immunoprecipitated with GFP-WIP, the WIP mutants and GFP-WIRE (Figure 4.3). Thus N-WASP binds to WIP independently of the interaction of Nck and WIP. Moreover, the presence of N-WASP was not sufficient to mediate Nck recruitment to these complexes in the absence of a WIP:Nck interaction.

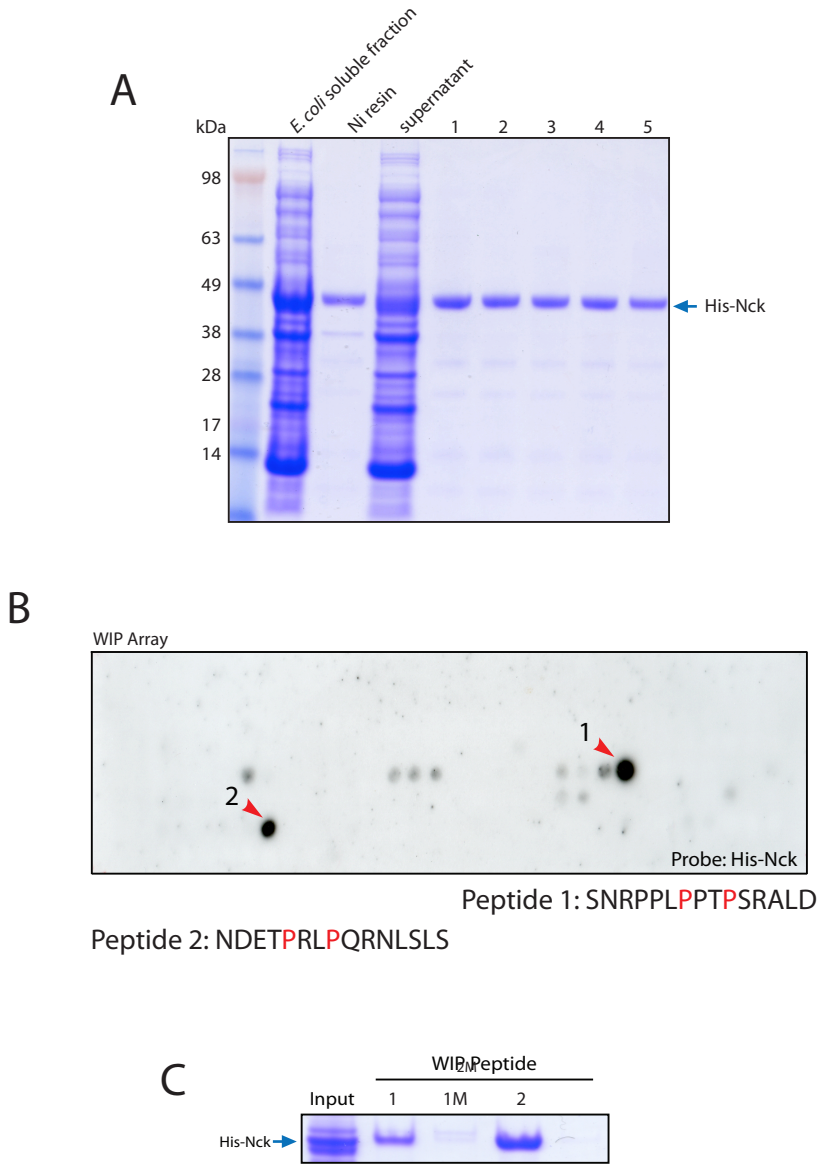

Figure 4.2. Nck1 interacts with two peptides in WIP

(A) Coomassie stained gel showing recombinant His-Nck1 purified from *E.coli* soluble fraction. Supernatant indicates the soluble fraction removed from the resin after binding for 1 hour at 4°C. 1-5 indicates the fractions eluted from the PD-10 desalting column. **(B)** Far western analysis of a peptide array covering the sequence of human WIP. The black spots indicate the peptides that interact with His-Nck1. The sequences of the identified peptides are below the array. Prolines in the canonical SH3 binding PxxPxR motif are indicated in red. **(C)** *In vitro* peptide pull down assay reveals that the peptides identified in the array retain His-Nck1 from bacterial soluble fraction. Mutation of the indicated prolines (red) to alanine disrupts binding.

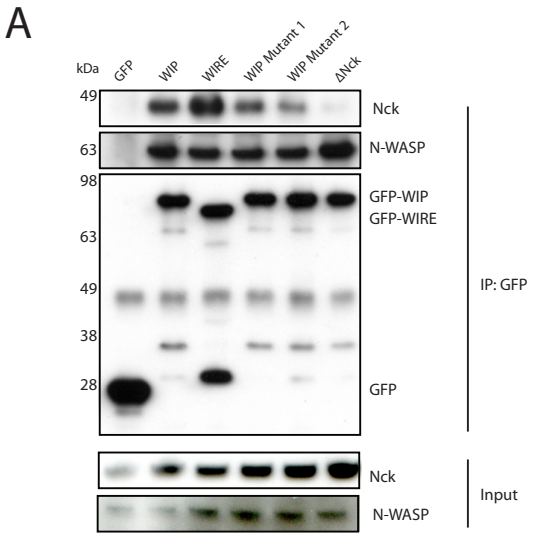

Figure 4.3. Mutation of both binding sites in WIP is required to abrogate Nck binding in cells

Immunoblot analysis reveals that endogenous N-WASP but not Nck interacts with GFP-WIPΔNck. GFP-WIP, GFP-WIRE or the indicated WIP mutants were expressed in HeLa cells and immunoprecipitated using a mouse monoclonal GFP antibody.

4.2.1 Disruption of the interaction of WIP and Nck impairs actin tail formation

Having identified the Nck binding site in WIP, I examined the functional consequences of abrogating this interaction during vaccinia actin tail formation. GFP, GFP-WIP or GFP-WIPΔNck constructs were transiently expressed in WIP-/- cells, in which WIRE had been depleted. As expected, after WR infection, cells expressing GFP alone did not have actin tails (Figure 4.4 B, data not shown). In contrast, wild type GFP-WIP was recruited to vaccinia virus particles and induced robust actin tail formation (Figure 4.4 A, B). GFP-WIPΔNck localised to virus particles and was capable of inducing actin tails. However, cells expressing GFP-WIPΔNck showed a marked reduction in the percentage of cells making actin tails, with only 59.5 ± 3.1% of cells having actin tails compared with 85.5 ± 1.0% in the control (Figure 4.4 A, B). In addition, these actin tails were significantly shorter than

the actin tails induced by wild type WIP (0.98 ± 0.04 and 2.50 ± 0.18μm respectively) (Figure 4.4 B).

To gain further insight into the effect of disrupting the Nck-WIP interaction, I used FRAP to analyse the exchange rate of GFP-WIPΔNck. Wild type GFP-WIP had a similar rate of exchange as I previously measured (0.91 ± 0.07 seconds) (compare Figures 3.7 A and Figure 4.5 A). In contrast, GFP-WIPΔNck had a 40% faster turnover, with a half-life of recovery of 0.55 ± 0.05 seconds (Figure 4.5 A). A slight difference was observed in the maximum fluorescence recovery for GFP-WIP and GFP-WIP∆Nck. As mentioned before (Chapter 3.2.3), decreased recovery of WIP has been observed in the absence of active actin polymerisation (Weisswange et al., 2009). This offers a possible explanation for the difference in recovery and is consistent with the shorter and slower moving actin tails observed for the GFP-WIP∆Nck mutant.

Furthermore, I quantified the speed of actin-based motility in WIP-/- cells treated with WIRE siRNA that were expressing GFP-WIP or GFP-WIP∆Nck. Actin tails in cells expressing wild type GFP-WIP had an average speed of 0.18 ± 0.01 μm/s, while those induced by GFP-WIPΔNck moved more slowly with an average speed of 0.12 ± 0.01μm/s (Figure 4.5 B). This represents a 40% decrease in the rate of actin-based motility, which correlates with the increased rate of exchange of WIP.

This data demonstrates that the interaction of WIP with Nck is important for stabilising WIP in the vaccinia actin polymerisation complex. The functional importance of this stabilisation is clear as fewer actin tails are formed and the rate of actin based motility is reduced in the absence of the Nck:WIP interaction. As WIP is still localised to the virus in the absence of an interaction with Nck, other factors must be involved in its recruitment. As Grb2 increases the efficiency of actin tail formation and I have previously shown that Grb2 stabilises WIP in the actin polymerisation complex (Chapter 3.2.3), I hypothesised that Grb2 may cooperate with Nck to recruit WIP to virus particles.

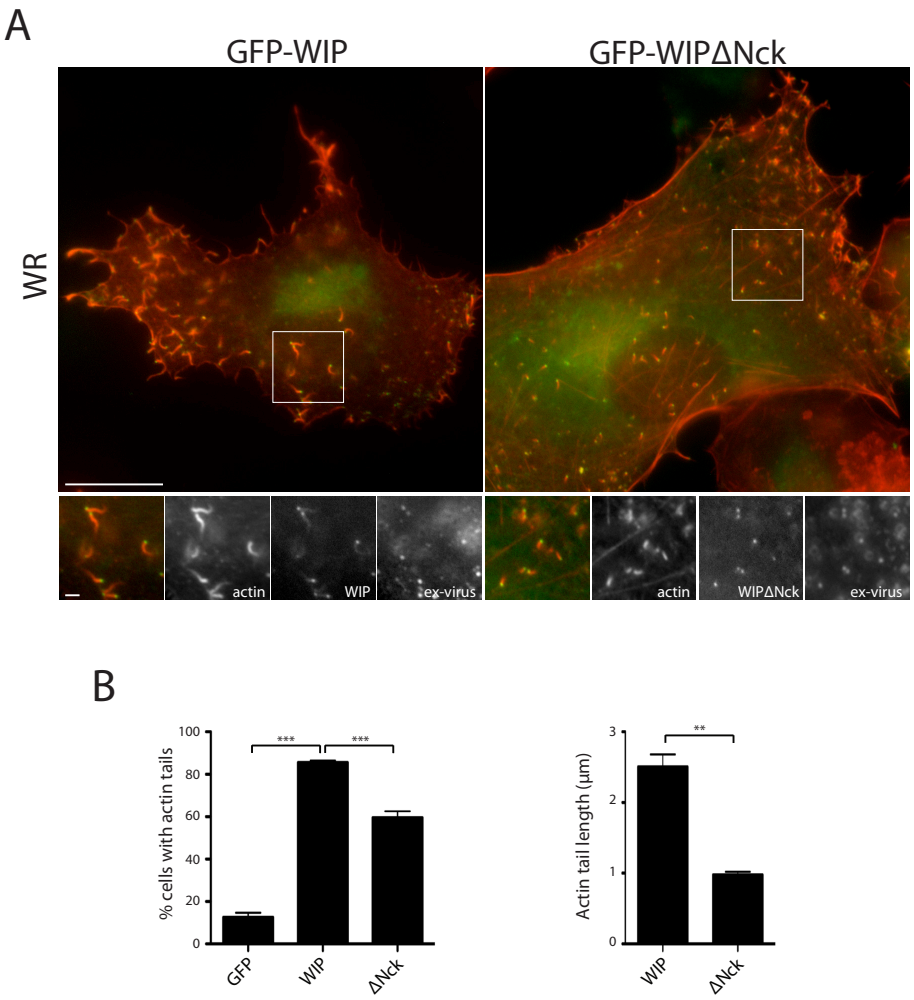

Figure 4.4. The interaction of WIP with Nck is important for actin tail formation

(A) Immunofluorescence analysis of WR infected WIP-/- cells treated with WIRE siRNA, reveals that expression of GFP-WIPΔNck induces fewer and shorter actin tails than GFP-WIP. Scale bars = 20 and 2μm. **(B)** Graphs show a quantification of the percentage of WR infected cells with actin tails (left panel) or the average length of actin tails (right panel) in WIP-/- cells treated with WIRE siRNA and transfected with the indicated construct. Error bars represent the SEM from three independent experiments. ** = $p<0.01$, *** = $p<0.001$.

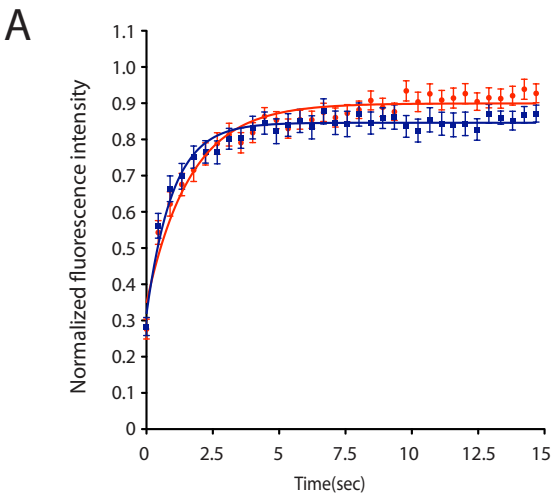

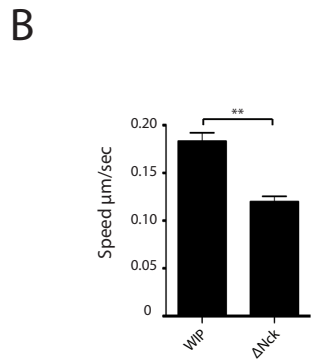

	% Recovery	$t_{1/2}$ (sec)
WIP	89.96 ± 0.6	0.91 ± 0.07
ΔNck	84.61 ± 0.6	0.55 ± 0.05**

Figure 4.5. The increased rate of exchange of WIPΔNck correlates with a slower rate of actin-based motility of vaccinia

(A) Comparison of the recovery kinetics of GFP-WIP (red) and GFP-WIPΔNck (purple) after photobleaching in WIP-/- cells treated with WIRE siRNA and infected with WR. The rate of exchange of GFP-WIPΔNck is more rapid than GFP-WIP. n=50 (WIP) or 44 (WIPΔNck) from three independent experiments. **(B)** Quantification of the rate of actin based motility of WR in WIP-/- cells treated with WIRE siRNA reveals that actin tails in cells expressing GFP-WIPΔNck have slower average speeds that those in cells expressing wild type GFP-WIP. Error bars represent the SEM from three independent experiments in which 50 virus particles were tracked in 5 cells. ** = $p<0.01$

4.2.2 Grb2 cooperates with Nck to recruit WIP and induce actin tail formation

To test whether Grb2 cooperates with Nck in recruiting WIP, I examined the consequences of abrogating the interaction between WIP and Nck in the absence of Grb2 recruitment using the A36-Y132F virus. In contrast to WR infection, the A36-Y132F virus showed a dramatic decrease in its ability to induce actin tails in cells expressing GFP-WIPΔNck (Figure 4.6 A, B). Only 17.00 ± 3.61% of cells expressing GFP-WIPΔNck had actin tails compared with 70.00 ± 1.53% of cells expressing wild type GFP-WIP (Figure 4.6 A, B). Moreover, in those cells that had actin tails, the tails were shorter than those found in control cells (1.39 ± 0.12 and 0.88 ± 0.02μm, respectively) (Figure 4.6 B). During A36-Y132F infection, the average speed of actin-based motility in cells expressing GFP-WIPΔNck was 0.06 ± 0.01 μm/s compared to 0.19 ±0.01 μm/s in control cells expressing GFP-WIP (Figure 4.7 A).

The recruitment of GFP-WIPΔNck to virus particles was also substantially reduced in the absence of Grb2 recruitment (Figure 4.7 B). The 50% decrease in fluorescence intensity compared to wild-type GFP-WIP made FRAP analysis impossible, as the signal was too weak to be detected consistently and accurately at the rapid imaging speeds required for this technique. To further characterise this mutant, the persistence of recruitment of GFP-WIPΔNck to virus particles was measured. In this assay, cells expressing either GFP-WIP or GFP-WIPΔNck were infected with an A36-Y132F virus tagged with RFP-A3 (RFP-A3/Y132F) and imaged for 90 seconds, with one image acquired every second. Virus particles were followed over the course of the movie and scored for whether the GFP signal was still associated at the indicated time points. The GFP-WIP signal remained associated with 69.33 ± 1.33% of virus particles for duration of the movie. In contrast, for GFP-WIPΔNck, this was the case for only 12.07 ± 2.66% of the analysed particles (Figure 4.7 C). This shows that in the absence of an interaction with Nck, the recruitment of WIP to virus particles is very transient.

Taken together, this data suggests that Nck and Grb2 co-operate to recruit WIP to virus particles. The recruitment of WIP by Grb2 may be direct or mediated by N-

WASP. Interestingly, even in the absence of Grb2 recruitment, weak and transient association of WIPΔNck with a small number of virus particles is observed. This localisation may be due to the presence of residual WIRE in the cells. Alternatively, as N-WASP can also interact with Nck, this may be sufficient to mediate the recruitment of N-WASP: WIP complexes in a small minority of virus particles.

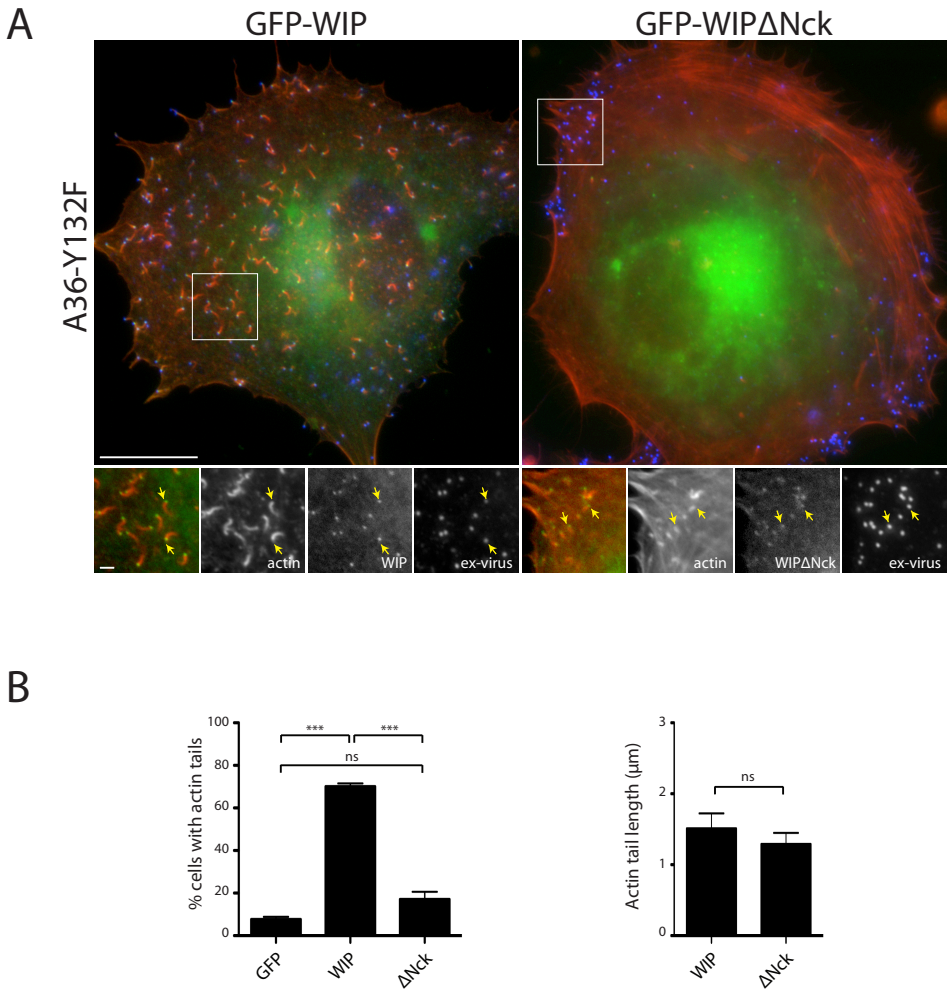

Figure 4.6. Lack of Grb2 recruitment results in decreased efficiency of actin tail formation

(A) Immunofluorescence analysis shows that significantly fewer actin tails are induced by the A36-Y132F virus in WIP-/- cells lacking WIRE but expressing GFP-WIPΔNck. Scale bars = 20 and 2μm. **(B)** Quantification of the percentage of A36-Y132F infected cells with actin tails (left panel) and the average length of actin tails (right panel) in WIP-/- cells treated with WIRE siRNA and expressing the indicated protein. Error bars represent the SEM from three independent experiments. *** = $p<0.001$, ns=not significant.

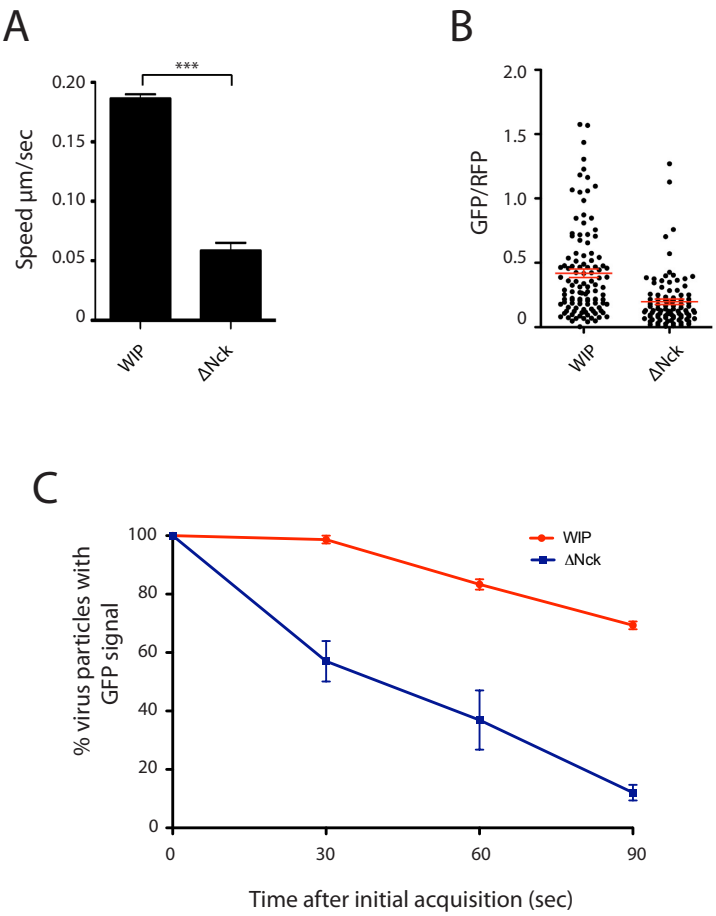

Figure 4.7. Grb2 cooperates with Nck to recruit WIP to virus particles

(A) Quantification showing that A36-Y132F virus particles move more slowly in WIP-/- cells lacking WIRE but expressing GFP-WIPΔNck. Error bars represent the SEM of three independent experiments in which 50 virus particles were tracked in 5 cells. *** = $p<0.001$ **(B)** In the absence of Grb2 recruitment, the localisation of GFP-WIPΔNck is weaker that that of GFP-WIP. The intensity of the RFP-A3 virus signal was used as a reference to which the GFP signal was compared. **(C)** The association of GFP-WIPΔNck with virus particles is more transient than that of GFP-WIP. Graph shows the percentage of virus particles still associated with GFP-WIP or GFP-WIPΔNck after the indicated time points.

4.3 Characterisation of the functional importance of the interaction of WIP and N-WASP

Having demonstrated that the interaction of Nck and WIP is important for vaccinia driven actin polymerisation, I now focussed on determining the function of the interaction of WIP with N-WASP. Previous work in our lab and others has identified the region required for the interaction of WIP and N-WASP. A combination of biochemical mapping and NMR showed that the C-terminal region of WIP wraps around the N-terminal WH1 domain of N-WASP forming extensive contacts during binding (Figure 4.8 A) (Peterson et al., 2007; Volkman et al., 2002; Zettl and Way, 2002). I utilised a construct of WIP in which two key phenylalanines at positions 454 and 456 are substituted with alanine (WIP-FFAA). These mutations have previously been shown to inhibit the binding of a peptide containing residues 451-456 of WIP to the WH1 domain of N-WASP (Zettl and Way, 2002). To confirm that this mutation disrupts binding between full length WIP and N-WASP, I used a GFP antibody to immunoprecipitate GFP-WIP or GFP-WIP-FFAA from HeLa cells. Immunoblot analysis showed that while endogenous N-WASP bound to WIP, the FFAA mutation abolished this interaction (Figure 4.8 B). In the absence of an interaction with N-WASP, WIP could still bind to Nck (Figure 4.8 B).

Next, I examined the consequences of expressing the GFP-WIP-FFAA mutant on vaccinia induced actin tail formation. Recruitment of this mutant to virus particles during WR infection was considerably weaker than wild type GFP-WIP or GFP-WIPΔNck (compare figures 4.9 A and 4.4 A). A dramatic drop in the number of infected cells with actin tails was also observed, when compared to either wild type GFP-WIP or GFP-WIPΔNck (36.67 ± 5.55 % compared with 87.00 ± 0.58 % and 59.5 ± 3.1%, respectively) (Figures 4.8 B and 4.4 B). The actin tails induced by GFP-WIP-FFAA were significantly shorter than those in cells expressing GFP-WIP (0.10 ± 0.03μm and 2.51 ± 0.30μm respectively). FRAP analysis of WR infected WIP-/- cells treated with WIRE siRNA, revealed that GFP-WIP-FFAA has a very rapid rate of exchange, with a half-life of fluorescence recovery of 0.27 ± 0.02 seconds (Figure 4.10 A) This represents an almost 70% increase in the rate of exchange of this mutant compared to wild type GFP-WIP (0.85 ± 0.06 seconds) and is also more rapid than the rate of exchange of GFP-WIPΔNck during WR

infection (0.55 ± 0.05) (Figure 4.5 A). As with GFP-WIP∆Nck, GFP-WIP-FFAA was observed to have a slightly lower maximum rate of recovery than GFP-WIP. A lower amount of active actin polymerisation could also account for this difference, as discussed before (Chapter 4.2.2). A decrease in the rate of actin-based motility was also observed, with the FFAA induced actin tails having an average speed of 0.071 ± 0.001μm/s compared with 0.180 ± 0.005μm/s in control actin tails (Figure 4.10 B). My data shows N-WASP plays a crucial role in stabilising the recruitment of WIP at virus particles. This is important for actin tail formation as the increased rate of exchange of WIP-FFAA results in fewer actin tails that are very short and move very slowly.

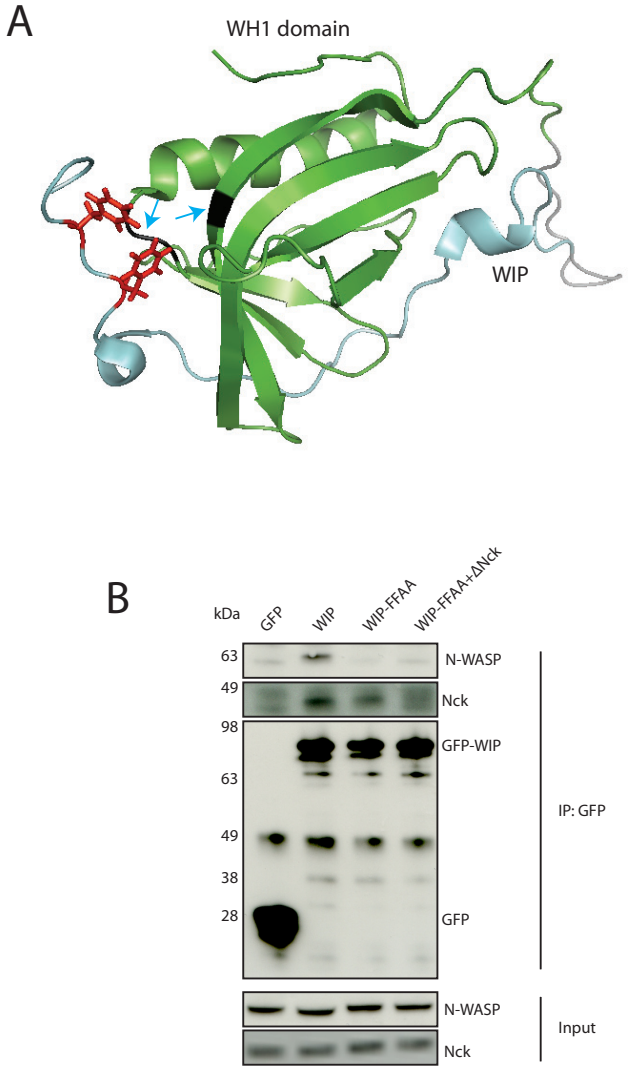

Figure 4.8. Substitution of phenylalanines 454 and 456 in WIP with alanine abrogates binding to N-WASP

(A) Cartoon representation of the structure of the WIP: N-WASP interface (WIP in blue, N-WASP in green). Phenylalanines 454 and 456 of WIP are highlighted in red. Blue arrows indicate the hydrophobic surface of N-WASP, which includes valine 42 and alanine 119, that mediates the interaction with phenylalanines 454 and 456 of WIP. **(B)** Immunoblot analysis reveals that endogenous N-WASP interacts with GFP-WIP but not with GFP-WIP-FFAA or GFP-WIP-FFAA+ΔNck immunoprecipitated from HeLa cells. Endogenous Nck interacts with GFP-N-WASP and GFP-N-WASP-FFAA but not GFP-WIP-FFAA+ΔNck.

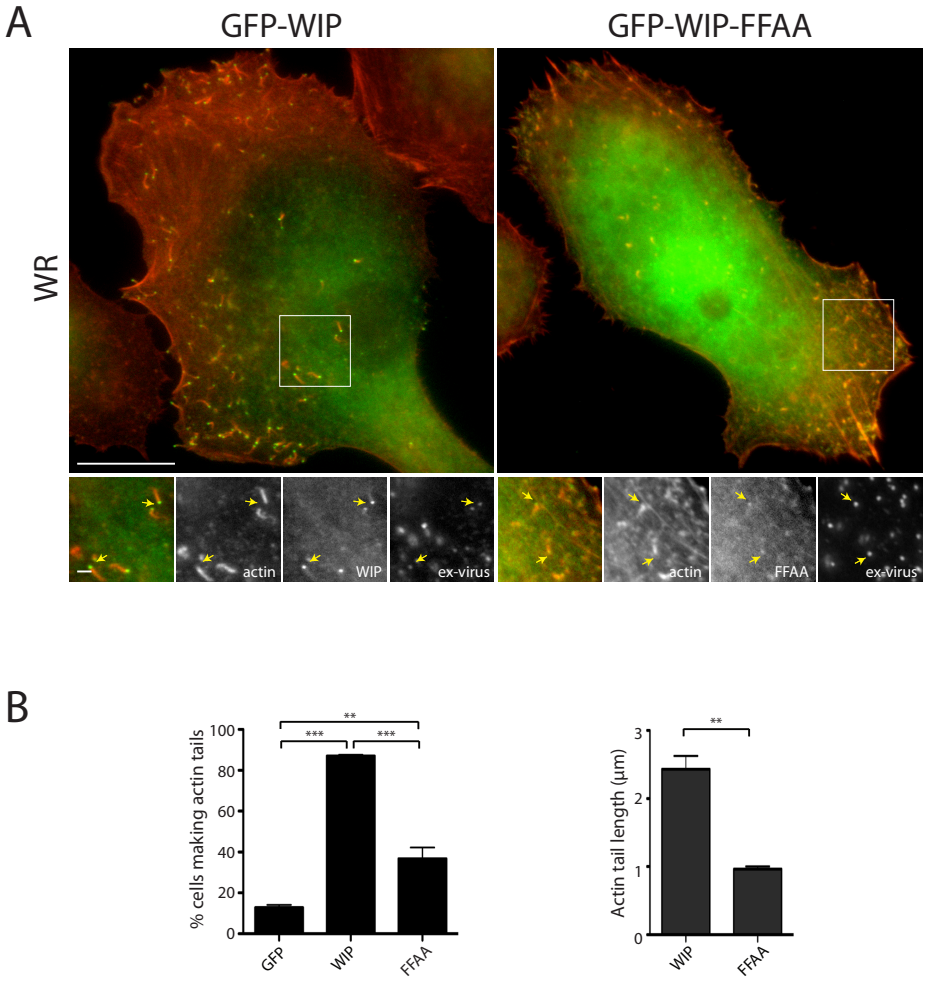

Figure 4.9. Disrupting the interaction of WIP and N-WASP leads to impaired actin tail formation

(A) Immunofluorescence analysis of WR infected WIP-/- cells treated with WIRE siRNA, reveals that expression of GFP-WIP-FFAA induces fewer and shorter actin tails than GFP-WIP. Scale bars = 20 and 2µm. **(B)** Graphs show a quantification of the percentage of WR infected cells with actin tails (left panel) or the average length of actin tails (right panel) in WIP-/- cells treated with WIRE siRNA and transfected with the indicated construct. Error bars represent the SEM from three independent experiments. ** = $p<0.01$, *** = $p<0.001$.

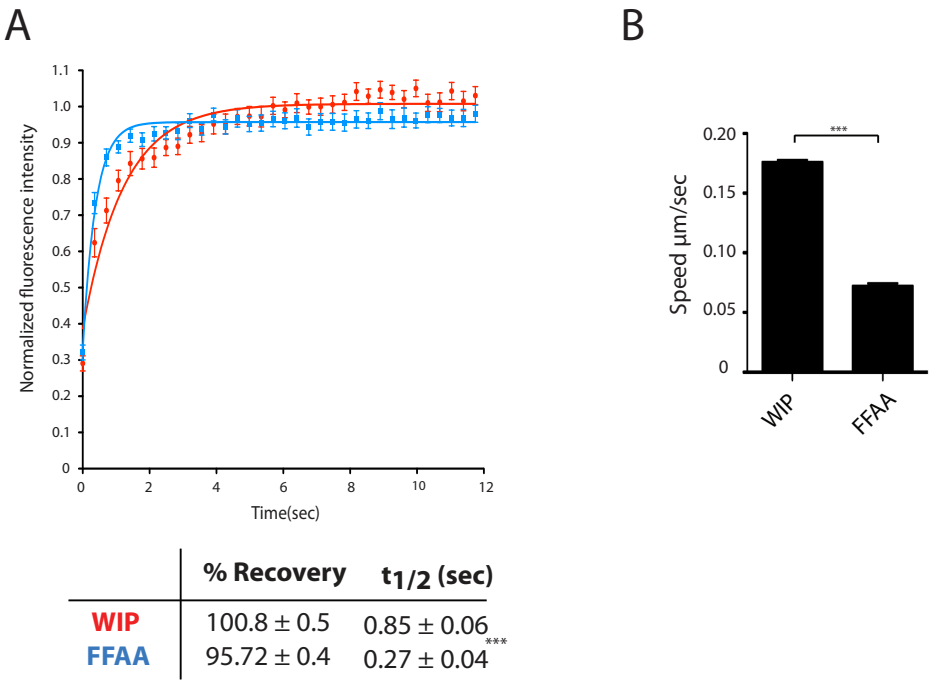

	% Recovery	$t_{1/2}$ (sec)
WIP	100.8 ± 0.5	0.85 ± 0.06
FFAA	95.72 ± 0.4	0.27 ± 0.04***

Figure 4.10. N-WASP stabilises WIP in the vaccinia actin polymerisation complex

(A) Comparison of the recovery kinetics of GFP-WIP (red) and GFP-WIP-FFAA (blue) after photobleaching in WIP-/- cells treated with WIRE siRNA and infected with WR. The rate of exchange of GFP-WIP-FFAA is more rapid than GFP-WIP. n=36 from three independent experiments. **(B)** Quantification of the rate of actin based motility of WR in WIP-/- cells treated with WIRE siRNA reveals that actin tails in cells expressing GFP-WIP-FFAA have slower average speeds that those in cells expressing GFP-WIP. Error bars represent the SEM from three independent experiments in which 50 virus particles were tracked in 5 cells. *** = p<0.001.

4.3.1 The interaction with Nck is not sufficient to recruit WIP to virus particles during infection

I examined the ability of the WIP-FFAA mutant to rescue actin tail formation in the absence of Grb2 recruitment. Immunofluorescence analysis revealed that during infection with the A36-Y132F virus, GFP-WIP-FFAA was not recruited to virus particles (Figure 4.10 A). Furthermore, actin tails were not induced by A36-Y132F in cells expressing GFP-WIP-FFAA (Figure 4.11 A, B). Thus in the absence of Grb2 recruitment, Nck is not sufficient to mediate recruitment of WIP to virus particles. To determine whether Grb2 is sufficient for the recruitment of WIP to virus particles, I constructed a WIP mutant in which both the Nck and N-WASP binding sites are mutated (WIPΔNck+FFAA). Immunoprecipitation of GFP-WIPΔNck+FFAA from HeLa cells revealed that neither Nck nor N-WASP could interact with this mutant (Figure 4.7 B). Immunofluorescence analysis of WR infected cells expressing GFP-WIPΔNck+FFAA demonstrated that this mutant was not recruited to virus particles and that actin tail formation was not rescued (Figure 4.12 A, B).

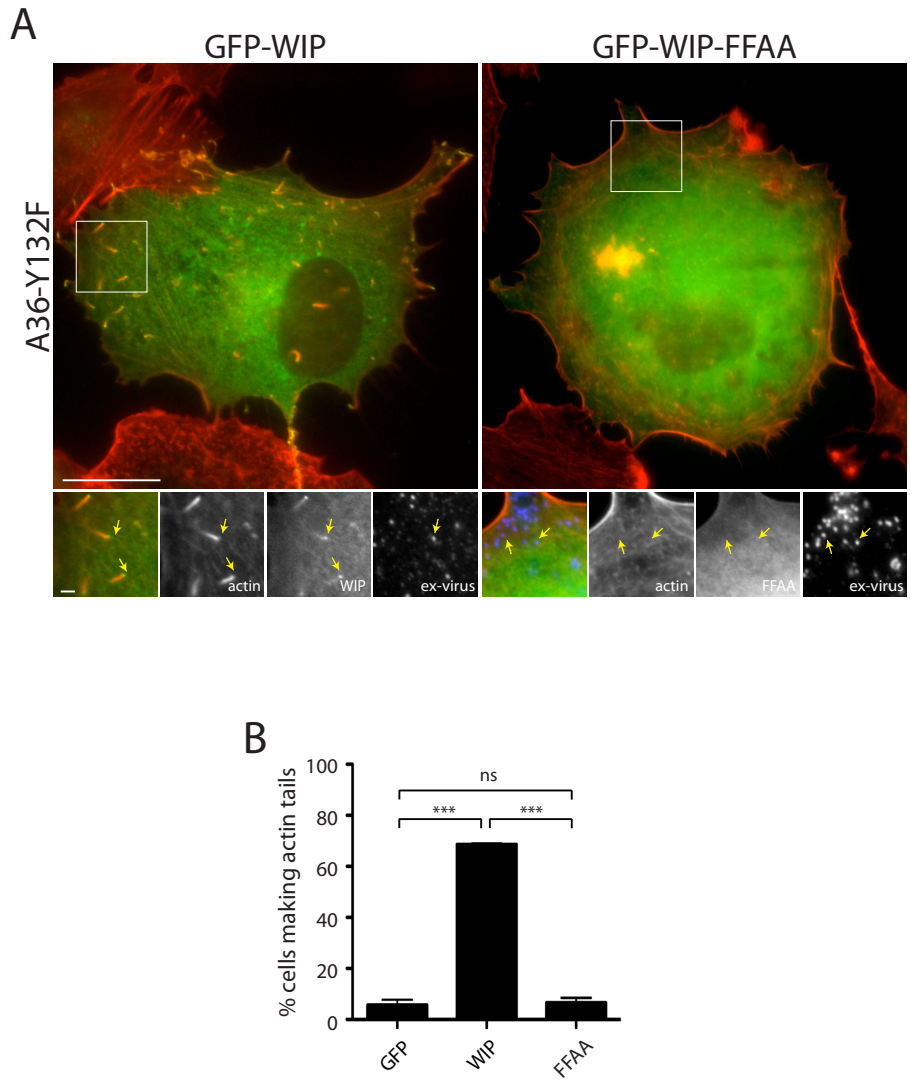

Figure 4.11. In the absence of Grb2 recruitment, the interaction of WIP and N-WASP is essential for actin tail formation

(A) Immunofluorescence analysis shows that significantly fewer actin tails are induced by the A36-Y132F virus in WIP-/- cells lacking WIRE but expressing GFP-WIP-FFAA. Scale bars = 20 and 2μm. **(B)** Quantification of the percentage of A36-Y132F infected cells with actin tails in WIP-/- cells treated with WIRE siRNA and expressing the indicated protein. Error bars represent the SEM from three independent experiments. *** = $p<0.001$, ns=not significant.

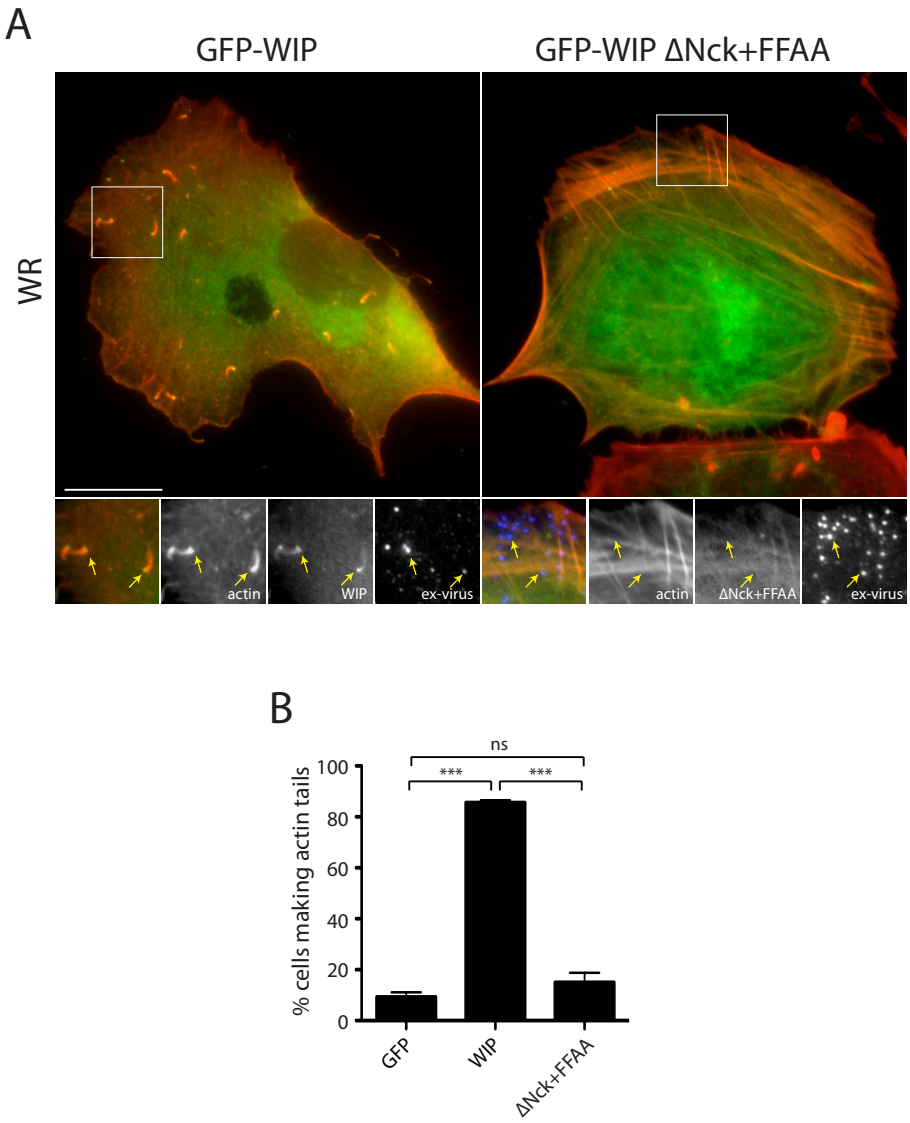

Figure 4.12. WIP is not recruited to virus particles in the absence of interactions with Nck and N-WASP

(A) Immunofluorescence analysis shows that significantly fewer actin tails are induced by WR in WIP-/- cells lacking WIRE but expressing GFP-WIP-FFAA+ΔNck. Scale bars = 20 and 2μm. **(B)** Quantification of the percentage of WR infected cells with actin tails in WIP-/- cells treated with WIRE siRNA and expressing the indicated protein. Error bars represent the SEM from three independent experiments. *** = $p<0.001$, ns=not significant.

4.4 Summary

In this chapter, I have investigated the importance of the interactions of WIP with Nck and N-WASP in vaccinia actin tail formation. I identified two Nck binding sites in WIP and demonstrated that both sites are important for the interaction of Nck and WIP. I have established that the interaction with Nck plays a vital role in stabilising the recruitment of WIP to virus particles and increasing the efficiency of actin tail formation. In the absence of Grb2 recruitment, the importance of the Nck:WIP interaction is highlighted, as very few actin tails are induced and recruitment of WIP is very weak. In addition, I have shown that the interaction of WIP and N-WASP is critical for actin tail formation. During WR infection, abrogating this interaction has a more severe effect on actin tail formation than disrupting the interaction between Nck and WIP. In the absence of Grb2 recruitment, WIP is not recruited to virus particles if it is not able to interact with N-WASP. This indicates that Nck is not sufficient to recruit WIP to vaccinia. Finally, Grb2 is also not sufficient to recruit WIP to vaccinia virus particles. Overall my data shows that two of the three interactions between WIP and Nck, N-WASP or Grb2 are required for recruitment of WIP to virus particles and the induction of actin polymerisation. My data also suggests that in the absence of WIP, Nck cannot recruit and activate N-WASP to induce actin polymerisation.

Chapter 5. The interaction of Nck and N-WASP is dispensable for actin tail formation

5.1 Introduction

In chapters three and four I demonstrated that, in the absence of WIP/WIRE, Nck is not sufficient to recruit and activate N-WASP to induce robust actin tail formation. N-WASP exists in an auto-inhibited conformation and interactions with other proteins, such as Cdc42, PIP_2 and SH3 adaptors, are required to relieve its intramolecular interactions and expose the WCA domain, which activates the Arp2/3 complex (Kim et al., 2000; Miki et al., 1998; Padrick and Rosen, 2010; Rohatgi et al., 1999; Sallee et al., 2008). Interestingly, while WIP has been shown to inhibit the activation of N-WASP by Cdc42 *in vitro*, Nck is a potent activator of N-WASP (Ho et al., 2004; Martinez-Quiles et al., 2001; Rohatgi et al., 2001; Tomasevic et al., 2007). Given this, I was interested to determine if the interaction of Nck and N-WASP is as important for promoting actin tail formation as the interaction between Nck and WIP (Chapter 4.2.2 and 4.2.3), Therefore, I decided to investigate the function of the interaction of Nck and N-WASP in actin tail formation by taking advantage of mouse embryo fibroblasts lacking expression of N-WASP (N-WASP-/-). Vaccinia virus cannot induce actin tails in these cells, although ectopic expression of GFP-N-WASP rescues this defect (Snapper et al., 2001; Weisswange et al., 2009). In addition, Nck, but not WIP or Grb2, is recruited to virus particles in the absence of N-WASP (Weisswange et al., 2009).

5.2 Identification of the Nck binding sites in N-WASP

To study the interaction of Nck and N-WASP, I first decided to identify the Nck binding site(s) in N-WASP. As is the case for WIP, the SH3 domains of Nck interact with the proline-rich region of N-WASP (Rohatgi et al., 2001). Given the success of the Far Western approach in identifying the Nck binding sites in WIP, as well as the presence of multiple putative SH3 binding motifs in N-WASP, I decided to use the same technique to identify the Nck binding sites in N-WASP (Figure 4.1). I used a peptide array that covers the entire sequence of N-WASP and consists of overlapping 15-mer peptides, with adjacent peptides shifted by three amino acids.

Following the same protocol as for the WIP array (chapter 4.2.1/2.7.4), purified recombinant His-tagged Nck (Figure 4.2 A) was incubated with the array and regions of binding were detected by immunoblot with an anti-His antibody. As with the WIP array, two potential binding sites were identified (Figure 5.1 A). These peptides both contained canonical SH3 binding motifs (PxxPxR) (Lim et al., 1994). In addition, the sequence of the second peptide corresponds to a Nck-binding site, which had previously been identified in N-WASP by probing an array covering the proline rich region of N-WASP with the isolated, GST-tagged, third SH3 domain of Nck (Weiss et al., 2009).

To confirm the interaction of these peptides with Nck, I performed peptide pulldown assays and found that both sequences retain His-Nck from bacterial soluble fraction (Figure 5.1 B). Mutating the key proline residues in the PxxPxR motif (shown in red in Figure 5.1 A) resulted in a substantial reduction in binding to His-Nck (Figure 5.1 B). The binding is not completely abolished, which may be due to the presence of multiple PxxP motifs in the peptides. To confirm that the interaction of Nck and N-WASP in cells depends on the identified sites, I introduced the same proline-to-alanine mutations in the PxxPxR motifs into full-length GFP-N-WASP. Next, I expressed GFP-N-WASP or the N-WASP mutants in HeLa cells and used the GFP-trap to pull down the GFP-tagged proteins. Immunoblot analysis revealed that while endogenous Nck interacts with wild type N-WASP, reduced binding of Nck to the second N-WASP mutant or the double mutant (N-WASPΔNck) is observed (Figure 5.2 A). To demonstrate that disrupting the interaction of Nck and N-WASP does not interfere with the binding of WIP to N-WASP, mCherry-WIP was co-expressed with the GFP-N-WASP mutants. Immunoblot analysis revealed that both N-WASP and the N-WASP mutants immunoprecipitated similar amounts of WIP (Figure 5.2 A). Data from the previous chapter suggests that the interaction of Nck and WIP is key to actin tail formation, therefore, I hypothesised that the residual binding between Nck and N-WASP may be due to the presence of WIP. To investigate this, I utilised of the WIP-/- cell line. Immunoblot analysis of immunoprecipitated GFP-N-WASP or its Nck binding mutants from WIP-/- cells that had been treated with WIRE siRNA revealed that the interaction of Nck with N-WASPΔNck depended on the presence of WIP or WIRE (Figure 5.2 B). Although these experiments indicate that the second mutation is sufficient to impede Nck

binding, all further experiments were carried out with the double mutant (N-WASPΔNck) to ensure that the binding between Nck and N-WASP was disrupted.

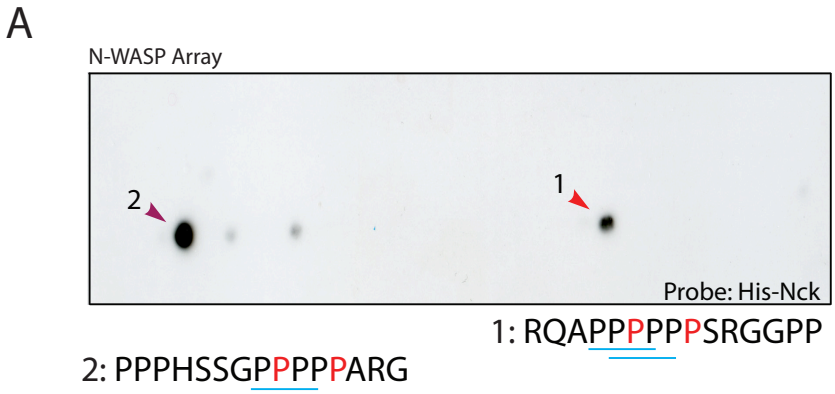

Figure 5.1. Identification of the Nck binding site in N-WASP

(A) Far Western analysis of a peptide array covering the whole sequence of rat N-WASP. Peptides were 15 amino acids in length and adjacent peptides are shifted by 3 residues. The array was probed with purified His-Nck1 and signal was detected by an anti-His antibody. Two potential binding sites are observed. The sequences of the identified peptides are below the array. The red prolines are part of the key PxxPxR motif. The blue lines highlight other PxxP sequeces present in the peptides. **(B)** Coomassie stained gel of an *In vitro* peptide pull down assay shows that N-WASP peptides 1 and 2, identified in the array, retain His-Nck1 from bacterial soluble fraction. Substitution of the indicated prolines (in red In **(A)**) to alanine reduces Nck binding. M = mutant

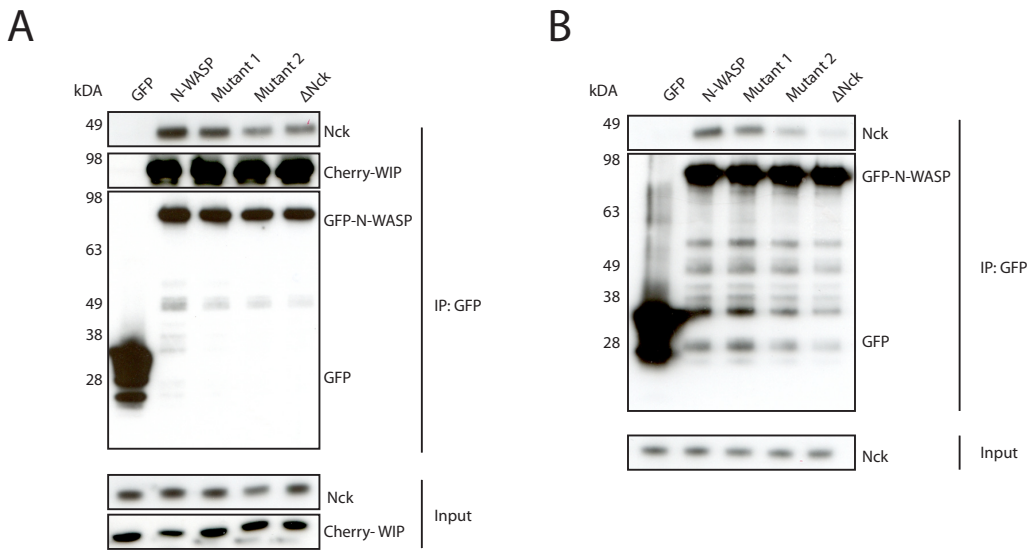

Figure 5.2. A single dominant Nck binding site is observed in N-WASP

(A) Immunoblot analysis of GFP-N-WASP pull downs from HeLa cells expressing Cherry-WIP reveals that binding of endogenous Nck, but not Cherry-WIP, is decreased for N-WASP mutant 2 and N-WASPΔNck. The GFP-trap was used to pull down the GFP-tagged proteins and endogenous Nck or Cherry-WIP were detected in both the bound fractions and the input cell lysates. **(B)** Immunoblot analysis of GFP-N-WASP pull downs from WIP-/- cells treated with WIRE siRNA shows that in the absence of WIP, endogenous Nck does not bind to N-WASP mutant 2 or N-WASPΔNck. Endogenous Nck was detected in all input cell lysates.

5.2.1 Disrupting the interaction of Nck and N-WASP does not inhibit actin tail formation

To examine the functional consequences of disrupting the interaction between Nck and N-WASP during vaccinia actin tail formation, I wanted to determine if expressing N-WASPΔNck rescued the ability of vaccinia virus to induce actin tails in N-WASP-/- cells. In order to investigate this I constructed stable cell lines expressing either GFP-tagged N-WASP or N-WASPΔNck (Figure 5.3 A). This was necessary as transient transfection of N-WASP-/- cells is very inefficient (data not shown). A lentiviral expression system was used to infect N-WASP -/- cells and generate cell lines expressing the desired proteins. Lentiviral systems are frequently used to make stable cell lines as they can infect a wide range of cell types including non-replicating cells. N-WASP or N-WASPΔNck was cloned into the pLVX expression vector such that GFP was fused to the N-terminal of the protein. This vector carries a puromycin resistance gene so that cells expressing the protein of interest can be easily and rapidly selected for by culturing in the presence of this drug (Chapter 2.5.2). These constructs were co-transfected into HEK293FT cells with the lentiviral packaging vector psPAX2 and the envelope vector pMD2.G. These plasmids are designed so that the virus particles produced are infectious but are unable to replicate. After two days, the culture medium from the 293FT cells was filtered and used to infect N-WASP-/- cells. The virus containing media was removed 48 hours later and the cells were subjected to puromycin selection. A survival curve had previously been carried out, which demonstrated that the presence of 1μg/ml of puromycin in the culture media is sufficient to kill all N-WASP-/- cells after 72 hours (data not shown). The lentivirus-infected cells were treated with the same concentration of puromycin so that any cells not expressing the pLVX-puromycin plasmid would die. In this way, I obtained a population of cells that all express the GFP-tagged protein of interest. The expression of the GFP-protein was then verified by a combination of immunoblot and immunofluorescence analysis (Figure 5.3 and 5.4 A). These cells were then expanded and a stock was frozen down at low passage number. The cell lines generated in this manner are maintained under constant selection pressure by supplementing the growth media with 1μg/ml of puromycin.

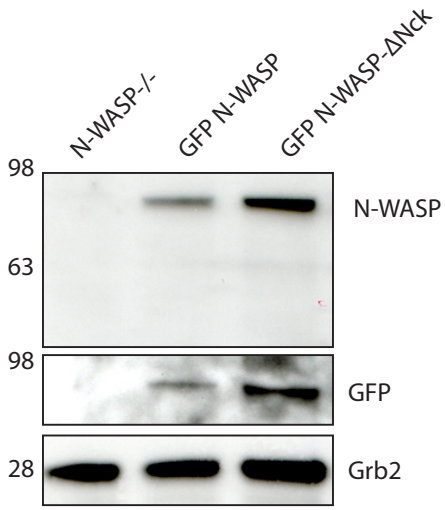

Figure 5.3. Expression of GFP-N-WASP and GFP-N-WASP∆Nck in N-WASP-/- cells

Immunoblot analysis shows that GFP-N-WASPΔNck is expressed at slightly higher levels than GFP-N-WASP in N-WASP-/- cells. Neither N-WASP nor GFP were detected in N-WASP-/- cells. Grb2 was used as a loading control.

5.2.2 Nck stabilises N-WASP in the vaccinia signalling network

To examine the consequences of mutating the Nck binding site in N-WASP, I investigated the ability of GFP-N-WASPΔNck to localise to virus particles and to rescue actin tail formation. Immunofluorescence analysis confirmed that GFP-N-WASP localised to virus particles during WR infection and could rescue actin tail formation in N-WASP-/- cells (Figure 5.4 A). Analysis of the N-WASP -/- cells expressing GFP-N-WASPΔNck showed that the localisation of N-WASP was not affected by the loss of Nck binding and that actin tails were also rescued in this case (Figure 5.4 A). Quantification of the percentage of infected cells containing even one actin tail revealed that GFP-N-WASPΔNck did not impair actin tail formation when compared to wild type N-WASP, with 92.45 ± 1.06% and 94.12 ± 1.61% of cells having actin tails, respectively (Figure 5.4 B). A more detailed analysis of the number of actin tails per cell revealed that cells expressing either GFP-N-WASP or GFP-N-WASPΔNck had a similar average number of actin tails (75.80 ± 1.86 and 72.67 ± 0.98 tails/cell respectively). While the ability of N-WASP to induce actin tails was not affected by the loss of Nck binding, the morphology of the actin tails was clearly different as the actin tails induced by GFP-N-WASPΔNck were slightly less than half the length of the wild-type actin tails (1.35 ± 0.02 and 2.38 ± 0.09μm respectively) (Figure 5.4 B).

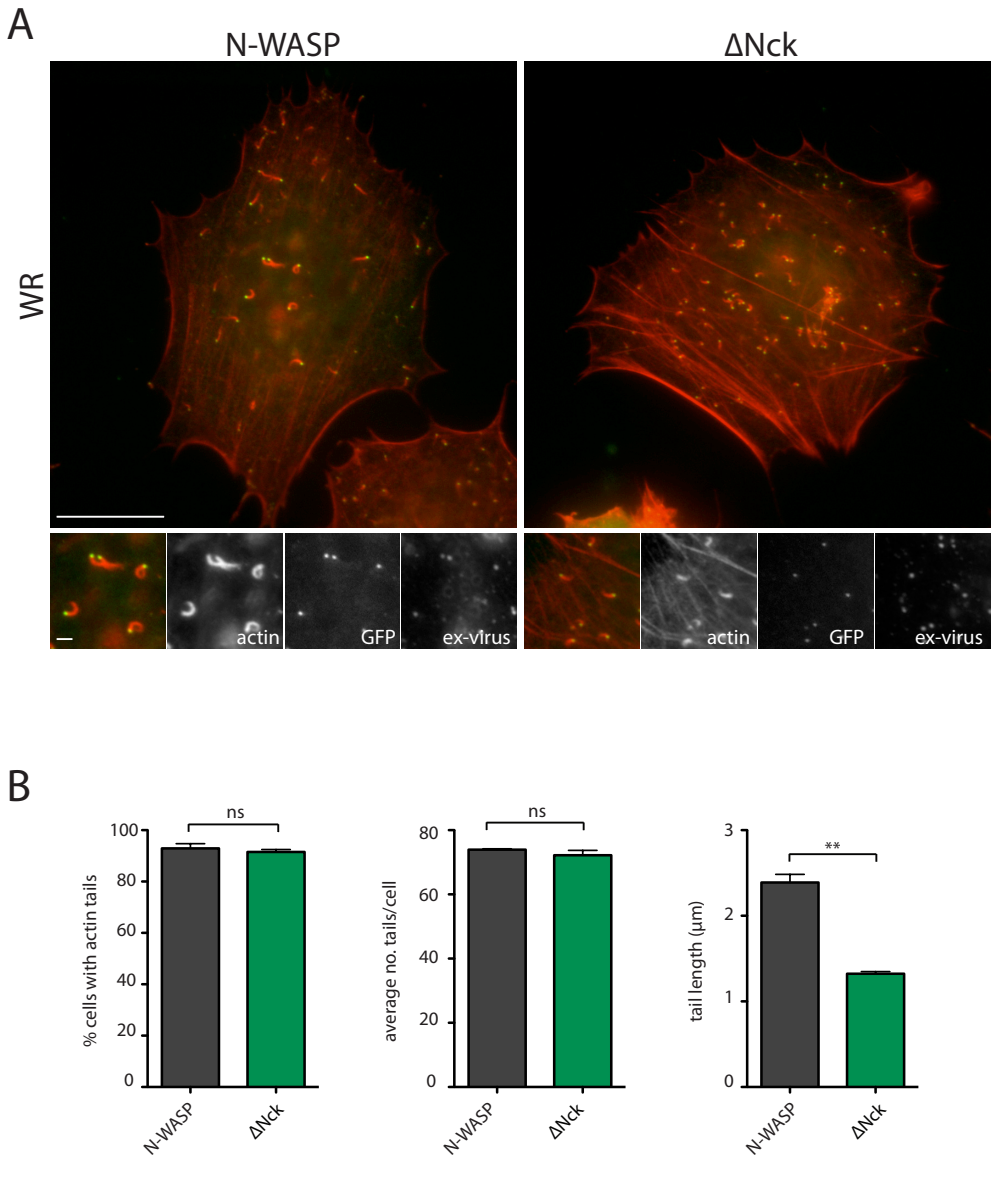

Figure 5.4. Abrogating the interaction of Nck and N-WASP results in shorter actin tails

(A) Immunofluorescence images showing the recruitment of GFP N-WASP and N-WASPΔNck to extracellular virus particles in WR infected cells. Shorter actin tails are observed in cells expressing GFP-N-WASPΔNck. Scale bars = 20 and 2μm. **(B)** Quantification of the percentage of WR infected cells with actin tails or the average number of actin tails per cell reveals that both GFP-N-WASP or GFP-N-WASPΔNck rescue actin tail formation to the same extent. Measurement of the average length of actin tails shows that actin tails are shorter in cells expressing GFP-N-WASPΔNck. Error bars represent the SEM of three independent experiments. ** = $p<0.01$, ns=not significant.

To further extend the characterisation of the N-WASPΔNck mutant, the stable cell lines were infected with WR expressing RFP-A3 (Chapter 3.2). The speed of actin-based motility of vaccinia virus was quantified by tracking RFP tagged virus particles that co-localise with the GFP signal from N-WASP or N-WASPΔNck. I found that virus particles in cells expressing N-WASPΔNck had an average rate of actin-based motility of 0.11 ± 0.008 μm/s compared with 0.15 ± 0.001μm/s in cells expressing wild type N-WASP (Figure 5.5 A). In addition, FRAP analysis revealed a small but significant increase in the rate of exchange of N-WASP when it lacks the ability to bind Nck (Figure 5.5 B). GFP-N-WASPΔNck has a half-time of recovery of 2.41 ± 0.13 seconds compared with 2.94 ± 0.17 seconds for wild type GFP-N-WASP (Figure 5.5 B). This value for the half time of fluorescence recovery of wild type N-WASP is similar to previously published values obtained in both HeLa and N-WASP-/- cells (Weisswange et al., 2009). Both GFP-N-WASP and GFP-N-WASPΔNck recovered to ~90%, indicating that an immobile fraction is not maintained at virus particles by either protein (Figure 5.5 B).

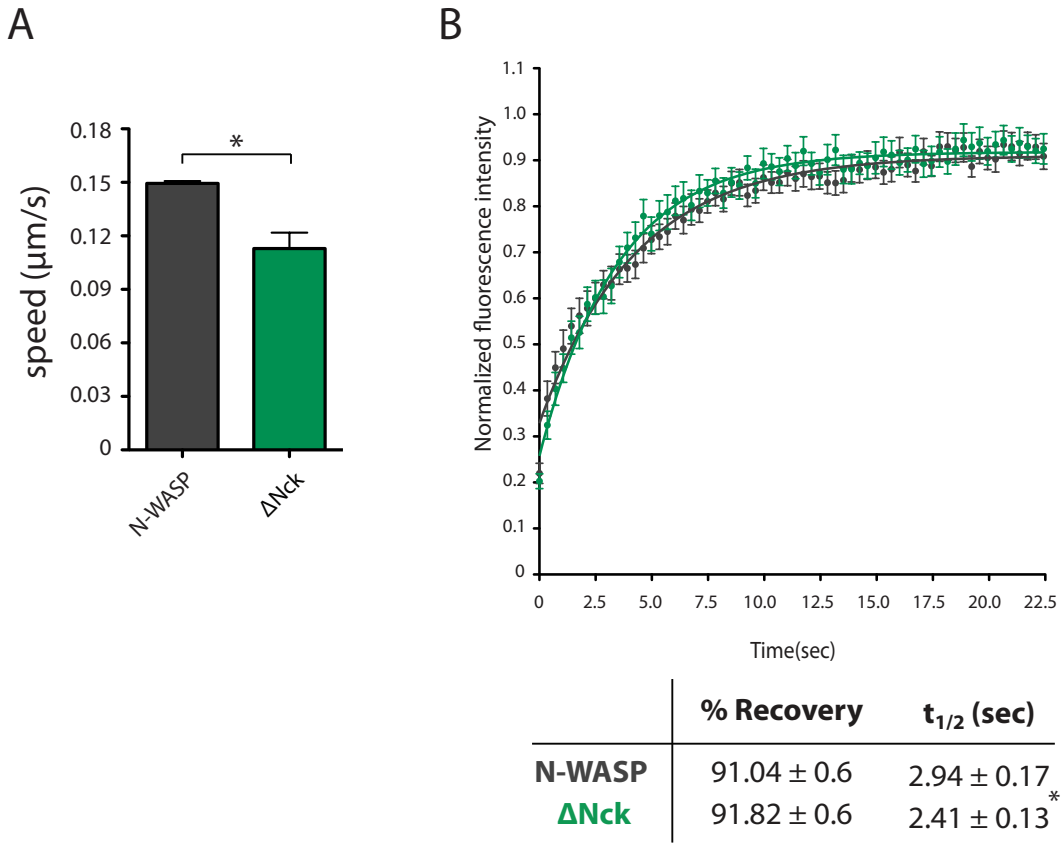

	% Recovery	$t_{1/2}$ (sec)
N-WASP	91.04 ± 0.6	2.94 ± 0.17
ΔNck	91.82 ± 0.6	2.41 ± 0.13*

Figure 5.5. Nck stabilises N-WASP at virus particles

(A) Quantification of the average speed of actin based motility of virus particles in N-WASP-/- cells expressing the indicated protein reveals that N-WASPΔNck dependent actin tails move more slowly than those in cells expressing GFP-N-WASP. Error bars represent the SEM of three independent experiments in which 50 virus particles were tracked. **(B)** Comparison of the recovery kinetics of GFP-N-WASP and GFP-N-WASPΔNck after photobleaching in N-WASP-/- cells infected with WR shows that GFP- N-WASPΔNck is less stable than GFP-N-WASP. n=45 from three independent experiments. Error bars represent the SEM * = $p<0.05$

Taken together this data indicates that the interaction of Nck and N-WASP is not essential for the recruitment of N-WASP to vaccinia virus particles and the induction of actin tails. However, this interaction is important for the stability of N-WASP in the vaccinia-signalling network. Together with an increased rate of exchange of N-WASP, shorter and slower moving actin tails are observed in N-WASP-/- cells expressing N-WASP∆Nck. This suggests that the interaction of Nck and N-WASP does play a role in promoting actin tail formation, by stabilising N-WASP.

As actin tails still form in the absence of an interaction of Nck and N-WASP, other signals must be present that can activate N-WASP at virus particles. Grb2 has been shown to have the ability to activate N-WASP *in vitro*; as well as stabilising N-WASP in the vaccinia actin polymerisation complex and promoting actin tail formation (Carlier et al., 2000; Weisswange et al., 2009). Therefore, I hypothesised that Grb2 is stabilising and activating N-WASP∆Nck during vaccinia virus infection. To investigate this, I infected N-WASP-/- cells expressing GFP-N-WASPΔNck with the A36-Y132F virus, which does not recruit Grb2 (Scaplehorn et al., 2002). I found that GFP-N-WASPΔNck was recruited to virus particles, although the localisation was much weaker than wild type N-WASP (Figure 5.6 A). The localisation was also weaker than GFP-N-WASPΔNck during WR infection (compare Figures 5.4 A and 5.6 A). As observed during WR infection, the percentage of cells with A36-Y132F virus induced actin tails was similar in cells expressing either GFP-N-WASPΔNck or GFP-N-WASP (Figure 5.6 B). The average number of actin tails per cell was also the same in both cell lines (Figure 5.6 B). The actin tails observed in A36-Y132F infected cells are shorter than those in WR infected cells (compare Figure 5.4 B and 5.6 B). While in cells expressing GFP-N-WASPΔNck, the A36-Y132F induced actin tails are even shorter (Figure 5.6 B).

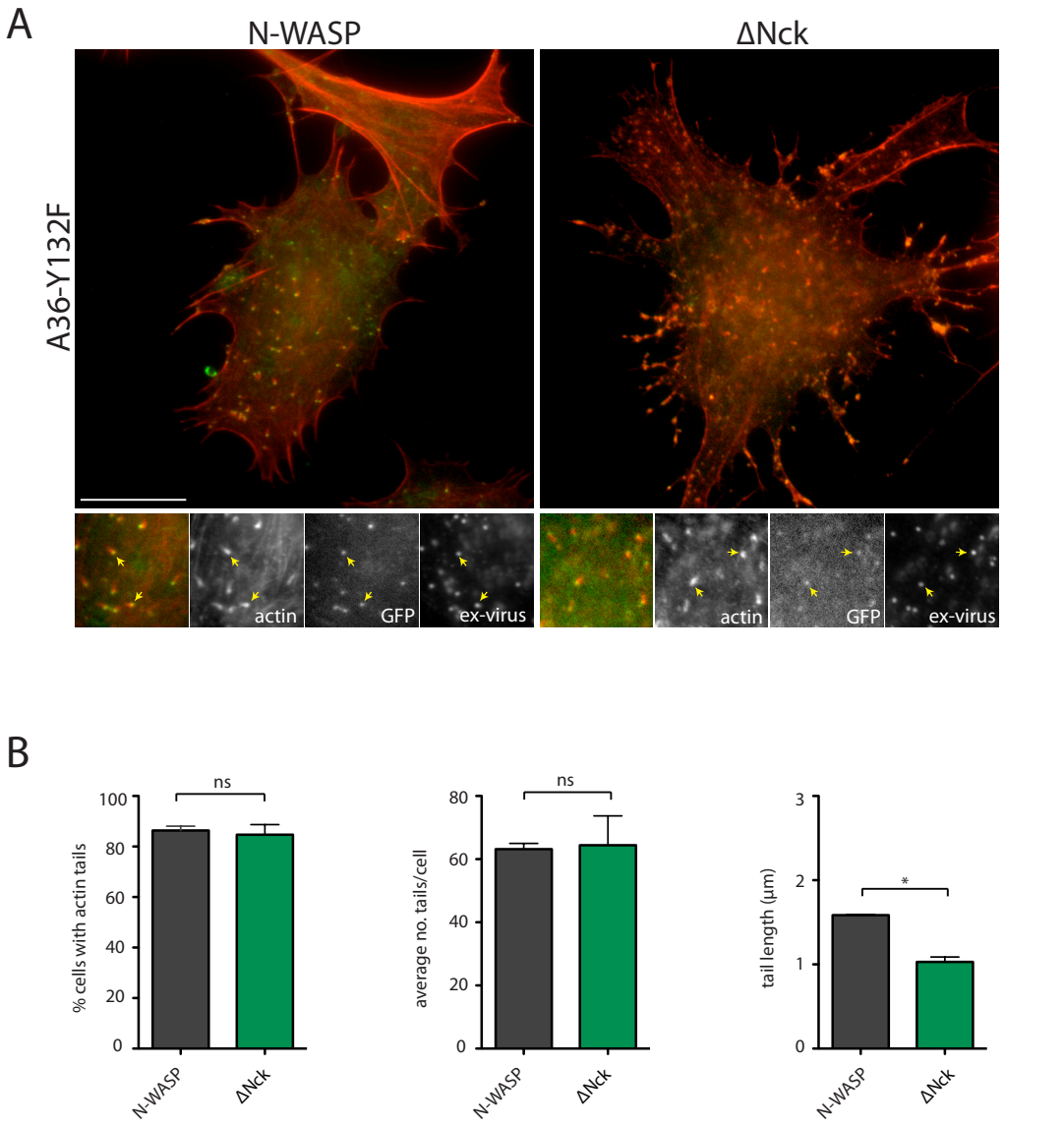

Figure 5.6. In the absence of Grb2 recruitment, N-WASPΔNck induces even shorter actin tails

(A) Immunofluorescence images showing that GFP-N-WASPΔNck is weakly recruited to virus particles in cells infected with the A36-Y132F virus. Very short actin tails are observed in N-WASP-/- cells expressing GFP-N-WASPΔNck and infected with A36-Y132F. Scale bars = 20 and 2μm. **(B)** Quantification of the percentage of A36-Y132F infected cells with actin tails or the average number of actin tails per cell reveals that both GFP-N-WASP or GFP-N-WASPΔNck rescue actin tail formation to the same extent. Measurement of the average length of actin tails induced by the A36-Y132F virus in N-WASP-/- cells expressing GFP-N-WASP or GFP-N-WASPΔNck shows that actin tails are even shorter in the absence of an interaction between N-WASP and Nck. Error bars represent the SEM of three independent experiments. * = $p<0.05$, ns=not significant.

As expected, in A36-Y132F infected cells, the rate of exchange of GFP-N-WASP increased 1.3 fold in the absence of Grb2 recruitment (compare Figures 5.7 A and 5.5 A) (Weisswange et al., 2009). The half-time of recovery of GFP-N-WASPΔNck at virus particles, in the absence of Grb2 recruitment, is 2.20 ± 0.12 seconds, which is very similar to that of GFP-N-WASP (2.11 ± 0.11) (Figure 5.7 A). In addition, both proteins recover to the same extent (Figure 5.7 A). Thus an additive increase in the rate of exchange of N-WASP is not observed upon loss of interactions with both Nck and Grb2.

Lack of Grb2 recruitment has previously been shown to result in an increase in the rate of actin based motility of virus particles (Weisswange et al., 2009). In agreement with this, in A36-Y132F infected N-WASP-/- cells expressing GFP-N-WASP, virus particles had an average speed of 0.16 ± 0.005 μm/s compared with 0.15 ± 0.001μm/s during WR infection (compare Figure 5.5 B and 5.7 B). In cells expressing GFP-N-WASPΔNck, an increase in the speed of actin-based motility to 0.17 ± 0.002 μm/s was observed during infection with the A36-Y132F virus (Figure 5.7 B). Thus, in the absence of Grb2 recruitment, both the speed of actin tails and the rate of exchange of N-WASP are similar in cells expressing either GFP-N-WASP or GFP-N-WASPΔNck. This is consistent with previous observations showing that the speed of actin-based motility of virus particles is determined by the rate of exchange of N-WASP (Weisswange et al., 2009). Furthermore, this data suggests that Nck plays a role in stabilising N-WASP in the presence but not the absence of Grb2.

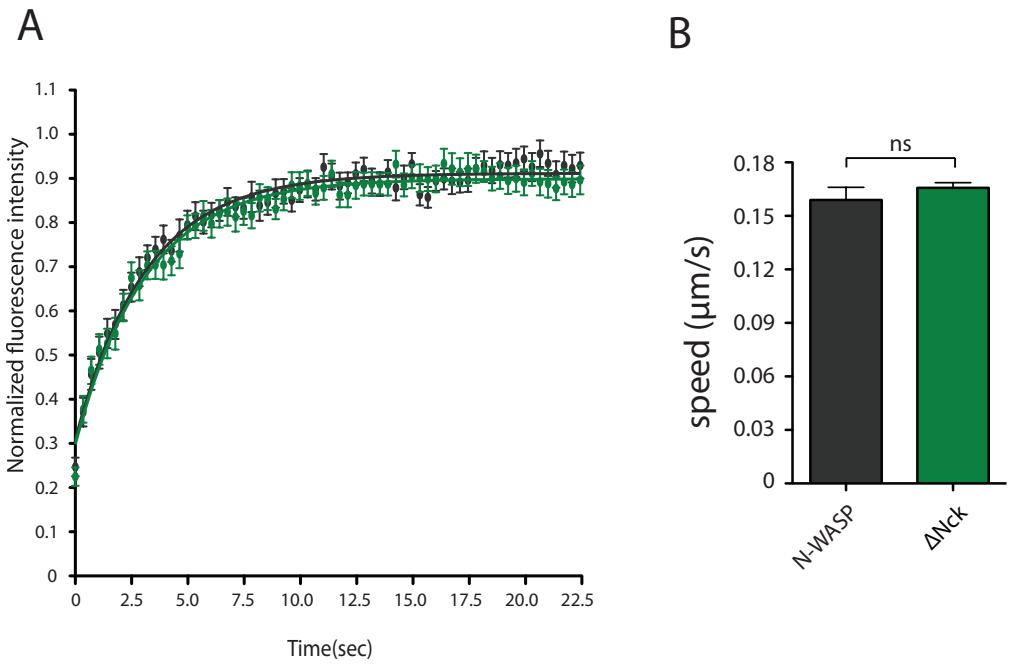

	% Recovery	$t_{1/2}$ (sec)
N-WASP	91.06 ± 0.5	2.11 ± 0.11
ΔNck	90.04 ± 0.6	2.20 ± 0.12

Figure 5.7. An additive increase in the rate of exchange of N-WASP is not observed in the absence of interactions with both Nck and Grb2

(A) Comparison of the recovery kinetics of GFP-N-WASP and GFP-N-WASPΔNck after photobleaching in N-WASP-/- cells infected with the A36-Y132F virus shows that GFP- N-WASPΔNck has a similar rate of exchange as GFP-N-WASP. n=40 virus particles from three independent experiments. Error bars represent the SEM. **(B)** Quantification of the average speed of actin based motility of virus particles in N-WASP-/- cells expressing the indicated protein reveals that N-WASPΔNck dependent actin tails move at a similar speed to those induced by the wild type protein. Error bars represent the SEM of three independent experiments. ns = not significant.

5.3 The 2nd SH3 domain of Nck is essential for actin tail formation.

My results indicate that Nck interacts with WIP to recruit the WIP:N-WASP complex to virus particles and subsequently interacts with N-WASP (Chapter 4.2). Nck then stabilises N-WASP and this promotes actin tail formation (Chapter 5.3). Nck contains three SH3 domains and a C-terminal SH2 domain. Recruitment of Nck to virus particles is dependent on the interaction of its SH2 domain with phosphorylated tyrosine 112 of A36 (Frischknecht et al., 1999b). As mentioned previously, Nck is recruited to virus particles in the absence of Grb2, WIP or N-WASP (Figure 3.13 A) (Weisswange et al., 2009). The SH3 domains then interact with WIP and N-WASP. As WIP contains two Nck binding sites, while N-WASP has a single dominant binding site, it is possible that each SH3 domain of Nck binds to a particular site in WIP or N-WASP (Figure 4.3; 5.2 A, B). Consistent with this, previous studies have indicated that each SH3 domain of Nck has preferences for different binding partners (Anton et al., 1998; Rivero-Lezcano et al., 1995; Rohatgi et al., 2001; Weiss et al., 2009). To determine the binding preferences of each SH3 domain with regard to WIP and N-WASP, I took advantage of point mutations that disrupt the function of the Nck SH3 domains. Substitution of a conserved tryptophan for lysine in each of the SH3 domains renders them unable to interact with proline rich motifs (Figure 5.8 A) (Blasutig et al., 2008; Ruusala et al., 2008; Tanaka et al., 1995; Wunderlich et al., 1999).

To investigate if the SH3 domains of Nck interact preferentially with the binding sites identified in WIP or N-WASP, I carried out peptide pulldown assays (Figure 5.8 B). Wild type His-tagged Nck or NckΔ1, Δ2 or Δ3 was expressed in BL21 (Rosetta) *E.coli*. As before, each of the peptides identified in the WIP peptide array retained wild type recombinant Nck from bacterial soluble fraction (Figures 4.2 C; 5.8 B). In contrast neither WIP peptide could interact with NckΔ2. In addition, Nck Δ1 and Δ3 also showed decreased binding to the 1st but not the 2nd WIP peptide (Figure 5.8 B). This analysis confirms and extends previous studies showing that WIP interacts preferentially with the 2nd SH3 domain of Nck (Anton et al., 1998; Weiss et al., 2009).

In agreement with my previous results, both N-WASP peptides also retained wild type His-Nck from bacterial soluble fraction (Figure 5.1 B, 5.8 B). Mutation of the 3rd SH3 domain of Nck resulted in a dramatic decrease in binding to both N-WASP peptides (Figure 5.8 B). In addition, NckΔ1 or Nck Δ2 also showed slightly reduced binding to both N-WASP peptides. This data demonstrates that the N-WASP peptides primarily interact with the third SH3 domain of Nck. This is consistent with data from a number of previous studies (Rohatgi et al., 2001; Weiss et al., 2009).

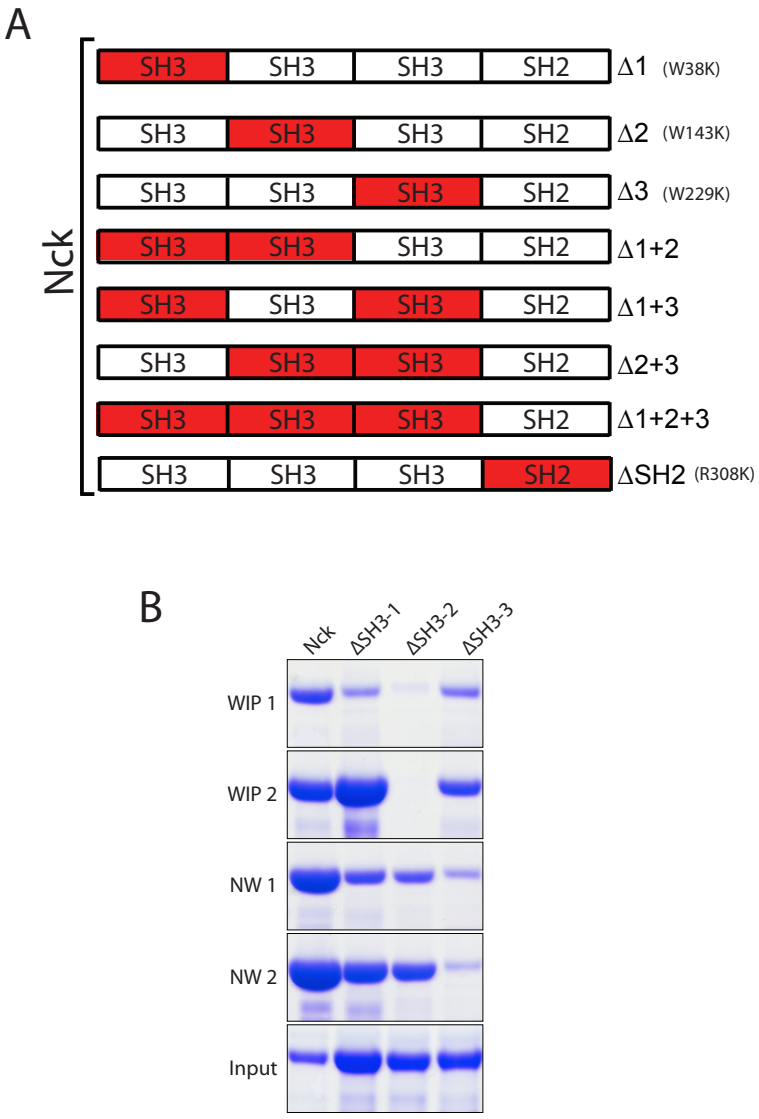

Figure 5.8. The SH3 domains of Nck show distinct preferences in binding WIP and N-WASP

(A) Schematic representation of the Nck mutant contructs. Red indicates the domain containing the loss of function mutation. The nomenclature used in this thesis is indicated on the right, followed by the point mutation used to disrupt the function of the domain. **(B)** Coomassie stained gels of peptide pull down assays using the WIP and N-WASP peptides identified as Nck binding sites in the peptide arrays (Figure 4.2 A and 5.3 B). All peptides retained wild type Nck from bacterial soluble fraction. The WIP peptides did not interact with NckΔ2, while N-WASP did not bind NckΔ3. The input represents 3% of the bacterial soluble fraction used in each pulldown.

5.3.1 Establishment of cell lines to study the function of Nck in actin tail formation

To study the importance of each Nck SH3 domain in actin tails formation, I took advantage of mouse embryonic fibroblasts (MEFs) lacking the expression of both isoforms of Nck (Nck-/-) (Bladt et al., 2003) Actin tails are not formed in these cells during vaccinia infection, however ectopic expression of GFP-Nck1 rescues this defect (Weisswange et al., 2009). Due to the poor efficiency of transfection observed in this cell line, I established cell lines that stably express the different Nck mutants (Figure 5.8 A). As with the N-WASP cell lines, a lentiviral system was used to generate these cell lines (Chapter 5.3). This differed slightly from the previous system in that the pL/ L expression vector was used (Chapter 2.5.1). This vector does not contain a puromycin resisistance cassette, thus FACS (fluorescence activated cell sorter) was used to obtain populations of cells that all express the GFP-tagged protein. Two days after infection of the Nck-/- cells with lentivirus, the culture media was changed and cells were checked for GFP expression by immunofluorescence microscopy. Cells were FACS sorted on the basis of GFP expression to eliminate cells not expressing GFP and to select a population of cells expressing similar levels of the GFP-tagged protein (Chapter 2.5.1.1).

After establishment of these cell lines, total cell lysates were collected and subjected to SDS-PAGE and immunoblot analysis to confirm expression of GFP-Nck or the Nck mutants (Figure 5.9). Nck-/- cell lines were used as a negative control. The GFP-tagged proteins were expressed in each cell line and migrated at the predicted molecular weight of 75kDa (Figure 5.9). The Nck antibody specifically detected a band at the expected size in each of the GFP positive cell lines but not in the Nck -/- cell lysates. Grb2 was used as a loading control. Wild type Nck and the Nck mutants were all expressed at similar levels (Figure 5.9).

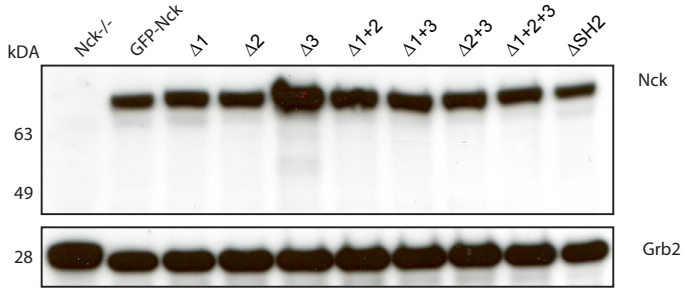

Figure 5.9. Expression of GFP-Nck and the GFP-Nck mutants in Nck-/- cells

Immunoblot analysis shows that the GFP-Nck mutants are expressed at similar levels to wild type GFP-Nck. As expected, Nck was not detected in Nck-/- cells. Grb2 was used as a loading control.

5.3.2 Functional analysis of the importance of the Nck SH3 domains in actin tail formation.

During WR infection, actin tails were not observed in Nck-/- cells expressing GFP alone (Figure 5.11 A, B). In contrast, wild type GFP-Nck was robustly recruited to vaccinia virus particles and actin tails were induced in 70.33 ± 3.77 % of infected cells (Figure 5.11 A, B). In cells expressing NckΔSH2, no GFP signal was observed at virus particles and actin tail formation was not rescued in this cell line. This agrees with previous reports that the SH2 domain of Nck is required for its recruitment to virus particles (Frischknecht et al., 1999b) (Figure 5.11 A, B). Recruitment of Nck to virus particles was observed for all constructs containing mutations in the SH3 domains, however if more than one of the SH3 domains was mutated, the localisation of GFP-Nck was weaker than the wild type (Figure 5.11 A). This suggests that the interaction of Nck with its downstream binding partners stabilises it at the virus. Consistent with this, Nck was found to have a more rapid rate of exchange in N-WASP-/- cells in which it is recruited to viruses in the absence of WIP, N-WASP and Grb2 (Weisswange et al., 2009). Actin tail formation was not rescued equally efficiently by all of the Nck SH3 mutants (figure 5.11 A, B). Mutation of any of the SH3 domains resulted in a ~10% decrease in the percentage of infected cells inducing actin tails compared to cells expressing wild type Nck. However, mutation of any two of the SH3 domains resulted in a significant

decrease in the number of actin tails formed. NckΔ1+2 rescued actin tail formation in only 13.33 ± 3.84 % of cells, while this was even less, at 7.33 ± 3.38%, for cells expressing NckΔ1+3. The most severe effects were observed in cells expressing NckΔ2+3 and NckΔ1+2+3, where actin tails were induced in only 3.33 ± 0.33% and 1.67 ± 0.67% of infected cells, respectively (Figure 5.11B). This suggests that at least two functioning Nck SH3 domains are required for WR induced actin tail formation.

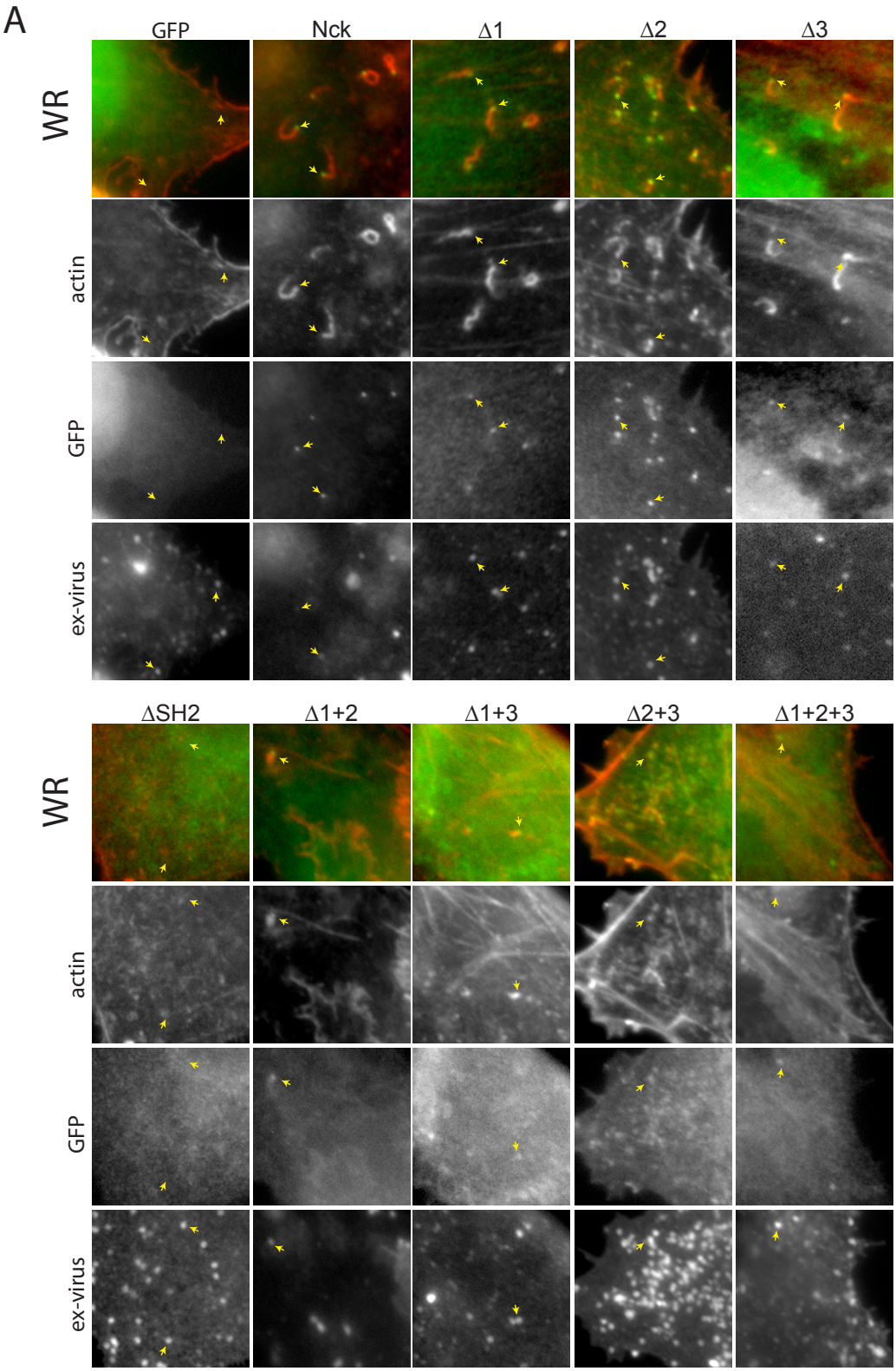
A
GFP
Nck
Δ1
Δ2
Δ3
WR
actin
GFP
ex-virus
ΔSH2
Δ1+2
Δ1+3
Δ2+3
Δ1+2+3
WR
actin
GFP
ex-virus

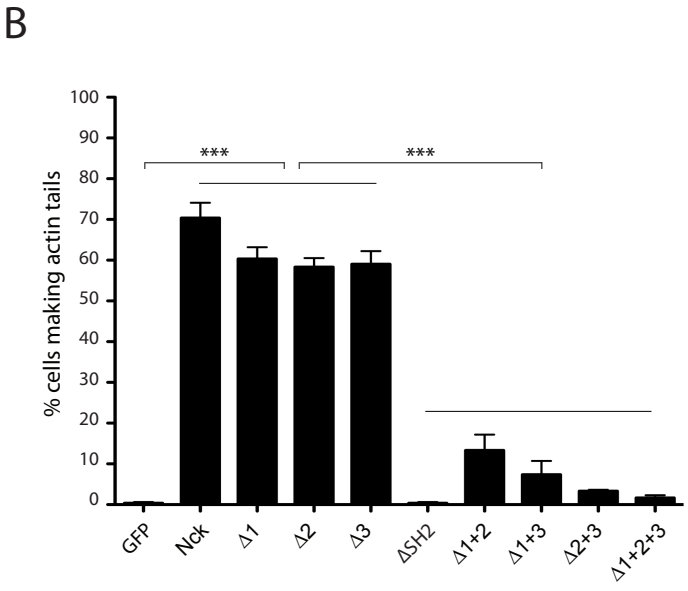

Figure 5.10. Two functioning Nck Sh3 domains are required for actin tail formation

(A) Immunofluorescence analysis shows that GFP-Nck or the Nck mutants are recruited to virus particles in WR infected cells. Loss of any two (or all three) SH3 domains results in a dramatic decrease in the ability of the virus to induce actin tails. Yellow arrows indicate the localisation of the GFP signal to virus particles. **(B)** Quantification of the percentage of WR infected cells with actin tails reveals that mutating the 2nd and 3rd SH3 domains, or all three SH3 domains has the biggest impact on actin tail formation. Error bars represent the SEM of three independent experiments. *** = $p<0.001$.

To gain further insight into the cooperation between Nck and Grb2 in actin tail formation, I infected the Nck mutant cell lines with the A36-Y132F virus. As expected, in the absence of Grb2, fewer actin tails were observed in cells rescued with wild type Nck than during WR infection (Scaplehorn et al., 2002). However, actin tails were still induced in 64.33 ± 6.89% of Nck-/- expressing wild type Nck (Figure 5.12 A, B). Interestingly, a significant effect on actin tail formation is observed upon the loss of the 2nd SH3 domain of Nck. In the absence of Grb2 recruitment, the A36-Y132F virus could induce actin tails in only 7.33 ± 2.03 % of cells expressing NckΔ2 (Figure 5.12 A, B). In contrast, actin tails were observed in 55 ± 4.73 % and 54 ± 7.51% of infected cells expressing NckΔ1 or NckΔ3, respectively. Mutation of any two, or all three of the Nck SH3 domains resulted in the loss of actin tail formation by the A36-Y132F virus. This is clearly demonstrated

by the observation that fewer than 2% of cells expressing NckΔ1+2, NckΔ1+3, NckΔ2+3 or NckΔ1+2+3 could support actin tails formation (Figure 5.11 A, B). This data shows that the 2nd SH3 domain of Nck is essential for actin tail formation. Taken together with my previous data demonstrating that this SH3 domain interacts with WIP, this is further evidence that WIP is essential to link Nck to N-WASP in order to promote Arp2/3 dependent actin polymerisation.

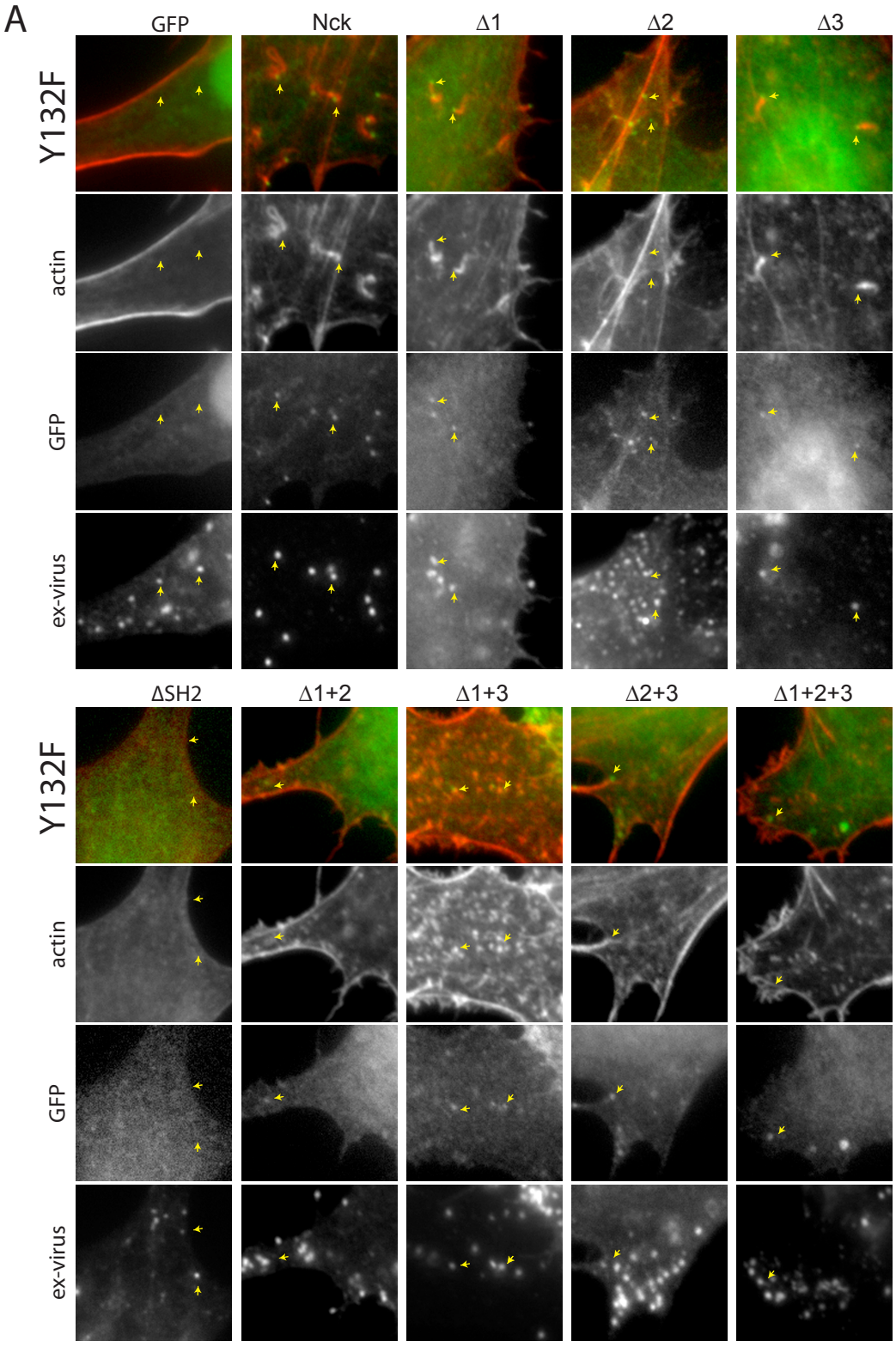
A
GFP
Nck
Δ1
Δ2
Δ3
Y132F
actin
GFP
ex-virus
ΔSH2
Δ1+2
Δ1+3
Δ2+3
Δ1+2+3
Y132F
actin
GFP
ex-virus

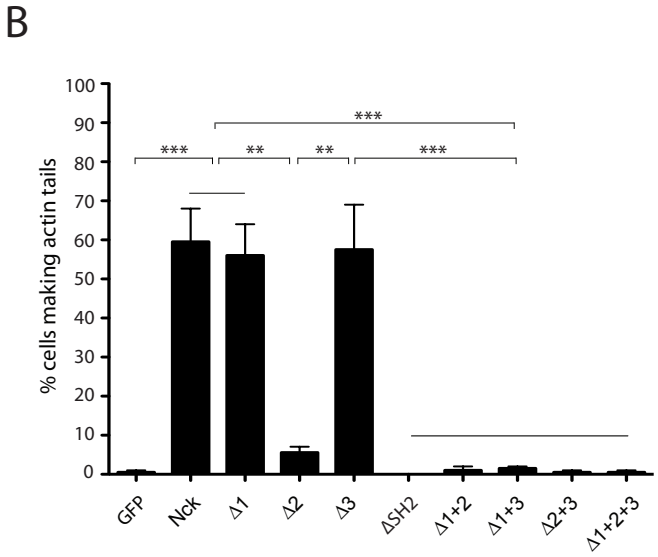

Figure 5.11. In the absence of Grb2 recruitment, the 2nd SH3 domain of Nck is essential for actin tail formation

(A) Immunofluorescence analysis shows that GFP-Nck or the Nck mutants are recruited to virus particles in A36-Y132F infected cells. Actin tails are no longer induced in cells expressing NckΔ2. Yellow arrows indicate the localisation of the GFP signal to virus particles. **(B)** Quantification of the percentage of A36-Y132F infected cells with actin tails reveals that mutating the 2nd SH3 domain alone, or any two SH3 domains inhibits actin tail formation in the absence of Grb2. Error bars represent the SEM of three independent experiments. ** = p< 0.01, *** = p<0.001.

5.4 Summary

In this chapter, I used a combination of Far Western blotting and immunoprecipitation to show that Nck interacts with N-WASP via a single dominant binding site. Furthermore, I demonstrated that the interaction of Nck and N-WASP is not essential for actin tail formation. However, Nck stabilises N-WASP at virus particles and the loss of this interaction results in an increased rate of exchange of N-WASP. This correlates with the induction of shorter actin tails and a slower rate of actin-based motility of virus particles. In the absence of Grb2 recruitment, GFP-N-WASPΔNck is weakly localised to virus particles and the resulting actin tails are very short. This indicates that Nck and Grb2 cooperate to recruit N-WASP to virus particles. However, a synergistic increase in the rate of exchange of N-WASP was not observed in the absence of interactions with both Nck and Grb2. In agreement with this, during infection with the A36-Y132F virus, the speed of virus particles is similar in cells expressing either GFP-N-WASP or GFP-N-WASPΔNck. Furthermore, I have demonstrated that the second SH3 domain of Nck interacts preferentially with WIP, while the third SH3 domain interacts with N-WASP. Consistent with an important role for WIP in recruiting N-WASP to vaccinia virus particles, loss of the 2nd, but not the 3rd SH3 domain of Nck inhibited actin tail formation during infection with A36-Y132F virus.

Chapter 6. Discussion

Nck and N-WASP signalling networks play an important role in regulating Arp2/3 dependent actin polymerisation in a variety of cellular contexts including cell migration and endocytosis (Anitei and Hoflack, 2012; Ridley, 2011). Deregulation of these networks results in aberrant cytoskeletal rearrangements leading to changes in cell adhesion and migration, which contribute to pathological conditions including metastatic cancer (Olson and Sahai, 2009). In order to gain a greater understanding of the connectivity and hierarchy within these networks, I have exploited the robust localisation of a Nck and N-WASP dependent signalling network to vaccinia virus. Examination of this network revealed an essential role for WIP in vaccinia actin tail formation. Furthermore, WIP was found to play an essential role in linking Nck to N-WASP in order to promote Arp2/3 dependent actin polymerisation. My findings have important implications for other Nck and N-WASP dependent signalling networks.

6.1 WIP or WIRE is essential for actin tail formation

Both Nck and N-WASP have previously been shown to be required for actin tail formation of vaccinia virus (Snapper et al., 2001; Weisswange et al., 2009). However, despite the robust localisation of WIP to virus particles undergoing actin-based motility, it was not clear if WIP plays an accessory or an essential role in this process (Moreau et al., 2000; Zettl and Way, 2002). Infection of MEFs lacking WIP expression revealed that vaccinia virus could still induce actin tails in the absence of WIP (Figure 3.2 A). However, these actin tails were shorter and moved more slowly than actin tails formed in wild type MEFs (Figure 3.2 B). This lead to two potential hypotheses, either WIP plays a non-essential, secondary role in the Nck and N-WASP signalling network or another protein can compensate for the loss of WIP. Consistent with the latter idea, recruitment of WIRE, a homologue of WIP (Aspenstrom, 2002; Kato et al., 2002), to the virus was strikingly increased in WIP deficient cells (Figure 3.3A). Treatment of WIP -/- cells with siRNA against WIRE confirmed that the actin tails observed in the absence of WIP were induced by WIRE (Figure 3.4 B, C). Furthermore, expression of GFP-tagged WIP or WIRE

rescues actin tails in WIP-/- MEFs treated with WIRE siRNA (Figure 3.5 A). In addition, the actin tails induced by vaccinia virus are longer in cells expressing GFP-WIP than those in cells expressing GFP-WIRE (Figure 3.5 B). Taken together, it is clear from my data that either WIP or WIRE is essential for the functioning of the signalling network. This agrees with data from a study showing that WIP is essential for actin comet formation induced by clustering the SH3 domains of Nck at the plasma membrane (Ditlev et al., 2012). However, in this study, WIRE was not observed to compensate for the loss of WIP. This is likely the result of differences in experimental set up. In their study, the SH3 domains of Nck were fused to a transmembrane domain and artificially clustered using an extracellular antibody. Thus, Nck is not freely exchanging in the system. Furthermore, in contrast to the situation in vaccinia virus, WIP is recruited to these Nck aggregates independently of N-WASP (Ditlev et al., 2012; Snapper et al., 2001; Weisswange et al., 2009).

WIRE can functionally replace WIP in vaccinia actin tail formation, however WIP is likely the predominant molecule. Expression of GFP-WIRE rescues the percentage of cells inducing actin tails to a similar extent as expression of GFP-WIP, but the WIP dependent actin tails are longer than those induced by GFP-WIRE. Thus, they more closely resemble the actin tails formed in the wild type cell line. Moreover, knockdown of WIRE in wild type cells that express WIP does not affect actin tail formation (Figure 3.6 A, B), which is consistent with the weak recruitment of WIRE to extracellular virus particles observed in these cells (Figure 3.3 B). The evidence that WIRE can replace WIP in the vaccinia signalling network has implications for the study of WIP in other systems. For example, WIP-/- cells were used to demonstrate that WIP is not essential for actin tail formation by *Mycobaterium marinum* (Stamm et al., 2005). This may because WIRE can also compensate for the loss of WIP in the N-WASP dependent actin-based motility of this pathogen. Furthermore, while loss of verprolin, the yeast orthologue of WIP, results in major defects in polarity, growth and endocytosis in *S. cerevisiae* (Naqvi et al., 2001; Naqvi et al., 1998; Thanabalu and Munn, 2001), WIP null mice do not exhibit any gross abnormalities, and the defects observed are mainly confined to the immune system (Anton et al., 2002; Curcio et al., 2007). A similarly mild phenotype has been observed for CR16 null mice, where the only documented defect is male

specific sterility (Suetsugu et al., 2007). Functional redundancy between WIP, WIRE and CR16 would account for the relatively minor defects in mammals.

WIP has previously been shown to inhibit the activity of N-WASP until the correct combination of activation signals is received (Ho et al., 2004; Martinez-Quiles et al., 2001). However in the absence of WIP, vaccinia virus cannot induce actin tails. This suggests that WIP fulfils other functions than repressing the activity of N-WASP. In the absence of WIP and WIRE, N-WASP is not observed at virus particles (Figure 3.12 B), suggesting that WIP is required to mediate the recruitment of N-WASP. Consistent with this, another study has also shown that WIP is important for the localisation of WASP to podosomes (Chou et al., 2006). Taken together with previous observations showing that WIP is not localised to virus particles in the absence of N-WASP, my data indicates that WIP and N-WASP are recruited as a complex (Snapper et al., 2001; Weisswange et al., 2009). Nck is recruited to virus particles independently of WIP, N-WASP and Grb2 (Figure 3.12 A) (Weisswange et al., 2009). Thus it is not unreasonable to assume that Nck is responsible for the recruitment of a complex consisting of WIP and N-WASP.

6.1.1 The dynamics of WIP

I used FRAP to analyse the rate of exchange of WIP in MEFs lacking expression of endogenous WIP and WIRE. GFP-WIP was found to have a half-time of fluorescence recovery of 0.93 ± 0.06 seconds (Figure 3.7 A). This is similar to the half-time of recovery of GFP-WIP in Hela cells expressing endogenous WIP, which was previously found to be 0.77 ± 0.06 seconds (Weisswange et al., 2009). As is the case for Nck and N-WASP, this demonstrates that the presence of endogenous protein does not affect the rate of exchange of the GFP-tagged protein (Weisswange et al., 2009). This is also evidence that the rate of exchange of WIP is independent of cell type. Furthermore, as observed before, the fluorescence intensity of WIP recovered to ~95% indicating that a stable population of WIP is not maintained at virus particles. Recovery of fluorescence to almost 100% was also observed for Nck, N-WASP and Grb2 (Figure 5.5 A) (Weisswange et al., 2009). A number of studies have shown that the signalling networks, which regulate Arp2/3 dependent actin polymerisation in the lamellipodia of migrating cells are also

constantly exchanging (Lai et al., 2008; Millius et al., 2009; Millius et al., 2012; Weiner et al., 2007). The perpetual renewal of the signalling networks involved in actin polymerisation is probably important to enable the cell to respond rapidly to environmental cues. Furthermore, the constant nucleation of actin filaments is likely to be important to generate the force required to propel virus particles, or the leading edge of the cell, forward (Pollard and Borisy, 2003). Interestingly, the dynamic turnover of these cellular networks is dependent on active actin polymerisation (Millius et al., 2009; Millius et al., 2012; Weiner et al., 2007). This is also true of the vaccinia actin-signalling network, as Cytochalasin D treatment decreases the recovery of WIP and N-WASP at virus particles. Thus, a general mechanism of regulation of these networks appears to involve the initiation of a positive feedback loop in which actin polymerisation stimulates the renewal of the signalling networks that promote Arp2/3 complex-dependent actin nucleation.

My FRAP analysis has shown that the rates of exchange of WIP and N-WASP in the signalling complex are very different (Figure 3.7A, 5.5A) (Weisswange et al., 2009). WIP has a half-time of recovery of 0.93 seconds, while N-WASP recovers more slowly at 2.9 seconds. If WIP and N-WASP are recruited as a complex, this data suggests that they dissociate at different rates. As inhibition of active actin polymerisation by Cytochalasin D decreased the recovery of both WIP and N-WASP to a similar extent, this may indicate that active actin polymerisation promotes the dissociation of the WIP/N-WASP complex. It would be interesting to examine if this is indeed the case and whether dissociation is required for actin polymerisation. FRET experiments could give insight into whether dissociation occurs. Moreover, a previous study employed a construct, in which full length WIP and N-WASP are fused, to demonstrate that dissociation is not required for IL-2 production (Dong et al., 2007). Thus, a similar approach could be used to determine if the same is true for actin polymerisation.

6.1.2 Comparison of WIP and WIRE

The actin tails induced by WIRE are shorter and move more slowly than those induced by WIP (Figure 3.1 A, B). This is curious given the similarities between the two molecules. Both WIP and WIRE have two actin-binding (WH2) domains, a

proline rich region and a WBD (Aspenstrom, 2005; Garcia et al., 2012). Despite this, FRAP analysis revealed that WIP and WIRE have different rates of exchange in the vaccinia signalling network. WIRE has a rate of exchange that is ~2.3 fold faster than WIP. Increased rate of exchange of a protein can reflect the loss interactions with other molecules. For, example, in the case of N-WASP, loss of interaction with Grb2 or with the actin cytoskeleton resulted in a more rapid exchange (Weisswange et al., 2009). Thus, the greater instability of WIRE compared to WIP may reflect a reduced capacity to interact with the other components of the network. Interestingly, the loss of Grb2 did not affect the actin tails formed in WIP-/- MEFs, although the actin tails in the WT cells were shorter and had reduced rates of actin based motility (Figure 3.8 A, B). Furthermore, the rate of exchange of WIP increased in the absence of Grb2 recruitment, but WIRE was unaffected (Figure 3.10 A). Thus, it is possible that Grb2 interacts only with WIP but not with WIRE.

At this time, a direct interaction between WIP and Grb2 has not been established, although it seems likely as WIP contains numerous PxxP motifs, which could bind to the SH3 domains of Grb2. Interestingly, a high stringency examination of WIP using Scansite (Obenauer et al., 2003), reveals eight potential Grb2 interaction motifs, while a similar scan of WIRE reveals only one potential site. Furthermore, the putative site in WIRE is located at the C-terminus of the protein, within the WBD making unlikely that WIRE could interact with both N-WASP and Grb2 simultaneously. This data must be interpreted with caution as these predicted sites are based on a consensus motif that may not be complete. Thus, further experiments are required to clarify the interaction of Grb2 with WIP or WIRE.

The Nck binding sites identified in WIP both contain the motif PxxPxRxL (Figure 4.1 B; Chapter 6.2, 6.5.1). This motif is present only once in WIRE (residues 271-282). The presence of only a single Nck binding site in WIRE could also contribute to increased dynamics of WIRE. A detailed comparison of the interactions of WIP and WIRE with Nck, N-WASP and Grb2 is required in order to understand the differences in their function in vaccinia actin tail formation. Distinct functions of WIP and WIRE have been observed in cells. For example, WIRE but not WIP synergizes with IRSp53 to induce the formation of filopodia (Lim et al., 2008; Misra et al., 2010). Furthermore, the stabilization of newly formed actin filaments at

adherens junctions is specifically dependent on WIRE (Kovacs et al., 2011). Thus understanding the differential regulation of WIP and WIRE in vaccinia actin tail formation may shed light on diverse cellular processes.

6.2 The recruitment of WIP to vaccinia virus

Having established the importance of the role of WIP in actin tail formation, I wanted to understand how it functions with Nck and N-WASP to induce actin polymerisation. Nck is recruited upstream of WIP, thus I hypothesised that it is important for localising WIP to virus particles (Figure 3.12 A) (Weisswange et al., 2009). While a previous study had demonstrated that the second SH3 domain of Nck interacts with a truncation of WIP (residues 321-503), the specific Nck binding sites in WIP had not been identified (Anton et al., 1998). WIP is a highly proline rich protein, which contains many putative SH3 binding motifs (Figure 3.3 A) (Ramesh et al., 1997). Due to this, I decided to take an unbiased approach to identify those that were specific for Nck. A previous study had successfully mapped the Nck binding site in PAK by performing Far Western analysis of a peptide array (Zhao et al., 2000). Thus, I probed a peptide array comprising the entire sequence of WIP with purified His-Nck1 and identified two potential binding sites (Figure 4.1 B). The second of these sites is contained in the truncation of WIP previously found to interact with the second SH3 domain of Nck (Anton et al., 1998). *In vitro* pulldown assays confirmed that these peptides could bind Nck. (Figure 4.1 C). Furthermore, while mutation of the key proline residues in each site in full length WIP resulted in decreased Nck binding, it was necessary to combine both mutations to abrogate the interaction completely (Figure 4.2). Thus both sites can mediate an interaction between WIP and Nck. Loss of the interaction between WIP and Nck did not affect the ability of WIP to bind to N-WASP. This agrees with previous studies showing that the Nck and N-WASP binding sites in WIP do not overlap (Anton et al., 1998; Martinez-Quiles et al., 2001). Interestingly, in the absence of an interaction between Nck and WIP, the presence of N-WASP is not sufficient to recruit Nck into the complex (Figure 4.2). This suggests that a prior interaction between Nck and WIP is required before N-WASP can interact with Nck. This is consistent with a model in which Nck interacts with WIP to recruit the WIP/N-WASP complex to the membrane, where other signals, for example PIP_2, cooperate with Nck to relieve

the autoinhibitory contacts in N-WASP. Alternatively, the interaction of Nck with WIP may induce a conformational change in the WIP/N-WASP complex that is required to promote the interaction of Nck and N-WASP (Figure 6.1).

Loss of the interaction between Nck and WIP did not result in loss of recruitment of WIP to virus particles, although a 25% decrease in the percentage of cells with actin tails was observed (Figure 4.3 A, B). However, the rate of exchange of WIP increased in the absence of an interaction with Nck (Figure 4.4 A). This demonstrates that WIP is stabilised in the signalling network by its interaction with Nck. In the absence of Grb2 recruitment, loss of the interaction between Nck and WIP resulted in extremely weak and transient recruitment of WIP to virus particles (Figure 4.7 B, C). Furthermore, there was a dramatic decrease in the ability of vaccinia virus to induce actin tails (Figure 4.6 A, B). Thus, Nck recruits WIP to virus particles, although Grb2 also contributes to its localisation and stabilisation. As mentioned above, the interaction of Grb2 and WIP has not been established (Chapter 6.1.2), but N-WASP may mediate the recruitment of WIP by Grb2. Consistent with this, WIP-FFAA, which cannot interact with N-WASP, is not recruited to virus particles during A36-Y132F infection (Figure 4.10 A, B). In addition, Grb2 alone is not sufficient for recruitment of WIP, as WIPΔNck+FFAA is not recruited to virus particles even during WR infection (Figure 4.11 A, B). This is not unexpected as in the absence of Nck Grb2 is not sufficient to induce actin tail formation (Scaplehorn et al., 2002). Taken together, this data demonstrates that cooperative interaction of WIP with at least two of Nck, N-WASP and Grb2 is required to recruit its recruitment to vaccinia virus.

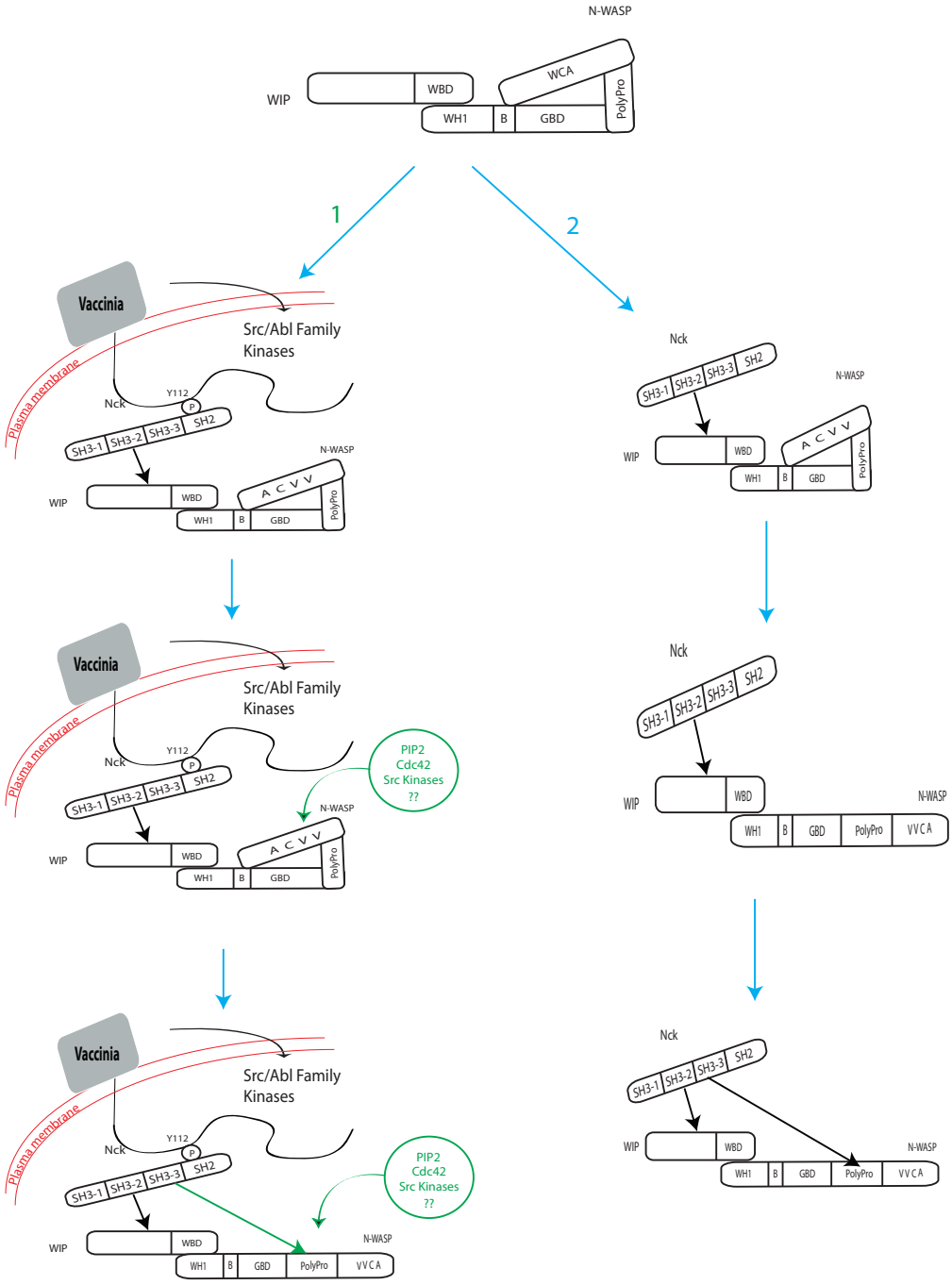

Figure 6.1. WIP promotes the interaction of Nck and N-WASP

The schematic shows two possible mechanisms by which the interaction of Nck and WIP could promote the interaction of Nck with N-WASP. **(1)** Nck interacts with WIP to recruit the WIP/N-WASP complex to vaccinia virus at the plasma membrane where other signals cooperate with Nck to relieve the autoinhibition of N-WASP. **(2)** The binding of Nck to WIP induces as conformational change in the WIP/N-WASP complex that helps to relieve the autoinhibition of N-WASP, thus allowing Nck to bind.

6.3 The interaction of WIP and N-WASP

My data indicates that the recruitment of WIP by Nck is important for the localisation of N-WASP to virus particles. To investigate this further, I examined the functional consequences of abrogating the direct interaction of WIP and N-WASP. Expression of GFP-WIP-FFAA, which does not interact with N-WASP (Figure 4.7 B) (Peterson et al., 2007; Zettl and Way, 2002), in WIP-/- cells treated with WIRE siRNA resulted in a significant inhibition of WR induced actin tails (Figure 4.8 A). Less than 40% of infected cells expressing WIP-FFAA could support actin tail formation and those actin tails that were induced were much shorter and moved extremely slowly in comparison to actin tails in cells expressing wild type WIP or WIP∆Nck (Figures 4.8 B, 4.9 B, 4.4 B). Furthermore, the recruitment of WIP-FFAA to virus particles was very weak (Figure 4.8 A).

My data suggests that WIP and N-WASP are recruited to virus particles as a complex (Figure 3.12 B). However, the localisation of WIP-FFAA to virus particles and the induction of weak actin polymerisation suggest that a direct interaction of the two proteins is not absolutely required. This seemingly contradictory data can be explained by the fact that WIP can still interact with Nck in the absence of an interaction with N-WASP (Figure 4.7 B). This interaction is likely to stabilise Nck at virus particles sufficiently to facilitate a low level of N-WASP recruitment by Nck. The presence of Grb2 will also recruit and stabilise N-WASP and WIP in the network. This model is consistent with data showing that the recruitment of WIP-FFAA is lost during infection with the A36-Y132F virus (Figure 4.10 A, B). Comparing the rate of exchange of Nck at virus particles in the absence of WIP/WIRE and in cells expressing WIP-FFAA would lend support to this theory.

The rate of exchange of WIP-FFAA is 0.27 ± 0.04 seconds, which is more rapid than either wild type WIP (0.85 ± 0.06) or WIP∆Nck (0.55 ± 0.05) (Figures 4.4 A, 4.9 A). In both cases, the increase in the rate of exchange of WIP correlated with a decrease in the actin-based motility of the virus particles (Figures 4.4 B, 4.9 B). Computational modelling studies have linked the rate of actin-based motility to the rate of actin filament nucleation by the Arp2/3 complex (Dawes et al., 2006). Consequently, this data suggests that the stability of WIP in the signalling network

may directly influence the rate of nucleation. Interestingly, in contrast to WIP, the increased rate of exchange of N-WASP was found to correspond to an increase in the rate of actin-based motility of vaccinia virus (Weisswange et al., 2009). This suggests a balance between the stabilities of WIP and N-WASP in the network is crucial for regulating actin polymerisation. It would be interesting to determine the rate of exchange of N-WASP at virus particles in cells expressing WIP-FFAA or WIP∆Nck to further investigate this hypothesis.

6.4 The interaction of Nck and N-WASP is not essential for actin tail formation

In the absence of Grb2 recruitment, abrogating the interaction between WIP and N-WASP results in a complete loss of actin polymerisation (Figure 4.10 A, B). This suggests that WIP is required to link N-WASP to Nck in order to promote Arp2/3 dependent actin polymerisation. However, Nck can also directly interact with and potently activate purified N-WASP *in vitro*, although these studies were done in the absence of WIP (Rohatgi et al., 2001; Tomasevic et al., 2007). To determine the importance of the interaction between Nck and N-WASP, I set out to identify the Nck binding site in N-WASP. Far western analysis of a peptide array comprising the sequence of N-WASP revealed two potential Nck binding sites (Figure 5.1 A). Each peptide contains a polyproline type II PxxPxR motif, which fits the consensus for SH3 domain binding (Li, 2005). *In vitro* pulldown assays confirmed that both peptides interact with recombinant His-Nck (Figure 5.1 B). Mutation of the two key proline residues in the PxxPxR motif resulted in a marked decrease in, but not complete loss of, Nck binding (Figure 5.1 B). In addition to the PxxPxR motif, the first peptide contains two extra PxxP motifs, while one other PxxP motif is present in the second peptide (Figure 5.1 A). These may account for the residual interaction of the mutant peptides with Nck. Mutation of the key proline residues in both potential binding sites reduced the interaction of Nck and N-WASP in HeLa cells, however the loss of this interaction did not affect binding of Nck to WIP (Figure 5.2 A). Based on this result, and my data suggesting that the binding of WIP and Nck promotes the interaction of Nck and N-WASP (Figure 4.2), I hypothesised that the residual Nck binding may be due to the presence of WIP.

This was confirmed by the immunoprecipitation experiments in WIP-/- cells treated with WIRE siRNA, which demonstrated that Nck could not interact with N-WASPΔNck (Figure 5.2 B). This data confirms and extends the analysis of Weiss and colleagues, who identified these binding sites by probing a peptide array corresponding to the proline rich region of N-WASP with the isolated third SH3 domain of Nck (Weiss et al., 2009). In this study the binding to the first peptide was very weak, furthermore my immunoprecipitation data suggests that the second Nck binding site is more important for mediating the interaction with N-WASP. Taken together, this suggests that N-WASP contains a single dominant Nck binding site.

Given the ability of Nck to activate N-WASP *in vitro*, it was surprising that a greater effect on actin tail formation was not observed after disrupting the interaction between Nck and N-WASP. The percentage of cells inducing actin tails, as well as the average number of actin tails per cell was similar in cells expressing either N-WASP or N-WASPΔNck (Figure 5.4 A, B). However, the actin tails induced were shorter and the rate of actin-based motility was reduced (Figure 5.4 A, B; Figure 5.5 B). As actin polymerisation still occurs in the absence of an interaction of Nck and N-WASP, this strongly suggests that Nck may not the sole activator of N-WASP in the signalling network. Furthermore, this is additional evidence that the major pathway of N-WASP recruitment to virus particles is mediated by WIP, not Nck. A small but significant increase in the rate of exchange of N-WASP was observed in the absence of an interaction with Nck suggesting that Nck does function to stabilise N-WASP in the signalling network (Figure 5.5 A).

As Grb2 also interacts with and activates N-WASP (Carlier et al., 2000), it is plausible that this interaction is sufficient to enable N-WASP to stimulate the Arp2/3 complex. However, surprisingly this was not the case. Infection with the A36-Y132F virus revealed that cells expressing N-WASPΔNck can still support actin tail formation as well as those expressing wild-type N-WASP (Figure 5.6 A, B). As expected, loss of Grb2 results in a decrease in actin tail length in cells expressing wild type N-WASP (Weisswange et al., 2009), while the N-WASPΔNck actin tails were even shorter (Figure 5.6 B). Thus neither Nck nor Grb2 is essential for the activation of N-WASP at virus particles. This raises the intriguing possibility that other, unknown molecules are involved in actin tail formation. Likely candidates are

Cdc42 or phosphatidylinositol (4,5)-bisphosphate (PIP_2), both of which are established activators of N-WASP (Miki et al., 1998; Papayannopoulos et al., 2005; Rohatgi et al., 1999; Rohatgi et al., 2001). Cdc42 has previously been observed at virus particles inducing actin tails (Moreau et al., 2000). However, expression of a dominant negative mutant of Cdc42 as well as treatment of the cells with Toxin B, an inhibitor of Rho GTPases, did not change the percentage of infected cells with actin tails (Moreau et al., 2000). Assuming the role of Cdc42 is to cooperate with Nck and Grb2 to activate N-WASP, it is not unexpected that a major defect in actin tail formation is not be observed upon inhibition of Cdc42. Consequently, a more detailed analysis of actin tail formation in the absence of functional Cdc42 or in cells expressing an N-WASP mutant that cannot interact with Cdc42 (N-WASP H208D) (Miki et al., 1998) may reveal a previously unappreciated role for this protein. The role of PIP_2 in the actin tail formation has never been investigated, however its ability to activate N-WASP, even in the presence of WIP, makes it an attractive candidate as a regulator of actin tails (Martinez-Quiles et al., 2001). It would be informative to determine if PIP_2 is enriched in the plasma membrane adjacent to virus particles that are inducing actin tails. Furthermore, analysis of actin tail formation in N-WASP-/- cells expressing N-WASP that is defective in PIP_2 binding (Papayannopoulos et al., 2005) would give insight into the importance of this interaction. Combining the ΔNck mutation with mutations that interfere with the interaction between N-WASP and Cdc42 or PIP_2, or both, during A36-Y132F infection would reveal if these are the only activators involved in actin tail formation.

Other potential candidates to cooperate with Nck and Grb2 to activate N-WASP are the Src and Abl family tyrosine kinases. These are recruited to extra-cellular virus particles and mediate the phosphorylation of A36 of tyrosines 112 and 132, which are essential for actin tail formation (Newsome et al., 2004; Newsome et al., 2006). These kinases also contain SH3 domains that could interact with N-WASP. Interestingly, Arg, an Abl family kinase that localises to vaccinia, can bind to the proline rich region of N-WASP and thus promote its activation of the Arp2/3 complex (Miller et al., 2010; Newsome et al., 2006). Furthermore, Src family kinases have been shown to phosphorylate N-WASP, resulting in the stimulation of Arp2/3 dependent actin polymerisation (Suetsugu et al., 2002; Torres and Rosen, 2003, 2006).

As expected, in the absence of Grb2 recruitment, the rate of exchange of N-WASP at virus particles is more rapid than during WR infection. This is consistent with the previously established role of Grb2 in stabilising the vaccinia signalling network (Weisswange et al., 2009). N-WASP∆Nck also had a faster rate of exchange in the absence of Grb2 recruitment, however, no synergistic increase in the half-life of fluorescence recovery due to the loss of Nck binding was observed (Figure 5.7 A). Furthermore, virus particles in cells expressing both N-WASP and N-WASP∆Nck moved at similar speeds (Figure 5.7 A). This implies that in the absence of Grb2 recruitment, another molecule can compensate for its loss. This molecule could be either Cdc42 or PIP_2, however as this factor is only important in the absence of Grb2, it seems likely that it would compete directly with Grb2 for binding to N-WASP. This suggests that another SH3 domain containing molecule is involved, which makes the Src and Abl family kinases attractive candidates. One way to test this hypothesis would be to identify the Grb2 binding sites in N-WASP. If another protein competes with Grb2 to bind and stabilise N-WASP, mutating this site(s) in combination with the Nck binding sites should result in an additional phenotype. One interesting possibility is that in the absence of Grb2 recruitment, Nck could interact with the Grb2 binding sites in N-WASP. *In vitro* binding and competition assays would be required to determine if this is the case. Alternatively, loss of Grb2 recruitment may simply remove a physical block that prevents the interaction of the unknown factor with N-WASP.

6.5 The second SH3 domain of Nck is essential for actin tail formation

My data suggests that the interaction of Nck with WIP is the most important interaction for the recruitment of the WIP/N-WASP complex, while a subsequent interaction of Nck with N-WASP plays a secondary role in stabilising and most likely activating N-WASP. As Nck contains three SH3 domains, a single Nck molecule could interact with WIP and N-WASP simultaneously. To investigate whether this is possible I set out to determine if any of the three Nck SH3 domains interact specifically with either WIP or N-WASP. *In vitro* pulldown assays showed that the second SH3 domain of Nck interacts specifically with the peptides identified in WIP, while the third SH3 domain preferentially interacts with the N-

WASP peptides (Figure 5.8). Thus a single Nck molecule could interact with both WIP and N-WASP. Alternatively, the second SH3 domain of one Nck molecule could recruit N-WASP via WIP, while the third SH3 domain of another Nck molecule subsequently directly interacts with the same N-WASP (Figure 6.2). Support for the latter model comes from a recent study in which a computational approach was used to estimate the ratio of Nck, N-WASP and the Arp2/3 complex present in comet tails generated by inducing aggregation of membrane bound Nck SH3 domains (Ditlev et al., 2012). This approach determined that the ratio of Nck:N-WASP:Arp2/3 complex is 4:2:1, which is consistent with the theory that optimal activation of the Arp2/3 complex occurs upon binding of two N-WASP molecules (Padrick et al., 2008; Padrick et al., 2011). Unfortunately, this study did not measure the ratio of WIP present in the complex. Moreover, the contribution of Grb2 to the vaccinia signalling network must also be taken into account. Thus, without knowing the relative amounts of each of the components, a complete picture of the vaccinia signalling network cannot be obtained. Ratio imaging is one way to determine the stoichiometry of the signalling network that is recruited to virus particles. In this technique, the fluorescence intensity of a GFP-tagged protein of interest, for example Nck, is measured and then referenced to the fluorescence intensity of an RFP-tagged viral core protein, which should remain constant. In this way, the relative amounts of a number of different GFP-tagged proteins in different cell lines can be compared.

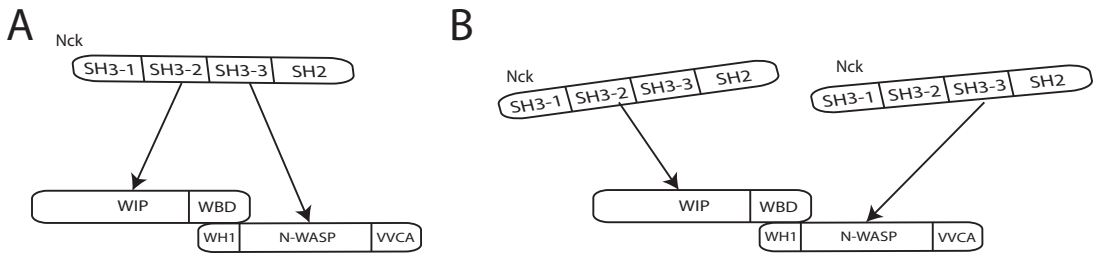

Figure 6.2. Stoichiometry of the Nck, WIP and N-WASP complex

The schematic shows two possible modes of interaction of Nck with WIP/N-WASP. (1) A single Nck molecule could interact with WIP and N-WASP simultaneously or (2) One molecule of Nck interacts with WIP, while a second Nck molecule interacts with N-WASP.

Two binding sites were identified for Nck in each of WIP and N-WASP, although one of the N-WASP binding sites appears to be more dominant. All four of these binding sites could be occupied if twice the amount of Nck is recruited to the virus as N-WASP and WIP. In addition, Nck and Grb2 could interact with adjacent WIP/N-WASP complexes resulting in crosstalk that would stabilise and organise these molecules into an array that results in maximal Arp2/3 complex activation. A number of studies have demonstrated the importance of spatial arrangement of molecules in Nck/N-WASP signalling networks in regulating actin polymerisation. Most recently, manipulating the density of A36 molecule on the virus particle was found to perturb the rate of exchange of N-WASP as well as its spatial organisation, resulting in longer, faster moving actin tails (Humphries et al., 2012). The density of PIP_2 molecules on rocketing vesicles and ActA on the surface of *Listeria* is also crucial for optimal actin based motility (Co et al., 2007; Footer et al., 2008). This is further incentive to determine the density and relative amounts of each protein in the network, as only with this information can the relationship between the spatial organisation of the complex and the regulation of actin polymerisation be more fully understood.

Examination of the functional importance of each of the SH3 domains of Nck in actin tail formation further reinforces the hypothesis that the interaction between Nck and WIP is critical for N-WASP recruitment. In the absence of Grb2 recruitment, the second SH3 domain of Nck, which interacts with WIP, is essential for actin tail formation (Figure 5.10 A, B). Furthermore, even during WR infection, mutation of any two Nck SH3 domains results in the loss of actin tail formation (Figure 5.9 A, B). This is consistent with a model in which the second SH3 domain of Nck recruits the WIP/N-WASP complex, but the presence of either the first or more likely the third SH3 domain is also required to activate N-WASP. In addition, while the third SH3 domain is clearly the most important for interacting with the N-WASP peptide, mutation of the first SH3 domain also resulted in a slight decrease in binding to both peptides, indicating it could also contribute to N-WASP activation (Figure 5.8 B). Analysis of the localisation of N-WASP to virus particles in cells expressing the Nck SH3 mutants during A36-Y132F infection would give further insight into this hypothesis. Mutation of the second SH3 domain would result in the loss of N-WASP recruitment, however in the absence of both the first and the third

SH3 domains (NckΔ1+3), N-WASP would still be recruited. As actin tails are not induced in cells expressing this mutant, this would demonstrate that loss of these SH3 domains results in a defect in the activation, rather than recruitment of N-WASP.

Clustering the SH3 domains of Nck is sufficient to induce N-WASP dependent actin polymerisation (Rivera et al., 2004). In this system, in contrast to my results, all three SH3 domains of Nck are necessary for efficient actin polymerization. However this study was carried out in cells expressing endogenous wild type Nck, and more importantly Nck cannot freely exchange as it is tethered to the plasma membrane. Another study demonstrated that either the second or the third SH3 domain of Nck is sufficient to induce actin polymerisation (Blasutig et al., 2008). While my data also demonstrates the second and third SH3 domains have key roles in the network, neither of them alone was sufficient to mediate actin polymerisation (Figure 5.9 A, B). In this system, as in my study, point mutations were used to disrupt the function of the SH3 domains of Nck and as Nck was recruited to the nephrin receptor in a phosphotyrosine dependent manner, it was able to freely exchange. However, in contrast to a single site in A36, the nephrin receptor contains three tyrosines that can recruit Nck (Blasutig et al., 2008). Thus the overall density of SH3 domains recruited by each nephrin receptor is likely to be higher than is recruited by A36. While the presence of the SH3 domains of Grb2 compensates somewhat for the loss of Nck SH3 domains, it is clearly not sufficient to fully replace it (Figure 5.10 A, B). In support of this hypothesis, Blasutig *et al*., demonstrated that if only one SH3 domain of Nck is functional, a single phosphotyrosine is not sufficient to induce actin polymerisation. It would be interesting to mutate the residues surrounding tyrosine 132 of A36 such that it can recruit Nck and then analyse the cooperativity between the SH3 domains of Nck in actin tail formation. Furthermore calculating the number of A36 molecules clustered at the virus, as well as what proportion of these are phosphorylated at any given time, would also give insight into the cooperativity within the system.

6.5.1 The binding specificities of the Nck SH3 domains

The results of my peptide pulldown assays clearly demonstrate that the SH3 domains of Nck have distinct binding preferences for the specific peptides identified in WIP and N-WASP. This data can be used to gain insight into the specificity determinants of the Nck SH3 domains. The second SH3 domain of Nck bound specifically to each of the peptides identified in WIP. Both of these peptides contained the motif PxxPxRxL (Figure 4.1 B). The second Nck binding peptide (NDETPRLPQRNLSLS) contains a sequence that precisely matches the consensus PxxPxRxxS, which was previously identified for the second SH3 domain (Zhao et al., 2000). This consensus was determined based on a detailed analysis of the interaction of Nck with PAK and it was found that negatively charged amino acids were poorly tolerated in positions C-terminal to the PxxP motif in PAK, while mutation of the serine residue resulted in loss of binding. Interestingly, my results show that the second SH3 domain of Nck can interact with a wider range of motifs, as the other peptide (SNRPPLPPTPSRALD), contains a negatively charged aspartic acid in place of the serine residue. The presence of a leucine residue in both peptides suggests that the combination of an arginine and a leucine may be more important for determining specificity than the serine residue. Phosphorylation of the consensus serine was also proposed to negatively regulate binding to the SH3 domain (Zhao et al., 2000). As the other Nck peptide also contains a serine residue, albeit at a different position, it is conceivable that phosphorylation could be a conserved mechanism for regulating SH3 domain binding. Interestingly, a search in the phosphosite database (www.phosphosite.org) revealed that serine 340 of WIP, which is contained in peptide two, has been identified as phosphorylated in a number of large scale proteomic investigations, including a study that characterised the phosphoproteosome of an acute myeloid leukaemia cell line (Weber et al., 2012).

In contrast to the WIP peptides, both of the peptides identified in N-WASP contain the motif PxxPxRG. As both of these peptides show a strong preference for interacting with the third SH3 domain of Nck, this consensus may be useful for identifying other proteins that specifically interact with this SH3 domain. Serine residues are also present in both these peptides suggesting that, as is the case for

the WIP peptides, phosphorylation is a possible mechanism for regulating the interactions between N-WASP and Nck (Zhao et al., 2000).

6.6 A model of the regulation of actin polymerisation by vaccinia virus

Taken together, my data demonstrates that WIP provides a crucial link between Nck and N-WASP. The second SH3 domain of Nck interacts with WIP, which subsequently recruits N-WASP via its WH1 domain. This facilitates the interaction of the first, or more likely the third, Nck SH3 domain with N-WASP, in order to promote its activation and stabilisation. This activation occurs in cooperation with Grb2 and other as yet unidentified molecules. Grb2 also functions to stabilise the recruitment of Nck and WIP to the virus, either directly or via N-WASP (Figure 6.2).

This is the first study that demonstrates that WIP (or WIRE) is essential for vaccinia actin based motility. Comparison of the hierarchy and connectivity within other Nck/WIP/N-WASP signalling networks is important to demonstrate that the mechanism uncovered in vaccinia actin tail formation is widespread. However, the importance of WIP in recruiting N-WASP to podosomes and in EPEC actin pedestal formation, as well as evidence that the interaction of WIP and N-WASP is required for invadopodia formation suggest that this is indeed the case (Chou et al., 2006; Wong et al., 2012; Yamaguchi et al., 2005). Furthermore, the majority of the causative mutations of Wiskott Aldrich Syndrome occur in the WH1 domain of WASP, suggesting that loss of binding of WIP is key to the pathogenesis of this condition (Jin et al., 2004; Moreau et al., 2000; Volkman et al., 2002). Thus, by exploiting the robust recruitment of this signalling network by vaccinia virus, we have been able to gain insights that have important implications for the Nck and N-WASP signalling networks that are key regulators of Arp2/3 dependent actin polymerisation in a variety of cellular contexts.

A number of unanswered questions remain, which are crucial for a complete understanding the regulation of Arp2/3 dependent actin polymerisation by Nck, WIP and N-WASP signalling networks. While the role of WIP in inhibiting the ability of N-WASP to stimulate Arp2/3 dependent actin polymerisation is clear (Ho et al., 2004;

Martinez-Quiles et al., 2001; Takano et al., 2008), the mechanism by which this inhibition occurs remains to be elucidated. Furthermore, the mechanisms employed by the activators of N-WASP to overcome this inhibition remain unknown. While many studies have examined the ability of Nck, Grb2 and other SH3 domain containing proteins to activate N-WASP, few have taken WIP into account. Furthermore, the finding that WIRE can functionally compensate for WIP raises interesting questions about the similarities and differences between these proteins. Importantly, it emphasises the importance of accounting for the contribution of both WIP and WIRE in any studies of these proteins. The induction of actin tail formation of vaccinia virus remains an important model for studying the regulation of Nck, WIP and N-WASP dependent signalling networks. Future studies should concentrate on determining the stoichiometry of the components in the network. Furthermore, carrying out FRET studies to determine the conformational changes in WIP and N-WASP during actin tail formation as well as elucidating the full complement of molecules involved in the signalling network will give important insights into the regulation of Arp2/3 dependent actin polymerisation. With this data in hand, it will be possible to use computational modelling methods to build up a complete picture of the spatial and temporal events that occur during vaccinia induced actin tail formation.

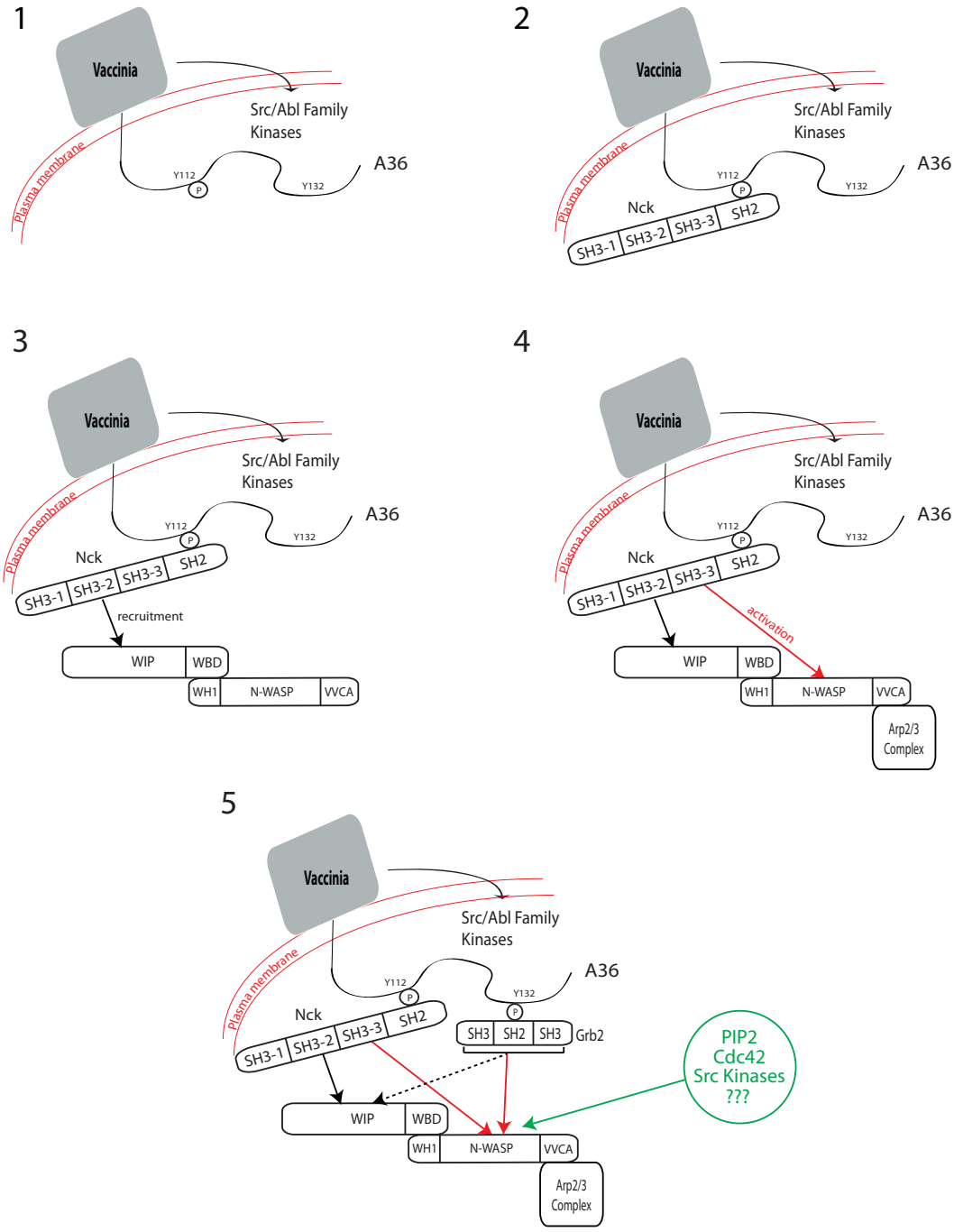

Figure 6.3. A model of the recruitment and activation of N-WASP during vaccinia actin tail formation

This schematic shows a possible mechanism for vaccinia induced actin polymerisation. Phosphorylation of A36 on Y112 by Src/Abl family kinases (1) recruits Nck (2). The second SH3 domain of Nck interacts with WIP, which recruits N-WASP via its WH1 domain (3). This allows the third SH3 domain of Nck to bind N-WASP resulting in its activation (4). Subsequently Grb2 and other, unknown molecules, interact with N-WASP to stabilise it and enhance its activation resulting in robust Arp2/3 dependent actin polymerisation (5).

Reference List

Abella, J.V., Parachoniak, C.A., Sangwan, V., and Park, M. (2010a). Dorsal ruffle microdomains potentiate Met receptor tyrosine kinase signaling and down-regulation. The Journal of biological chemistry *285*, 24956-24967.

Abella, J.V., Vaillancourt, R., Frigault, M.M., Ponzo, M.G., Zuo, D., Sangwan, V., Larose, L., and Park, M. (2010b). The Gab1 scaffold regulates RTK-dependent dorsal ruffle formation through the adaptor Nck. Journal of cell science *123*, 1306-1319.

Abercrombie, M., Heaysman, J.E., and Pegrum, S.M. (1970a). The locomotion of fibroblasts in culture. I. Movements of the leading edge. Experimental cell research *59*, 393-398.

Abercrombie, M., Heaysman, J.E., and Pegrum, S.M. (1970b). The locomotion of fibroblasts in culture. II. "RRuffling". Experimental cell research *60*, 437-444.

Ahuja, R., Pinyol, R., Reichenbach, N., Custer, L., Klingensmith, J., Kessels, M.M., and Qualmann, B. (2007). Cordon-bleu is an actin nucleation factor and controls neuronal morphology. Cell *131*, 337-350.

Aitio, O., Hellman, M., Kazlauskas, A., Vingadassalom, D.F., Leong, J.M., Saksela, K., and Permi, P. (2010). Recognition of tandem PxxP motifs as a unique Src homology 3-binding mode triggers pathogen-driven actin assembly. Proceedings of the National Academy of Sciences of the United States of America *107*, 21743-21748.

Aizawa, H., Sutoh, K., and Yahara, I. (1996). Overexpression of cofilin stimulates bundling of actin filaments, membrane ruffling, and cell movement in Dictyostelium. The Journal of cell biology *132*, 335-344.

Akin, O., and Mullins, R.D. (2008). Capping protein increases the rate of actin-based motility by promoting filament nucleation by the Arp2/3 complex. Cell *133*, 841-851.

Alexandropoulos, K., Cheng, G., and Baltimore, D. (1995). Proline-rich sequences that bind to Src homology 3 domains with individual specificities. Proceedings of the National Academy of Sciences of the United States of America *92*, 3110-3114.

Alvarez, D.E., and Agaisse, H. (2012). Casein kinase 2 regulates vaccinia virus actin tail formation. Virology *423*, 143-151.

Amann, K.J., and Pollard, T.D. (2001). Direct real-time observation of actin filament branching mediated by Arp2/3 complex using total internal reflection fluorescence microscopy. Proceedings of the National Academy of Sciences of the United States of America *98*, 15009-15013.

Anderson, B.L., Boldogh, I., Evangelista, M., Boone, C., Greene, L.A., and Pon, L.A. (1998). The Src homology domain 3 (SH3) of a yeast type I myosin, Myo5p, binds to verprolin and is required for targeting to sites of actin polarization. The Journal of cell biology *141*, 1357-1370.

Andrianantoandro, E., and Pollard, T.D. (2006). Mechanism of actin filament turnover by severing and nucleation at different concentrations of ADF/cofilin. Molecular cell *24*, 13-23.

Anitei, M., and Hoflack, B. (2012). Bridging membrane and cytoskeleton dynamics in the secretory and endocytic pathways. Nature cell biology *14*, 11-19.

Anton, I.M., de la Fuente, M.A., Sims, T.N., Freeman, S., Ramesh, N., Hartwig, J.H., Dustin, M.L., and Geha, R.S. (2002). WIP deficiency reveals a differential role for WIP and the actin cytoskeleton in T and B cell activation. Immunity *16*, 193-204.

Anton, I.M., Jones, G.E., Wandosell, F., Geha, R., and Ramesh, N. (2007). WASP-interacting protein (WIP): working in polymerisation and much more. Trends in cell biology *17*, 555-562.

Anton, I.M., Lu, W., Mayer, B.J., Ramesh, N., and Geha, R.S. (1998). The Wiskott-Aldrich syndrome protein-interacting protein (WIP) binds to the adaptor protein Nck. The Journal of biological chemistry *273*, 20992-20995.

Anton, I.M., Saville, S.P., Byrne, M.J., Curcio, C., Ramesh, N., Hartwig, J.H., and Geha, R.S. (2003). WIP participates in actin reorganization and ruffle formation induced by PDGF. Journal of cell science *116*, 2443-2451.

Arakawa, Y., Cordeiro, J.V., Schleich, S., Newsome, T.P., and Way, M. (2007a). The release of vaccinia virus from infected cells requires RhoA-mDia modulation of cortical actin. Cell host & microbe *1*, 227-240.

Arakawa, Y., Cordeiro, J.V., and Way, M. (2007b). F11L-mediated inhibition of RhoA-mDia signaling stimulates microtubule dynamics during vaccinia virus infection. Cell host & microbe *1*, 213-226.

Arjonen, A., Kaukonen, R., and Ivaska, J. (2011). Filopodia and adhesion in cancer cell motility. Cell adhesion & migration *5*, 421-430.

Armstrong, J.A., Metz, D.H., and Young, M.R. (1973). The mode of entry of vaccinia virus into L cells. The Journal of general virology *21*, 533-537.

Aspenstrom, P. (2002). The WASP-binding protein WIRE has a role in the regulation of the actin filament system downstream of the platelet-derived growth factor receptor. Experimental cell research *279*, 21-33.

Aspenstrom, P. (2004). The mammalian verprolin homologue WIRE participates in receptor-mediated endocytosis and regulation of the actin filament system by distinct mechanisms. Experimental cell research *298*, 485-498.

Aspenstrom, P. (2005). The verprolin family of proteins: regulators of cell morphogenesis and endocytosis. FEBS letters *579*, 5253-5259.

Baba, Y., Nonoyama, S., Matsushita, M., Yamadori, T., Hashimoto, S., Imai, K., Arai, S., Kunikata, T., Kurimoto, M., Kurosaki, T.*, et al.* (1999). Involvement of wiskott-aldrich syndrome protein in B-cell cytoplasmic tyrosine kinase pathway. Blood *93*, 2003-2012.

Badour, K., Zhang, J., Shi, F., Leng, Y., Collins, M., and Siminovitch, K.A. (2004). Fyn and PTP-PEST-mediated regulation of Wiskott-Aldrich syndrome protein (WASp) tyrosine phosphorylation is required for coupling T cell antigen receptor engagement to WASp effector function and T cell activation. The Journal of experimental medicine *199*, 99-112.

Bailly, M., Ichetovkin, I., Grant, W., Zebda, N., Machesky, L.M., Segall, J.E., and Condeelis, J. (2001). The F-actin side binding activity of the Arp2/3 complex is essential for actin nucleation and lamellipod extension. Current biology : CB *11*, 620-625.

Bailly, M., Macaluso, F., Cammer, M., Chan, A., Segall, J.E., and Condeelis, J.S. (1999). Relationship between Arp2/3 complex and the barbed ends of actin filaments at the leading edge of carcinoma cells after epidermal growth factor stimulation. The Journal of cell biology *145*, 331-345.

Balcer, H.I., Goodman, A.L., Rodal, A.A., Smith, E., Kugler, J., Heuser, J.E., and Goode, B.L. (2003). Coordinated regulation of actin filament turnover by a high-molecular-weight Srv2/CAP complex, cofilin, profilin, and Aip1. Current biology : CB *13*, 2159-2169.

Banon-Rodriguez, I., Monypenny, J., Ragazzini, C., Franco, A., Calle, Y., Jones, G.E., and Anton, I.M. (2011). The cortactin-binding domain of WIP is essential for podosome formation and extracellular matrix degradation by murine dendritic cells. European journal of cell biology *90*, 213-223.

Barnett, P., Bottger, G., Klein, A.T., Tabak, H.F., and Distel, B. (2000). The peroxisomal membrane protein Pex13p shows a novel mode of SH3 interaction. The EMBO journal *19*, 6382-6391.

Bartolini, F., and Gundersen, G.G. (2010). Formins and microtubules. Biochimica et biophysica acta *1803*, 164-173.

Bear, J.E., Rawls, J.F., and Saxe, C.L., 3rd (1998). SCAR, a WASP-related protein, isolated as a suppressor of receptor defects in late Dictyostelium development. The Journal of cell biology *142*, 1325-1335.

Becker-Herman, S., Meyer-Bahlburg, A., Schwartz, M.A., Jackson, S.W., Hudkins, K.L., Liu, C., Sather, B.D., Khim, S., Liggitt, D., Song, W.*, et al.* (2011). WASp-deficient B cells play a critical, cell-intrinsic role in triggering autoimmunity. The Journal of experimental medicine *208*, 2033-2042.

Benesch, S., Lommel, S., Steffen, A., Stradal, T.E., Scaplehorn, N., Way, M., Wehland, J., and Rottner, K. (2002). Phosphatidylinositol 4,5-biphosphate (PIP2)-induced vesicle movement depends on N-WASP and involves Nck, WIP, and Grb2. The Journal of biological chemistry *277*, 37771-37776.

Bernardini, M.L., Mounier, J., d'Hauteville, H., Coquis-Rondon, M., and Sansonetti, P.J. (1989). Identification of icsA, a plasmid locus of Shigella flexneri that governs bacterial intra- and intercellular spread through interaction with F-actin. Proceedings of the National Academy of Sciences of the United States of America *86*, 3867-3871.

Bernstein, B.W., and Bamburg, J.R. (2010). ADF/cofilin: a functional node in cell biology. Trends in cell biology *20*, 187-195.

Bladt, F., Aippersbach, E., Gelkop, S., Strasser, G.A., Nash, P., Tafuri, A., Gertler, F.B., and Pawson, T. (2003). The murine Nck SH2/SH3 adaptors are important for the development of mesoderm-derived embryonic structures and for regulating the cellular actin network. Molecular and cellular biology *23*, 4586-4597.

Blanchoin, L., Amann, K.J., Higgs, H.N., Marchand, J.B., Kaiser, D.A., and Pollard, T.D. (2000). Direct observation of dendritic actin filament networks nucleated by Arp2/3 complex and WASP/Scar proteins. Nature *404*, 1007-1011.

Blanchoin, L., and Pollard, T.D. (1998). Interaction of actin monomers with Acanthamoeba actophorin (ADF/cofilin) and profilin. The Journal of biological chemistry *273*, 25106-25111.

Blanchoin, L., and Pollard, T.D. (1999). Mechanism of interaction of Acanthamoeba actophorin (ADF/Cofilin) with actin filaments. The Journal of biological chemistry *274*, 15538-15546.

Blanchoin, L., and Pollard, T.D. (2002). Hydrolysis of ATP by polymerized actin depends on the bound divalent cation but not profilin. Biochemistry *41*, 597-602.

Blasco, R., and Moss, B. (1992). Role of cell-associated enveloped vaccinia virus in cell-to-cell spread. Journal of virology *66*, 4170-4179.

Blasutig, I.M., New, L.A., Thanabalasuriar, A., Dayarathna, T.K., Goudreault, M., Quaggin, S.E., Li, S.S., Gruenheid, S., Jones, N., and Pawson, T. (2008). Phosphorylated YDXV motifs and Nck SH2/SH3 adaptors act cooperatively to induce actin reorganization. Molecular and cellular biology *28*, 2035-2046.

Boczkowska, M., Rebowski, G., Petoukhov, M.V., Hayes, D.B., Svergun, D.I., and Dominguez, R. (2008). X-ray scattering study of activated Arp2/3 complex with bound actin-WCA. Structure *16*, 695-704.

Bonder, E.M., Fishkind, D.J., and Mooseker, M.S. (1983). Direct measurement of critical concentrations and assembly rate constants at the two ends of an actin filament. Cell *34*, 491-501.

Boujemaa-Paterski, R., Gouin, E., Hansen, G., Samarin, S., Le Clainche, C., Didry, D., Dehoux, P., Cossart, P., Kocks, C., Carlier, M.F*., et al.* (2001). Listeria protein ActA mimics WASp family proteins: it activates filament barbed end branching by Arp2/3 complex. Biochemistry *40*, 11390-11404.

Bouma, G., Burns, S.O., and Thrasher, A.J. (2009). Wiskott-Aldrich Syndrome: Immunodeficiency resulting from defective cell migration and impaired immunostimulatory activation. Immunobiology *214*, 778-790.

Brady, M.J., Campellone, K.G., Ghildiyal, M., and Leong, J.M. (2007). Enterohaemorrhagic and enteropathogenic Escherichia coli Tir proteins trigger a common Nck-independent actin assembly pathway. Cellular microbiology *9*, 2242-2253.

Braverman, L.E., and Quilliam, L.A. (1999). Identification of Grb4/Nckbeta, a src homology 2 and 3 domain-containing adapter protein having similar binding and biological properties to Nck. The Journal of biological chemistry *274*, 5542-5549.

Breitsprecher, D., Jaiswal, R., Bombardier, J.P., Gould, C.J., Gelles, J., and Goode, B.L. (2012). Rocket launcher mechanism of collaborative actin assembly defined by single-molecule imaging. Science *336*, 1164-1168.

Breitsprecher, D., Kiesewetter, A.K., Linkner, J., and Faix, J. (2009). Analysis of actin assembly by in vitro TIRF microscopy. Methods Mol Biol *571*, 401-415.

Bu, W., Lim, K.B., Yu, Y.H., Chou, A.M., Sudhaharan, T., and Ahmed, S. (2010). Cdc42 interaction with N-WASP and Toca-1 regulates membrane tubulation, vesicle formation and vesicle motility: implications for endocytosis. PloS one *5*, e12153.

Buday, L., Wunderlich, L., and Tamas, P. (2002). The Nck family of adapter proteins: regulators of actin cytoskeleton. Cellular signalling *14*, 723-731.

Cai, L., Makhov, A.M., Schafer, D.A., and Bear, J.E. (2008). Coronin 1B antagonizes cortactin and remodels Arp2/3-containing actin branches in lamellipodia. Cell *134*, 828-842.

Cameron, L.A., Footer, M.J., van Oudenaarden, A., and Theriot, J.A. (1999). Motility of ActA protein-coated microspheres driven by actin polymerization. Proceedings of the National Academy of Sciences of the United States of America *96*, 4908-4913.

Campellone, K.G., Cheng, H.C., Robbins, D., Siripala, A.D., McGhie, E.J., Hayward, R.D., Welch, M.D., Rosen, M.K., Koronakis, V., and Leong, J.M. (2008a). Repetitive N-WASP-binding elements of the enterohemorrhagic Escherichia coli effector EspF(U) synergistically activate actin assembly. PLoS pathogens *4*, e1000191.

Campellone, K.G., and Leong, J.M. (2005). Nck-independent actin assembly is mediated by two phosphorylated tyrosines within enteropathogenic Escherichia coli Tir. Molecular microbiology *56*, 416-432.

Campellone, K.G., Robbins, D., and Leong, J.M. (2004). EspFU is a translocated EHEC effector that interacts with Tir and N-WASP and promotes Nck-independent actin assembly. Developmental cell *7*, 217-228.

Campellone, K.G., Webb, N.J., Znameroski, E.A., and Welch, M.D. (2008b). WHAMM is an Arp2/3 complex activator that binds microtubules and functions in ER to Golgi transport. Cell *134*, 148-161.

Campellone, K.G., and Welch, M.D. (2010). A nucleator arms race: cellular control of actin assembly. Nature reviews Molecular cell biology *11*, 237-251.

Cao, H., Orth, J.D., Chen, J., Weller, S.G., Heuser, J.E., and McNiven, M.A. (2003). Cortactin is a component of clathrin-coated pits and participates in receptor-mediated endocytosis. Molecular and cellular biology *23*, 2162-2170.

Carlier, M.F., Laurent, V., Santolini, J., Melki, R., Didry, D., Xia, G.X., Hong, Y., Chua, N.H., and Pantaloni, D. (1997). Actin depolymerizing factor (ADF/cofilin) enhances the rate of filament turnover: implication in actin-based motility. The Journal of cell biology *136*, 1307-1322.

Carlier, M.F., Nioche, P., Broutin-L'Hermite, I., Boujemaa, R., Le Clainche, C., Egile, C., Garbay, C., Ducruix, A., Sansonetti, P., and Pantaloni, D. (2000). GRB2 links signaling to actin assembly by enhancing interaction of neural Wiskott-Aldrich syndrome protein (N-WASp) with actin-related protein (ARP2/3) complex. The Journal of biological chemistry *275*, 21946-21952.

Carlier, M.F., and Pantaloni, D. (1986). Direct evidence for ADP-Pi-F-actin as the major intermediate in ATP-actin polymerization. Rate of dissociation of Pi from actin filaments. Biochemistry *25*, 7789-7792.

Carlier, M.F., and Pantaloni, D. (1997). Control of actin dynamics in cell motility. Journal of molecular biology *269*, 459-467.

Carlier, M.F., Pantaloni, D., Evans, J.A., Lambooy, P.K., Korn, E.D., and Webb, M.R. (1988). The hydrolysis of ATP that accompanies actin polymerization is essentially irreversible. FEBS letters *235*, 211-214.

Carlsson, L., Nystrom, L.E., Lindberg, U., Kannan, K.K., Cid-Dresdner, H., and Lovgren, S. (1976). Crystallization of a non-muscle actin. Journal of molecular biology *105*, 353-366.

Carlsson, L., Nystrom, L.E., Sundkvist, I., Markey, F., and Lindberg, U. (1977). Actin polymerizability is influenced by profilin, a low molecular weight protein in non-muscle cells. Journal of molecular biology *115*, 465-483.

Carter, G.C., Law, M., Hollinshead, M., and Smith, G.L. (2005). Entry of the vaccinia virus intracellular mature virion and its interactions with glycosaminoglycans. The Journal of general virology *86*, 1279-1290.

Carter, G.C., Rodger, G., Murphy, B.J., Law, M., Krauss, O., Hollinshead, M., and Smith, G.L. (2003). Vaccinia virus cores are transported on microtubules. The Journal of general virology *84*, 2443-2458.

Castagnoli, L., Costantini, A., Dall'Armi, C., Gonfloni, S., Montecchi-Palazzi, L., Panni, S., Paoluzi, S., Santonico, E., and Cesareni, G. (2004). Selectivity and promiscuity in

the interaction network mediated by protein recognition modules. FEBS letters *567*, 74-79.

Cavnar, P.J., Mogen, K., Berthier, E., Beebe, D.J., and Huttenlocher, A. (2012). The Actin Regulatory Protein HS1 Interacts with Arp2/3 and Mediates Efficient Neutrophil Chemotaxis. The Journal of biological chemistry *287*, 25466-25477.

Chakrabarti, S., Sisler, J.R., and Moss, B. (1997). Compact, synthetic, vaccinia virus early/late promoter for protein expression. BioTechniques *23*, 1094-1097.

Chan, K.T., Creed, S.J., and Bear, J.E. (2011). Unraveling the enigma: progress towards understanding the coronin family of actin regulators. Trends in cell biology *21*, 481-488.

Chen, M., She, H., Davis, E.M., Spicer, C.M., Kim, L., Ren, R., Le Beau, M.M., and Li, W. (1998). Identification of Nck family genes, chromosomal localization, expression, and signaling specificity. The Journal of biological chemistry *273*, 25171-25178.

Cheng, H.C., Skehan, B.M., Campellone, K.G., Leong, J.M., and Rosen, M.K. (2008). Structural mechanism of WASP activation by the enterohaemorrhagic E. coli effector EspF(U). Nature *454*, 1009-1013.

Chereau, D., Boczkowska, M., Skwarek-Maruszewska, A., Fujiwara, I., Hayes, D.B., Rebowski, G., Lappalainen, P., Pollard, T.D., and Dominguez, R. (2008). Leiomodin is an actin filament nucleator in muscle cells. Science *320*, 239-243.

Chereau, D., Kerff, F., Graceffa, P., Grabarek, Z., Langsetmo, K., and Dominguez, R. (2005). Actin-bound structures of Wiskott-Aldrich syndrome protein (WASP)-homology domain 2 and the implications for filament assembly. Proceedings of the National Academy of Sciences of the United States of America *102*, 16644-16649.

Chesarone, M.A., DuPage, A.G., and Goode, B.L. (2010). Unleashing formins to remodel the actin and microtubule cytoskeletons. Nature reviews Molecular cell biology *11*, 62-74.

Chhabra, E.S., and Higgs, H.N. (2007). The many faces of actin: matching assembly factors with cellular structures. Nature cell biology *9*, 1110-1121.

Chong, R., Swiss, R., Briones, G., Stone, K.L., Gulcicek, E.E., and Agaisse, H. (2009). Regulatory mimicry in Listeria monocytogenes actin-based motility. Cell host & microbe *6*, 268-278.

Chou, H.C., Anton, I.M., Holt, M.R., Curcio, C., Lanzardo, S., Worth, A., Burns, S., Thrasher, A.J., Jones, G.E., and Calle, Y. (2006). WIP regulates the stability and localization of WASP to podosomes in migrating dendritic cells. Current biology : CB *16*, 2337-2344.

Co, C., Wong, D.T., Gierke, S., Chang, V., and Taunton, J. (2007). Mechanism of actin network attachment to moving membranes: barbed end capture by N-WASP WH2 domains. Cell *128*, 901-913.

Conley, C.A., Fritz-Six, K.L., Almenar-Queralt, A., and Fowler, V.M. (2001). Leiomodins: larger members of the tropomodulin (Tmod) gene family. Genomics *73*, 127-139.

Cooper, J.A., and Pollard, T.D. (1982). Methods to measure actin polymerization. Methods in enzymology *85 Pt B*, 182-210.

Cooper, J.A., and Sept, D. (2008). New insights into mechanism and regulation of actin capping protein. International review of cell and molecular biology *267*, 183-206.

Cooper, J.A., Walker, S.B., and Pollard, T.D. (1983). Pyrene actin: documentation of the validity of a sensitive assay for actin polymerization. Journal of muscle research and cell motility *4*, 253-262.

Cornfine, S., Himmel, M., Kopp, P., El Azzouzi, K., Wiesner, C., Kruger, M., Rudel, T., and Linder, S. (2011). The kinesin KIF9 and reggie/flotillin proteins regulate matrix degradation by macrophage podosomes. Molecular biology of the cell *22*, 202-215.

Cortesio, C.L., Perrin, B.J., Bennin, D.A., and Huttenlocher, A. (2010). Actin-binding protein-1 interacts with WASp-interacting protein to regulate growth factor-induced dorsal ruffle formation. Molecular biology of the cell *21*, 186-197.

Cory, G.O., Garg, R., Cramer, R., and Ridley, A.J. (2002). Phosphorylation of tyrosine 291 enhances the ability of WASp to stimulate actin polymerization and filopodium formation. Wiskott-Aldrich Syndrome protein. The Journal of biological chemistry *277*, 45115-45121.

Courtemanche, N., and Pollard, T.D. (2012). Determinants of Formin Homology 1 (FH1) domain function in actin filament elongation by formins. The Journal of biological chemistry *287*, 7812-7820.

Cudmore, S., Cossart, P., Griffiths, G., and Way, M. (1995). Actin-based motility of vaccinia virus. Nature *378*, 636-638.

Curcio, C., Pannellini, T., Lanzardo, S., Forni, G., Musiani, P., and Anton, I.M. (2007). WIP null mice display a progressive immunological disorder that resembles Wiskott-Aldrich syndrome. The Journal of pathology *211*, 67-75.

da Silva, M.L., Mortara, R.A., Barros, H.C., de Souza, W., and Trabulsi, L.R. (1989). Aggregation of membrane-associated actin filaments following localized adherence of enteropathogenic Escherichia coli to HeLa cells. Journal of cell science *93 (Pt 3)*, 439-446.

Dalhaimer, P., and Pollard, T.D. (2010). Molecular dynamics simulations of Arp2/3 complex activation. Biophysical journal *99*, 2568-2576.

Dart, A.E., Donnelly, S.K., Holden, D.W., Way, M., and Caron, E. (2012). Nck and Cdc42 co-operate to recruit N-WASP to promote FcgammaR-mediated phagocytosis. Journal of cell science *125*, 2825-2830.

Dawes, A.T., Bard Ermentrout, G., Cytrynbaum, E.N., and Edelstein-Keshet, L. (2006). Actin filament branching and protrusion velocity in a simple 1D model of a motile cell. Journal of theoretical biology *242*, 265-279.

Dayel, M.J., Holleran, E.A., and Mullins, R.D. (2001). Arp2/3 complex requires hydrolyzable ATP for nucleation of new actin filaments. Proceedings of the National Academy of Sciences of the United States of America *98*, 14871-14876.

De La Cruz, E.M., Mandinova, A., Steinmetz, M.O., Stoffler, D., Aebi, U., and Pollard, T.D. (2000). Polymerization and structure of nucleotide-free actin filaments. Journal of molecular biology *295*, 517-526.

de la Fuente, M.A., Sasahara, Y., Calamito, M., Anton, I.M., Elkhal, A., Gallego, M.D., Suresh, K., Siminovitch, K., Ochs, H.D., Anderson, K.C.*, et al.* (2007). WIP is a chaperone for Wiskott-Aldrich syndrome protein (WASP). Proceedings of the National Academy of Sciences of the United States of America *104*, 926-931.

Delatour, V., Helfer, E., Didry, D., Le, K.H., Gaucher, J.F., Carlier, M.F., and Romet-Lemonne, G. (2008). Arp2/3 controls the motile behavior of N-WASP-functionalized

GUVs and modulates N-WASP surface distribution by mediating transient links with actin filaments. Biophysical journal *94*, 4890-4905.

Derivery, E., and Gautreau, A. (2010). Generation of branched actin networks: assembly and regulation of the N-WASP and WAVE molecular machines. BioEssays : news and reviews in molecular, cellular and developmental biology *32*, 119-131.

Derry, J.M., Ochs, H.D., and Francke, U. (1994). Isolation of a novel gene mutated in Wiskott-Aldrich syndrome. Cell *78*, 635-644.

DeVinney, R., Stein, M., Reinscheid, D., Abe, A., Ruschkowski, S., and Finlay, B.B. (1999). Enterohemorrhagic Escherichia coli O157:H7 produces Tir, which is translocated to the host cell membrane but is not tyrosine phosphorylated. Infection and immunity *67*, 2389-2398.

Didry, D., Carlier, M.F., and Pantaloni, D. (1998). Synergy between actin depolymerizing factor/cofilin and profilin in increasing actin filament turnover. The Journal of biological chemistry *273*, 25602-25611.

Ditlev, J.A., Michalski, P.J., Huber, G., Rivera, G.M., Mohler, W.A., Loew, L.M., and Mayer, B.J. (2012). Stoichiometry of Nck-dependent actin polymerization in living cells. The Journal of cell biology *197*, 643-658.

Doceul, V., Hollinshead, M., Breiman, A., Laval, K., and Smith, G.L. (2012). Protein B5 is required on extracellular enveloped vaccinia virus for repulsion of superinfecting virions. The Journal of general virology *93*, 1876-1886.

Doceul, V., Hollinshead, M., van der Linden, L., and Smith, G.L. (2010). Repulsion of superinfecting virions: a mechanism for rapid virus spread. Science *327*, 873-876.

Dodding, M.P., Mitter, R., Humphries, A.C., and Way, M. (2011). A kinesin-1 binding motif in vaccinia virus that is widespread throughout the human genome. The EMBO journal *30*, 4523-4538.

Dodding, M.P., Newsome, T.P., Collinson, L.M., Edwards, C., and Way, M. (2009). An E2-F12 complex is required for intracellular enveloped virus morphogenesis during vaccinia infection. Cellular microbiology *11*, 808-824.

Dodding, M.P., and Way, M. (2009). Nck- and N-WASP-dependent actin-based motility is conserved in divergent vertebrate poxviruses. Cell host & microbe *6*, 536-550.

Domi, A., and Beaud, G. (2000). The punctate sites of accumulation of vaccinia virus early proteins are precursors of sites of viral DNA synthesis. The Journal of general virology *81*, 1231-1235.

Dominguez, R., and Holmes, K.C. (2011). Actin structure and function. Annual review of biophysics *40*, 169-186.

Dong, X., Patino-Lopez, G., Candotti, F., and Shaw, S. (2007). Structure-function analysis of the WIP role in T cell receptor-stimulated NFAT activation: evidence that WIP-WASP dissociation is not required and that the WIP NH2 terminus is inhibitory. The Journal of biological chemistry *282*, 30303-30310.

Donnelly, S.F., Pocklington, M.J., Pallotta, D., and Orr, E. (1993). A proline-rich protein, verprolin, involved in cytoskeletal organization and cellular growth in the yeast Saccharomyces cerevisiae. Molecular microbiology *10*, 585-596.

Douangamath, A., Filipp, F.V., Klein, A.T., Barnett, P., Zou, P., Voorn-Brouwer, T., Vega, M.C., Mayans, O.M., Sattler, M., Distel, B.*, et al.* (2002). Topography for

independent binding of alpha-helical and PPII-helical ligands to a peroxisomal SH3 domain. Molecular cell *10*, 1007-1017.

Ducka, A.M., Joel, P., Popowicz, G.M., Trybus, K.M., Schleicher, M., Noegel, A.A., Huber, R., Holak, T.A., and Sitar, T. (2010). Structures of actin-bound Wiskott-Aldrich syndrome protein homology 2 (WH2) domains of Spire and the implication for filament nucleation. Proceedings of the National Academy of Sciences of the United States of America *107*, 11757-11762.

Dustin, M.L., and Depoil, D. (2011). New insights into the T cell synapse from single molecule techniques. Nature reviews Immunology *11*, 672-684.

Eck, M.J., Shoelson, S.E., and Harrison, S.C. (1993). Recognition of a high-affinity phosphotyrosyl peptide by the Src homology-2 domain of p56lck. Nature *362*, 87-91.

Edds, K.T. (1993). Effects of cytochalasin and colcemid on cortical flow in coelomocytes. Cell motility and the cytoskeleton *26*, 262-273.

Egile, C., Loisel, T.P., Laurent, V., Li, R., Pantaloni, D., Sansonetti, P.J., and Carlier, M.F. (1999). Activation of the CDC42 effector N-WASP by the Shigella flexneri IcsA protein promotes actin nucleation by Arp2/3 complex and bacterial actin-based motility. The Journal of cell biology *146*, 1319-1332.

Erickson, H.P. (2007). Evolution of the cytoskeleton. BioEssays : news and reviews in molecular, cellular and developmental biology *29*, 668-677.

Faix, J., and Rottner, K. (2006). The making of filopodia. Current opinion in cell biology *18*, 18-25.

Fedorov, A.A., Fedorov, E., Gertler, F., and Almo, S.C. (1999). Structure of EVH1, a novel proline-rich ligand-binding module involved in cytoskeletal dynamics and neural function. Nature structural biology *6*, 661-665.

Feng, S., Chen, J.K., Yu, H., Simon, J.A., and Schreiber, S.L. (1994). Two binding orientations for peptides to the Src SH3 domain: development of a general model for SH3-ligand interactions. Science *266*, 1241-1247.

Firat-Karalar, E.N., Hsiue, P.P., and Welch, M.D. (2011). The actin nucleation factor JMY is a negative regulator of neuritogenesis. Molecular biology of the cell *22*, 4563-4574.

Firat-Karalar, E.N., and Welch, M.D. (2011). New mechanisms and functions of actin nucleation. Current opinion in cell biology *23*, 4-13.

Footer, M.J., Lyo, J.K., and Theriot, J.A. (2008). Close packing of Listeria monocytogenes ActA, a natively unfolded protein, enhances F-actin assembly without dimerization. The Journal of biological chemistry *283*, 23852-23862.

Franco, A., Knafo, S., Banon-Rodriguez, I., Merino-Serrais, P., Fernaud-Espinosa, I., Nieto, M., Garrido, J.J., Esteban, J.A., Wandosell, F., and Anton, I.M. (2012). WIP is a negative regulator of neuronal maturation and synaptic activity. Cereb Cortex *22*, 1191-1202.

Frese, S., Schubert, W.D., Findeis, A.C., Marquardt, T., Roske, Y.S., Stradal, T.E., and Heinz, D.W. (2006). The phosphotyrosine peptide binding specificity of Nck1 and Nck2 Src homology 2 domains. The Journal of biological chemistry *281*, 18236-18245.

Frischknecht, F., Cudmore, S., Moreau, V., Reckmann, I., Rottger, S., and Way, M. (1999a). Tyrosine phosphorylation is required for actin-based motility of vaccinia but not Listeria or Shigella. Current biology : CB *9*, 89-92.

Frischknecht, F., Moreau, V., Rottger, S., Gonfloni, S., Reckmann, I., Superti-Furga, G., and Way, M. (1999b). Actin-based motility of vaccinia virus mimics receptor tyrosine kinase signalling. Nature *401*, 926-929.

Fujiwara, I., Takahashi, S., Tadakuma, H., Funatsu, T., and Ishiwata, S. (2002). Microscopic analysis of polymerization dynamics with individual actin filaments. Nature cell biology *4*, 666-673.

Fujiwara, I., Vavylonis, D., and Pollard, T.D. (2007). Polymerization kinetics of ADP-and ADP-Pi-actin determined by fluorescence microscopy. Proceedings of the National Academy of Sciences of the United States of America *104*, 8827-8832.

Galkin, V.E., Orlova, A., Kudryashov, D.S., Solodukhin, A., Reisler, E., Schroder, G.F., and Egelman, E.H. (2011). Remodeling of actin filaments by ADF/cofilin proteins. Proceedings of the National Academy of Sciences of the United States of America *108*, 20568-20572.

Gallego, M.D., de la Fuente, M.A., Anton, I.M., Snapper, S., Fuhlbrigge, R., and Geha, R.S. (2006). WIP and WASP play complementary roles in T cell homing and chemotaxis to SDF-1alpha. International immunology *18*, 221-232.

Garcia, E., Jones, G.E., Machesky, L.M., and Anton, I.M. (2012). WIP: WASP-interacting proteins at invadopodia and podosomes. European journal of cell biology.

Garrity, P.A., Rao, Y., Salecker, I., McGlade, J., Pawson, T., and Zipursky, S.L. (1996). Drosophila photoreceptor axon guidance and targeting requires the dreadlocks SH2/SH3 adapter protein. Cell *85*, 639-650.

Gates, M.A., Kannan, R., and Giniger, E. (2011). A genome-wide analysis reveals that the Drosophila transcription factor Lola promotes axon growth in part by suppressing expression of the actin nucleation factor Spire. Neural development *6*, 37.

Gaucher, J.F., Mauge, C., Didry, D., Guichard, B., Renault, L., and Carlier, M.F. (2012). Interactions of isolated C-terminal fragments of Neural Wiskott-Aldrich Syndrome Protein (N-WASP) with actin and Arp2/3 complex. The Journal of biological chemistry.

Gilbert, H.R., and Frieden, C. (1983). Preparation, purification and properties of a crosslinked trimer of G-actin. Biochemical and biophysical research communications *111*, 404-408.

Goebel, S.J., Johnson, G.P., Perkus, M.E., Davis, S.W., Winslow, J.P., and Paoletti, E. (1990). The complete DNA sequence of vaccinia virus. Virology *179*, 247-266, 517-263.

Goldberg, M.B., and Theriot, J.A. (1995). Shigella flexneri surface protein IcsA is sufficient to direct actin-based motility. Proceedings of the National Academy of Sciences of the United States of America *92*, 6572-6576.

Goley, E.D., Rodenbusch, S.E., Martin, A.C., and Welch, M.D. (2004). Critical conformational changes in the Arp2/3 complex are induced by nucleotide and nucleation promoting factor. Molecular cell *16*, 269-279.

Goley, E.D., and Welch, M.D. (2006). The ARP2/3 complex: an actin nucleator comes of age. Nature reviews Molecular cell biology *7*, 713-726.

Gruenheid, S., DeVinney, R., Bladt, F., Goosney, D., Gelkop, S., Gish, G.D., Pawson, T., and Finlay, B.B. (2001). Enteropathogenic E. coli Tir binds Nck to initiate actin pedestal formation in host cells. Nature cell biology *3*, 856-859.

Gu, X., Zerbini, L.F., Otu, H.H., Bhasin, M., Yang, Q., Joseph, M.G., Grall, F., Onatunde, T., Correa, R.G., and Libermann, T.A. (2007). Reduced PDEF expression

increases invasion and expression of mesenchymal genes in prostate cancer cells. Cancer research *67*, 4219-4226.

Hammer, J.A., 3rd, and Sellers, J.R. (2012). Walking to work: roles for class V myosins as cargo transporters. Nature reviews Molecular cell biology *13*, 13-26.

Hanson, J., and Lowy, J. (1964). The Structure of Actin Filaments and the Origin of the Axial Periodicity in the I-Substance of Vertebrate Striated Muscle. Proc R Soc Lond B Biol Sci *160*, 449-460.

Hartland, E.L., Batchelor, M., Delahay, R.M., Hale, C., Matthews, S., Dougan, G., Knutton, S., Connerton, I., and Frankel, G. (1999). Binding of intimin from enteropathogenic Escherichia coli to Tir and to host cells. Molecular microbiology *32*, 151-158.

Hayward, R.D., Leong, J.M., Koronakis, V., and Campellone, K.G. (2006). Exploiting pathogenic Escherichia coli to model transmembrane receptor signalling. Nature reviews Microbiology *4*, 358-370.

Herrera, E., Lorenzo, M.M., Blasco, R., and Isaacs, S.N. (1998). Functional analysis of vaccinia virus B5R protein: essential role in virus envelopment is independent of a large portion of the extracellular domain. Journal of virology *72*, 294-302.

Higgs, H.N., Blanchoin, L., and Pollard, T.D. (1999). Influence of the C terminus of Wiskott-Aldrich syndrome protein (WASp) and the Arp2/3 complex on actin polymerization. Biochemistry *38*, 15212-15222.

Higgs, H.N., and Pollard, T.D. (1999). Regulation of actin polymerization by Arp2/3 complex and WASp/Scar proteins. The Journal of biological chemistry *274*, 32531-32534.

Higgs, H.N., and Pollard, T.D. (2000). Activation by Cdc42 and PIP(2) of Wiskott-Aldrich syndrome protein (WASp) stimulates actin nucleation by Arp2/3 complex. The Journal of cell biology *150*, 1311-1320.

Hiller, G., and Weber, K. (1985). Golgi-derived membranes that contain an acylated viral polypeptide are used for vaccinia virus envelopment. Journal of virology *55*, 651-659.

Hiroaki, H., Ago, T., Ito, T., Sumimoto, H., and Kohda, D. (2001). Solution structure of the PX domain, a target of the SH3 domain. Nature structural biology *8*, 526-530.

Ho, H.Y., Rohatgi, R., Lebensohn, A.M., Le, M., Li, J., Gygi, S.P., and Kirschner, M.W. (2004). Toca-1 mediates Cdc42-dependent actin nucleation by activating the N-WASP-WIP complex. Cell *118*, 203-216.

Ho, H.Y., Rohatgi, R., Ma, L., and Kirschner, M.W. (2001). CR16 forms a complex with N-WASP in brain and is a novel member of a conserved proline-rich actin-binding protein family. Proceedings of the National Academy of Sciences of the United States of America *98*, 11306-11311.

Hollinshead, M., Rodger, G., Van Eijl, H., Law, M., Hollinshead, R., Vaux, D.J., and Smith, G.L. (2001). Vaccinia virus utilizes microtubules for movement to the cell surface. The Journal of cell biology *154*, 389-402.

Hotulainen, P., and Hoogenraad, C.C. (2010). Actin in dendritic spines: connecting dynamics to function. The Journal of cell biology *189*, 619-629.

Hotulainen, P., and Lappalainen, P. (2006). Stress fibers are generated by two distinct actin assembly mechanisms in motile cells. The Journal of cell biology *173*, 383-394.

Hubbard, S.R., and Miller, W.T. (2007). Receptor tyrosine kinases: mechanisms of activation and signaling. Current opinion in cell biology *19*, 117-123.

Hug, C., Jay, P.Y., Reddy, I., McNally, J.G., Bridgman, P.C., Elson, E.L., and Cooper, J.A. (1995). Capping protein levels influence actin assembly and cell motility in dictyostelium. Cell *81*, 591-600.

Humphries, A.C., Dodding, M.P., Barry, D.J., Collinson, L.M., Durkin, C.H., and Way, M. (2012). Clathrin potentiates vaccinia-induced actin polymerization to facilitate viral spread. Cell host & microbe *12*, 346-359.

Humphries, C.L., Balcer, H.I., D'Agostino, J.L., Winsor, B., Drubin, D.G., Barnes, G., Andrews, B.J., and Goode, B.L. (2002). Direct regulation of Arp2/3 complex activity and function by the actin binding protein coronin. The Journal of cell biology *159*, 993-1004.

Husson, C., Renault, L., Didry, D., Pantaloni, D., and Carlier, M.F. (2011). Cordon-Bleu uses WH2 domains as multifunctional dynamizers of actin filament assembly. Molecular cell *43*, 464-477.

Huxley, H.E. (1963). Electron Microscope Studies on the Structure of Natural and Synthetic Protein Filaments from Striated Muscle. Journal of molecular biology *7*, 281-308.

Innocenti, M., Gerboth, S., Rottner, K., Lai, F.P., Hertzog, M., Stradal, T.E., Frittoli, E., Didry, D., Polo, S., Disanza, A.*, et al.* (2005). Abi1 regulates the activity of N-WASP and WAVE in distinct actin-based processes. Nature cell biology *7*, 969-976.

Isenberg, G., Aebi, U., and Pollard, T.D. (1980). An actin-binding protein from Acanthamoeba regulates actin filament polymerization and interactions. Nature *288*, 455-459.

Janmey, P.A., Hvidt, S., Oster, G.F., Lamb, J., Stossel, T.P., and Hartwig, J.H. (1990). Effect of ATP on actin filament stiffness. Nature *347*, 95-99.

Jaumouille, V., and Grinstein, S. (2011). Receptor mobility, the cytoskeleton, and particle binding during phagocytosis. Current opinion in cell biology *23*, 22-29.

Jin, P., Duan, R., Luo, F., Zhang, G., Hong, S.N., and Chen, E.H. (2011). Competition between Blown fuse and WASP for WIP binding regulates the dynamics of WASP-dependent actin polymerization in vivo. Developmental cell *20*, 623-638.

Jin, Y., Mazza, C., Christie, J.R., Giliani, S., Fiorini, M., Mella, P., Gandellini, F., Stewart, D.M., Zhu, Q., Nelson, D.L.*, et al.* (2004). Mutations of the Wiskott-Aldrich Syndrome Protein (WASP): hotspots, effect on transcription, and translation and phenotype/genotype correlation. Blood *104*, 4010-4019.

Jones, G.E., Zicha, D., Dunn, G.A., Blundell, M., and Thrasher, A. (2002). Restoration of podosomes and chemotaxis in Wiskott-Aldrich syndrome macrophages following induced expression of WASp. The international journal of biochemistry & cell biology *34*, 806-815.

Kabsch, W., Mannherz, H.G., Suck, D., Pai, E.F., and Holmes, K.C. (1990). Atomic structure of the actin:DNase I complex. Nature *347*, 37-44.

Kalman, D., Weiner, O.D., Goosney, D.L., Sedat, J.W., Finlay, B.B., Abo, A., and Bishop, J.M. (1999). Enteropathogenic E. coli acts through WASP and Arp2/3 complex to form actin pedestals. Nature cell biology *1*, 389-391.

Kang, H., Freund, C., Duke-Cohan, J.S., Musacchio, A., Wagner, G., and Rudd, C.E. (2000). SH3 domain recognition of a proline-independent tyrosine-based RKxxYxxY motif in immune cell adaptor SKAP55. The EMBO journal *19*, 2889-2899.

Kardos, R., Pozsonyi, K., Nevalainen, E., Lappalainen, P., Nyitrai, M., and Hild, G. (2009). The effects of ADF/cofilin and profilin on the conformation of the ATP-binding cleft of monomeric actin. Biophysical journal *96*, 2335-2343.

Kato, M., Miki, H., Kurita, S., Endo, T., Nakagawa, H., Miyamoto, S., and Takenawa, T. (2002). WICH, a novel verprolin homology domain-containing protein that functions cooperatively with N-WASP in actin-microspike formation. Biochemical and biophysical research communications *291*, 41-47.

Kato, M., and Takenawa, T. (2005). WICH, a member of WASP-interacting protein family, cross-links actin filaments. Biochemical and biophysical research communications *328*, 1058-1066.

Kay, B.K. (2012). SH3 domains come of age. FEBS letters *586*, 2606-2608.

Kelleher, J.F., Atkinson, S.J., and Pollard, T.D. (1995). Sequences, structural models, and cellular localization of the actin-related proteins Arp2 and Arp3 from Acanthamoeba. The Journal of cell biology *131*, 385-397.

Kelly, A.E., Kranitz, H., Dotsch, V., and Mullins, R.D. (2006). Actin binding to the central domain of WASP/Scar proteins plays a critical role in the activation of the Arp2/3 complex. The Journal of biological chemistry *281*, 10589-10597.

Kempiak, S.J., Yip, S.C., Backer, J.M., and Segall, J.E. (2003). Local signaling by the EGF receptor. The Journal of cell biology *162*, 781-787.

Kenny, B. (1999). Phosphorylation of tyrosine 474 of the enteropathogenic Escherichia coli (EPEC) Tir receptor molecule is essential for actin nucleating activity and is preceded by additional host modifications. Molecular microbiology *31*, 1229-1241.

Kenny, B., DeVinney, R., Stein, M., Reinscheid, D.J., Frey, E.A., and Finlay, B.B. (1997). Enteropathogenic E. coli (EPEC) transfers its receptor for intimate adherence into mammalian cells. Cell *91*, 511-520.

Kespichayawattana, W., Rattanachetkul, S., Wanun, T., Utaisincharoen, P., and Sirisinha, S. (2000). Burkholderia pseudomallei induces cell fusion and actin-associated membrane protrusion: a possible mechanism for cell-to-cell spreading. Infection and immunity *68*, 5377-5384.

Kessels, H.W., Ward, A.C., and Schumacher, T.N. (2002). Specificity and affinity motifs for Grb2 SH2-ligand interactions. Proceedings of the National Academy of Sciences of the United States of America *99*, 8524-8529.

Kessels, M.M., and Qualmann, B. (2004). The syndapin protein family: linking membrane trafficking with the cytoskeleton. Journal of cell science *117*, 3077-3086.

Kim, A.S., Kakalis, L.T., Abdul-Manan, N., Liu, G.A., and Rosen, M.K. (2000). Autoinhibition and activation mechanisms of the Wiskott-Aldrich syndrome protein. Nature *404*, 151-158.

King, S.J., Worth, D.C., Scales, T.M., Monypenny, J., Jones, G.E., and Parsons, M. (2011). beta1 integrins regulate fibroblast chemotaxis through control of N-WASP stability. The EMBO journal *30*, 1705-1718.

Kinley, A.W., Weed, S.A., Weaver, A.M., Karginov, A.V., Bissonette, E., Cooper, J.A., and Parsons, J.T. (2003). Cortactin interacts with WIP in regulating Arp2/3 activation and membrane protrusion. Current biology : CB *13*, 384-393.

Kirkbride, K.C., Sung, B.H., Sinha, S., and Weaver, A.M. (2011). Cortactin: a multifunctional regulator of cellular invasiveness. Cell adhesion & migration *5*, 187-198.

Knutton, S., Baldwin, T., Williams, P.H., and McNeish, A.S. (1989). Actin accumulation at sites of bacterial adhesion to tissue culture cells: basis of a new diagnostic test for enteropathogenic and enterohemorrhagic Escherichia coli. Infection and immunity *57*, 1290-1298.

Koduru, S., Massaad, M., Wilbur, C., Kumar, L., Geha, R., and Ramesh, N. (2007). A novel anti-WIP monoclonal antibody detects an isoform of WIP that lacks the WASP binding domain. Biochemical and biophysical research communications *353*, 875-881.

Kovacs, E.M., Verma, S., Ali, R.G., Ratheesh, A., Hamilton, N.A., Akhmanova, A., and Yap, A.S. (2011). N-WASP regulates the epithelial junctional actin cytoskeleton through a non-canonical post-nucleation pathway. Nature cell biology *13*, 934-943.

Kreishman-Deitrick, M., Goley, E.D., Burdine, L., Denison, C., Egile, C., Li, R., Murali, N., Kodadek, T.J., Welch, M.D., and Rosen, M.K. (2005). NMR analyses of the activation of the Arp2/3 complex by neuronal Wiskott-Aldrich syndrome protein. Biochemistry *44*, 15247-15256.

Krzewski, K., Chen, X., Orange, J.S., and Strominger, J.L. (2006). Formation of a WIP-, WASp-, actin-, and myosin IIA-containing multiprotein complex in activated NK cells and its alteration by KIR inhibitory signaling. The Journal of cell biology *173*, 121-132.

Krzewski, K., Chen, X., and Strominger, J.L. (2008). WIP is essential for lytic granule polarization and NK cell cytotoxicity. Proceedings of the National Academy of Sciences of the United States of America *105*, 2568-2573.

Kumar, A., Crawford, K., Close, L., Madison, M., Lorenz, J., Doetschman, T., Pawlowski, S., Duffy, J., Neumann, J., Robbins, J*., et al.* (1997). Rescue of cardiac alpha-actin-deficient mice by enteric smooth muscle gamma-actin. Proceedings of the National Academy of Sciences of the United States of America *94*, 4406-4411.

Lai, F.P., Szczodrak, M., Block, J., Faix, J., Breitsprecher, D., Mannherz, H.G., Stradal, T.E., Dunn, G.A., Small, J.V., and Rottner, K. (2008). Arp2/3 complex interactions and actin network turnover in lamellipodia. The EMBO journal *27*, 982-992.

Lanzardo, S., Curcio, C., Forni, G., and Anton, I.M. (2007). A role for WASP Interacting Protein, WIP, in fibroblast adhesion, spreading and migration. The international journal of biochemistry & cell biology *39*, 262-274.

Lanzi, G., Moratto, D., Vairo, D., Masneri, S., Delmonte, O., Paganini, T., Parolini, S., Tabellini, G., Mazza, C., Savoldi, G*., et al.* (2012). A novel primary human immunodeficiency due to deficiency in the WASP-interacting protein WIP. The Journal of experimental medicine *209*, 29-34.

Latour, S., Roncagalli, R., Chen, R., Bakinowski, M., Shi, X., Schwartzberg, P.L., Davidson, D., and Veillette, A. (2003). Binding of SAP SH2 domain to FynT SH3 domain reveals a novel mechanism of receptor signalling in immune regulation. Nature cell biology *5*, 149-154.

Le Bras, S., Massaad, M., Koduru, S., Kumar, L., Oyoshi, M.K., Hartwig, J., and Geha, R.S. (2009). WIP is critical for T cell responsiveness to IL-2. Proceedings of the National Academy of Sciences of the United States of America *106*, 7519-7524.

Le Clainche, C., and Carlier, M.F. (2008). Regulation of actin assembly associated with protrusion and adhesion in cell migration. Physiological reviews *88*, 489-513.

Le Clainche, C., Didry, D., Carlier, M.F., and Pantaloni, D. (2001). Activation of Arp2/3 complex by Wiskott-Aldrich Syndrome protein is linked to enhanced binding of ATP to Arp2. The Journal of biological chemistry *276*, 46689-46692.

LeClaire, L.L., 3rd, Baumgartner, M., Iwasa, J.H., Mullins, R.D., and Barber, D.L. (2008). Phosphorylation of the Arp2/3 complex is necessary to nucleate actin filaments. The Journal of cell biology *182*, 647-654.

Lee, S.H., Kerff, F., Chereau, D., Ferron, F., Klug, A., and Dominguez, R. (2007). Structural basis for the actin-binding function of missing-in-metastasis. Structure *15*, 145-155.

Legg, J.A., Bompard, G., Dawson, J., Morris, H.L., Andrew, N., Cooper, L., Johnston, S.A., Tramountanis, G., and Machesky, L.M. (2007). N-WASP involvement in dorsal ruffle formation in mouse embryonic fibroblasts. Molecular biology of the cell *18*, 678-687.

Lemmon, M.A., and Schlessinger, J. (2010). Cell signaling by receptor tyrosine kinases. Cell *141*, 1117-1134.

Lettau, M., Pieper, J., and Janssen, O. (2009). Nck adapter proteins: functional versatility in T cells. Cell communication and signaling : CCS *7*, 1.

Leung, Y., Ally, S., and Goldberg, M.B. (2008). Bacterial actin assembly requires toca-1 to relieve N-wasp autoinhibition. Cell host & microbe *3*, 39-47.

Li, F., and Higgs, H.N. (2003). The mouse Formin mDia1 is a potent actin nucleation factor regulated by autoinhibition. Current biology : CB *13*, 1335-1340.

Li, P., Banjade, S., Cheng, H.C., Kim, S., Chen, B., Guo, L., Llaguno, M., Hollingsworth, J.V., King, D.S., Banani, S.F.*, et al.* (2012). Phase transitions in the assembly of multivalent signalling proteins. Nature *483*, 336-340.

Li, S.S. (2005). Specificity and versatility of SH3 and other proline-recognition domains: structural basis and implications for cellular signal transduction. The Biochemical journal *390*, 641-653.

Li, Y., Grenklo, S., Higgins, T., and Karlsson, R. (2008). The profilin:actin complex localizes to sites of dynamic actin polymerization at the leading edge of migrating cells and pathogen-induced actin tails. European journal of cell biology *87*, 893-904.

Lim, K.B., Bu, W., Goh, W.I., Koh, E., Ong, S.H., Pawson, T., Sudhaharan, T., and Ahmed, S. (2008). The Cdc42 effector IRSp53 generates filopodia by coupling membrane protrusion with actin dynamics. The Journal of biological chemistry *283*, 20454-20472.

Lim, W.A., Richards, F.M., and Fox, R.O. (1994). Structural determinants of peptide-binding orientation and of sequence specificity in SH3 domains. Nature *372*, 375-379.

Linardopoulou, E.V., Parghi, S.S., Friedman, C., Osborn, G.E., Parkhurst, S.M., and Trask, B.J. (2007). Human subtelomeric WASH genes encode a new subclass of the WASP family. PLoS genetics *3*, e237.

Liu, Q., Berry, D., Nash, P., Pawson, T., McGlade, C.J., and Li, S.S. (2003). Structural basis for specific binding of the Gads SH3 domain to an RxxK motif-containing SLP-76 peptide: a novel mode of peptide recognition. Molecular cell *11*, 471-481.

Loisel, T.P., Boujemaa, R., Pantaloni, D., and Carlier, M.F. (1999). Reconstitution of actin-based motility of Listeria and Shigella using pure proteins. Nature *401*, 613-616.

Lommel, S., Benesch, S., Rohde, M., Wehland, J., and Rottner, K. (2004). Enterohaemorrhagic and enteropathogenic Escherichia coli use different mechanisms for actin pedestal formation that converge on N-WASP. Cellular microbiology *6*, 243-254.

Lommel, S., Benesch, S., Rottner, K., Franz, T., Wehland, J., and Kuhn, R. (2001). Actin pedestal formation by enteropathogenic Escherichia coli and intracellular motility of Shigella flexneri are abolished in N-WASP-defective cells. EMBO reports *2*, 850-857.

Lu, J., and Pollard, T.D. (2001). Profilin binding to poly-L-proline and actin monomers along with ability to catalyze actin nucleotide exchange is required for viability of fission yeast. Molecular biology of the cell *12*, 1161-1175.

Lu, W., Katz, S., Gupta, R., and Mayer, B.J. (1997). Activation of Pak by membrane localization mediated by an SH3 domain from the adaptor protein Nck. Current biology : CB *7*, 85-94.

Ma, L., Rohatgi, R., and Kirschner, M.W. (1998). The Arp2/3 complex mediates actin polymerization induced by the small GTP-binding protein Cdc42. Proceedings of the National Academy of Sciences of the United States of America *95*, 15362-15367.

Machesky, L.M., Atkinson, S.J., Ampe, C., Vandekerckhove, J., and Pollard, T.D. (1994). Purification of a cortical complex containing two unconventional actins from Acanthamoeba by affinity chromatography on profilin-agarose. The Journal of cell biology *127*, 107-115.

Machesky, L.M., and Insall, R.H. (1998). Scar1 and the related Wiskott-Aldrich syndrome protein, WASP, regulate the actin cytoskeleton through the Arp2/3 complex. Current biology : CB *8*, 1347-1356.

Marchand, J.B., Kaiser, D.A., Pollard, T.D., and Higgs, H.N. (2001). Interaction of WASP/Scar proteins with actin and vertebrate Arp2/3 complex. Nature cell biology *3*, 76-82.

Marengere, L.E., Songyang, Z., Gish, G.D., Schaller, M.D., Parsons, J.T., Stern, M.J., Cantley, L.C., and Pawson, T. (1994). SH2 domain specificity and activity modified by a single residue. Nature *369*, 502-505.

Martinez-Quiles, N., Rohatgi, R., Anton, I.M., Medina, M., Saville, S.P., Miki, H., Yamaguchi, H., Takenawa, T., Hartwig, J.H., Geha, R.S.*, et al.* (2001). WIP regulates N-WASP-mediated actin polymerization and filopodium formation. Nature cell biology *3*, 484-491.

Masters, J.N., Cotman, S.L., Osterburg, H.H., Nichols, N.R., and Finch, C.E. (1996). Modulation of a novel RNA in brain neurons by glucocorticoid and mineralocorticoid receptors. Neuroendocrinology *63*, 28-38.

Mathew, E., Sanderson, C.M., Hollinshead, M., and Smith, G.L. (1998). The extracellular domain of vaccinia virus protein B5R affects plaque phenotype, extracellular enveloped virus release, and intracellular actin tail formation. Journal of virology *72*, 2429-2438.

Matozaki, T., Murata, Y., Saito, Y., Okazawa, H., and Ohnishi, H. (2009). Protein tyrosine phosphatase SHP-2: a proto-oncogene product that promotes Ras activation. Cancer science *100*, 1786-1793.

Mayer, B.J. (2001). SH3 domains: complexity in moderation. Journal of cell science *114*, 1253-1263.

Mayer, B.J., Hamaguchi, M., and Hanafusa, H. (1988a). Characterization of p47gag-crk, a novel oncogene product with sequence similarity to a putative modulatory domain of protein-tyrosine kinases and phospholipase C. Cold Spring Harbor symposia on quantitative biology *53 Pt 2*, 907-914.

Mayer, B.J., Hamaguchi, M., and Hanafusa, H. (1988b). A novel viral oncogene with structural similarity to phospholipase C. Nature *332*, 272-275.

McGough, A., Pope, B., Chiu, W., and Weeds, A. (1997). Cofilin changes the twist of F-actin: implications for actin filament dynamics and cellular function. The Journal of cell biology *138*, 771-781.

Mejillano, M.R., Kojima, S., Applewhite, D.A., Gertler, F.B., Svitkina, T.M., and Borisy, G.G. (2004). Lamellipodial versus filopodial mode of the actin nanomachinery: pivotal role of the filament barbed end. Cell *118*, 363-373.

Meng, L., Rajmohan, R., Yu, S., and Thanabalu, T. (2007). Actin binding and proline rich motifs of CR16 play redundant role in growth of vrp1Delta cells. Biochemical and biophysical research communications *357*, 289-294.

Mercer, J., and Helenius, A. (2008). Vaccinia virus uses macropinocytosis and apoptotic mimicry to enter host cells. Science *320*, 531-535.

Miki, H., Miura, K., and Takenawa, T. (1996). N-WASP, a novel actin-depolymerizing protein, regulates the cortical cytoskeletal rearrangement in a PIP2-dependent manner downstream of tyrosine kinases. The EMBO journal *15*, 5326-5335.

Miki, H., Sasaki, T., Takai, Y., and Takenawa, T. (1998). Induction of filopodium formation by a WASP-related actin-depolymerizing protein N-WASP. Nature *391*, 93-96.

Miki, H., and Takenawa, T. (1998). Direct binding of the verprolin-homology domain in N-WASP to actin is essential for cytoskeletal reorganization. Biochemical and biophysical research communications *243*, 73-78.

Miller, M.M., Lapetina, S., MacGrath, S.M., Sfakianos, M.K., Pollard, T.D., and Koleske, A.J. (2010). Regulation of actin polymerization and adhesion-dependent cell edge protrusion by the Abl-related gene (Arg) tyrosine kinase and N-WASp. Biochemistry *49*, 2227-2234.

Millius, A., Dandekar, S.N., Houk, A.R., and Weiner, O.D. (2009). Neutrophils establish rapid and robust WAVE complex polarity in an actin-dependent fashion. Current biology : CB *19*, 253-259.

Millius, A., Watanabe, N., and Weiner, O.D. (2012). Diffusion, capture and recycling of SCAR/WAVE and Arp2/3 complexes observed in cells by single-molecule imaging. Journal of cell science *125*, 1165-1176.

Misra, A., Rajmohan, R., Lim, R.P., Bhattacharyya, S., and Thanabalu, T. (2010). The mammalian verprolin, WIRE induces filopodia independent of N-WASP through IRSp53. Experimental cell research *316*, 2810-2824.

Mogilner, A., and Oster, G. (1996). Cell motility driven by actin polymerization. Biophysical journal *71*, 3030-3045.

Mooren, O.L., Galletta, B.J., and Cooper, J.A. (2012). Roles for actin assembly in endocytosis. Annual review of biochemistry *81*, 661-686.

Moreau, V., Frischknecht, F., Reckmann, I., Vincentelli, R., Rabut, G., Stewart, D., and Way, M. (2000). A complex of N-WASP and WIP integrates signalling cascades that lead to actin polymerization. Nature cell biology *2*, 441-448.

Morgan, G.W., Hollinshead, M., Ferguson, B.J., Murphy, B.J., Carpentier, D.C., and Smith, G.L. (2010). Vaccinia protein F12 has structural similarity to kinesin light chain and contains a motor binding motif required for virion export. PLoS pathogens *6*, e1000785.

Moriyama, K., and Yahara, I. (2002). Human CAP1 is a key factor in the recycling of cofilin and actin for rapid actin turnover. Journal of cell science *115*, 1591-1601.

Mouilleron, S., Guettler, S., Langer, C.A., Treisman, R., and McDonald, N.Q. (2008). Molecular basis for G-actin binding to RPEL motifs from the serum response factor coactivator MAL. The EMBO journal *27*, 3198-3208.

Mounier, J., Ryter, A., Coquis-Rondon, M., and Sansonetti, P.J. (1990). Intracellular and cell-to-cell spread of Listeria monocytogenes involves interaction with F-actin in the enterocytelike cell line Caco-2. Infection and immunity *58*, 1048-1058.

Mullins, R.D., Heuser, J.A., and Pollard, T.D. (1998). The interaction of Arp2/3 complex with actin: nucleation, high affinity pointed end capping, and formation of branching networks of filaments. Proceedings of the National Academy of Sciences of the United States of America *95*, 6181-6186.

Mullins, R.D., Stafford, W.F., and Pollard, T.D. (1997). Structure, subunit topology, and actin-binding activity of the Arp2/3 complex from Acanthamoeba. The Journal of cell biology *136*, 331-343.

Munemitsu, S., Souza, B., Muller, O., Albert, I., Rubinfeld, B., and Polakis, P. (1994). The APC gene product associates with microtubules in vivo and promotes their assembly in vitro. Cancer research *54*, 3676-3681.

Munn, A.L., and Thanabalu, T. (2009). Verprolin: a cool set of actin-binding sites and some very HOT prolines. IUBMB life *61*, 707-712.

Munter, S., Way, M., and Frischknecht, F. (2006). Signaling during pathogen infection. Science's STKE : signal transduction knowledge environment *2006*, re5.

Murphy, D.A., and Courtneidge, S.A. (2011). The 'ins' and 'outs' of podosomes and invadopodia: characteristics, formation and function. Nature reviews Molecular cell biology *12*, 413-426.

Musacchio, A., Noble, M., Pauptit, R., Wierenga, R., and Saraste, M. (1992). Crystal structure of a Src-homology 3 (SH3) domain. Nature *359*, 851-855.

Naqvi, S.N., Feng, Q., Boulton, V.J., Zahn, R., and Munn, A.L. (2001). Vrp1p functions in both actomyosin ring-dependent and Hof1p-dependent pathways of cytokinesis. Traffic *2*, 189-201.

Naqvi, S.N., Zahn, R., Mitchell, D.A., Stevenson, B.J., and Munn, A.L. (1998). The WASp homologue Las17p functions with the WIP homologue End5p/verprolin and is essential for endocytosis in yeast. Current biology : CB *8*, 959-962.

Narayanan, A., LeClaire, L.L., 3rd, Barber, D.L., and Jacobson, M.P. (2011). Phosphorylation of the Arp2 subunit relieves auto-inhibitory interactions for Arp2/3 complex activation. PLoS computational biology *7*, e1002226.

Newsome, T.P., Scaplehorn, N., and Way, M. (2004). SRC mediates a switch from microtubule- to actin-based motility of vaccinia virus. Science *306*, 124-129.

Newsome, T.P., Weisswange, I., Frischknecht, F., and Way, M. (2006). Abl collaborates with Src family kinases to stimulate actin-based motility of vaccinia virus. Cellular microbiology *8*, 233-241.

Nichols, N.R., Masters, J.N., and Finch, C.E. (1990). Changes in gene expression in hippocampus in response to glucocorticoids and stress. Brain research bulletin *24*, 659-662.

Nishida, E., and Sakai, H. (1983). Kinetic analysis of actin polymerization. Journal of biochemistry *93*, 1011-1020.

Noble, M.E., Musacchio, A., Saraste, M., Courtneidge, S.A., and Wierenga, R.K. (1993). Crystal structure of the SH3 domain in human Fyn; comparison of the three-dimensional structures of SH3 domains in tyrosine kinases and spectrin. The EMBO journal *12*, 2617-2624.

Noy, E., Fried, S., Matalon, O., and Barda-Saad, M. (2012). WIP Remodeling Actin behind the Scenes: How WIP Reshapes Immune and Other Functions. International journal of molecular sciences *13*, 7629-7647.

Nurnberg, A., Kitzing, T., and Grosse, R. (2011). Nucleating actin for invasion. Nature reviews Cancer *11*, 177-187.

Nusblat, L.M., Dovas, A., and Cox, D. (2011). The non-redundant role of N-WASP in podosome-mediated matrix degradation in macrophages. European journal of cell biology *90*, 205-212.

Obenauer, J.C., Cantley, L.C., and Yaffe, M.B. (2003). Scansite 2.0: Proteome-wide prediction of cell signaling interactions using short sequence motifs. Nucleic acids research *31*, 3635-3641.

Obermann, H., Raabe, I., Balvers, M., Brunswig, B., Schulze, W., and Kirchhoff, C. (2005). Novel testis-expressed profilin IV associated with acrosome biogenesis and spermatid elongation. Molecular human reproduction *11*, 53-64.

Okada, K., Bartolini, F., Deaconescu, A.M., Moseley, J.B., Dogic, Z., Grigorieff, N., Gundersen, G.G., and Goode, B.L. (2010). Adenomatous polyposis coli protein nucleates actin assembly and synergizes with the formin mDia1. The Journal of cell biology *189*, 1087-1096.

Okreglak, V., and Drubin, D.G. (2007). Cofilin recruitment and function during actin-mediated endocytosis dictated by actin nucleotide state. The Journal of cell biology *178*, 1251-1264.

Olivier, A., Jeanson-Leh, L., Bouma, G., Compagno, D., Blondeau, J., Seye, K., Charrier, S., Burns, S., Thrasher, A.J., Danos, O.*, et al.* (2006). A partial down-regulation of WASP is sufficient to inhibit podosome formation in dendritic cells. Molecular therapy : the journal of the American Society of Gene Therapy *13*, 729-737.

Olson, M.F., and Sahai, E. (2009). The actin cytoskeleton in cancer cell motility. Clinical & experimental metastasis *26*, 273-287.

Orlova, A., and Egelman, E.H. (1992). Structural basis for the destabilization of F-actin by phosphate release following ATP hydrolysis. Journal of molecular biology *227*, 1043-1053.

Oser, M., Dovas, A., Cox, D., and Condeelis, J. (2011). Nck1 and Grb2 localization patterns can distinguish invadopodia from podosomes. European journal of cell biology *90*, 181-188.

Oser, M., Mader, C.C., Gil-Henn, H., Magalhaes, M., Bravo-Cordero, J.J., Koleske, A.J., and Condeelis, J. (2010). Specific tyrosine phosphorylation sites on cortactin regulate Nck1-dependent actin polymerization in invadopodia. Journal of cell science *123*, 3662-3673.

Otomo, T., Tomchick, D.R., Otomo, C., Panchal, S.C., Machius, M., and Rosen, M.K. (2005). Structural basis of actin filament nucleation and processive capping by a formin homology 2 domain. Nature *433*, 488-494.

Padrick, S.B., Cheng, H.C., Ismail, A.M., Panchal, S.C., Doolittle, L.K., Kim, S., Skehan, B.M., Umetani, J., Brautigam, C.A., Leong, J.M.*, et al.* (2008). Hierarchical regulation of WASP/WAVE proteins. Molecular cell *32*, 426-438.

Padrick, S.B., Doolittle, L.K., Brautigam, C.A., King, D.S., and Rosen, M.K. (2011). Arp2/3 complex is bound and activated by two WASP proteins. Proceedings of the National Academy of Sciences of the United States of America *108*, E472-479.

Padrick, S.B., and Rosen, M.K. (2010). Physical mechanisms of signal integration by WASP family proteins. Annual review of biochemistry *79*, 707-735.

Panchal, S.C., Kaiser, D.A., Torres, E., Pollard, T.D., and Rosen, M.K. (2003). A conserved amphipathic helix in WASP/Scar proteins is essential for activation of Arp2/3 complex. Nature structural biology *10*, 591-598.

Pantaloni, D., Boujemaa, R., Didry, D., Gounon, P., and Carlier, M.F. (2000). The Arp2/3 complex branches filament barbed ends: functional antagonism with capping proteins. Nature cell biology *2*, 385-391.

Pantaloni, D., Le Clainche, C., and Carlier, M.F. (2001). Mechanism of actin-based motility. Science *292*, 1502-1506.

Papayannopoulos, V., Co, C., Prehoda, K.E., Snapper, S., Taunton, J., and Lim, W.A. (2005). A polybasic motif allows N-WASP to act as a sensor of PIP(2) density. Molecular cell *17*, 181-191.

Pardee, J.D., and Spudich, J.A. (1982). Mechanism of K+-induced actin assembly. The Journal of cell biology *93*, 648-654.

Park, H., and Cox, D. (2009). Cdc42 regulates Fc gamma receptor-mediated phagocytosis through the activation and phosphorylation of Wiskott-Aldrich syndrome protein (WASP) and neural-WASP. Molecular biology of the cell *20*, 4500-4508.

Pauker, M.H., Reicher, B., Fried, S., Perl, O., and Barda-Saad, M. (2011). Functional cooperation between the proteins Nck and ADAP is fundamental for actin reorganization. Molecular and cellular biology *31*, 2653-2666.

Paul, A.S., and Pollard, T.D. (2008). The role of the FH1 domain and profilin in formin-mediated actin-filament elongation and nucleation. Current biology : CB *18*, 9-19.

Pawson, T. (2004). Specificity in signal transduction: from phosphotyrosine-SH2 domain interactions to complex cellular systems. Cell *116*, 191-203.

Pawson, T. (2007). Dynamic control of signaling by modular adaptor proteins. Current opinion in cell biology *19*, 112-116.

Pellegrin, S., and Mellor, H. (2007). Actin stress fibres. Journal of cell science *120*, 3491-3499.

Perrin, B.J., and Ervasti, J.M. (2010). The actin gene family: function follows isoform. Cytoskeleton (Hoboken) *67*, 630-634.

Peterson, F.C., Deng, Q., Zettl, M., Prehoda, K.E., Lim, W.A., Way, M., and Volkman, B.F. (2007). Multiple WASP-interacting protein recognition motifs are required for a functional interaction with N-WASP. The Journal of biological chemistry *282*, 8446-8453.

Pfender, S., Kuznetsov, V., Pleiser, S., Kerkhoff, E., and Schuh, M. (2011). Spire-type actin nucleators cooperate with Formin-2 to drive asymmetric oocyte division. Current biology : CB *21*, 955-960.

Phillips, N., Hayward, R.D., and Koronakis, V. (2004). Phosphorylation of the enteropathogenic E. coli receptor by the Src-family kinase c-Fyn triggers actin pedestal formation. Nature cell biology *6*, 618-625.

Pinyol, R., Haeckel, A., Ritter, A., Qualmann, B., and Kessels, M.M. (2007). Regulation of N-WASP and the Arp2/3 complex by Abp1 controls neuronal morphology. PloS one *2*, e400.

Pollard, T.D. (1983). Measurement of rate constants for actin filament elongation in solution. Analytical biochemistry *134*, 406-412.

Pollard, T.D. (1986). Rate constants for the reactions of ATP- and ADP-actin with the ends of actin filaments. The Journal of cell biology *103*, 2747-2754.

Pollard, T.D. (2007). Regulation of actin filament assembly by Arp2/3 complex and formins. Annual review of biophysics and biomolecular structure *36*, 451-477.

Pollard, T.D., and Borisy, G.G. (2003). Cellular motility driven by assembly and disassembly of actin filaments. Cell *112*, 453-465.

Pollard, T.D., and Cooper, J.A. (1984). Quantitative analysis of the effect of Acanthamoeba profilin on actin filament nucleation and elongation. Biochemistry *23*, 6631-6641.

Pollard, T.D., and Cooper, J.A. (2009). Actin, a central player in cell shape and movement. Science *326*, 1208-1212.

Pollard, T.D., and Weeds, A.G. (1984). The rate constant for ATP hydrolysis by polymerized actin. FEBS letters *170*, 94-98.

Porta, J.C., and Borgstahl, G.E. (2012). Structural basis for profilin-mediated actin nucleotide exchange. Journal of molecular biology *418*, 103-116.

Prehoda, K.E., Lee, D.J., and Lim, W.A. (1999). Structure of the enabled/VASP homology 1 domain-peptide complex: a key component in the spatial control of actin assembly. Cell *97*, 471-480.

Prehoda, K.E., Scott, J.A., Mullins, R.D., and Lim, W.A. (2000). Integration of multiple signals through cooperative regulation of the N-WASP-Arp2/3 complex. Science *290*, 801-806.

Pruyne, D., Evangelista, M., Yang, C., Bi, E., Zigmond, S., Bretscher, A., and Boone, C. (2002). Role of formins in actin assembly: nucleation and barbed-end association. Science *297*, 612-615.

Qualmann, B., and Kessels, M.M. (2002). Endocytosis and the cytoskeleton. International review of cytology *220*, 93-144.

Qualmann, B., and Kessels, M.M. (2009). New players in actin polymerization--WH2-domain-containing actin nucleators. Trends in cell biology *19*, 276-285.

Quinlan, M.E., Heuser, J.E., Kerkhoff, E., and Mullins, R.D. (2005). Drosophila Spire is an actin nucleation factor. Nature *433*, 382-388.

Quinlan, M.E., Hilgert, S., Bedrossian, A., Mullins, R.D., and Kerkhoff, E. (2007). Regulatory interactions between two actin nucleators, Spire and Cappuccino. The Journal of cell biology *179*, 117-128.

Ramesh, N., Anton, I.M., Hartwig, J.H., and Geha, R.S. (1997). WIP, a protein associated with wiskott-aldrich syndrome protein, induces actin polymerization and redistribution in lymphoid cells. Proceedings of the National Academy of Sciences of the United States of America *94*, 14671-14676.

Reebye, V., Frilling, A., Hajitou, A., Nicholls, J.P., Habib, N.A., and Mintz, P.J. (2012). A perspective on non-catalytic Src homology (SH) adaptor signalling proteins. Cellular signalling *24*, 388-392.

Reeves, P.M., Bommarius, B., Lebeis, S., McNulty, S., Christensen, J., Swimm, A., Chahroudi, A., Chavan, R., Feinberg, M.B., Veach, D.*, et al.* (2005). Disabling poxvirus pathogenesis by inhibition of Abl-family tyrosine kinases. Nature medicine *11*, 731-739.

Reicher, B., and Barda-Saad, M. (2010). Multiple pathways leading from the T-cell antigen receptor to the actin cytoskeleton network. FEBS letters *584*, 4858-4864.

Ren, R., Mayer, B.J., Cicchetti, P., and Baltimore, D. (1993). Identification of a ten-amino acid proline-rich SH3 binding site. Science *259*, 1157-1161.

Ridley, A.J. (2011). Life at the leading edge. Cell *145*, 1012-1022.

Rietdorf, J., Ploubidou, A., Reckmann, I., Holmstrom, A., Frischknecht, F., Zettl, M., Zimmermann, T., and Way, M. (2001). Kinesin-dependent movement on microtubules precedes actin-based motility of vaccinia virus. Nature cell biology *3*, 992-1000.

Rivera, G.M., Briceno, C.A., Takeshima, F., Snapper, S.B., and Mayer, B.J. (2004). Inducible clustering of membrane-targeted SH3 domains of the adaptor protein Nck triggers localized actin polymerization. Current biology : CB *14*, 11-22.

Rivera, G.M., Vasilescu, D., Papayannopoulos, V., Lim, W.A., and Mayer, B.J. (2009). A reciprocal interdependence between Nck and PI(4,5)P(2) promotes localized N-WASp-mediated actin polymerization in living cells. Molecular cell *36*, 525-535.

Rivero-Lezcano, O.M., Marcilla, A., Sameshima, J.H., and Robbins, K.C. (1995). Wiskott-Aldrich syndrome protein physically associates with Nck through Src homology 3 domains. Molecular and cellular biology *15*, 5725-5731.

Roberts, K.L., and Smith, G.L. (2008). Vaccinia virus morphogenesis and dissemination. Trends in microbiology *16*, 472-479.

Robinson, R.C., Turbedsky, K., Kaiser, D.A., Marchand, J.B., Higgs, H.N., Choe, S., and Pollard, T.D. (2001). Crystal structure of Arp2/3 complex. Science *294*, 1679-1684.

Rodal, A.A., Sokolova, O., Robins, D.B., Daugherty, K.M., Hippenmeyer, S., Riezman, H., Grigorieff, N., and Goode, B.L. (2005). Conformational changes in the Arp2/3 complex leading to actin nucleation. Nature structural & molecular biology *12*, 26-31.

Rodger, G., and Smith, G.L. (2002). Replacing the SCR domains of vaccinia virus protein B5R with EGFP causes a reduction in plaque size and actin tail formation but enveloped virions are still transported to the cell surface. The Journal of general virology *83*, 323-332.

Rohatgi, R., Ho, H.Y., and Kirschner, M.W. (2000). Mechanism of N-WASP activation by CDC42 and phosphatidylinositol 4, 5-bisphosphate. The Journal of cell biology *150*, 1299-1310.

Rohatgi, R., Ma, L., Miki, H., Lopez, M., Kirchhausen, T., Takenawa, T., and Kirschner, M.W. (1999). The interaction between N-WASP and the Arp2/3 complex links Cdc42-dependent signals to actin assembly. Cell *97*, 221-231.

Rohatgi, R., Nollau, P., Ho, H.Y., Kirschner, M.W., and Mayer, B.J. (2001). Nck and phosphatidylinositol 4,5-bisphosphate synergistically activate actin polymerization through the N-WASP-Arp2/3 pathway. The Journal of biological chemistry *276*, 26448-26452.

Romero, S., Le Clainche, C., Didry, D., Egile, C., Pantaloni, D., and Carlier, M.F. (2004). Formin is a processive motor that requires profilin to accelerate actin assembly and associated ATP hydrolysis. Cell *119*, 419-429.

Rosenshine, I., Ruschkowski, S., Stein, M., Reinscheid, D.J., Mills, S.D., and Finlay, B.B. (1996). A pathogenic bacterium triggers epithelial signals to form a functional bacterial receptor that mediates actin pseudopod formation. The EMBO journal *15*, 2613-2624.

Rottger, S., Frischknecht, F., Reckmann, I., Smith, G.L., and Way, M. (1999). Interactions between vaccinia virus IEV membrane proteins and their roles in IEV assembly and actin tail formation. Journal of virology *73*, 2863-2875.

Rouiller, I., Xu, X.P., Amann, K.J., Egile, C., Nickell, S., Nicastro, D., Li, R., Pollard, T.D., Volkmann, N., and Hanein, D. (2008). The structural basis of actin filament branching by the Arp2/3 complex. The Journal of cell biology *180*, 887-895.

Ruusala, A., Pawson, T., Heldin, C.H., and Aspenstrom, P. (2008). Nck adapters are involved in the formation of dorsal ruffles, cell migration, and Rho signaling downstream of the platelet-derived growth factor beta receptor. The Journal of biological chemistry *283*, 30034-30044.

Sadowski, I., Stone, J.C., and Pawson, T. (1986). A noncatalytic domain conserved among cytoplasmic protein-tyrosine kinases modifies the kinase function and transforming activity of Fujinami sarcoma virus P130gag-fps. Molecular and cellular biology *6*, 4396-4408.

Sagot, I., Rodal, A.A., Moseley, J., Goode, B.L., and Pellman, D. (2002). An actin nucleation mechanism mediated by Bni1 and profilin. Nature cell biology *4*, 626-631.

Saksela, K., and Permi, P. (2012). SH3 domain ligand binding: What's the consensus and where's the specificity? FEBS letters *586*, 2609-2614.

Sallee, N.A., Rivera, G.M., Dueber, J.E., Vasilescu, D., Mullins, R.D., Mayer, B.J., and Lim, W.A. (2008). The pathogen protein EspF(U) hijacks actin polymerization using mimicry and multivalency. Nature *454*, 1005-1008.

Sasahara, Y., Rachid, R., Byrne, M.J., de la Fuente, M.A., Abraham, R.T., Ramesh, N., and Geha, R.S. (2002). Mechanism of recruitment of WASP to the immunological synapse and of its activation following TCR ligation. Molecular cell *10*, 1269-1281.

Sato, M., Sawahata, R., Takenouchi, T., and Kitani, H. (2011). Identification of Fyn as the binding partner for the WASP N-terminal domain in T cells. International immunology *23*, 493-502.

Savoy, D.N., Billadeau, D.D., and Leibson, P.J. (2000). Cutting edge: WIP, a binding partner for Wiskott-Aldrich syndrome protein, cooperates with Vav in the regulation of T cell activation. J Immunol *164*, 2866-2870.

Scaplehorn, N., Holmstrom, A., Moreau, V., Frischknecht, F., Reckmann, I., and Way, M. (2002). Grb2 and Nck act cooperatively to promote actin-based motility of vaccinia virus. Current biology : CB *12*, 740-745.

Schmelz, M., Sodeik, B., Ericsson, M., Wolffe, E.J., Shida, H., Hiller, G., and Griffiths, G. (1994). Assembly of vaccinia virus: the second wrapping cisterna is derived from the trans Golgi network. Journal of virology *68*, 130-147.

Schmidt, F.I., Bleck, C.K., Helenius, A., and Mercer, J. (2011). Vaccinia extracellular virions enter cells by macropinocytosis and acid-activated membrane rupture. The EMBO journal *30*, 3647-3661.

Schutt, C.E., Myslik, J.C., Rozycki, M.D., Goonesekere, N.C., and Lindberg, U. (1993). The structure of crystalline profilin-beta-actin. Nature *365*, 810-816.

Schwintzer, L., Koch, N., Ahuja, R., Grimm, J., Kessels, M.M., and Qualmann, B. (2011). The functions of the actin nucleator Cobl in cellular morphogenesis critically depend on syndapin I. The EMBO journal *30*, 3147-3159.

Scita, G., Confalonieri, S., Lappalainen, P., and Suetsugu, S. (2008). IRSp53: crossing the road of membrane and actin dynamics in the formation of membrane protrusions. Trends in cell biology *18*, 52-60.

Selden, L.A., Kinosian, H.J., Estes, J.E., and Gershman, L.C. (1999). Impact of profilin on actin-bound nucleotide exchange and actin polymerization dynamics. Biochemistry *38*, 2769-2778.

Serio, A.W., Jeng, R.L., Haglund, C.M., Reed, S.C., and Welch, M.D. (2010). Defining a core set of actin cytoskeletal proteins critical for actin-based motility of Rickettsia. Cell host & microbe *7*, 388-398.

Shawlot, W., Deng, J.M., Fohn, L.E., and Behringer, R.R. (1998). Restricted beta-galactosidase expression of a hygromycin-lacZ gene targeted to the beta-actin locus and embryonic lethality of beta-actin mutant mice. Transgenic research *7*, 95-103.

Shibata, T., Takeshima, F., Chen, F., Alt, F.W., and Snapper, S.B. (2002). Cdc42 facilitates invasion but not the actin-based motility of Shigella. Current biology : CB *12*, 341-345.

Shin, N., Lee, S., Ahn, N., Kim, S.A., Ahn, S.G., YongPark, Z., and Chang, S. (2007). Sorting nexin 9 interacts with dynamin 1 and N-WASP and coordinates synaptic vesicle endocytosis. The Journal of biological chemistry *282*, 28939-28950.

Silvin, C., Belisle, B., and Abo, A. (2001). A role for Wiskott-Aldrich syndrome protein in T-cell receptor-mediated transcriptional activation independent of actin polymerization. The Journal of biological chemistry *276*, 21450-21457.

Skoble, J., Auerbuch, V., Goley, E.D., Welch, M.D., and Portnoy, D.A. (2001). Pivotal role of VASP in Arp2/3 complex-mediated actin nucleation, actin branch-formation, and Listeria monocytogenes motility. The Journal of cell biology *155*, 89-100.

Skoble, J., Portnoy, D.A., and Welch, M.D. (2000). Three regions within ActA promote Arp2/3 complex-mediated actin nucleation and Listeria monocytogenes motility. The Journal of cell biology *150*, 527-538.

Small, J.V., Isenberg, G., and Celis, J.E. (1978). Polarity of actin at the leading edge of cultured cells. Nature *272*, 638-639.

Small, J.V., Stradal, T., Vignal, E., and Rottner, K. (2002). The lamellipodium: where motility begins. Trends in cell biology *12*, 112-120.

Snapper, S.B., Rosen, F.S., Mizoguchi, E., Cohen, P., Khan, W., Liu, C.H., Hagemann, T.L., Kwan, S.P., Ferrini, R., Davidson, L.*, et al.* (1998). Wiskott-Aldrich syndrome protein-deficient mice reveal a role for WASP in T but not B cell activation. Immunity *9*, 81-91.

Snapper, S.B., Takeshima, F., Anton, I., Liu, C.H., Thomas, S.M., Nguyen, D., Dudley, D., Fraser, H., Purich, D., Lopez-Ilasaca, M.*, et al.* (2001). N-WASP deficiency reveals distinct pathways for cell surface projections and microbial actin-based motility. Nature cell biology *3*, 897-904.

Songyang, Z., Shoelson, S.E., Chaudhuri, M., Gish, G., Pawson, T., Haser, W.G., King, F., Roberts, T., Ratnofsky, S., Lechleider, R.J.*, et al.* (1993). SH2 domains recognize specific phosphopeptide sequences. Cell *72*, 767-778.

Songyang, Z., Shoelson, S.E., McGlade, J., Olivier, P., Pawson, T., Bustelo, X.R., Barbacid, M., Sabe, H., Hanafusa, H., Yi, T.*, et al.* (1994). Specific motifs recognized by the SH2 domains of Csk, 3BP2, fps/fes, GRB-2, HCP, SHC, Syk, and Vav. Molecular and cellular biology *14*, 2777-2785.

Sparks, A.B., Rider, J.E., Hoffman, N.G., Fowlkes, D.M., Quillam, L.A., and Kay, B.K. (1996). Distinct ligand preferences of Src homology 3 domains from Src, Yes, Abl, Cortactin, p53bp2, PLCgamma, Crk, and Grb2. Proceedings of the National Academy of Sciences of the United States of America *93*, 1540-1544.

Stamm, L.M., Pak, M.A., Morisaki, J.H., Snapper, S.B., Rottner, K., Lommel, S., and Brown, E.J. (2005). Role of the WASP family proteins for Mycobacterium marinum actin tail formation. Proceedings of the National Academy of Sciences of the United States of America *102*, 14837-14842.

Staub, E., Groene, J., Heinze, M., Mennerich, D., Roepcke, S., Klaman, I., Hinzmann, B., Castanos-Velez, E., Pilarsky, C., Mann, B.*, et al.* (2009). An expression module of WIPF1-coexpressed genes identifies patients with favorable prognosis in three tumor types. J Mol Med (Berl) *87*, 633-644.

Stewart, D.M., Tian, L., and Nelson, D.L. (1999). Mutations that cause the Wiskott-Aldrich syndrome impair the interaction of Wiskott-Aldrich syndrome protein (WASP) with WASP interacting protein. J Immunol *162*, 5019-5024.

Stoletov, K.V., Ratcliffe, K.E., Spring, S.C., and Terman, B.I. (2001). NCK and PAK participate in the signaling pathway by which vascular endothelial growth factor stimulates the assembly of focal adhesions. The Journal of biological chemistry *276*, 22748-22755.

Stylli, S.S., Stacey, T.T., Verhagen, A.M., Xu, S.S., Pass, I., Courtneidge, S.A., and Lock, P. (2009). Nck adaptor proteins link Tks5 to invadopodia actin regulation and ECM degradation. Journal of cell science *122*, 2727-2740.

Suarez, C., Roland, J., Boujemaa-Paterski, R., Kang, H., McCullough, B.R., Reymann, A.C., Guerin, C., Martiel, J.L., De la Cruz, E.M., and Blanchoin, L. (2011). Cofilin tunes the nucleotide state of actin filaments and severs at bare and decorated segment boundaries. Current biology : CB *21*, 862-868.

Suetsugu, S., Banzai, Y., Kato, M., Fukami, K., Kataoka, Y., Takai, Y., Yoshida, N., and Takenawa, T. (2007). Male-specific sterility caused by the loss of CR16. Genes to cells : devoted to molecular & cellular mechanisms *12*, 721-733.

Suetsugu, S., Hattori, M., Miki, H., Tezuka, T., Yamamoto, T., Mikoshiba, K., and Takenawa, T. (2002). Sustained activation of N-WASP through phosphorylation is essential for neurite extension. Developmental cell *3*, 645-658.

Suzuki, M., Morita, H., and Ueno, N. (2012). Molecular mechanisms of cell shape changes that contribute to vertebrate neural tube closure. Development, growth & differentiation *54*, 266-276.

Suzuki, T., Miki, H., Takenawa, T., and Sasakawa, C. (1998). Neural Wiskott-Aldrich syndrome protein is implicated in the actin-based motility of Shigella flexneri. The EMBO journal *17*, 2767-2776.

Suzuki, T., Mimuro, H., Miki, H., Takenawa, T., Sasaki, T., Nakanishi, H., Takai, Y., and Sasakawa, C. (2000). Rho family GTPase Cdc42 is essential for the actin-based motility of Shigella in mammalian cells. The Journal of experimental medicine *191*, 1905-1920.

Suzuki, T., Mimuro, H., Suetsugu, S., Miki, H., Takenawa, T., and Sasakawa, C. (2002). Neural Wiskott-Aldrich syndrome protein (N-WASP) is the specific ligand for Shigella VirG among the WASP family and determines the host cell type allowing actin-based spreading. Cellular microbiology *4*, 223-233.

Svitkina, T.M., and Borisy, G.G. (1999). Arp2/3 complex and actin depolymerizing factor/cofilin in dendritic organization and treadmilling of actin filament array in lamellipodia. The Journal of cell biology *145*, 1009-1026.

Svitkina, T.M., Verkhovsky, A.B., McQuade, K.M., and Borisy, G.G. (1997). Analysis of the actin-myosin II system in fish epidermal keratocytes: mechanism of cell body translocation. The Journal of cell biology *139*, 397-415.

Swimm, A., Bommarius, B., Li, Y., Cheng, D., Reeves, P., Sherman, M., Veach, D., Bornmann, W., and Kalman, D. (2004). Enteropathogenic Escherichia coli use redundant tyrosine kinases to form actin pedestals. Molecular biology of the cell *15*, 3520-3529.

Symons, M., Derry, J.M., Karlak, B., Jiang, S., Lemahieu, V., McCormick, F., Francke, U., and Abo, A. (1996). Wiskott-Aldrich syndrome protein, a novel effector for the GTPase CDC42Hs, is implicated in actin polymerization. Cell *84*, 723-734.

Symons, M.H., and Mitchison, T.J. (1991). Control of actin polymerization in live and permeabilized fibroblasts. The Journal of cell biology *114*, 503-513.

Takano, K., Toyooka, K., and Suetsugu, S. (2008). EFC/F-BAR proteins and the N-WASP-WIP complex induce membrane curvature-dependent actin polymerization. The EMBO journal *27*, 2817-2828.

Tanaka, M., Gupta, R., and Mayer, B.J. (1995). Differential inhibition of signaling pathways by dominant-negative SH2/SH3 adapter proteins. Molecular and cellular biology *15*, 6829-6837.

Tatarova, Z., Brabek, J., Rosel, D., and Novotny, M. (2012). SH3 domain tyrosine phosphorylation--sites, role and evolution. PloS one *7*, e36310.

Thanabalu, T., and Munn, A.L. (2001). Functions of Vrp1p in cytokinesis and actin patches are distinct and neither requires a WH2/V domain. The EMBO journal *20*, 6979-6989.

Theriot, J.A., and Mitchison, T.J. (1991). Actin microfilament dynamics in locomoting cells. Nature *352*, 126-131.

Thevenot, E., Moreau, A.W., Rousseau, V., Combeau, G., Domenichini, F., Jacquet, C., Goupille, O., Amar, M., Kreis, P., Fossier, P.*, et al.* (2011). p21-Activated kinase 3 (PAK3) protein regulates synaptic transmission through its interaction with the Nck2/Grb4 protein adaptor. The Journal of biological chemistry *286*, 40044-40059.

Thrasher, A.J., and Burns, S.O. (2010). WASP: a key immunological multitasker. Nature reviews Immunology *10*, 182-192.

Ti, S.C., Jurgenson, C.T., Nolen, B.J., and Pollard, T.D. (2011). Structural and biochemical characterization of two binding sites for nucleation-promoting factor WASp-VCA on Arp2/3 complex. Proceedings of the National Academy of Sciences of the United States of America *108*, E463-471.

Tilney, L.G., Bonder, E.M., Coluccio, L.M., and Mooseker, M.S. (1983). Actin from Thyone sperm assembles on only one end of an actin filament: a behavior regulated by profilin. The Journal of cell biology *97*, 112-124.

Tilney, L.G., and Portnoy, D.A. (1989). Actin filaments and the growth, movement, and spread of the intracellular bacterial parasite, Listeria monocytogenes. The Journal of cell biology *109*, 1597-1608.

Tolonen, N., Doglio, L., Schleich, S., and Krijnse Locker, J. (2001). Vaccinia virus DNA replication occurs in endoplasmic reticulum-enclosed cytoplasmic mini-nuclei. Molecular biology of the cell *12*, 2031-2046.

Tomasevic, N., Jia, Z., Russell, A., Fujii, T., Hartman, J.J., Clancy, S., Wang, M., Beraud, C., Wood, K.W., and Sakowicz, R. (2007). Differential regulation of WASP and N-WASP by Cdc42, Rac1, Nck, and PI(4,5)P2. Biochemistry *46*, 3494-3502.

Tondeleir, D., Vandamme, D., Vandekerckhove, J., Ampe, C., and Lambrechts, A. (2009). Actin isoform expression patterns during mammalian development and in pathology: insights from mouse models. Cell motility and the cytoskeleton *66*, 798-815.

Tong, A.H., Drees, B., Nardelli, G., Bader, G.D., Brannetti, B., Castagnoli, L., Evangelista, M., Ferracuti, S., Nelson, B., Paoluzi, S.*, et al.* (2002). A combined experimental and computational strategy to define protein interaction networks for peptide recognition modules. Science *295*, 321-324.

Tooze, J., Hollinshead, M., Reis, B., Radsak, K., and Kern, H. (1993). Progeny vaccinia and human cytomegalovirus particles utilize early endosomal cisternae for their envelopes. European journal of cell biology *60*, 163-178.

Torres, E., and Rosen, M.K. (2003). Contingent phosphorylation/dephosphorylation provides a mechanism of molecular memory in WASP. Molecular cell *11*, 1215-1227.

Torres, E., and Rosen, M.K. (2006). Protein-tyrosine kinase and GTPase signals cooperate to phosphorylate and activate Wiskott-Aldrich syndrome protein (WASP)/neuronal WASP. The Journal of biological chemistry *281*, 3513-3520.

Tsuboi, S. (2006). A complex of Wiskott-Aldrich syndrome protein with mammalian verprolins plays an important role in monocyte chemotaxis. J Immunol *176*, 6576-6585.

Tybulewicz, V.L., Ardouin, L., Prisco, A., and Reynolds, L.F. (2003). Vav1: a key signal transducer downstream of the TCR. Immunological reviews *192*, 42-52.

Urban, E., Jacob, S., Nemethova, M., Resch, G.P., and Small, J.V. (2010). Electron tomography reveals unbranched networks of actin filaments in lamellipodia. Nature cell biology *12*, 429-435.

Uruno, T., Zhang, P., Liu, J., Hao, J.J., and Zhan, X. (2003). Haematopoietic lineage cell-specific protein 1 (HS1) promotes actin-related protein (Arp) 2/3 complex-mediated actin polymerization. The Biochemical journal *371*, 485-493.

Vadlamudi, R.K., Li, F., Barnes, C.J., Bagheri-Yarmand, R., and Kumar, R. (2004). p41-Arc subunit of human Arp2/3 complex is a p21-activated kinase-1-interacting substrate. EMBO reports *5*, 154-160.

Vaduva, G., Martin, N.C., and Hopper, A.K. (1997). Actin-binding verprolin is a polarity development protein required for the morphogenesis and function of the yeast actin cytoskeleton. The Journal of cell biology *139*, 1821-1833.

Vaduva, G., Martinez-Quiles, N., Anton, I.M., Martin, N.C., Geha, R.S., Hopper, A.K., and Ramesh, N. (1999). The human WASP-interacting protein, WIP, activates the cell polarity pathway in yeast. The Journal of biological chemistry *274*, 17103-17108.

van Eijl, H., Hollinshead, M., and Smith, G.L. (2000). The vaccinia virus A36R protein is a type Ib membrane protein present on intracellular but not extracellular enveloped virus particles. Virology *271*, 26-36.

Vaynberg, J., Fukuda, T., Chen, K., Vinogradova, O., Velyvis, A., Tu, Y., Ng, L., Wu, C., and Qin, J. (2005). Structure of an ultraweak protein-protein complex and its crucial role in regulation of cell morphology and motility. Molecular cell *17*, 513-523.

Veltman, D.M., and Insall, R.H. (2010). WASP family proteins: their evolution and its physiological implications. Molecular biology of the cell *21*, 2880-2893.

Vetterkind, S., Miki, H., Takenawa, T., Klawitz, I., Scheidtmann, K.H., and Preuss, U. (2002). The rat homologue of Wiskott-Aldrich syndrome protein (WASP)-interacting protein (WIP) associates with actin filaments, recruits N-WASP from the nucleus, and mediates mobilization of actin from stress fibers in favor of filopodia formation. The Journal of biological chemistry *277*, 87-95.

Vingadassalom, D., Campellone, K.G., Brady, M.J., Skehan, B., Battle, S.E., Robbins, D., Kapoor, A., Hecht, G., Snapper, S.B., and Leong, J.M. (2010). Enterohemorrhagic E. coli requires N-WASP for efficient type III translocation but not for EspFU-mediated actin pedestal formation. PLoS pathogens *6*, e1001056.

Vingadassalom, D., Kazlauskas, A., Skehan, B., Cheng, H.C., Magoun, L., Robbins, D., Rosen, M.K., Saksela, K., and Leong, J.M. (2009). Insulin receptor tyrosine kinase substrate links the E. coli O157:H7 actin assembly effectors Tir and EspF(U) during pedestal formation. Proceedings of the National Academy of Sciences of the United States of America *106*, 6754-6759.

Vinzenz, M., Nemethova, M., Schur, F., Mueller, J., Narita, A., Urban, E., Winkler, C., Schmeiser, C., Koestler, S.A., Rottner, K.*, et al.* (2012). Actin branching in the initiation and maintenance of lamellipodia. Journal of cell science *125*, 2775-2785.

Volkman, B.F., Prehoda, K.E., Scott, J.A., Peterson, F.C., and Lim, W.A. (2002). Structure of the N-WASP EVH1 domain-WIP complex: insight into the molecular basis of Wiskott-Aldrich Syndrome. Cell *111*, 565-576.

Volkmer, R. (2009). Synthesis and application of peptide arrays: quo vadis SPOT technology. Chembiochem *10*, 1431-1442.

Waksman, G., Kominos, D., Robertson, S.C., Pant, N., Baltimore, D., Birge, R.B., Cowburn, D., Hanafusa, H., Mayer, B.J., Overduin, M.*, et al.* (1992). Crystal structure of the phosphotyrosine recognition domain SH2 of v-src complexed with tyrosine-phosphorylated peptides. Nature *358*, 646-653.

Waksman, G., Shoelson, S.E., Pant, N., Cowburn, D., and Kuriyan, J. (1993). Binding of a high affinity phosphotyrosyl peptide to the Src SH2 domain: crystal structures of the complexed and peptide-free forms. Cell *72*, 779-790.

Wang, Y.L. (1985). Exchange of actin subunits at the leading edge of living fibroblasts: possible role of treadmilling. The Journal of cell biology *101*, 597-602.

Watanabe, N., and Mitchison, T.J. (2002). Single-molecule speckle analysis of actin filament turnover in lamellipodia. Science *295*, 1083-1086.

Waterman-Storer, C.M., Desai, A., Bulinski, J.C., and Salmon, E.D. (1998). Fluorescent speckle microscopy, a method to visualize the dynamics of protein assemblies in living cells. Current biology : CB *8*, 1227-1230.

Way, M., Pope, B., Gooch, J., Hawkins, M., and Weeds, A.G. (1990). Identification of a region in segment 1 of gelsolin critical for actin binding. The EMBO journal *9*, 4103-4109.

Wear, M.A., Yamashita, A., Kim, K., Maeda, Y., and Cooper, J.A. (2003). How capping protein binds the barbed end of the actin filament. Current biology : CB *13*, 1531-1537.

Weaver, A.M., Heuser, J.E., Karginov, A.V., Lee, W.L., Parsons, J.T., and Cooper, J.A. (2002). Interaction of cortactin and N-WASp with Arp2/3 complex. Current biology : CB *12*, 1270-1278.

Weaver, A.M., Karginov, A.V., Kinley, A.W., Weed, S.A., Li, Y., Parsons, J.T., and Cooper, J.A. (2001). Cortactin promotes and stabilizes Arp2/3-induced actin filament network formation. Current biology : CB *11*, 370-374.

Weber, C., Schreiber, T.B., and Daub, H. (2012). Dual phosphoproteomics and chemical proteomics analysis of erlotinib and gefitinib interference in acute myeloid leukemia cells. Journal of proteomics *75*, 1343-1356.

Weed, S.A., Karginov, A.V., Schafer, D.A., Weaver, A.M., Kinley, A.W., Cooper, J.A., and Parsons, J.T. (2000). Cortactin localization to sites of actin assembly in lamellipodia requires interactions with F-actin and the Arp2/3 complex. The Journal of cell biology *151*, 29-40.

Wegner, A. (1976). Head to tail polymerization of actin. Journal of molecular biology *108*, 139-150.

Wegner, A., and Isenberg, G. (1983). 12-fold difference between the critical monomer concentrations of the two ends of actin filaments in physiological salt conditions. Proceedings of the National Academy of Sciences of the United States of America *80*, 4922-4925.

Weiler, M.C., Smith, J.L., and Masters, J.N. (1996). CR16, a novel proline-rich protein expressed in rat brain neurons, binds to SH3 domains and is a MAP kinase substrate. Journal of molecular neuroscience : MN *7*, 203-215.

Weiner, O.D., Marganski, W.A., Wu, L.F., Altschuler, S.J., and Kirschner, M.W. (2007). An actin-based wave generator organizes cell motility. PLoS biology *5*, e221.

Weiss, S.M., Ladwein, M., Schmidt, D., Ehinger, J., Lommel, S., Stading, K., Beutling, U., Disanza, A., Frank, R., Jansch, L.*, et al.* (2009). IRSp53 links the enterohemorrhagic E. coli effectors Tir and EspFU for actin pedestal formation. Cell host & microbe *5*, 244-258.

Weisswange, I., Newsome, T.P., Schleich, S., and Way, M. (2009). The rate of N-WASP exchange limits the extent of ARP2/3-complex-dependent actin-based motility. Nature *458*, 87-91.

Welch, M.D., DePace, A.H., Verma, S., Iwamatsu, A., and Mitchison, T.J. (1997a). The human Arp2/3 complex is composed of evolutionarily conserved subunits and is

localized to cellular regions of dynamic actin filament assembly. The Journal of cell biology *138*, 375-384.

Welch, M.D., Iwamatsu, A., and Mitchison, T.J. (1997b). Actin polymerization is induced by Arp2/3 protein complex at the surface of Listeria monocytogenes. Nature *385*, 265-269.

Welch, M.D., Rosenblatt, J., Skoble, J., Portnoy, D.A., and Mitchison, T.J. (1998). Interaction of human Arp2/3 complex and the Listeria monocytogenes ActA protein in actin filament nucleation. Science *281*, 105-108.

Weng, Z., Rickles, R.J., Feng, S., Richard, S., Shaw, A.S., Schreiber, S.L., and Brugge, J.S. (1995). Structure-function analysis of SH3 domains: SH3 binding specificity altered by single amino acid substitutions. Molecular and cellular biology *15*, 5627-5634.

Winter, D., Lechler, T., and Li, R. (1999). Activation of the yeast Arp2/3 complex by Bee1p, a WASP-family protein. Current biology : CB *9*, 501-504.

Winter, D., Podtelejnikov, A.V., Mann, M., and Li, R. (1997). The complex containing actin-related proteins Arp2 and Arp3 is required for the motility and integrity of yeast actin patches. Current biology : CB *7*, 519-529.

Witke, W. (2004). The role of profilin complexes in cell motility and other cellular processes. Trends in cell biology *14*, 461-469.

Witke, W., Sutherland, J.D., Sharpe, A., Arai, M., and Kwiatkowski, D.J. (2001). Profilin I is essential for cell survival and cell division in early mouse development. Proceedings of the National Academy of Sciences of the United States of America *98*, 3832-3836.

Wong, A.R., Pearson, J.S., Bright, M.D., Munera, D., Robinson, K.S., Lee, S.F., Frankel, G., and Hartland, E.L. (2011). Enteropathogenic and enterohaemorrhagic Escherichia coli: even more subversive elements. Molecular microbiology *80*, 1420-1438.

Wong, A.R., Raymond, B., Collins, J.W., Crepin, V.F., and Frankel, G. (2012). The enteropathogenic E. coli effector EspH promotes actin pedestal formation and elongation via WASP-interacting protein (WIP). Cellular microbiology *14*, 1051-1070.

Woodrum, D.T., Rich, S.A., and Pollard, T.D. (1975). Evidence for biased bidirectional polymerization of actin filaments using heavy meromyosin prepared by an improved method. The Journal of cell biology *67*, 231-237.

Wu, C., Asokan, S.B., Berginski, M.E., Haynes, E.M., Sharpless, N.E., Griffith, J.D., Gomez, S.M., and Bear, J.E. (2012). Arp2/3 is critical for lamellipodia and response to extracellular matrix cues but is dispensable for chemotaxis. Cell *148*, 973-987.

Wunderlich, L., Goher, A., Farago, A., Downward, J., and Buday, L. (1999). Requirement of multiple SH3 domains of Nck for ligand binding. Cellular signalling *11*, 253-262.

Xiang, W., Wen, Z., Pang, W., Hu, L., Xiong, C., and Zhang, Y. (2011). CR16 forms a complex with N-WASP in human testes. Cell and tissue research *344*, 519-526.

Xu, P., Johnson, T.L., Stoller-Conrad, J.R., and Schulz, R.A. (2012a). Spire, an actin nucleation factor, regulates cell division during Drosophila heart development. PloS one *7*, e30565.

Xu, X.P., Rouiller, I., Slaughter, B.D., Egile, C., Kim, E., Unruh, J.R., Fan, X., Pollard, T.D., Li, R., Hanein, D.*, et al.* (2012b). Three-dimensional reconstructions of Arp2/3 complex with bound nucleation promoting factors. The EMBO journal *31*, 236-247.

Yamaguchi, H., Lorenz, M., Kempiak, S., Sarmiento, C., Coniglio, S., Symons, M., Segall, J., Eddy, R., Miki, H., Takenawa, T.*, et al.* (2005). Molecular mechanisms of invadopodium formation: the role of the N-WASP-Arp2/3 complex pathway and cofilin. The Journal of cell biology *168*, 441-452.

Yu, H., Chen, J.K., Feng, S., Dalgarno, D.C., Brauer, A.W., and Schreiber, S.L. (1994). Structural basis for the binding of proline-rich peptides to SH3 domains. Cell *76*, 933-945.

Zalevsky, J., Grigorova, I., and Mullins, R.D. (2001a). Activation of the Arp2/3 complex by the Listeria acta protein. Acta binds two actin monomers and three subunits of the Arp2/3 complex. The Journal of biological chemistry *276*, 3468-3475.

Zalevsky, J., Lempert, L., Kranitz, H., and Mullins, R.D. (2001b). Different WASP family proteins stimulate different Arp2/3 complex-dependent actin-nucleating activities. Current biology : CB *11*, 1903-1913.

Zarrinpar, A., Bhattacharyya, R.P., and Lim, W.A. (2003). The structure and function of proline recognition domains. Science's STKE : signal transduction knowledge environment *2003*, RE8.

Zettl, M., and Way, M. (2002). The WH1 and EVH1 domains of WASP and Ena/VASP family members bind distinct sequence motifs. Current biology : CB *12*, 1617-1622.

Zhang, J., Shehabeldin, A., da Cruz, L.A., Butler, J., Somani, A.K., McGavin, M., Kozieradzki, I., dos Santos, A.O., Nagy, A., Grinstein, S.*, et al.* (1999). Antigen receptor-induced activation and cytoskeletal rearrangement are impaired in Wiskott-Aldrich syndrome protein-deficient lymphocytes. The Journal of experimental medicine *190*, 1329-1342.

Zhao, Z.S., Manser, E., and Lim, L. (2000). Interaction between PAK and nck: a template for Nck targets and role of PAK autophosphorylation. Molecular and cellular biology *20*, 3906-3917.

Zheng, J.Q., Wan, J.J., and Poo, M.M. (1996). Essential role of filopodia in chemotropic turning of nerve growth cone induced by a glutamate gradient. The Journal of neuroscience : the official journal of the Society for Neuroscience *16*, 1140-1149.

Zuchero, J.B., Coutts, A.S., Quinlan, M.E., Thangue, N.B., and Mullins, R.D. (2009). p53-cofactor JMY is a multifunctional actin nucleation factor. Nature cell biology *11*, 451-459.